Department of
Organic Chemistry
Faculty of Chemistry

Department of Lipids
Characterization and Quality
Instituto de la Grasa

Phenolics as carbonyl scavengers: an additional protection against lipid oxidative damage in foods.

Mª ISABEL AGUILAR TÉLLEZ

Rosario Zamora Corchero, Profesora de Investigación del Consejo Superior de Investigaciones Científicas (CSIC), y **Francisco Javier Hidalgo García,** Profesor de Investigación del Consejo Superior de Investigaciones Científicas (CSIC),

INFORMAN que el presente trabajo titulado "Phenolics as carbonyl scavengers: an additional protection against lipid oxidative damage in foods" ha sido realizado bajo nuestra dirección y asesoramiento en los laboratorios del Departamento de Caracterización y Calidad de Lípidos del Instituto de la Grasa (CSIC) de Sevilla durante los cursos académicos 2013-2014 al 2017-2018, constituyendo la Memoria que presenta la Lcda. Mª Isabel Aguilar Téllez para aspirar al grado de Doctor con la mención "Doctor Internacional" por la Universidad de Sevilla.

Consideramos que el trabajo realizado es original y ha dado lugar a cinco artículos científicos en revistas con amplio reconocimiento internacional. La excelente labor realizada por la Lcda. Mª Isabel Aguilar Téllez, tanto en tareas experimentales como en las discusiones de los resultados, acredita una formación adecuada para la obtención del título de Doctor con la mención "Doctor Internacional" por la Universidad de Sevilla.

Y para que conste a efectos de tramitación de la referida Tesis, firmamos el presente informe en Sevilla a ocho de Febrero de dos mil dieciocho.

Prof. Rosario Zamora Corchero Prof. Francisco J. Hidalgo García

VºBº

Tutora de la Tesis

Prof. Mª Carmen Ortíz Mellet.
Catedrática de la Universidad de Sevilla

Department of
Organic Chemistry
Faculty of Chemistry

Department of Lipids
Characterization and Quality
Instituto de la Grasa

Phenolics as carbonyl scavengers: an additional protection against lipid oxidative damage in foods.

Doctoral thesis for the degree of Philosophiae Doctor

presented by Mª Isabel Aguilar Téllez

Seville, 2018.

Department of
Organic Chemistry
Faculty of Chemistry

Department of Lipids
Characterization and Quality
Instituto de la Grasa

Thesis Supervisor Approval

Prof. Francisco J. Hidalgo García
Instituto de la Grasa
Spanish National Research Council (CSIC)
Seville, Spain

Thesis Supervisor Approval

Prof. Rosario Zamora Corchero
Instituto de la Grasa
Spanish National Research Council (CSIC)
Seville, Spain

Tutor: Professor Mª Carmen Ortiz Mellet
Department of Organic Chemistry
Faculty of Chemistry
University of Seville
Seville, Spain

Supervisors: Professor Francisco Javier Hidalgo García
Instituto de la Grasa
Spanish National Research Council (CSIC)
Seville, Spain

Professor Rosario Zamora Corchero
Instituto de la Grasa
Spanish National Research Council (CSIC)
Seville, Spain

Reviewers: Dr. Stephen Elmore
Department of Food and Nutritional Sciences
University of Reading
Whiteknights, Reading, UK.

Dr. Pedro Jesús García Moreno
National Food Institute
Technical University of Denmark
Lyngby, Denmark

University of Seville
Seville, 2018.

I would like to acknowledge personally everyone who has been by my side during these years. I feel really lucky to be able to count on such wonderful people.

Firstly, I wish to express my sincere gratitude to my supervisors Prof. Francisco J. Hidalgo and Prof. Rosario Zamora. I cannot thank them enough for giving me the chance to work with them and helping me as much as possible during all the process of this thesis. Thanks for your patience and understanding.

I am also very grateful to Prof. Mª Carmen Ortiz Mellet for being the tutor of this thesis and for receiving me and solving problems whenever I have needed it.

I would also like to thank Dr. Maurizio Servili for giving me the opportunity to stay for a short period of time at Università degli Studi di Perugia (Italy). I am grateful to everyone in the group for their kindness, especially to Beatrice, who was always available to help me, and to Dr. Roberto Selvaggini, for his interesting explanations about chromatography.

Thanks to Dr. Stephen Elmore and Dr. Pedro Jesús García Moreno for their careful pre-examination of this thesis.

To Prof. Inmaculada Robina, I truly appreciate that you gave me the first opportunity to work in science and, to Dr. Fernando Monje, thanks for allowing me to discover the fascinating world of Molecular Biology.

Thanks to all my colleagues at the Instituto de la Grasa, especially to Cristina, Esme and Rosa, for sharing laughters, conversations and experiences. I am happy to have shared such a good time with you and I wish we had spent more time working together. I am also grateful to Mere and Mercedes, because although we have not shared any time in the laboratory, they gave me advice and support a lot of times. And, of course, special thanks to Jose Luis for listening to me and helping me, and always receiving me with a smile. Besides, thanks to José J. Ríos for the LC-HRMS analyses.

To my university friends (Ana, Marta, Pilis, Rocío, Samuel and Sheila), because you are the proof that demonstrate that chemists can be good-

looking and funny. You are the best thing Chemistry has given to me. Thanks for so many unforgettable moments. "*Without Chemistry, this reaction would have not been possible*".

And, my deepest gratitude goes to my family and my husband.

To my parents, for their love, for doing their best to bring me up, and make me be the person that I am today. I am so proud of you.

To my sister, for being not only my sister, but my friend and my teacher, for guiding me and looking after me. Words cannot express how grateful I am.

To my husband, Álvaro, for having chosen me to share your life and for your understanding. Thanks for being so optimistic, for valuing me and making me feel self-confident.

Finally, I wish to pay special thanks to the Ministerio de Economía, Industria y Competitividad of Spain for granting my fellowship (BES-2013-063600). The study was supported partly by the European Union (FEDER funds), and the Plan Nacional de I+D of the Ministerio de Economía, Industria y Competitividad of Spain (Projects AGL2012-35627 and AGL2015-68186-R); this financial support is gratefully acknowledged.

INDEXES

LIST OF FIGURES

LIST OF TABLES

LIST OF ABBREVIATIONS

AGEs. Advanced glycation end-products

ALEs. Advanced lipoxidation end-products

E_a. Activation energy

EI. Electron ionization

ESI. Electrospray ionization

FRS. Free radical scavengers

GC-MS. Gas chromatography-mass spectrometry.

HAAs. Heterocyclic aromatic amines

HNE. 4-Hydroxy-*trans*-2-nonenal

$L^{\bullet}$. Lipid radical

LC-HRMS. Liquid chromatography-high resolution mass spectrometry.

LC-MS/MS. Liquid chromatography-tandem mass spectrometry.

LH. Lipid

$LO^{\bullet}$. Lipid alcoxyl radical

$LOO^{\bullet}$. Lipid peroxyl radical

LOOH. Lipid hydroperoxide

LOPs. Lipid oxidation products

MRM. Multiple reaction monitoring

MS. Mass spectrometry

MSD. Mass selective detector

NMR. Nuclear magnetic resonance spectroscopy

$OH^{\bullet}$. Hydroxyl radical.

PhIP. 2-Amino-1-methyl-6-phenylimidazo[4,5-*b*]pyridine

PUFAs. Polyunsaturated fatty acids

RNS. Reactive nitrogen species

ROS. Reactive oxygen species

SAR. Structure-activity relationships

TAG. Triacylglycerol.

TOF. Time-of-flight

LIST OF ISOLATED AND CHARACTERIZED COMPOUNDS

Compound 2. 4-(1-Methoxypentyl)-2-methyl-1,3-phenylene diacetate

Compound 3. 2-Methyl-4-(pent-1-en-1-yl)-1,3-phenylene diacetate

Compound 4. 4-(1-Acetoxypentyl)-2-methyl-1,3-phenylene diacetate

Compound 5. 4-Butyl-8-methyl-3-propylchroman-2,7-diyl diacetate

Compound 6. 4-(1-Methoxypropyl)benzene-1,3-diol

Compound 7. 4-(1-Methoxypentyl)benzene-1,3-diol

Compound 8. 2-(1-Hydroxypentyl)benzene-1,3-diol

Compound 9a and 9b 4-(1-Methoxy-2-methylbutyl)benzene-1,3-diol

Compound 10. 4-(1-Methoxyhexyl)benzene-1,3-diol

Compound 11. 4-(1-Methoxypropyl)-2-methylbenzene-1,3-diol

Compound 12. 4-(1-Methoxypentyl)-2-methylbenzene-1,3-diol

Compound 13. 2-Methyl-4-(pent-1-en-1-yl)benzene-1,3-diol

Compound 14a and 14b. 4-(1-Methoxy-2-methylbutyl)-2-methylbenzene-1,3-diol

Compound 15. 4-(1-Methoxy-3-methylbutyl)-2-methylbenzene-1,3-diol

Compound 16. 4-(Hex-1-en-1-yl)-2-methylbenzene-1,3-diol

Compound 17. 1-(2,4-Dihydroxyphenyl)-2-hydroxyethan-1-one

Compound 18. 1-(2,4-dihydroxy-3-methylphenyl)-2-hydroxyethan-1-one

Compound 19. 2-Ethyl-3-methyl-2*H*-chromen-7-ol

Compound 20a and 20b. 4-Ethyl-2-hydroxy-6-methyl-1,3a,4,9b-tetrahydro-2*H*-furo[2,3-*c*]chromen-7-yl acetate

Compound 21. 2-Ethyl-8-methyl-4-(2-oxoethyl)-2*H*-chromen-7-yl acetate

Compound 22. 2-Hydroxy-6,9-dimethyl-4-pentyl-1,3a,4,9b-tetrahydro-2*H*-furo[2,3-*c*]chromen-7-yl acetate

Compound 23. 8-Methyl-4-(2-oxoethyl)-2-pentyl-2*H*-chromen-7-yl acetate

Compound 24. 1,8-Dimethyl-3,4,4a,9a-tetrahydro-1*H*-pyrano[3,4-*b*]benzofuran-3,7-diyl diacetate

Compound 25a and 25b. 1-Ethyl-8-methyl-3,4,4a,9a-tetrahydro-1*H*-pyrano[3,4-*b*]benzofuran-3,7-diyl diacetate

Compound 26. 1-Ethyl-5,8-dimethyl-3,4,4a,9a-tetrahydro-1*H*-pyrano[3,4-*b*]benzofuran-3,7-diyl diacetate

Compound 29. 7-Methyl-2-(2-oxobutyl)benzofuran-6-yl acetate

Compound 30a and 30b. 8a-Ethyl-7-methyl-2,3,3a,8a-tetrahydrofuro[2,3-*b*]benzofuran-2,6-diyl diacetate

Compound 31a and 31b. 8-Methyl-4-propionylchromane-2,7-diyl diacetate

Compound 32. 7-Methyl-2-(2-oxoheptyl)benzofuran-6-yl acetate

Compound 33a and 33b. 7-Methyl-8a-pentyl-2,3,3a,8a-tetrahydrofuro[2,3-*b*]benzofuran-2,6-diyl diacetate

Compound 34a and 34b. 4-Hexanoyl-8-methylchromane-2,7-diyl diacetate

Compound 35. 2-(2-Hydroxyheptyl)-7-methylbenzofuran-6-ol

Compound 36. 2-(2-Hydroxyheptyl)benzofuran-6-ol

Compound 37. 2-(2-Hydroxyethyl)-7-methylbenzofuran-6-ol

Compound 38. 2-(2-Hydroxyethyl)-7-methyl-2,3-dihydrobenzofuran-3,6-diol

Compound 39. 2-(2-Hydroxyethyl)benzofuran-6-ol

Compound 56. 2-(3,4-Dihydroxyphenyl)-3,5,8-trihydroxy-9,10-dihydro-4*H*,8*H*-pyrano[2,3-*f*]chromen-4-one

Compound 57. 2-(3,4-Dihydroxyphenyl)-3,5,8-trihydroxy-10-methyl-9,10-dihydro- 4*H*,8*H*-pyrano[2,3-*f*]chromen-4-one

Compound 61. 2-(3,4-Dihydroxyphenyl)-3,5-dihydroxy-8-methyl-4*H*,8*H*-pyrano-[2,3-*f*]chromen-4-one

Compound 62. 2-(3,4-Dihydroxyphenyl)- 3,5-dihydroxy-8-ethyl-4*H*,8*H*-pyrano-[2,3-*f*]chromen-4-one

LIST OF ORIGINAL PUBLICATIONS

Paper 1. Zamora, R., Navarro, J. L., Aguilar, I., & Hidalgo, F. J. (2015). Lipid-derived aldehyde degradation under thermal conditions. *Food Chemistry*, 174, 89-96.

Paper 2. Zamora, R., Aguilar, I., Granvogl, M., & Hidalgo, F. J. (2016). Toxicologically relevant aldehydes produced during frying process are trapped by food phenolics. *Journal of Agricultural and Food Chemistry*, 64, 5583-5589.

Paper 3. Zamora, R., Aguilar, I., & Hidalgo, F. J. (2017). Epoxyalkenal-trapping ability of phenolic compounds. *Food Chemistry*, 237, 444-452.

Paper 4. Hidalgo, F. J., Aguilar, I., & Zamora, R. (2017). Model studies on the effect of aldehyde structure on their selective trapping by phenolic compounds**.** *Journal of Agricultural and Food Chemistry*, 65, 4736-4743.

Paper 5. Hidalgo, F. J., Aguilar, I., & Zamora, R. (2017). Phenolic trapping of lipid oxidation products 4-oxo-2-alkenals. *Food Chemistry*, 240, 822-830.

1. INTRODUCTION

1.1. Lipids as a source of reactive carbonyls in foods.

1.1.1. Lipids.

Lipids are a complex group of organic compounds that are insoluble in water but soluble in organic solvents (e.g., chloroform, ether), and are present or are derived from living organisms (Nichols & Sanderson, 2003; Coultate, 2016). Therefore, this broad definition includes many chemically heterogeneous substances, such as acylglycerols, waxes, phospholipids, sphingolipids, steroids, tocopherols, carotenoids, terpenes and polycyclic hydrocarbons.

Lipids can be classified on the basis of their physical properties at room temperature (oils are liquid and fats are solid), their polarity [neutral (e.g., triacylglycerols) or polar (e.g., phospholipids)], or their essentiality for humans (essential or nonessential fatty acids). Besides, based on structure, lipids can be classified as simple (acylglycerols, waxes and esters of sterols), complex (glycerophospholipids, glyceroglycolipids and sphingolipids) and derived (fatty alcohols, fatty acids, steroids, fat-soluble vitamins and hydrocarbons) (Mara Block & Barrera-Arellano, 2012; O´Keefe, 2008).

Lipids are necessary components in our diet because of their relation to our health. Thus, they are sources of fat-soluble vitamins (A, D, E, and K) and other functional compounds such as essential fatty acids, and provide energy for organic functions. In addition, foods lipids play an important role in food quality by contributing to sensory attributes such as color, rheological properties, and flavor. In general, lipids have a desirable impact on the sensory properties of foods by affecting the mouth-feel. On the other hand, this desirable contribution may be easily lost as a consequence of deteriorative reactions, mainly oxidation and hydrolysis (Kolakowska & Sikorski, 2003; McClements & Decker, 2017).

1.1.2. Fatty acids as major lipid components.

The major components of lipids are fatty acids. They are aliphatic compounds that contain a hydrocarbon chain with a carboxylic group. Most fatty acids in nature range from 14 to 24 carbons. While over 500 individual fatty acids have been described from animal, plant, and microbial sources, only a few of them are quantitatively significant. Thus, approximately 95% of the fatty acids from plant oils consist of only seven components: lauric, myristic, palmitic, stearic, oleic, linoleic, and α-linolenic acids (Nichols & Sanderson, 2003).

Fatty acids are generally classified as either saturated or unsaturated, depending on the presence or not of double bonds in their structure. Those with more than one double bond in the carbon chain are known as polyunsaturated fatty acids (PUFAs). The most common PUFAs present in plants and animals have an even number of carbons (predominantly 16 and 18) and non-conjugated double bonds, with a methylene group that is inserted between each two *cis*-double bonds (Mara Block & Barrera-Arellano, 2012; O´Keefe, 2008; McClements & Decker, 2017; Coultate, 2016).

PUFAs can be classified into different families depending on the position of the first carbon-carbon double bond by counting from the methyl end of the chain. Thus, there are three main families of PUFAs: ω3 (linolenic type), ω6 (linoleic type) and ω9 (oleic acid type) (**Figure 1**).

Some PUFAs cannot be synthesized by the human body. Thus, linoleic acid is considered an essential fatty acid required as building blocks for biologically active membranes. α-Linolenic acid, which belongs to the ω3 family and is synthesized only by plants, also plays a nutritional role as essential fatty acid (Belitz et al., 2009).

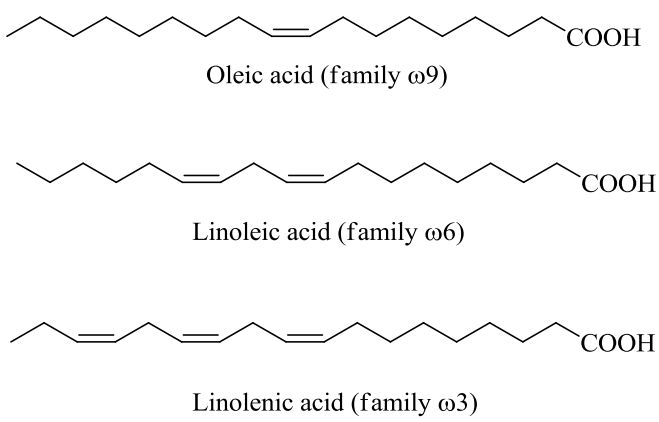

***Figure 1**. Chemical structures of some fatty acids corresponding to main PUFAs families.*

1.1.3. Lipid oxidation as a major deteriorative process in foods.

All food components are susceptible to oxidation. However, lipids are affected by oxidation more easily than proteins, carbohydrates, or nucleic acids. This process leads to important deteriorative changes in food properties, such as nutritional losses (PUFAs, vitamins, carotenoids,…) and production of undesirable flavor, color, and toxic compounds, which causes consumer rejection and potential safety problems (Kim & Min, 2008; Márquez-Ruiz et al., 2014; Uluata et al., 2015; Lee et al., 2014; Kim et al., 2016).

Lipid oxidation depends on numerous internal and external factors such as fatty acid composition, content and activity of pro- and antioxidants, light, temperature, concentration of oxygen, surface area in contact with oxygen, water activity, food structure and distribution of lipids in the food (Márquez-Ruiz et al., 2014; Kolakowska, 2003; Tenyang et al., 2017).

Lipid oxidation process is induced by different mechanisms, including free-radical reactions (autooxidation), light energy (photooxidation), enzyme action (lipoxygenase), and the presence of trace metals (Márquez-Ruiz et al., 2014). Among them, autooxidation is the most common process leading to

oxidative deterioration of food lipids (Senanayake, 2013). This process takes place through a sequential free radical chain reaction mechanism, which implies the well-known stages of initiation, propagation and termination (Erickson, 2008; Frankel, 2005; Coultate, 2016). It is schematically represented in **Figure 2**.

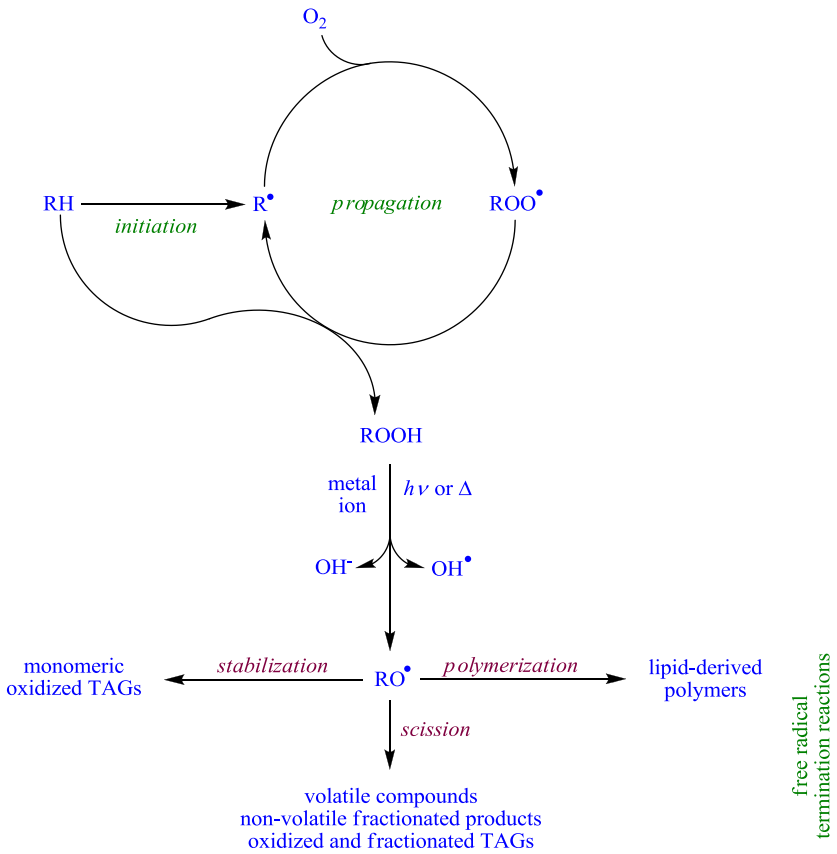

***Figure 2**. Lipid oxidation pathway. RH, lipid; R•, lipid radical; RO•, lipid alcoxyl radical; ROO•, lipid peroxyl radical; ROOH, lipid hydroperoxide; OH•, hydroxyl radical; OH^-, hydroxide ion*; *TAG, triacylglycerol.*

The initiation step involves the abstraction of a hydrogen from a fatty acid (RH) to form a fatty acid radical known as the alkyl radical (R•)

(McClements, & Decker, 2017). The generation of primary free radicals is a thermodynamically unfavorable reaction and needs to be facilitated by the presence of oxidation initiators such as light, heat, ionizing radiation, transition metals, metalloproteins, oxidants, various hemolysis-prone substances and enzymes (Senanayake, 2013).

$$RH + \text{initiator} \longrightarrow R^{\bullet}$$

The free radicals are formed at the carbon that requires least energy for a hydrogen atom removal**.** In fatty acids, allylic hydrogens have the lowest C-H bond energies, so they are the preferred sites for H removal and formation of a free radical. The methylene groups between two double bonds in lipids are doubly activated so C-H bond energies drop dramatically and radicals are formed at these positions (Schaich, 2013; Coultate, 2016).

Once the alkyl radical is produced, it is stabilized by delocalization over the double bond(s), which results in double bonds shifting and conjugation. This process is shown in **Figure 3**.

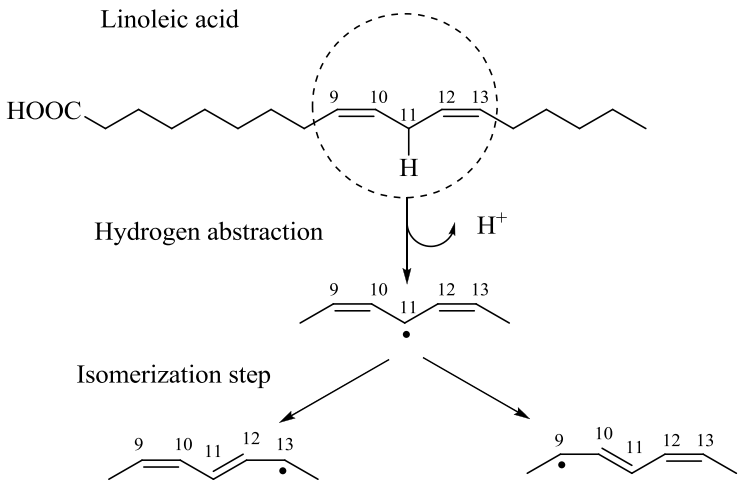

Figure 3. *The initiation step of lipid oxidation for linoleic acid (McClements, & Decker, 2017).*

The propagation step involves the addition of oxygen to the alkyl radical ($R^{\bullet}$) to form a peroxyl radical ($ROO^{\bullet}$) (McClements & Decker, 2017).

$$R^{\bullet} + O_2 \longrightarrow ROO^{\bullet}$$

This new radical triggers the chain reaction by abstracting a hydrogen atom from another unsaturated lipid molecule and giving rise to a hydroperoxide (ROOH), as the primary oxidation product, and a new alkyl radical ($R^{\bullet}$) that propagates the reaction chain (Márquez-Ruiz et al., 2014). This later step is slow and rate-limiting. Therefore, hydrogen abstraction from unsaturated lipids becomes selective for the most weakly bound hydrogen atoms.

$$ROO^{\bullet} + RH \longrightarrow ROOH + R^{\bullet}$$

In addition to hydroperoxide formation, peroxyl radicals may also be involved in alternate pathways. These competing reactions include β-elimination of oxygen, disproportionation, and addition to double bonds. In this last case, if the double bond belongs to the same molecule, a cyclic product is formed, whereas dimers and oligomers are formed if the carbon-carbon double bond belongs to a different molecule (Gardner, 1989; Porter et al., 1995; Schaich, 2013). The favored pathways are determined by the reaction conditions, the solvent, and the lipid concentration and conformation (Schaich, 2013).

Hydroperoxides are relatively stable at room temperature and in the absence of metals. However, at high temperature or in the presence of metals, they can be degraded to alkoxyl radicals ($RO^{\bullet}$) (Erickson, 2008; Márquez-Ruiz et al., 2014). Metal-mediated decompositions are heterolytic producing one radical and one ion per event, whereas homolytic decompositions by heat and UV light yield two radical species that are considerably more reactive

than the original ROO•: alkoxyl (RO•) and hydroxyl radicals (OH•) (Schaich, 2013).

$$ROOH \longrightarrow RO^{\bullet} + OH^{\bullet} \quad \text{(heat and UV)}$$

$$ROOH \longrightarrow RO^{\bullet} + OH^{-} \quad \text{(metals)}$$

Alcoxyl radicals (RO•) can also follow different pathways and their decomposition produce a great variety of secondary oxidation products which are described in the next section.

Finally, in the termination stage, radicals react among them to yield relatively stable nonradical products (Márquez-Ruiz et al., 2014). Three types of reaction are produced: stabilization reactions to produce compounds of analogous molecular weights to the original lipid; scission reactions to produce molecules of a molecular weight lower than the original lipid; and polymerization reactions to produce polymers of higher molecular weights than the initial lipid. Some of these polymerization and stabilization reactions are:

$$ROO^{\bullet} + ROO^{\bullet} \longrightarrow ROOR + O_2$$

$$R^{\bullet} + ROO^{\bullet} \longrightarrow ROOR$$

$$R^{\bullet} + RO^{\bullet} \longrightarrow ROR$$

$$R^{\bullet} + H^{\bullet} \longrightarrow RH$$

$$RO^{\bullet} + H^{\bullet} \longrightarrow ROH$$

$$ROO^{\bullet} + H^{\bullet} \longrightarrow ROOH$$

$$R^{\bullet} + OH^{\bullet} \longrightarrow ROH$$

1.1.4. The formed lipid oxidation products (LOPs).

As described above, lipid hydroperoxides are the primary oxidation products. Nevertheless, these compounds are easily decomposed and a very

complex mixture of LOPs is produced (McClements, & Decker, 2017; Bastos et al., 2017). Because of their complexity, LOPs are usually classified depending on their oxidation level into primary, secondary, and tertiary LOPs.

A. Primary LOPs.

Hydroperoxides, which are produced in the propagation and termination steps, are the primary LOPs. These products are odorless and tasteless since they are not volatiles. However, they are degraded into compounds that are responsible for off-flavors (Erickson, 2008; Márquez-Ruiz et al., 2014; Belitz et al., 2009). They are produced at the initial step of oxidation and their concentration decreases afterwards. Nevertheless, they are an important fraction of LOPs at low and moderate temperatures. **Figure 4** shows the hydroperoxides formed as a consequence of linoleic acid oxidation.

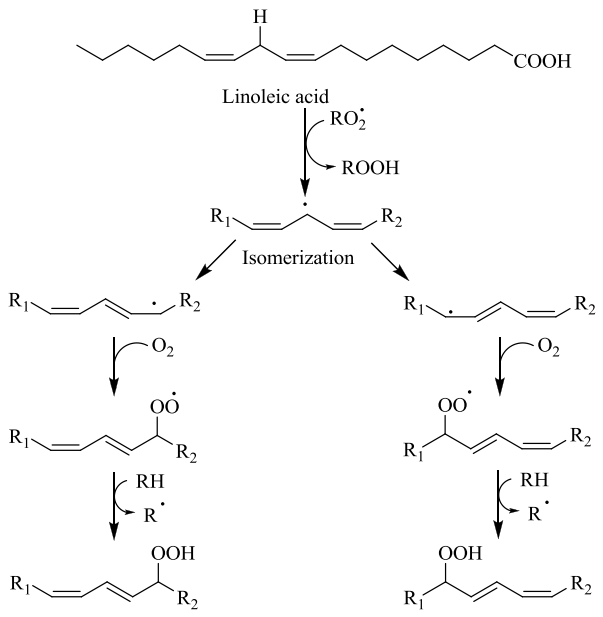

Figure 4. *Primary lipid oxidation products of linoleic acid. R_1 = C_5H_{11} and R_2 = $C_8H_{15}O_2$.*

B. Secondary LOPs.

Secondary LOPs are formed from hydroperoxides by different transformations and cleavages (**Figure 5**). This cascade of reactions, which includes abstraction of hydrogens, cyclization, addition to double bonds and scissions, generates hundreds of different compounds, including volatile and non-volatile products (such as aldehydes, ketones, acids, esters, alcohols, and short-chain hydrocarbons) (McClements, & Decker, 2017; Schaich, 2013).

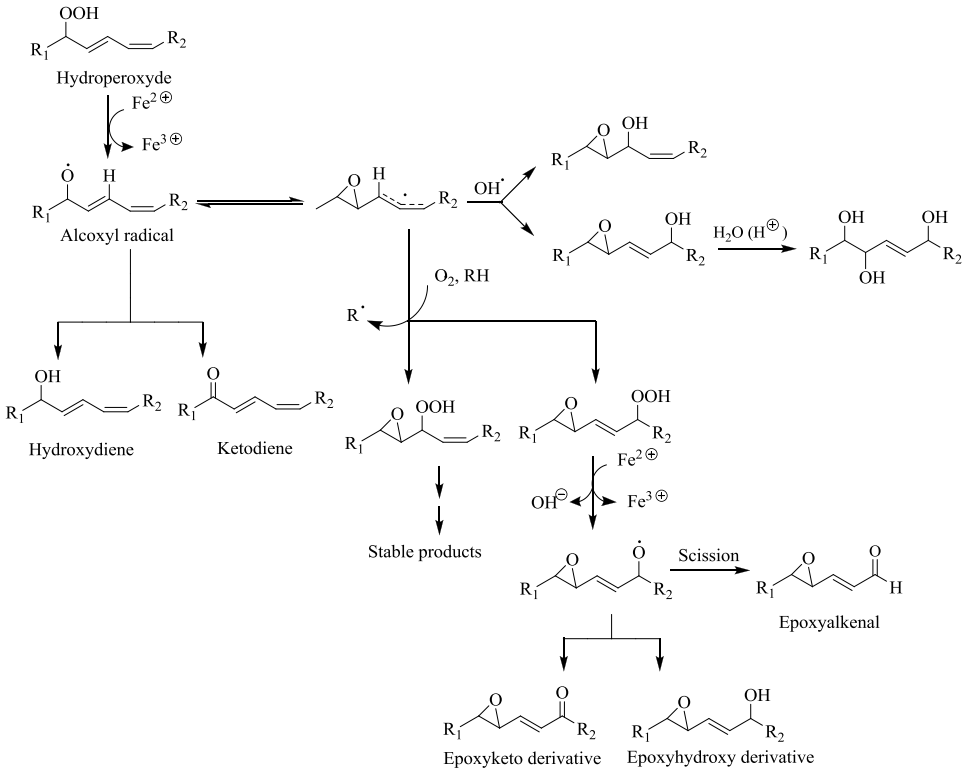

Figure 5. *Degradation of linoleic acid hydroperoxides to hydroxy-, epoxy- and oxo-fatty acids.* R_1 *=* C_5H_{11} *and* R_2 *=* $C_8H_{15}O_2$ *(Belitz et al., 2009).*

These compounds can be classified according to their molecular weights within three groups: compounds with molecular weights lower than the non-oxidized lipid, oxidized monomers or compounds with molecular weights similar to those of the non-oxidized lipid, and dimeric and polymeric compounds with molecular weights higher than the non-oxidized lipid.

The compounds with molecular weights lower than the non-oxidized lipid are produced by alkoxyl radical breakdown (Márquez-Ruiz et al., 2014). Alkoxyl radicals can suffer scission of the C-C bond on either side of the RO• group producing an oxo compound and an alkyl or alkenyl radical on the aliphatic chain (McClements, & Decker, 2017; Schaich, 2013; Kim & Min, 2008).

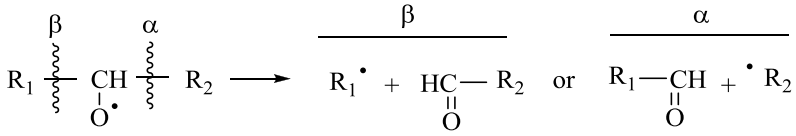

The formed radical can then either abstract one hydrogen atom to form a stable compound (alkanes, alkenes, fatty acids) and propagate the radical chain, or react with a hydroxyl radical to form an alcohol or with oxygen to form a hydroperoxide, which might be further decomposed.

Figure 6 shows some of the scission products produced during linoleic acid oxidation. It includes the formation of 2,4-decadienal, a secondary LOP used in the experiments described in this thesis. 2,4-Heptadienal, also used in this study, is produced similarly from linolenic acid.

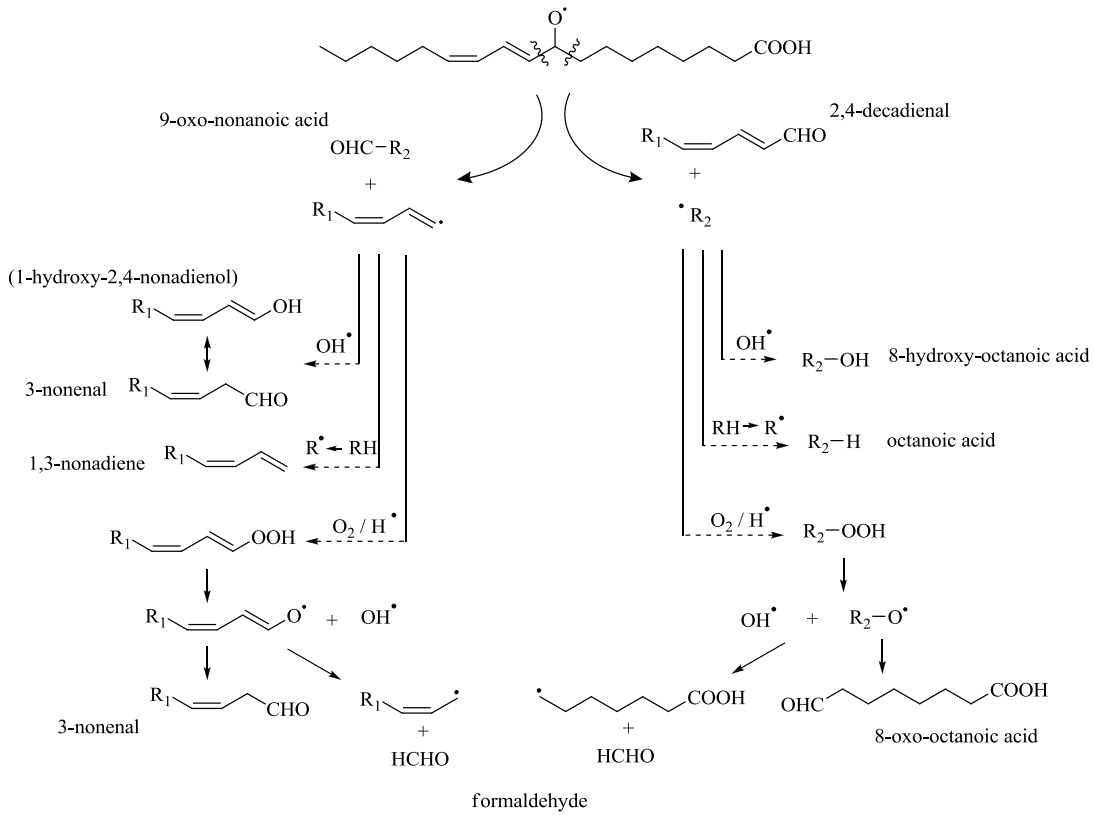

Figure 6. *Some typical scission products of 9-hydroperoxy linoleic acid. $R_1 = C_5H_{11}$ and $R_2 = C_8H_{15}O_2$. (Adapted from Schaich, 2013).*

Fragments containing the oxygen atom (mainly aldehydes) become the volatile and flavor compounds most strongly associated with rancidity, and they have an impact even at extremely low concentrations (Belitz et al., 2009; Schaich, 2013). The main volatile compounds produced by oleic acid, linoleic acid and linolenic acid are summarized in **Table 1**.

Table 1. *Volatile compounds formed by lipid oxidation of unsaturated fatty acids.*

Oleic acid	**Linoleic acid**	**Linolenic acid**
Heptanal	Pentane	Propanal
Octanal	Pentanal	1-Penten-3-one
Nonanal	Hexanal	2-Butenal
Decanal	Heptanal	2-Pentenal
2-Decenal	2-Heptenal	2-Hexenal
2-Undecenal	Octanal	3-Hexenal
	1-Octen-3-one	2-Heptenal
	1-Octen-3-hydroperoxide	2,4-Heptadienal
	2-Octenal	2,4-Octadienal
	3-Nonenal	3,5-Octadien-2-one
	2-Nonenal	1,5-Octadien-3-one
	2-Decenal	1,5-Octadien-3-hydroperoxide
	2,4-Nonadienal	2,6-Nonadienal
	2,4-Decadienal	2,4,7-Decatrienal
	4,5-Epoxy-2-decenal	

Adapted from Belitz et al. (2009).

This table includes some of the carbonyl compounds used in the experiments described in this work, such as propanal, pentanal, hexanal, 2-pentenal, 2-octenal, 2,4- heptadienal and 2,4-decadienal. The mechanism for alkadienal formation is shown in **Figure 6**. The mechanism proposed for the formation of 2-alkenals and alkanals from linolenic acid is summarized in **Figure 7**. Other alkenals and alkanals are produced similarly.

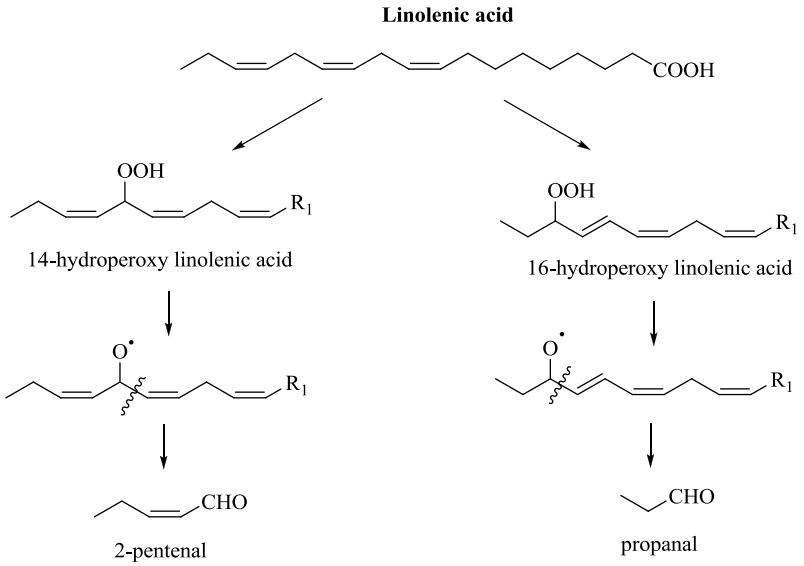

***Figure 7**. Proposed mechanism for 2-pentenal and propanal formation from linolenic acid. $R_1 = C_8H_{15}O_2$ (Frankel, 2005).*

When these reactions occur without scission of the carbon chain, compounds with molecular weights similar to those of non-oxidized lipids are produced (**Figure 5**). They have an oxygenated function (usually epoxy, hydroxyl or oxo group). These compounds are the most abundant LOPs formed at ambient or moderate temperatures (Márquez-Ruiz et al., 2014; Gardner, 1989).

Finally, the reaction of two or more lipid radicals produce dimeric and polymeric compounds (Márquez-Ruiz et al., 2014).

C. Tertiary LOPs.

Secondary LOPs can suffer further oxidations to produce new products with two oxygenated functions, which are named tertiary LOPs. For example, an alcoxyl radical can form either secondary stable products or tertiary products if it suffers a new oxidation. These compounds usually have two of the following functional groups: hydroperoxy, epoxy, hydroxyl or oxo,

and they are very reactive. These products play a major role in the color and flavor changes produced in food as a consequence of lipid oxidation (Hidalgo, & Zamora, 2004). **Figure 8** collects the structures of the tertiary LOPs used in this investigation. 4,5-Epoxy-2-heptenal and 4-oxo-2-hexenal are both oxidation products of ω3 fatty acyl chains, while 4,5-epoxy-2-decenal and 4-oxo-2-nonenal are derived from ω6 fatty acyl chains. In addition, fumaraldehyde and 4,5-epoxy-2-hexenal were also used as models of 4-oxo-2-alkenals and 4,5-epoxy-2-alkenals, respectively, in some experiments. The mechanism of formation of 4,5-epoxy-2-alkenals is shown in **Figure 5**.

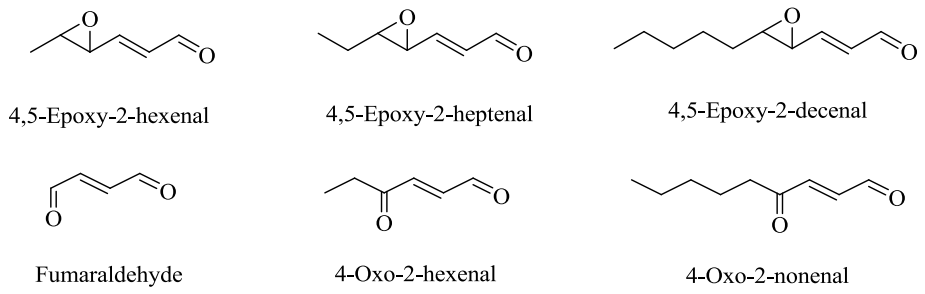

Figure 8. *Structures of the tertiary LOPs and analogues employed in this study.*

1.1.5. Consequences of lipid oxidation.

Lipid oxidation strongly impacts on food properties and quality (Schaich, 2013; Brewer, 2014; Steel et al., 2012; Correddu et al., 2015; Liu et al., 2016; Sainsbury et al., 2016). Thus, LOPs affect food sensory properties generating flavors, off-odors, browning, texture alterations and color loss. In general, volatile compounds produced during lipid oxidation are detrimental to food quality although there are some food products, such as fried foods, dried cereals, and cheeses, for which small amounts of LOPs are important positive components for their flavor profile (McClements & Decker, 2017).

Aldehydes are main responsible for the formation of off-flavors as a consequence of lipid oxidation. Undesirable odors resulting from oxidation are commonly described as stale, wet cardboard, painty, grassy, or rancid (Brewer, 2014).

In addition, lipid oxidation causes a reduction in the nutritional value of the food, and it can seriously impact toxicity and safety due to the formation of potentially toxic compounds, including α,β-unsaturated aldehydes (Guillén & Goicoechea, 2008a; Guillén & Uriarte, 2012; Liu et al., 2003; Zarkovic, 2003; Guillén & Goicoechea, 2008b; Picklo et al., 2011; Kawai et al., 2006; Kasai & Kawai, 2008; Demir et al., 2013; Lee et al., 2002; Van Hecke et al., 2015; Zeng et al., 2015). Some α,β-unsaturated aldehydes, such as acrolein or crotonaldehyde, have been related to an adverse effect on human health. These relevant aldehydes have been found in both frying oils and fried foods (Ewert et al., 2011; Granvogl, 2014; Ewert et al., 2014). They have been employed in this study. Other toxic aldehydes employed in this research have been 4,5-epoxy-2-alkenals and 4-oxo-2-alkenals.

1.2. The broadcasting of lipid oxidative damage.

The formation of LOPs is neither the only consequence of lipid oxidation nor the final step of the lipid oxidative process. In fact, this is the initial step of a very complex cascade of reactions. Thus, many of the produced LOPs are not stable, and they react with the surrounding food components, broadcasting the oxidative damage from lipids to all kind of molecules. Among the different produced reactions, carbonyl-amine reactions are particularly important because they have been shown to produce significant changes in food with both positive and negative consequences (Zamora, & Hidalgo, 2016).

1.2.1. Carbonyl-amine reactions produced by LOPs.

Analogously to the reactive carbonyl compounds derived from carbohydrates, the lipid-derived reactive carbonyls are also able to react with the amino groups of amines, amino acids, aminophospholipids, and proteins, among other food macromolecules, producing a complex cascade of reactions and numerous compounds. Many of these compounds have been traditionally considered exclusive of Maillard reaction (Zamora & Hidalgo, 2011).

These reactions are the final step of the oxidation pathway when lipid oxidation occurs in the presence of amino compounds. Thus, lipid-derived carbonyls react with amino compounds producing nonenzymatic browning and the formation of advanced lipoxidation end-products (ALEs), which can be defined as carbonyl-amine adducts originated from lipids.

1.2.2. Formation of carbonyl-amine adducts.

The initial step of carbonyl-amine reactions is the formation of the corresponding imine. The stabilization of this imine can occur without the loss of any portion of either the lipid or the amino compound, and the formation of low molecular weight monomeric ALEs is produced (Hidalgo & Zamora, 2000a; Hidalgo & Zamora, 2017). Particularly, the formation of diverse heterocyclic aromatic structures having five and six atoms has been described.

One of the first carbonyl-amine adducts described was a pyridinium salt (**A** and **B** in **Figure 9**) formed between amino compounds and aldehydes (Suyama & Adachi, 1979). The formation is shown in **Figure 9**. Pyridinium salts are the products formed at low temperature. Nevertheless, upon heating, pyridinium salts suffer a Strecker elimination and the corresponding pyridines (**C** and **D**) are formed.

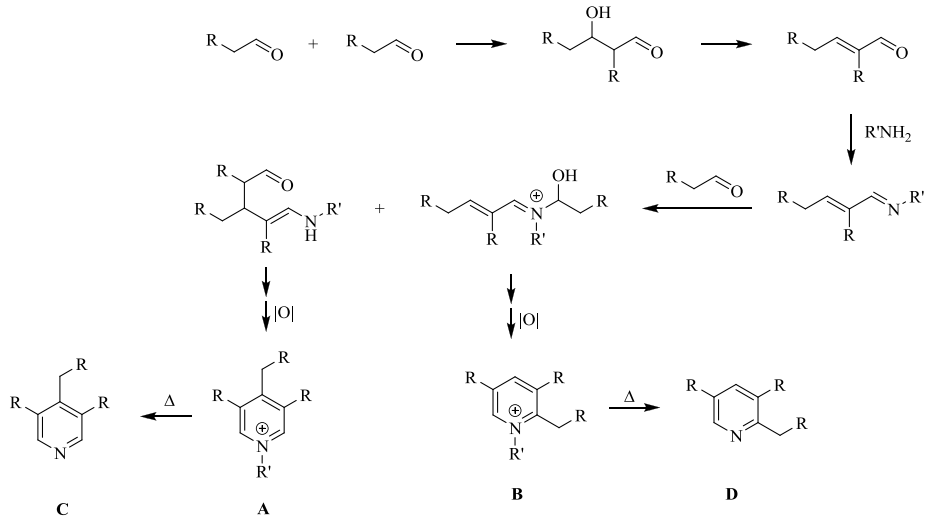

Figure 9. *Formation of pyridinium salts **A** and **B** by carbonyl-amine reactions involving alkanals. Pyridinium salts **A** and **B** are converted into pyridines **C** and **D**, respectively, by heat treatment.*

Formation of other pyridines has also been described in these reactions. Thus, 2-alkylpyridines (**E**) are also produced at low temperatures as secondary products in the Strecker degradation of amino acids initiated by different carbonyls including 2,4-alkadienals, 4,5-epoxy-2-alkenals, and non-volatile long-chain LOPs having epoxy and oxo functions (Hidalgo & Zamora, 2004; Zamora et al., 2007; Zamora et al., 2005). The reaction takes place in several steps as indicated in **Figure 10** (Zamora et al., 2015).

In addition, 2-alkylpyridines (**E**) can also be produced at high temperatures when starting from 2,4-alkadienals as indicated in **Figure 10** (Zamora et al., 2009).

Two 2-alkylpyridines are always produced in reactions collected in **Figure 10**. 2-Pentylpyridine is the product derived from ω6 fatty acyl chains and 2-ethylpyridine is the product derived from ω3 fatty acyl chains.

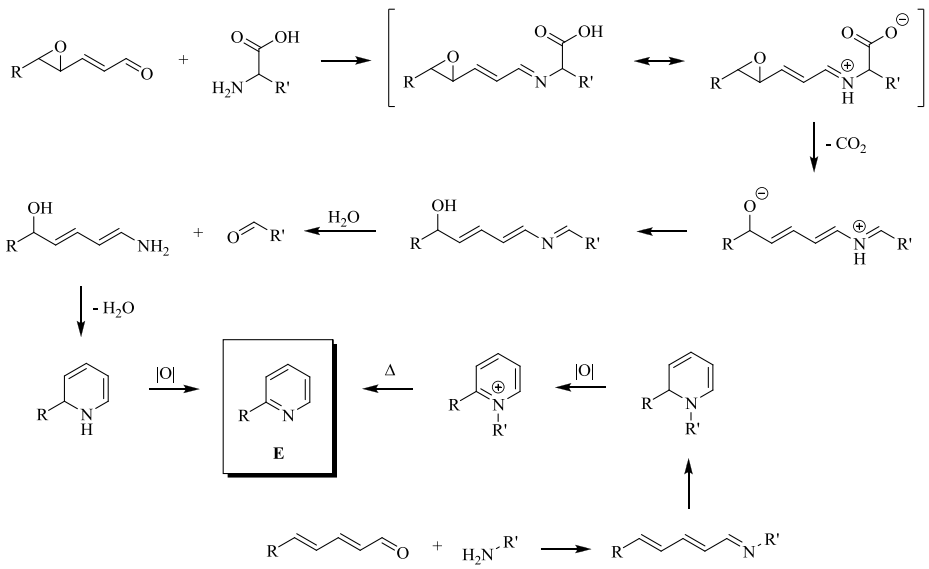

***Figure 10**. Formation of 2-alkylpyridines (**E**) by carbonyl-amine reactions involving different lipid-derived reactive carbonyls.*

Another special type of pyridine (the dihydropyridine **F**) is produced when the involved lipid oxidation product is malondialdehyde (**Figure 11**) (Kikugawa et al., 1984).

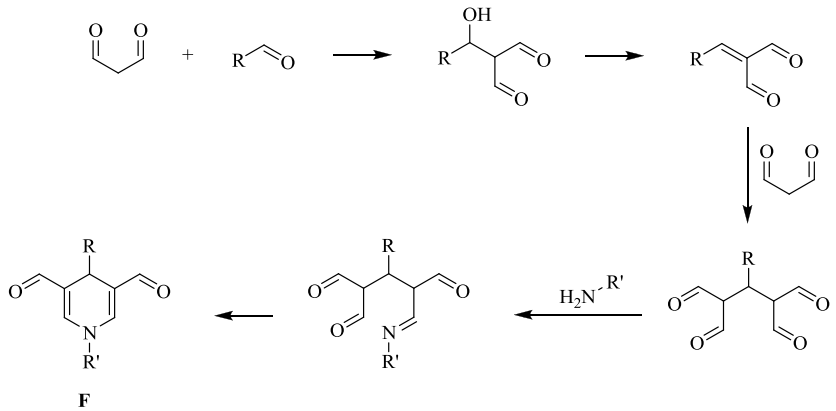

***Figure 11**. Formation of dihydropyridines (**F**) by oligomerization of malondialdehyde in the presence of alkanals and later reaction with amino compounds.*

In addition to six-membered heterocycles, the formation of five-membered heterocycles has also been described. Among them, the formation of pyrroles is likely the most studied.

Different types of pyrroles can be formed depending on the initial LOP. As shown in **Figure 12**, the reaction between epoxyalkenals and amino compounds produces hydroxyalkylpyrroles (**G)** and *N*-substituted pyrroles (**H**). However, hydroxyalkylpyrroles are not stable and polymerize spontaneously (Hidalgo & Zamora, 1993).

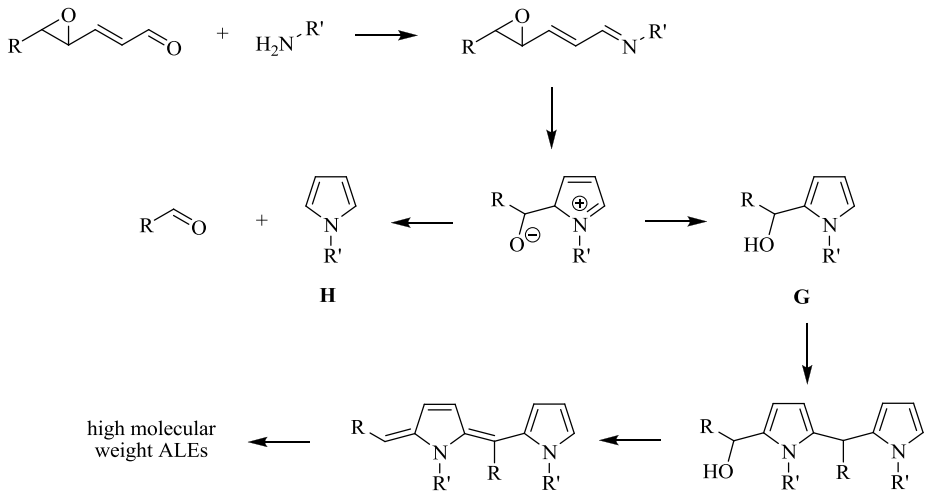

***Figure 12**. Formation of 1-alkylpyrroles (**H**) and 1-alkyl-2-(1'-hydroxyalkyl)pyrroles (**G**) by reaction of 4,5-epoxy-2-alkenals with amino compounds. The figure also shows the polymerization of 1-alkyl-2-(1'-hydroxyalkyl)pyrroles to produce high molecular weight ALEs.*

Other pyrrole derivatives produced in these reactions are 1,2-disubstituted pyrroles (**I**). These compounds have been shown to be produced in the reaction of amino compounds with hydroxyalkenals (Sayre et al., 1993) and epoxyalkenals (Zamora & Hidalgo, 2005), as shown in **Figure 13**.

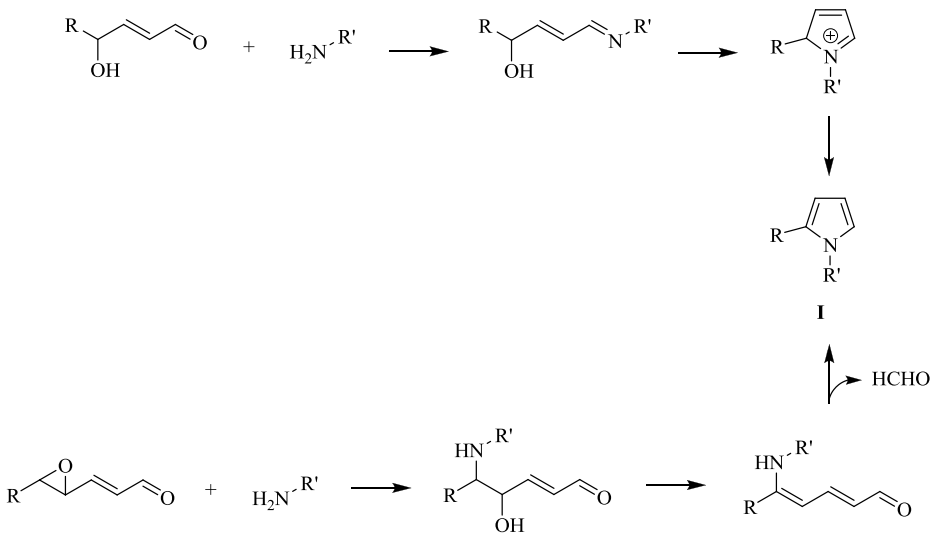

Figure 13. *Formation of 1,2-dialkylpyrroles (**I**) by carbonyl-amine reactions involving different lipid-derived reactive carbonyls.*

In addition to pyrroles, other five-membered heterocycles produced in these reactions are imidazoles. Imidazolium salts (**J**) can be produced by reaction between glyoxal and amino compounds as shown in **Figure 14** (Wells-Knecht et al., 1995). The reaction mechanism is general for different amino compounds and can also be extended to other 1,2-dicarbonyl compounds.

Also, carbonyl-amine adducts containing an imidazole ring (**K** and **L**) are also produced when the amino acid histidine is involved. The imidazole ring of the amino acid is added to the carbon–carbon double bond of different lipid-derived reactive carbonyls as shown in **Figure 15** (Zamora, et al., 1999). This reaction is usually reversible, but the adduct can be stabilized by reduction of the carbonyl group with sodium borohydride.

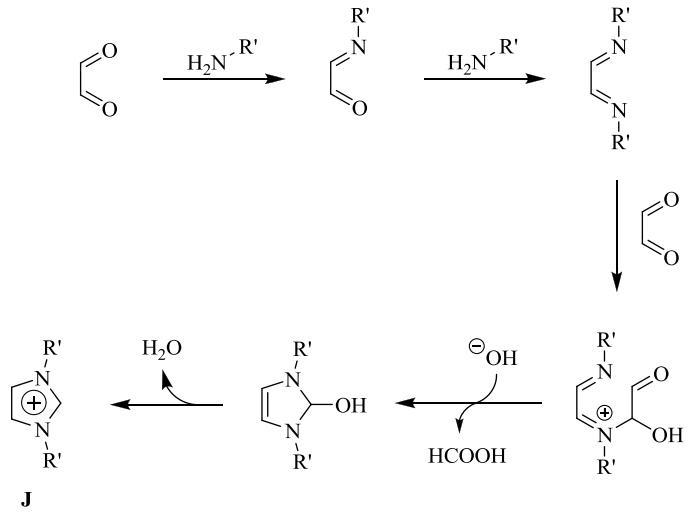

***Figure 14**. Formation of imidazolium salts (**J**) by carbonyl-amine reactions involving glyoxal.*

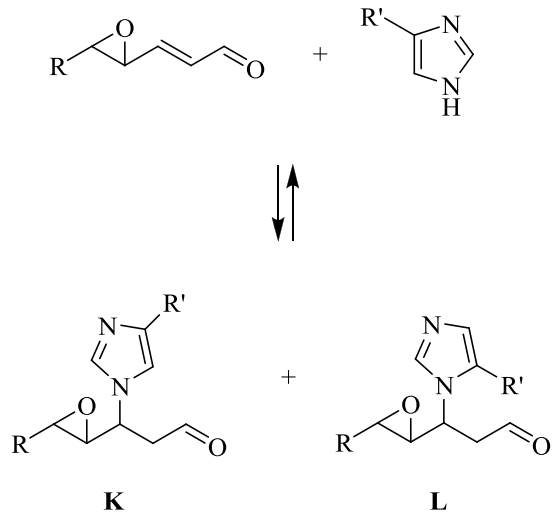

***Figure 15**. Formation of Michael adducts by addition of an imidazole ring, such as the present in the side chain of histidine, to 4,5-epoxy-2-alkenals.*

1.2.3. Formation of amino acid degradation products.

Amino acids are easily degraded by LOPs producing different compounds, some of which are volatile. Different to the volatile compounds formed in cleavage of alkoxyl radicals, which have been related to rancid flavors, the flavors produced by carbonyl-amine reactions are usually positive in many foods.

These degradation reactions produce three kinds of compounds in a first step: Strecker aldehydes, α-keto acids, and amines. However, they are not final compounds and these compounds are involved in further reactions. Thus, α-keto acids are transformed into Strecker aldehydes and other aldehydes having two carbons less than the original amino acid; the amines are transformed into Strecker aldehydes and olefins; and the Strecker aldehydes can be oxidized to shorter aldehydes. Finally, olefins are susceptible to suffer addition of nucleophilic compounds. All these reactions are shown in **Figure 16**. Although they are interconnected, it is possible to modify the ratio among the different formed products as a function of the oxidized lipid and the amino acid involved, as well as the reaction conditions (pH, water activity, presence of oxygen, time, and temperature) (Zamora et al., 2015; Hidalgo et al., 2016). By playing with these tools it is possible to favor the formation of the desirable compounds produced in these reactions and to decrease the amount of the undesired products that are also formed.

The main reaction pathways by which these compounds are produced are briefly described below. A more extensive description can be found somewhere else (Hidalgo et al., 2016).

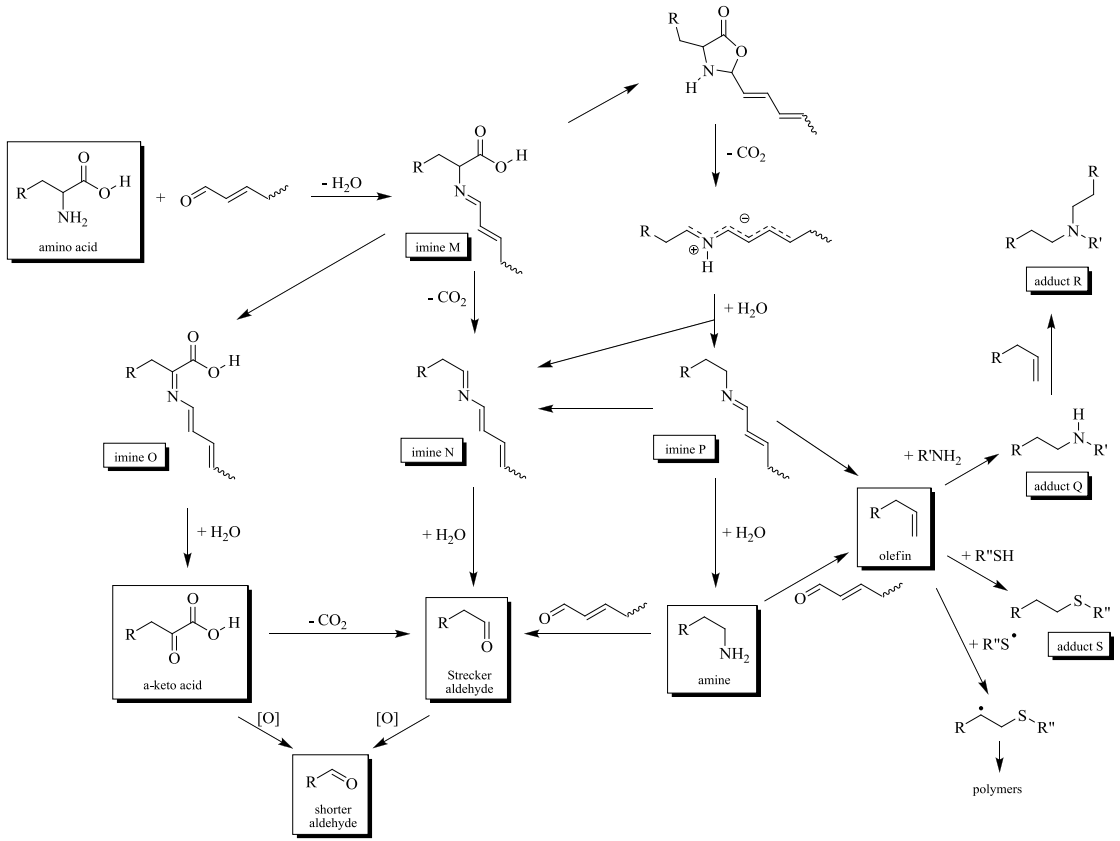

Figure 16*. General scheme for amino acid degradations induced by lipid-derived reactive carbonyls (Hidalgo & Zamora, 2016)*

The Strecker degradation of amino acids produced by secondary and tertiary LOPs was firstly described in 2004 for the formation of phenylacetaldehyde by phenylalanine degradation in the presence of epoxyalkenals (Hidalgo & Zamora, 2004), and later extended to other lipid-derived reactive carbonyls (Hidalgo et al., 2005; Zamora et al., 2005; Zamora et al., 2007; Zamora et al., 2008). However, the reaction is produced to different extents depending on the LOPs involved. This is likely a consequence of both the influence of the lipid-derived carbonyl on the reaction pathway and the existence of parallel reactions in which these oxidized lipids may be involved and that compete with the Strecker reaction (Hidalgo & Zamora, 2016; Zamora et al., 2008).

A general mechanism for the Strecker degradation of amino acids produced by lipid-derived reactive carbonyls is shown in **Figure 17**. The reaction starts with the formation of the corresponding imine (**M**), followed by a decarboxylation and hydrolysis of the new imine (**N**) produced.

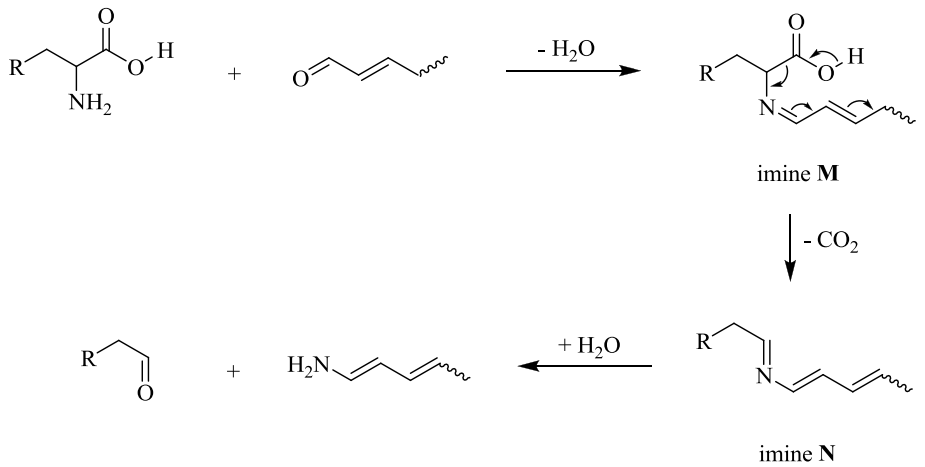

Figure 17. *Proposed pathway for the conversion of amino acids into Strecker aldehydes in the presence of lipid-derived reactive carbonyls (Hidalgo & Zamora, 2016).*

In addition to aldehydes, some LOPs, which are ketones, can also produce the Strecker degradation of amino acids (Zamora et al., 2005; Zamora et al., 2007). The obtained results showed that the ability of aldehydes and ketones for degrading amino acids was similar in most experiments and differences found might be more related to the different solubility of the LOPs assayed than to a different reactivity.

Although hydroperoxides do not have a carbonyl group, they also produce the Strecker degradation of amino acids, because they are easily decomposed and converted into free radicals and carbonyl compounds that react as described above (Hidalgo & Zamora, 2016).

Under aerobic conditions, the formation of Strecker aldehydes is favored. However, they can suffer further reactions. Thus, they can also be oxidized to shorter aldehydes having two carbons less than the original amino acid or, under appropriate conditions, they can react with other food components. As an example, the Strecker aldehydes are involved in the production of heterocyclic aromatic amines (HAAs) such as 2-amino-1-methyl-6-phenylimidazo[4,5-*b*]pyridine (PhIP). This compound is produced by reaction of phenylacetaldehyde, the Strecker aldehyde of phenylalanine, and creati(ni)ne in the presence of the *in situ* formed formaldehyde and ammonia (Zamora & Hidalgo, 2015).

If this degradation of amino acids takes place without decarboxylation, the produced compounds are α-keto acids (Zamora et al., 2006a; Zamora & Hidalgo, 2011; Hidalgo & Zamora, 2016). The pathway for this reaction is shown in **Figure 18**. These compounds are also an important source of flavor compounds in foods.

α-Keto acids are not thermally stable compounds, and they produce new flavors under mild conditions. Among them, their degradation to Strecker aldehydes and other aldehydes having two fewer carbon atoms than the original amino acid has been described (Hidalgo & Zamora, 2016).

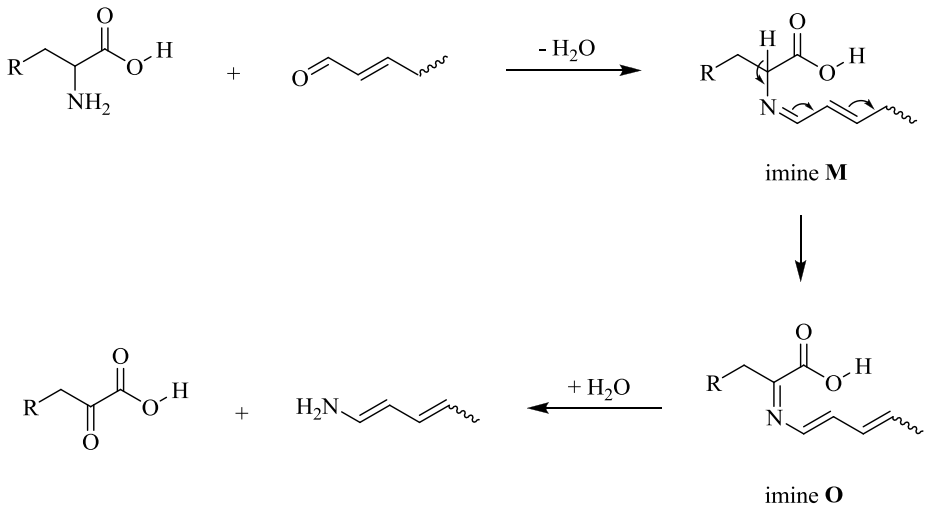

***Figure 18**. Proposed pathway for the conversion of amino acids into a-keto acids in the presence of lipid-derived reactive carbonyls (Hidalgo & Zamora, 2016).*

Amino acids can also be converted into amines by action of reactive carbonyls. These amines are usually known as biogenic amines because they have been traditionally considered to be produced as a consequence of the action of microorganisms (Hidalgo et al., 2010; Hidalgo & Zamora, 2016; Zamora & Hidalgo, 2011). The reaction pathway proposed for this reaction is shown in **Figure 19.**

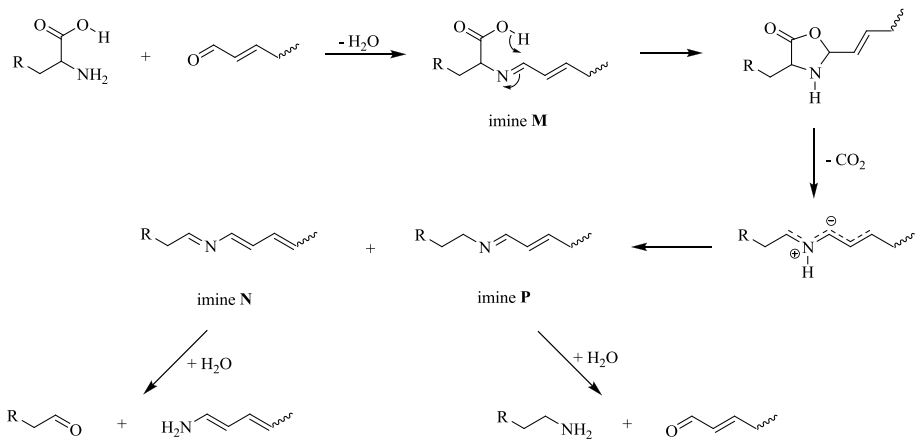

Figure 19. *Proposed pathway for the conversion of amino acids into amines and Strecker aldehydes in the presence of lipid-derived reactive carbonyls (Hidalgo & Zamora, 2016).*

These amines can suffer later reactions in the presence of lipid-derived reactive carbonyls. One of them is their conversion into the corresponding Strecker aldehydes, which seems to takes place according to the reaction pathway shown in **Figure 20** (Zamora et al., 2012).

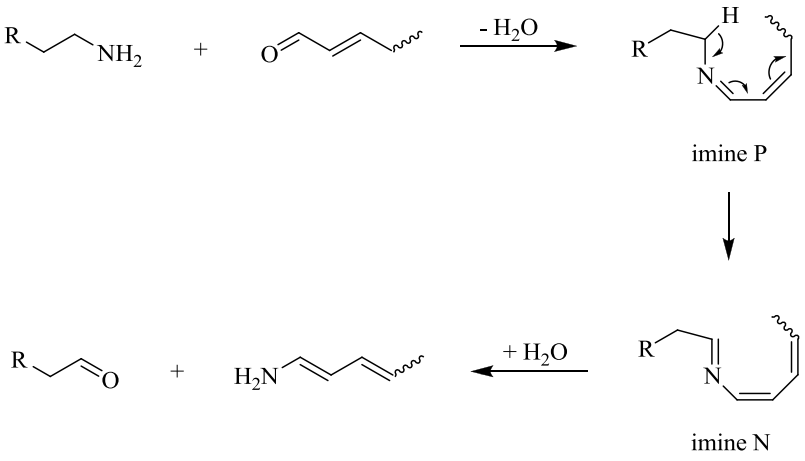

Figure 20. *Proposed pathway for the conversion of amines into Strecker aldehydes in the presence of lipid-derived reactive carbonyls (Hidalgo & Zamora, 2016).*

Another reaction suffered by amines is an elimination reaction that converts them into olefins: the corresponding vinylogous derivatives of the amino acids. The reaction takes place as shown in **Figure 21**. In the presence of the lipid-derived reactive carbonyl, the amine produces first the corresponding imine (**P**), which may be then converted into an iminium ion that suffer a elimination. This conversion is favored by the lipid because a reactive carbon in the lipid chain may react with the nitrogen of the imine to produce the corresponding iminium ion (Hidalgo & Zamora, 2016).

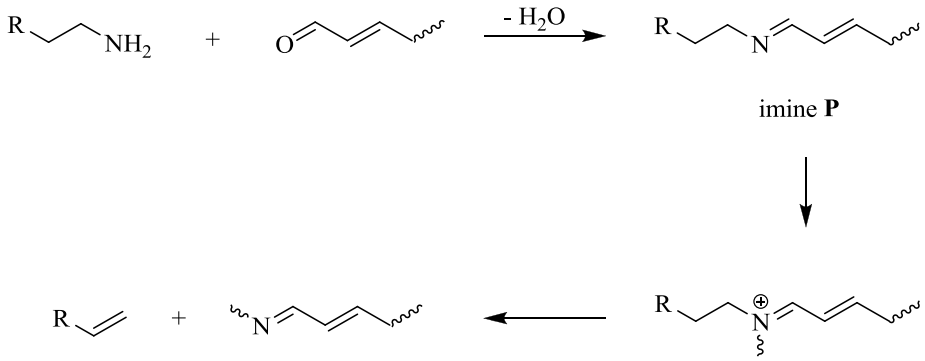

Figure 21. *Proposed pathway for the conversion of amines into olefins in the presence of lipid-derived reactive carbonyls (Hidalgo & Zamora, 2016).*

This reaction has lately received a considerable attention because of its potential implication in the formation of acrylamide as a consequence of asparagine degradation in the presence of reactive carbonyl compounds, including lipid-derived reactive carbonyls (Zamora & Hidalgo, 2011; Zamora & Hidalgo, 2008; Xu et al., 2016; Muttucumaru et al., 2017). Although only deamination reactions of phenylethylamine and 3-aminopropionamide by lipid carbonyls have been studied to date (Zamora et al., 2009), other biogenic amines are likely to suffer similar eliminations.

These vinylogous derivatives of amino acids are not stable compounds and can suffer the addition of nucleophiles. This reaction has recently received a considerable attention because of its possible use in the elimination of acrylamide (Zamora et al., 2010; Zamora et al., 2011; Salazar et al., 2012). Compounds having either amino or sulfhydryl groups are added to these vinylogous derivatives, and there are significant differences between the addition of either amino or sulfhydryl groups. These differences have been described by Hidalgo & Zamora (2016).

1.2.4. Formation of polymers.

The imine produced between lipid-derived reactive carbonyls and amino compounds can also evolve into the formation of polymers, which are responsible (at least to a significant extent) for the browning developed in these reactions.

Different kinds of colored polymers with a variable nitrogen content are produced in these reactions by different pathways as shown in **Figure 22** (Hidalgo & Zamora, 2000a).

One of these pathways is the reaction of proteins with lipid-derived reactive carbonyls. This reaction produces the formation of carbonyl-amine adducts in the terminal amino acid residues of the protein, and some of these adducts can also suffer later polymerizations (Hidalgo & Zamora, 2000b).

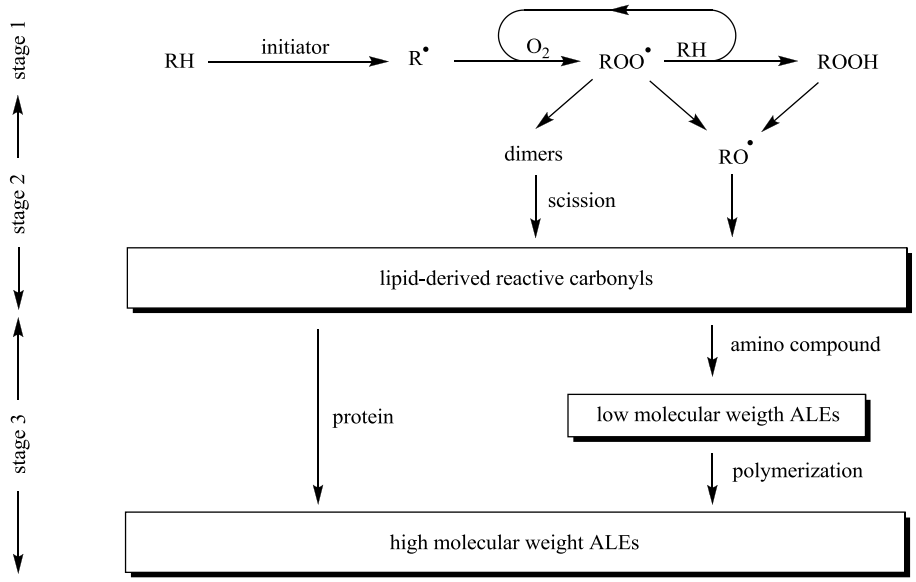

***Figure 22**. The formation of carbonyl-amine adducts (advanced lipoxidation end-products, ALEs) in the course of lipid oxidation.*

The other pathway is the polymerization of some of the low molecular weight ALEs described in previous subsections. Within this last pathway, two main mechanisms have been described for the formation of high molecular weight ALEs. The first one is a repeated aldol condensation which is shown in **Figure 23** (Hidalgo & Zamora, 2000a; Hidalgo & Zamora, 2017). The produced polymeric brown materials are unstable and generate volatiles by scission or dehydration, which affect the flavor characteristics of foods during cooking and processing. The second one is based on the polymerization of *N*-substituted hydroxyalkylpyrroles (**Figure 12 and 23**) (Hidalgo & Zamora, 1995). These compounds polymerize spontaneously forming dimers, trimers, tetramers, and higher polymers as shown in **Figure 23** (Hidalgo & Zamora, 1993).

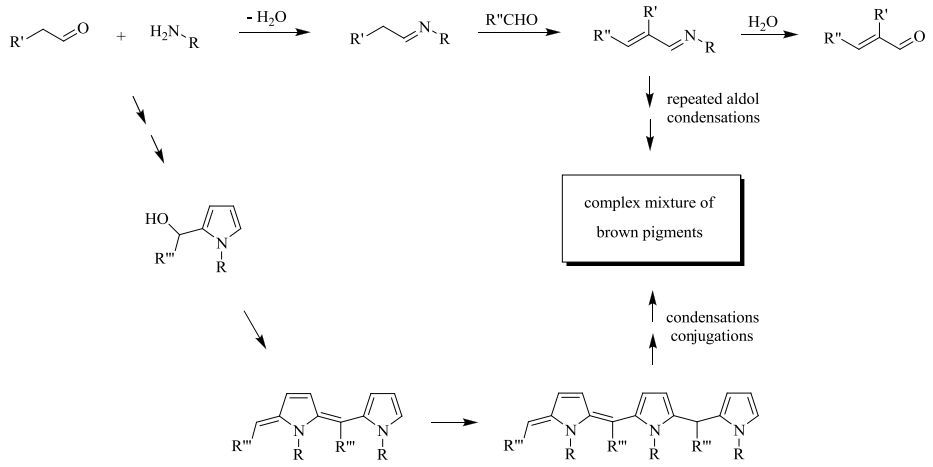

***Figure 23**. Proposed mechanisms for the formation of brown pigments by carbonyl–amine reactions. Lipid carbonyls react with amino compounds either forming imines or hydroxyalkylpyrroles depending on the lipid carbonyl involved (Zamora & Hidalgo, 2011).*

All reactions described in this section show that **Figure 2** should be completed by including the broadcasting of the lipid oxidative damage by means of the carbonyl compounds produced in the course of lipid oxidation. This has been collected in **Figure 24**. As observed in this figure, the initial product formed between the carbonyl compound and the amino compound is the corresponding imine which can suffer then three kinds of reactions: stabilization reactions to produce the corresponding carbonyl-amine adducts of a molecular weight similar to the addition of the molecular weights of the reagents; scission reactions to produce volatile compounds; and polymerization reactions to produce the polymers responsible for the browning formation in these reactions (**Figure 24**).

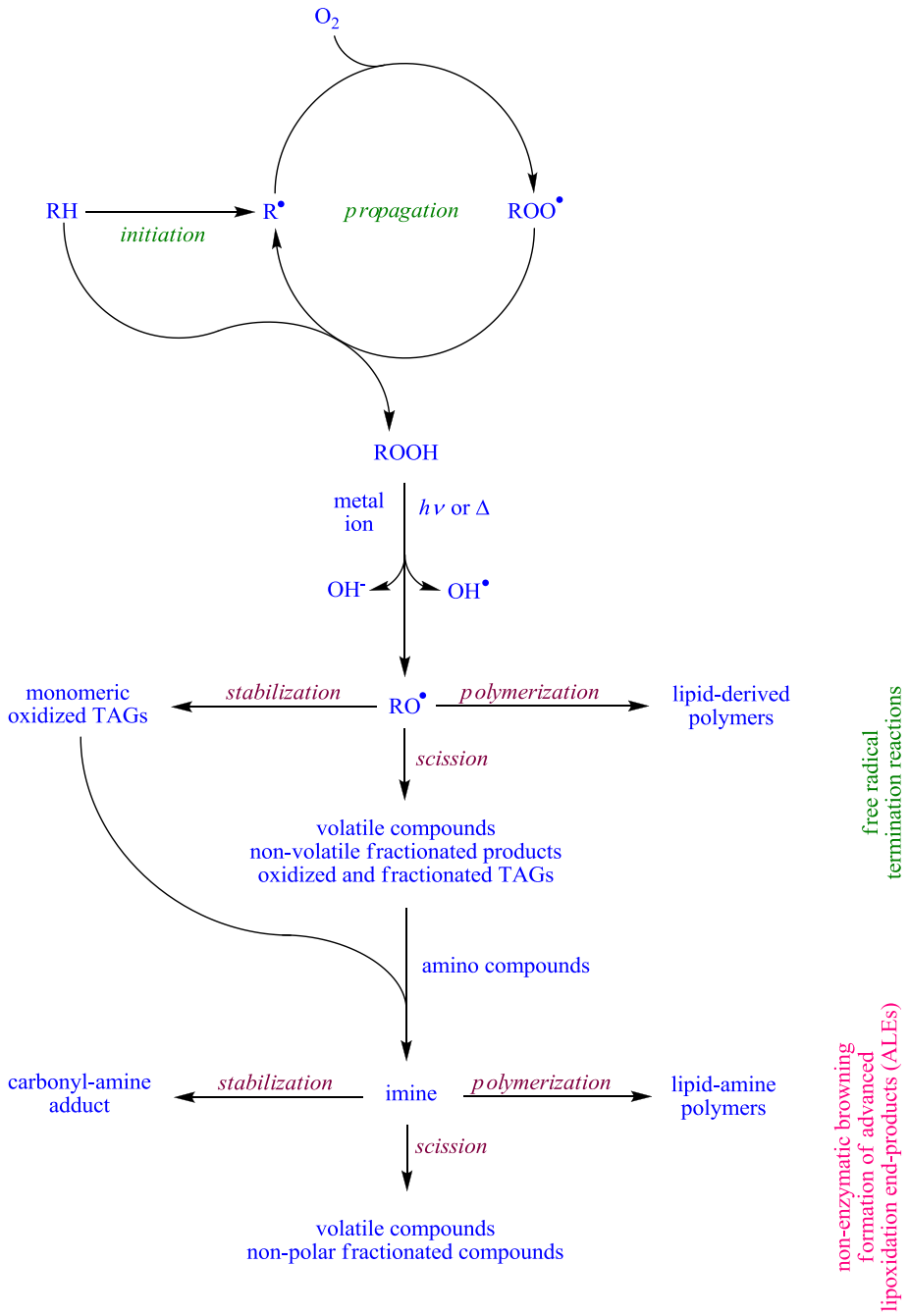

Figure 24. *Carbonyl-amine reactions as a broadcasting of lipid oxidative damage to food macromolecules containing amino groups (Adapted from Zamora & Hidalgo, 2016).*

1.3. The control of lipid oxidative damage by phenolics.

1.3.1. Phenolic compounds.

Phenols are a large group of compounds (more than 8000 phenolic compounds have been reported (Crozier et al., 2009)) characterized by having at least one aromatic ring with one or more hydroxyl groups attached. They are plant secondary metabolites commonly found in many herbs, fruits, vegetables, grains and cereals, green and black teas, coffee beans, propolis, and red and white wines (Leopoldini et al., 2011).

Phenolics can be classified by the number and arrangement of their phenol subunits into simple phenols and polyphenols. Simple phenols can have only hydroxyl groups or also a carboxylic group such as in phenolic acids. In addition, polyphenols, which possess at least two phenol subunits, include flavonoids and stilbenes among others (**Figure 25**). Polyphenols possessing three or more phenol subunits are known as tannins (Leopoldini et al., 2011).

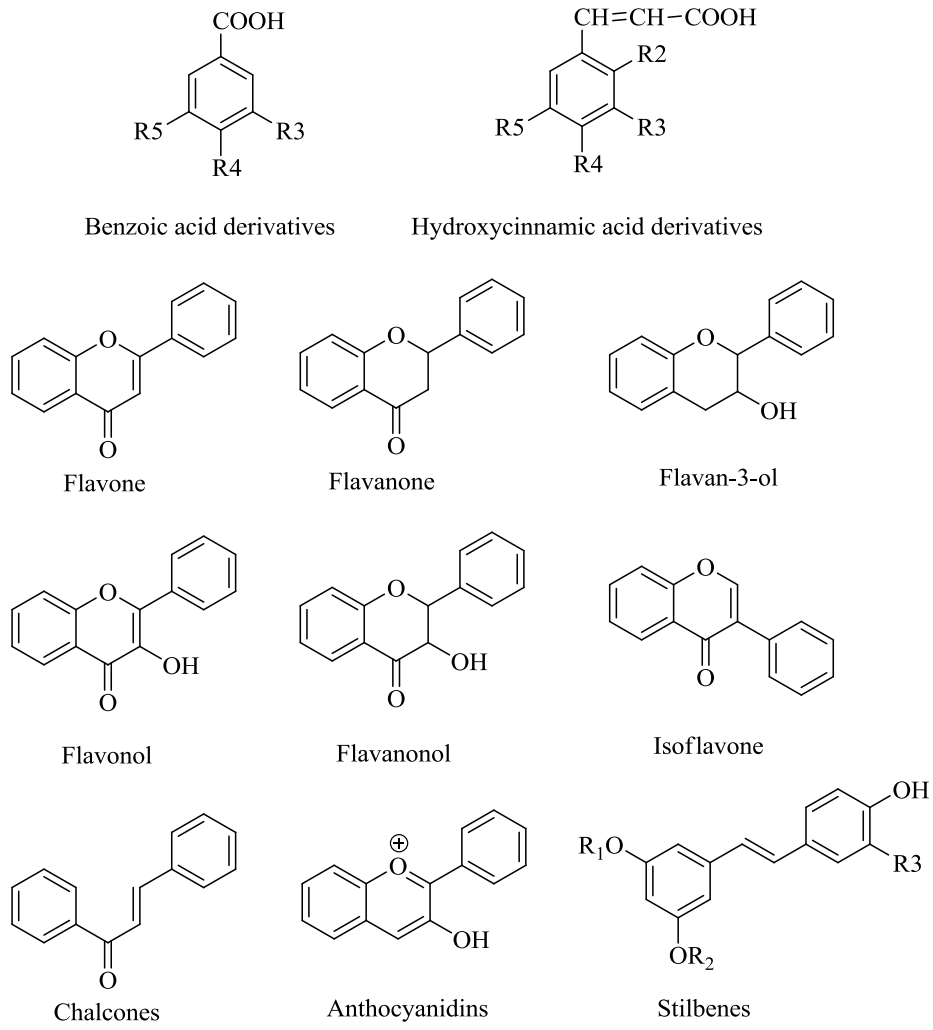

Figure 25. *Structures of benzoic and hydroxycinnamic acids, flavonoids and stilbenes.*

Simple phenols include *o*-, *m*-, *p*-diphenols as well as compounds having three or more hydroxyl groups. Among these phenolics, resorcinol, 2-methylresorcinol, 2,5-dimethylresorcinol, and orcinol have been used in this study. The structures of these compounds are given in **Figure 26**.

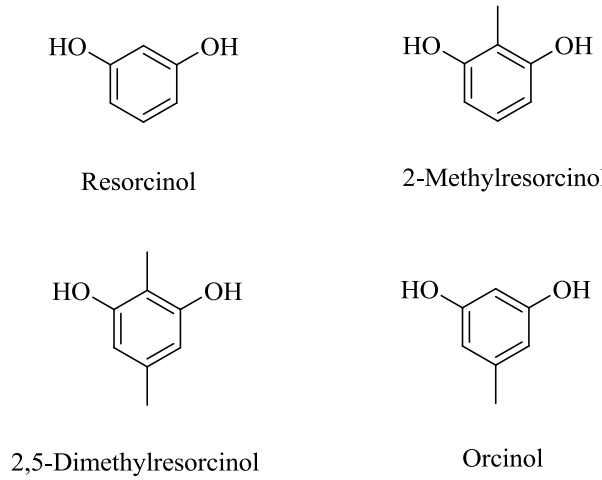

***Figure 26**. Chemical structures of model phenolic compounds used in this study.*

Phenolic acids can have either hydroxycinnamic or hydroxybenzoic structures (**Figure 25**). Hydroxycinnamic acids are more common than hydroxybenzoic acids and include *p*-coumaric, caffeic, ferulic, and sinapic acids. Hydroxybenzoic acids include gallic acid. Phenolic acids are commonly present under two principal forms in all plant-derived foods: a free and a bound form. The latter is found more frequently and occurs in the form of esters, glycosides and bound complexes (Andjelkovic et al., 2006).

Flavonoids are the most widely distributed phenolic compounds in plant foods and also the most studied ones. They possess a common tricyclic carbon skeleton with rings A, B, and C. The basic structural feature of all flavonoids is the flavane (2-phenyl-benzo-γ-pyran) nucleus, a system of two benzene rings (rings A and B) linked by an oxygen-containing pyran ring (ring C) (**Figure 27**).

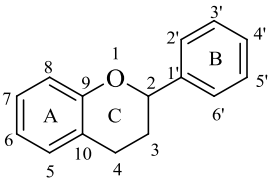

Figure 27. *Carbon skeleton of flavane.*

According to the degree of oxidation of the C ring, the hydroxylation pattern of the nucleus, and the substituent at carbon 3, the flavonoids can be categorized into different subclasses: flavones, flavanones, flavan-3-ols (catechins), flavonols, flavanonols, isoflavones, anthocyanidins and chalcones (**Figure 25**). Anthocyanidins differ from the other flavonoids by possessing a charged oxygen atom in the ring C. In addition, the ring C is open in chalcones. Many flavonoids occur naturally in food as *O*-glycosides with glucose being the most common sugar residue. On the other hand, flavan-3-ols, unlike most flavonoids, are not glycosylated (Gliszczynska-Swiglo & Oszmianski, 2014). Some foods containing different types of flavonoids and the main phenolics present in them are shown in **Table 2**.

The flavonol quercetin, which is the major flavonoid in onions (*Allium cepa* L.) (Price & Rhodes, 1997; Crozier et al., 1997; Price et al., 1997; Marotti & Piccaglia, 2002; Patil et al., 1995), was used in this study. **Figure 28** shows the chemical structure of quercetin.

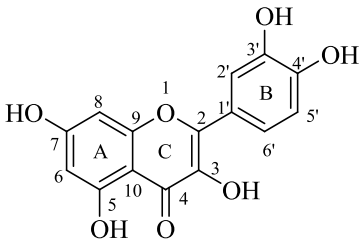

Figure 28*. Chemical structure of quercetin.*

Table 2. *Class, dietary source and main phenolics of different flavonoid classes.*

Flavonoid Class	Dietary source	Main Representatives
Flavonols	Onion, tomato, apple, broccoli, red wine	Kaempferol Quercetin Myricetin Rutin
Flavones	Herbs, celery, parsley, fruit skins	Luteonin Apigenin Chrysin
Flavan-3-ols	Tea, cacao	(+)-Catechin (C) (−)-Epicatechin (EC) (−)-Epicatechin gallate (ECG) (−)-Epigallocatechin (EGC) (−)-Epigallocatechin gallate (EGCG)
Flavanones	Citrus fruits and juices	Hesperetin Herperidin Naringenin Naringin Eriodictyol
Isoflavones	Soybean	Genistein Genistin Daidzein Daidzin
Anthocyanidins	Apple, pear, tomato	Pelargonidin Cyanidin Delphinidin Maldivin

Adapted from Gliszczynska-Swiglo & Oszmianski (2014).

The family of stilbenes includes several compounds among which resveratrol, pterostilbene and piceatannol are the main derivatives, characterized by a double bond connecting the phenolic rings (**Figure 25**).

Polymeric compounds, called tannins, are divided into two groups: condensed and hydrolyzable. Condensed tannins are polymers of flavonoids, and hydrolyzable tannins contain gallic acid, or similar compounds, esterified to a carbohydrate.

1.3.2. The chelating ability of phenolic compounds and the control of lipid oxidative damage.

Phenolic compounds have been used to control lipid oxidation based on different properties. One of them is their ability to chelate metals (Hermund et al., 2016; Sulaiman & Ooi, 2012).

Transition metals are found in all foods since they are common constituents of biological materials, water, ingredients, and packaging materials. They often exist chelated to other compounds, such as magnesium in chlorophyll, copper, zinc and manganese in various enzymes; or iron in proteins such as ferritin. When these ions are released by hydrolytic or other degradative reactions, they participate in reactions responsible for food spoiling (Lindsay, 2017).

Two mechanisms of the promotion of oxidation by metals have been proposed. Thus, metals are believed to either interact with hydroperoxides, favoring their decomposition, or to react directly with lipid molecules, favoring the formation of primary hydroperoxides (Reische et al., 2008).

The prooxidative activity of metals can be altered by chelating agents to form complexes (Lindsay, 2017). Thus, metallic ions are entrapped in these complexes and cannot participate in reactions involving production of free radicals species. This inhibition is produced, among others, by prevention of metal redox cycling; occupation of all metal coordination sites; formation of insoluble complexes; and/or steric hindrance of interactions between metals and lipids or oxidation intermediates (e.g., hydroperoxides). On the other hand, in some cases, metals chelators can increase oxidative reactions by increasing metal solubility and/or altering the redox potential (McClements & Decker, 2017).

In general, any molecule or ion with an unshared electron pair can coordinate or form complexes with metal ions, as occurs in phenolics. Thus, many phenolics have a strong capacity for binding ferric (Fe^{3+}) ions due to the presence of iron-binding motifs. It has been shown that the following

functional groups are important for Fe-binding: *o*-dihydroxyl groups, e.g., 3', 4', and 7, 8 dihydroxy groups (catechol); the presence of 5-OH and/or 3-OH in conjunction with a C4 keto group (e. g., quercetin), and a large number of OH groups (e. g., tannic acid). Some of these binding places are shown in **Figure 29**. Besides, the presence of a 3',4',5'-trihydroxy (galloyl) group on ring B and the substitution for a galloyl group on ring C was associated with reduced Fe-binding (Khokhar & Owusu Apenten, 2003; Leopoldini et al., 2011; Satterfield & Brodbelt, 2000).

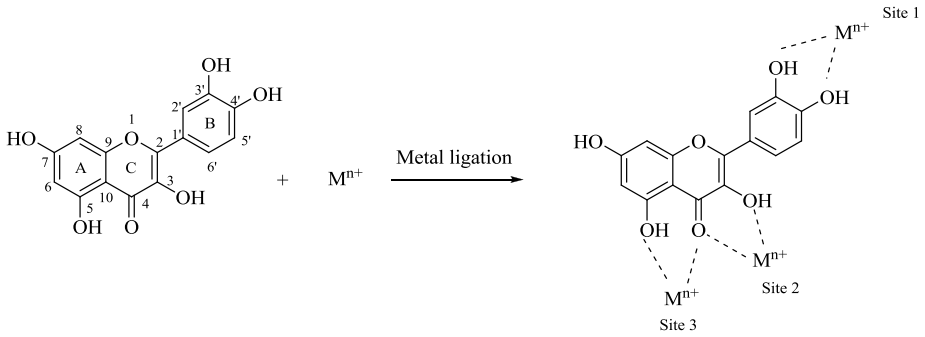

Figure 29. *Mechanism for the transition metal chelation by flavonoids.*

Although polyphenols may offer several chelating sites, when the carbonyl group is available, commonly the metal ion complexes are preferentially formed between the keto group at C4 and the hydroxyl group at C5. In some cases, other complexes are formed involving the keto group at C4 and the hydroxyl group at C3 (Selvaraj et al., 2013; Malesev & Kuntic, 2007; Mira et al., 2002; Leopoldini et al., 2011; Bukhari et al., 2009;).

The structure of the formed flavonoid-metal ion complex depends on numerous factors. These include the coordination number and oxidation state of the central metal ion, the number of electron donors in the flavonoid, the proximity of the electron donors in the flavonoid, and chelating conditions

such as temperature and pH (Selvaraj et al., 2013; Malesev & Kuntic, 2007). In addition, the formation of complexes of various stoichiometries is possible.

1.3.3. The free radical scavenging ability of phenolic compounds and the control of lipid oxidative damage.

Phenolic compounds also delay the lipid oxidation process by scavenging the free radicals that either initiate the lipid oxidation or take part in the propagation of the free radical chain (Zamora & Hidalgo, 2016). This is consequence of their well-known ability of scavenging a wide range of free radical species, including reactive oxygen (ROS), nitrogen (RNS), and chlorine species, such as superoxide, hydroxyl, peroxyl and alkoxyl radicals, and peroxynitrous and hypochlorous acids (Maqsood et al., 2014; Abeywickrama et al., 2016; Rouphael et al., 2016).

Phenolic compounds interact with peroxyl ($ROO^{\bullet}$) or alkoxyl ($RO^{\bullet}$) radicals, and also directly with lipid radicals ($R^{\bullet}$), to convert them to more stable, nonradical products by the following reactions where AH is the phenolic compound (Reische et al., 2008; McClements & Decker, 2017):

$$ROO^{\bullet} + AH \longrightarrow ROOH + A^{\bullet}$$
$$RO^{\bullet} + AH \longrightarrow ROH + A^{\bullet}$$
$$R^{\bullet} + AH \longrightarrow RH + A^{\bullet}$$

The reaction is produced by donation of a hydrogen atom to the radical at the same time that the phenolic compound is converted into a phenolic free radical (phenoxyl radical). Phenolic antioxidants are thought to interact mainly with peroxyl radicals because they have a longer lifetime (they are less reactive). On the contrary, hydroxyl radicals ($OH^{\bullet}$) are so reactive that they interact with the molecules closest to their site of production. Since

phenolic compounds are generally found at low concentrations they would be less likely to react with these highly reactive free radicals.

Antioxidant efficiency is dependent on the ability of the phenolic compound to donate hydrogen to a free radical. As bond energy of a hydrogen in a free radical scavengers (FRS) decreases, the transfer of the hydrogen to a free radical is more energetically favorable and thus more rapid. The efficiency of the FRS is also dependent on the energy of the resulting FRS radical. Effective FRS, such as phenolic compounds, form low energy radicals (phenoxyl radicals in this case) due to resonance delocalization. The phenoxyl radical is stabilized by electron delocalization around a phenolic ring(s) to form stable resonance hybrids (**Figure 30**).

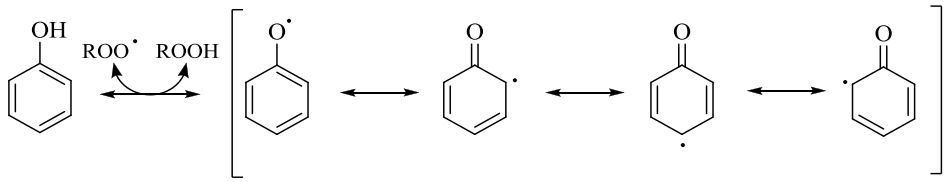

Figure 30. *Resonance delocalization of phenoxyl radical. (Adapted from McClements & Decker, 2017).*

Effective FRS also produce radicals that do not react rapidly with oxygen to form hydroperoxides. Therefore, the phenoxyl radical produced by hydrogen donation has a very low reactivity with oxygen and lipids. Thus, they reduce the rate of propagation of the free radical chain.

Besides, phenoxyl radicals may participate in termination reactions with other phenoxyl radicals or lipid radicals to form nonradical species by the following reactions:

$$ROO^{\bullet} + A^{\bullet} \longrightarrow ROOA$$

$$RO^{\bullet} + A^{\bullet} \longrightarrow ROA$$

$$A^{\bullet} + A^{\bullet} \longrightarrow AA$$

Therefore, each FRS is capable of inactivating at least two free radicals. The first radical is inactivated when the FRS interacts with peroxyl, alkoxyl, or lipid radicals. The second radical is inactivated when the FRS takes part in termination reactions with another FRS radical or lipid radical (**Figure 31**).

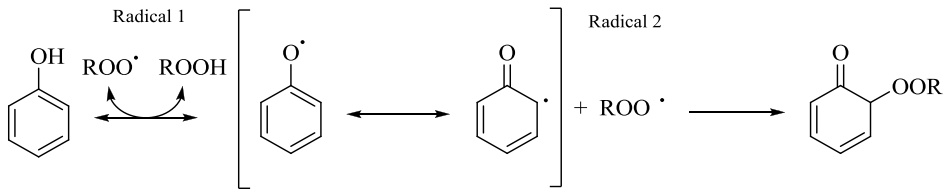

Figure 31. *A termination reaction between a phenoxyl radical and a lipid peroxyl radical (ROO•) (Adapted from McClements & Decker, 2017).*

In foods, the efficiency of phenolic FRS depends on additional factors other than chemical reactivity. Thus, factors such as volatility, pH, sensitivity, and polarity can influence the activity of the FRS in stored and processed foods (Decker, 2008).

The free radical-scavenging potential of natural polyphenolic compounds appears to depend on the pattern (both number and location) of free hydroxyl groups on the flavonoid skeleton (Brewer, 2011). This distribution seems to be more important than the flavan backbone alone (Heim et al., 2002). Besides, other types of substituents can influence the free radical scavenging activity.

The hydroxyl configuration in the B-ring plays the main role in the scavenging of ROS and RNS (Heim et al., 2002). Hydroxyl groups in the B-ring donate hydrogen and an electron to free radicals, stabilizing them and giving rise to a relatively stable flavonoid radical. A 3',4'-catechol structure in the B-ring strongly enhances lipid oxidation inhibition because it yields a fairly stable *o*-semiquinone radical stabilized by electron delocalization.

Furthermore, phenolics containing three adjacent hydroxyl groups are more effective FRS than their dihydroxyl counterparts. Flavonoids lacking catechol or *o*-trihydroxyl (pyrogallol) systems form relatively unstable radicals and are weak scavengers (Pannala et al., 2001).

The significance of other hydroxyl configurations is less clear. It seems that A-ring substitution correlates little with antioxidant activity and compared to the B-ring hydroxylation pattern, the impact of the A-ring arrangement on antioxidant activity is of questionable significance.

Regarding *O*-methylation, the differences in antioxidant activity between polyhydroxylated and polymethoxylated flavonoids are most likely due to differences in both hydrophobicity and molecular planarity. Suppression of antioxidant activity by *O*-methylation may reflect steric effects that perturb planarity (Heim et al., 2002).

In the presence of glycosides, it has been shown that aglycones are more potent antioxidants than their corresponding glycosides. Like methylation, *O*-glycosylation interferes with the coplanarity of the B-ring with the rest of the flavonoid and its ability to delocalize electrons (Heim et al., 2002).

1.3.4. The carbonyl scavenging ability of phenolic compounds and the control of lipid oxidative damage.

Free radical scavenging and chelating properties of phenolics do not explain the ability of these compounds to inhibit some processes in which free radicals are not involved. Thus, the formation of the heterocyclic aromatic amine (HAA) PhIP is a consequence of carbonyl chemistry. This reaction is inhibited in the presence of phenolic compounds (Murkovic et al., 1998; Janoszka, 2010; Persson et al., 2003; Salazar et al., 2014), but this inhibition did not correlate with the antioxidant/free radical scavenging capacity of the phenolic compounds responsible for its inhibition. For example, Cheng et al.

(2007) evaluated the relative activities of 12 food-derived dietary phenolic compounds (including naringenin, quercetin, and epigallocatechin gallate, among others) in inhibiting HAAs formation in model systems and beef patties. The data clearly showed the inhibitory activity of a few phenolic compounds on PhIP formation in model system and all of them in beef patties. In fact, naringenin, a flavonoid found in many citrus fruits, was found to be the most promising inhibitor in both chemical model system and beef patties, suggesting its great potential for practical application in daily cuisine. However, a good positive correlation with their free radical scavenging activities could not be established suggesting that radical scavenging activity may not be the principal mechanism of intervention of these phytochemicals. In fact, recent studies have shown that this effect seems to be a consequence of the ability of phenolic compounds to scavenge lipid-derived reactive carbonyls (Salazar et al., 2014; Cheng et al., 2008).

1.3.4.1. The carbonyl compounds scavenged by phenolics.

The ability of phenolics to react with carbonyl compounds has been long known (Lo et al., 2011; Peng et al., 2008; Totlani & Peterson, 2005). In fact, recent studies have shown that they can act as natural inhibitors against the formation of advanced glycation end-products (AGEs) by trapping or scavenging reactive carbonyls (Wu et al., 2011; Peng et al., 2011; Mesías et al., 2014; Liu et al., 2014).

The reactive carbonyls mostly studied in this sense have been glyoxal and methylglyoxal. Thus, the *in vitro* capacity of numerous phenolics to scavenge these aldehydes has been shown, including hydroxytyrosol (Navarro & Morales, 2015), a mixture of quercitrin, chlorogenic acid and rutin (Yoon & Shim, 2015), genistein (Lv et al., 2011); phlorotannins extracted from brown algae *Fucus Vesiculosus* (Liu & Gu, 2012), and tea polyphenols, particularly epicatechins in green tea and theaflavins in black tea (Lo et al., 2006; Totlani & Peterson, 2006).

In addition, the reaction between phenylacetaldehyde and phenols has also been studied, mostly in relation to the inhibition of PhIP formation (Cheng et al., 2009, 2008; Delgado et al., 2016). Thus, Cheng et al. (2008) demonstrated that naringenin exhibited a dose-dependent reduction of phenylacetaldehyde, a key intermediate in PhIP formation. The capability of naringenin to form adducts with phenylacetaldehyde was confirmed by isolating and characterizing two phenylacetaldehyde-naringenin adducts.

Although lesser studied than the highly reactive short dicarbonyl compounds glyoxal and methylglyoxal, some reports have also shown that lipid-derived reactive carbonyls are potential compounds to be trapped by phenolic compounds. Thus, Delgado et al. (2016) studied the Strecker-type degradation of phenylalanine to produce phenylacetaldehyde in the presence of 2-pentenal and phenolic compounds, and they observed an antagonism when the aldehyde and the phenolics were simultaneously present, which suggested an ability of phenolics to react with both 2-pentenal and phenylacetaldehyde. In fact, Hidalgo and Zamora (2014) investigated the reaction between *m*-diphenols (resorcinol, 2-methylresorcinol, 2,5-dimethylresorcinol, 3-methylphenol, orcinol, and phloroglucinol) and 2-alkenals (2-pentenal and 2-octenal) and isolated and characterized the formed carbonyl-phenol adducts. Zhu et al. (2009a) also evaluated the carbonyl trapping capacity of 21 natural polyphenols against two cytotoxic lipid-derived α,β-unsaturated aldehydes, acrolein and 4-hydroxy-*trans*-2-nonenal (HNE). They found that flavan-3-ols, theaflavins, cyanomaclurins, and dihydrochalcones effectively trapped acrolein and/or HNE, and the most effective one was phloretin. In addition, Zhu et al. (2009b) employed green and black tea extracts to stabilize seal blubber oil and they showed that with the addition of green/black tea extracts, the contents of acetaldehyde, acrolein, malondialdehyde, and propanal, four major lipid peroxidation products, were reduced.

All these results have pointed out that some lipid-derived carbonyls, including alkanals (acetaldehyde and propanal), dialdehydes

(malondialdehyde), alkenals (acrolein, 2-pentenal, 2-octenal), and HNE can be trapped by phenolics. However, unequivocal structures for the produced adducts were not determined in most cases. Moreover, the ability of phenolic compounds to trap many other carbonyl compounds produced in the lipid oxidation, such as the very reactive and toxic epoxyalkenals or oxoalkenals, remains to be investigated.

1.3.4.2. The structure-activity relationships (SAR) for the carbonyl-scavenging function of phenolics.

Analogously to the observed chelating and free radical scavenging activities, the carbonyl trapping potential of phenolic compounds depends on the pattern (both number and location) of free hydroxyl groups.

In a study investigating the SAR of phenolic compounds for the inhibition of PhIP formation, Salazar et al. (2014) analyzed the role of twenty-five phenolic compounds on the PhIP produced in phenylalanine/creatinine/oxidized lipid reaction mixtures. They found that phenols having two hydroxyl groups at *meta* positions of the aromatic ring were the most efficient inhibitors. Besides, they observed that the presence of alkyl or carboxylic groups as additional substituents in the aromatic ring slightly reduced the inhibitory effect. On the other hand, the introduction of additional hydroxyl and amino groups mostly cancelled the inhibitory effect, which was also mostly absent in *o*- and *p*-dihydroxy derivatives. In complex phenols, the presence of several rings with opposite effects produced a reduced inhibitory effect. Nevertheless, although reduced with respect to resorcinol and its simple derivatives, the assayed complex phenols still exhibited a significant PhIP inhibitory effect.

This ability of *m*-diphenols to reduce PhIP formation was a consequence of the formation of carbonyl-phenol adducts as shown by Hidalgo and Zamora (2014) when studying the reaction between 2-alkenals

and *m*-diphenols. Thus, any substituent or substitution pattern that favors the nucleophilicity of some phenolic carbons, will favor the carbonyl-trapping ability of these compounds.

This reaction is mainly favored in *m*-diphenols and not in *o*- or *p*-diphenols because *m*-diphenols have aromatic carbons with a higher nucleophilicity than *o*- and *p*-diphenols due to the electronic delocalization shown in **Figure 32**. The position of the two hydroxyl groups of *m*-diphenols in the aromatic ring favors the loss of the aromatic proton at positions 2, 4 or 6. These positions are activated by the two hydroxyl groups. On the other hand, each hydroxyl group in *o*- and *p*-diphenols activates different aromatic carbons, which reduces their nucleophilicity.

By using the same reasoning, the lower electronic density in the carbonyl compound will facilitate the reaction. This is the reason of the high reactivity of glyoxal and methylglyoxal.

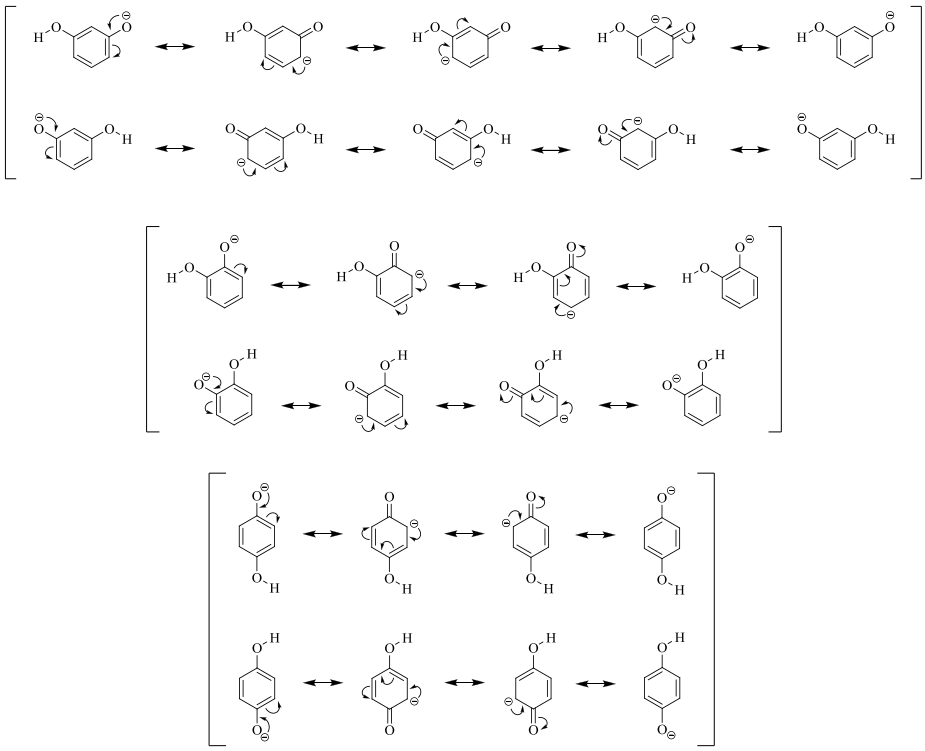

***Figure 32**. Comparative electronic delocalization produced in m- (top), o- (centre), and p-diphenols (bottom) after proton loss (Hidalgo & Zamora, 2014).*

1.3.4.3. The chemical structures of produced carbonyl-phenol adducts.

Carbonyl-phenol reactions are produced as a consequence of the high nucleophilicity of some phenolic carbons and the low electronic density in the carbonyl carbon. Therefore, the reaction should start with the addition of the aromatic carbon or hydroxyl group of the phenol to the carbonyl carbon, or the conjugated carbon-carbon double bond in the case of α,β-unsaturated carbonyls. The formed products should be produced by stabilization of this initial addition product. This has been observed in the reactions studied until now (Sang et al., 2007; Lv et al., 2011; Shao et al., 2008; Hidalgo & Zamora, 2014; Zhu et al., 2009a; Beretta et al., 2008).

Thus, saturated carbonyl compounds suffer the addition of the phenolic compound and the corresponding alcohol is produced (**Figure 33**). Depending on the reaction conditions and both the carbonyl and the phenolic compound involved, the formed adduct can suffer then a dehydration reaction to produce a more stable conjugated compound. An example of this dehydration has been observed in the reaction of phenylacetaldehyde with different flavonoids (Cheng et al., 2008; Zheng et al., 2016).

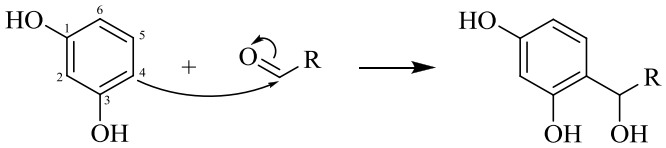

resorcinol

***Figure 33**. Alkanal addition to resorcinol.*

In the case of the highly reactive short dicarbonyl compounds glyoxal and methylglyoxal, the reaction occurs similarly (Wang & Ho, 2012; Lv et al., 2011; Sang et al., 2007; Lo et al., 2006; Yoon & Shim, 2015; Shao et al., 2008; Totlani & Peterson, 2006; Navarro & Morales, 2015).

Although much more complex, the reaction of 2-alkenals with phenolic compounds also occurs similarly, as shown in **Figure 34**. Thus, the reaction takes place by initial addition of either the aromatic carbon or hydroxyl group of the phenolic to the carbon-carbon double bond of the carbonyl compound and later stabilization of these initial addition products. The adduct produced by the initial addition of the aromatic carbon to the aldehyde is relatively stable after formation of a hemiacetal structure. However, the adduct produced by the initial addition of the hydroxyl group to the aldehyde is more unstable and suffers a dehydration. These compounds have been isolated and characterized by nuclear magnetic resonance spectroscopy (NMR) and mass spectrometry (MS) for a significant number of

phenolic compounds (Hidalgo & Zamora, 2014). In addition, this new adduct can suffer further polymerization reactions that have been related to the browning development produced in these reactions (Zamora & Hidalgo, 2016).

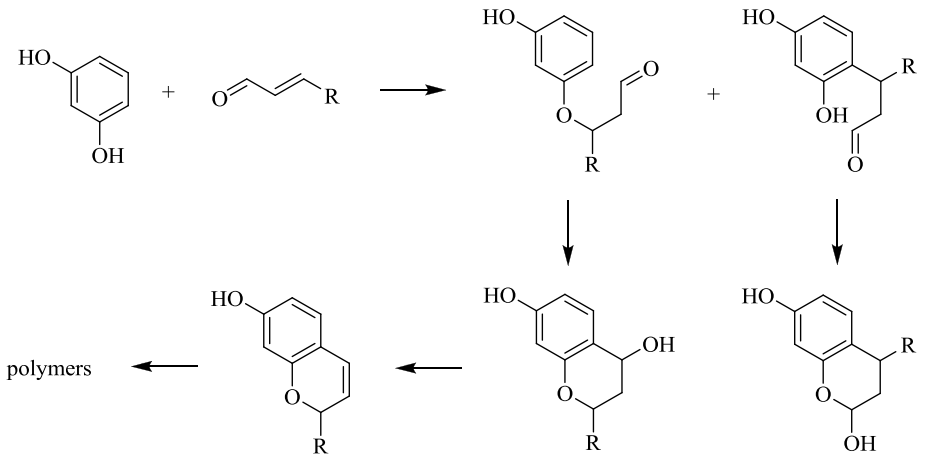

***Figure 34**. Reaction of 2-alkenals with resorcinol (Zamora & Hidalgo, 2016).*

These results are in agreement with those obtained by Zhu et al. (2009a), who purified an adduct formed in the reaction of the dihydrochalcone phloretin and acrolein. It was identified as a diacrolein-conjugated phloretin (**Figure 35**).

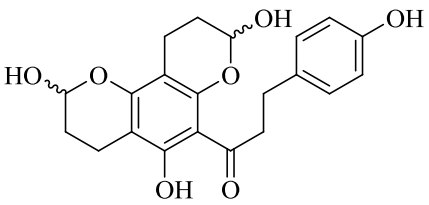

***Figure 35**. Structure of diACR-conjugated phloretin adduct.*

Nevertheless, at present only the structures of carbonyl-phenol adducts with these simple carbonyl compounds have been proposed. The structures of the adducts that might be produced with more complex LOPs remain to be elucidated.

1.3.5. The hypothesis of the triple defensive barrier of phenolic compounds against the lipid oxidative damage produced in foods.

Based on the above described abilities of phenolic compounds to act as metal chelators, free radical scavengers, and carbonyl-trapping agents, Zamora and Hidalgo (2016) have recently hypothesized that phenolic compounds might be acting as a triple defensive barrier against the lipid oxidative damage produced in foods.

As described above, in the presence of metal ions, among other initiators, lipids are oxidized producing a complex cascade of reactions and the formation of a myriad of LOPs (**Figure 2**). Some of the produced LOPs are stable, but others are highly reactive and broadcast the lipid oxidative damage to all kind of molecules. Among them, the production of carbonyl-amine reactions is particularly important because of the consequences produced in foods (**Figure 24**).

According to the reactions described in sections 1.3.2, 1.3.3, and 1.3.4, Zamora and Hidalgo (2016) have hypothesized that phenolics can be acting at different steps of this process according to their different structures and functions. Thus, they would be able successively to chelate metals and to avoid the formation of free radicals, scavenge free radicals and to avoid the formation of secondary and tertiary LOPs, and trap lipid-derived reactive carbonyls avoiding in this way the carbonyl-amine reactions produced as a consequence of the lipid oxidation pathway.

This hypothesis assumes that the carbonyl-trapping ability of phenolic compounds is general for all LOPs. Furthermore, it supposes that the

structural requirements for this carbonyl-trapping function are common for all lipid-derived reactive carbonyls (Zamora & Hidalgo, 2016).

This can be observed in **Figure 36**, in which four flavones with different hydroxylation pattern are shown. The main groups involved in the different protective functions of phenolic compounds have been marked by using different ellipses.

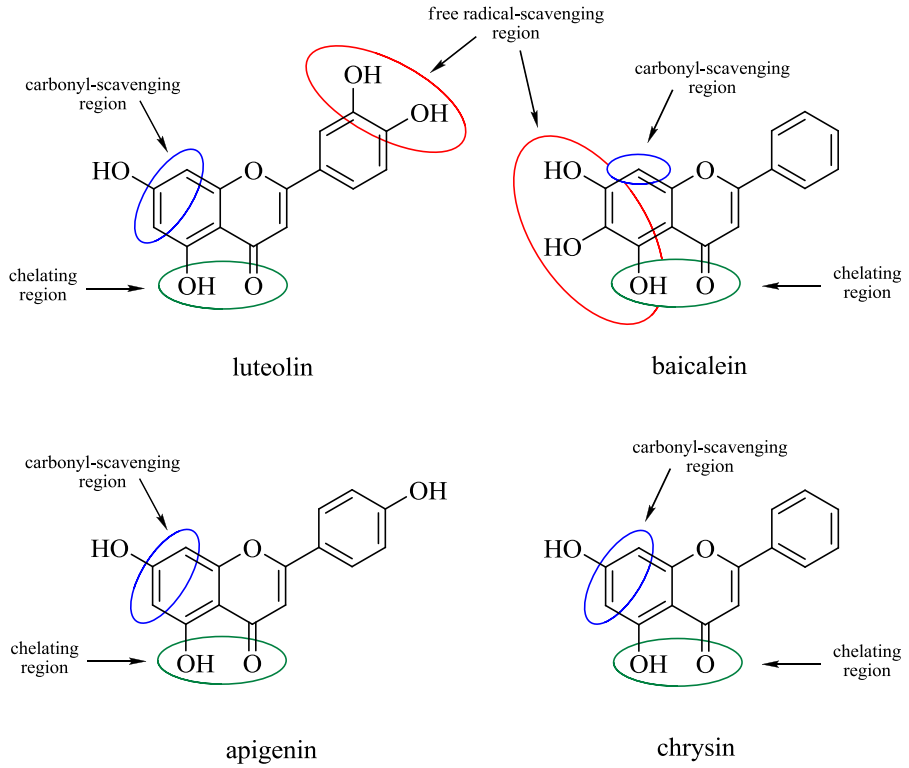

***Figure 36**. Presence of chelating, free radical-scavenging, and carbonyl-scavenging regions in selected flavonoids (Zamora & Hidalgo, 2016).*

Regarding the transition metal chelating activity, the metal ion complexes are preferentially formed between the keto group at C4 and the hydroxyl group at C5 when the carbonyl group is available. In some cases,

other complexes are formed involving the keto group at C4 and the hydroxyl group at C3. This activity should be present in the four selected flavones because the keto group at C4 and the hydroxyl group at C5 are present in all of them.

The free-radical scavenging activity of flavonoids depends on the presence of catechol or *o*-trihydroxyl (pyrogallol) systems. For that reason, when Cai et al. (2006) studied the free-radical scavenging activity of the four flavones collected in **Figure 36**, only luteolin and baicalein exhibited activity. These two compounds are the only compounds among those included in the figure that have catechol or pyrogallol systems.

Finally, the carbonyl-scavenging activity needs the presence of phenolic carbons with a high electronic density. It occurs in luteolin, apigenin, chrysin and, to a lower extent, also in baicalein.

All regions marked in **Figure 36** correspond to the most active regions for that protective effect. However, other regions can also play a role under determined circumstances.

As observed in **Figure 36**, not all phenolics have all the protective functions. According to the presence or not of these protective functions, phenolics might be divided, at least, into seven groups as a function of their activities: chelating agents, free radical scavengers, carbonyl scavengers, chelating and free radical scavengers, chelating and carbonyl scavengers, free radical and carbonyl scavengers, and chelating and free radical and carbonyl scavengers.

2. AIMS OF THE STUDY

As described in the Introduction section, phenolic compounds might, in addition to chelating metals and scavenging free radicals, also be limiting the produced lipid oxidative damage by trapping the lipid-derived reactive carbonyls formed in the course of lipid oxidation. Furthermore, this trapping would constitute a third protective barrier of phenolic compounds against the broadcasting of the consequences of lipid oxidation to other food macromolecules. However, this barrier is still poorly understood because neither the carbonyl-trapping ability of all LOPs has been studied nor the possibility that this carbonyl-trapping might be produced under usual cooking conditions has been investigated. Therefore, the general objective of this thesis is to determine whether the carbonyl-trapping ability of phenolics is general for main LOPs, and to study the presence of carbonyl-phenol adducts in processed food products.

To carry out this general objective, different specific objectives have been proposed:

1. To study the reaction among phenolic compounds and the main groups of carbonyl compounds produced as a consequence of lipid oxidation, including alkanals, alkadienals, 4,5-epoxy-2-alkenals, and 4-oxo-2-alkenals.
2. To investigate the reaction conditions that favor the formation of the corresponding carbonyl-phenol adducts.
3. To understand the structure-activity relationships (SAR) of both phenolics and carbonyl compounds that favor the formation of carbonyl-phenol adducts.
4. To determine the reaction pathways by which carbonyl-phenol reactions are produced.
5. To study the lipid-derived carbonyl-trapping ability of phenolic compounds under common food processing conditions in order to

know whether carbonyl-phenol adducts might be usual food components in processed foods.

3. MATERIALS AND METHODS

3.1. Materials.

3.1.1. Commercial products.

A series of aldehydes having different number of carbons and unsaturations were employed in these studies. These aldehydes included alkanals such as propanal, butanal, 2-methylpropanal, pentanal, 2-methylbutanal, 3-methylbutanal, hexanal, and glyoxal; 2-alkenals such as acrolein, crotonaldehyde, 2-pentenal, 2-octenal, and 2-methyl-2-pentenal; and alkadienals, such as 2,4-heptadienal and 2,4-decadienal. Fumaraldehyde was also used in some experiments. It was prepared from commercial fumaraldehyde bis(dimethyl acetal) by treating an aqueous solution of the acetal with acid resin (Dowex 50WX8) for 1 h. The chemical structures of all these compounds are given in **Figure 37**.

As model phenolic compounds, resorcinol, 2-methylresorcinol, 2,5-dimethylresorcinol, orcinol, and quercetin were employed. The chemical structures of these phenolic compounds are given in **Figure 26** and **Figure 28** in the Introduction section 1.3.1.

All these compounds were purchased from Sigma-Aldrich (St. Louis, MO), Fluka (Buchs, Switzerland), Alfa Aesar (HaverHill, MA), or TCI Chemicals (Zwijndrecht, Belgium), and were of either analytical grade or the highest available quality.

Citric acid (99.5%), boric acid, sodium hydroxide (99%) and the sodium phosphate used to prepare the different buffers were obtained from Merck (Darmstadt, Germany).

Rapeseed oil, red onions (*Allium cepa L.*), and commercially crispy fried onions were purchased at local supermarkets.

Sephadex LH-20 was obtained from GE Healthcare Europe (Freiburg, Germany). Silica gel, alumina, and thin-layer chromatography plates (thickness of 0.2 mm) were purchased from Macherey Nagel (Gmbh, Düren, Germany).

All solvents used in these studies (methanol, hexane, diethyl ether, acetonitrile, chloroform, acetone) were analytical grade and were purchased from Merck.

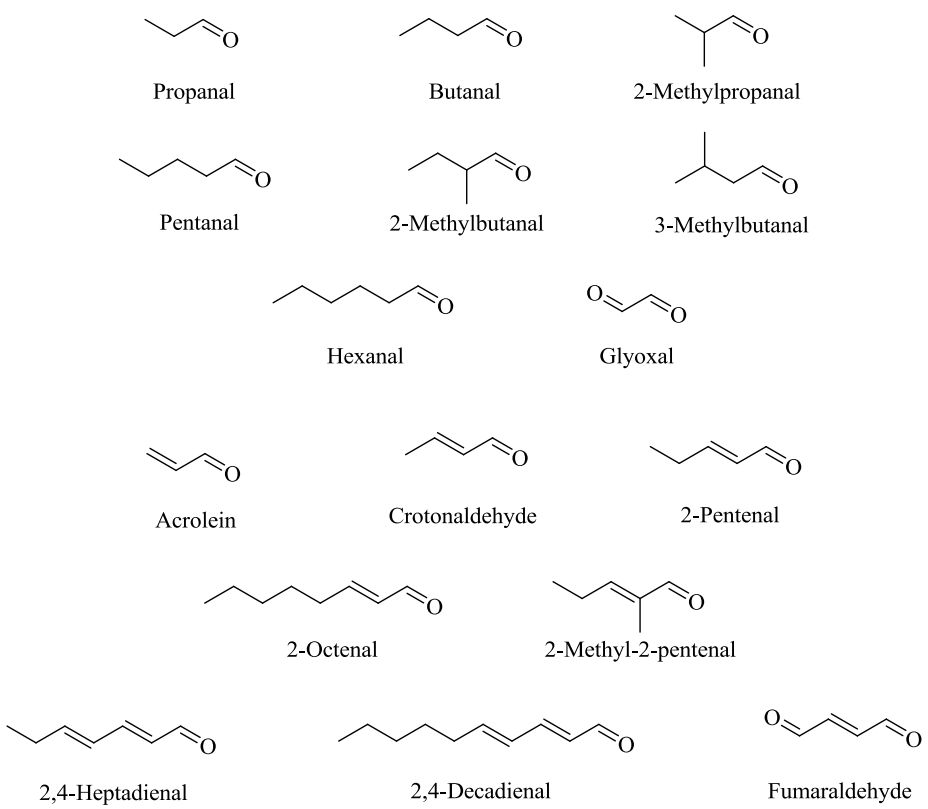

Figure 37. *Chemical structures of some of the aldehydes employed in this study.*

3.1.2. Syntheses of epoxyalkenals.

Three 4,5-epoxy-2-alkenals were employed in this study. They were 4,5-epoxy-2-hexenal, 4,5-epoxy-2-heptenal, and 4,5-epoxy-2-decenal. Their syntheses were carried out from the corresponding 2,4-alkadienals (2,4-

hexadienal, 2,4-heptadienal, and 2,4-decadienal, respectively) by epoxidation with 3-chloroperoxybenzoic acid (Zamora et al., 2006b) (**Figure 38**).

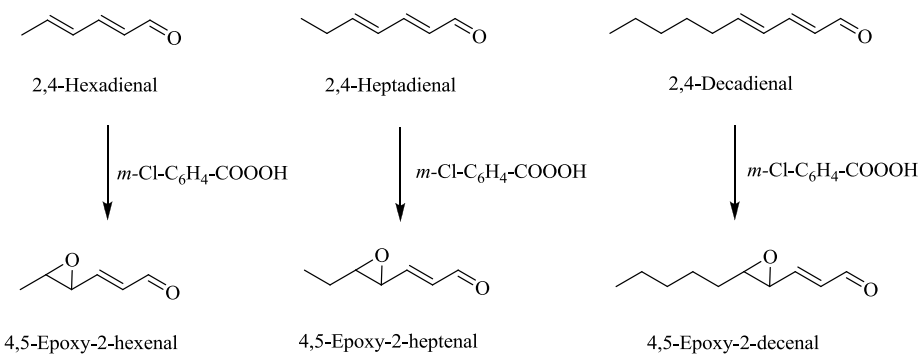

***Figure 38**. Synthesis of epoxyalkenals used in this study.*

In short, 3-chloroperoxybenzoic acid (69.5 mmol) was dissolved in chloroform (175 ml), washed three times with 100 ml of buffer (0.2 M $Na_2HPO_4 \cdot 12H_2O$ adjusted to pH 7.5 with 0.1 M citric acid) followed by three 100 ml portions of water, and dried with anhydrous sodium sulfate. This solution was added slowly to a solution of 2,4-alkadienal (39.9 mmol) in chloroform (30 ml), which was stirred at room temperature overnight and, finally, washed three times with 100 ml of buffer (0.2 M $Na_2HPO_4 \cdot 12H_2O$ adjusted to pH 7.5 with 0.1 M citric acid monohydrate) followed by three extractions with 100 ml of water. The organic solution was dried over anhydrous sodium sulfate and concentrated under vacuum. The residue was fractionated by column chromatography on silica gel 60 (230-400 mesh; Macherey-Nagel) using mixtures of hexane and acetone as eluent. The separation was controlled by thin-layer chromatography. 4,5-Epoxy-2-alkenals were obtained chromatographically pure. Confirmations of identity and purity were obtained by gas chromatography-mass spectrometry (GC-MS) by comparing retention times and mass spectra with authentic standards prepared previously in the laboratory.

3.1.3. Syntheses of oxoalkenals.

Two 4-oxo-2-alkenals were employed in this study. They were 4-oxo-2-hexenal and 4-oxo-2-nonenal, which were prepared by ring opening of the corresponding 2-alkylfuran: 2-ethylfuran and 2-pentylfuran, respectively (Shimozu et al., 2009) (**Figure 39**).

Briefly, *N*-bromosuccinimide (10.7 mmol) and pyridine (10 ml) were added to a solution of 2-alkylfuran (16.6 mmol) in 11 ml of tetrahydrofuran/acetone/water (5:4:2) in an ice bath. The reaction mixture was stirred for 1 h at this temperature and, then, kept on stirring at room temperature for 2 h. After this time, the mixture was diluted with 10 ml of water and extracted three times with 50 ml of chloroform. The combined chloroformic extracts were washed succesively with hydrochloric acid and water in order to remove pyridine, then dried over anhydrous sodium sulfate, and finally concentrated under vacuum. The residue was fractionated by column chromatography on silica gel 60 (230-400 mesh; Macherey-Nagel) using mixtures of hexane and ethyl acetate as eluent. The separation was controlled by thin-layer chromatography. 4-Oxo-2-alkenals were obtained chromatographically pure. Confirmations of identity and purity were obtained by GC-MS as described above.

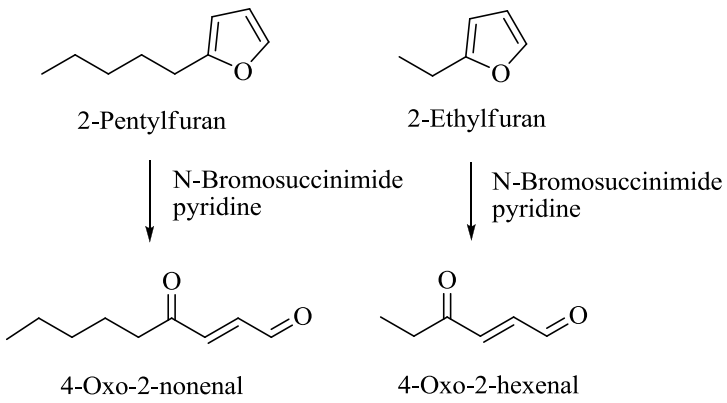

Figure 39. *Syntheses of 4-oxo-2-nonenal and 4-oxo-2-hexenal.*

3.2. Analytical instrumentation.

3.2.1. Gas chromatography-mass spectrometry (GC-MS).

GC-MS analyses were conducted with two instruments. Some GC-MS analyses were carried out with a Hewlett-Packard 6890 GC Plus coupled with an Agilent 5973 MSD (mass selective detector, quadrupole type). A fused-silica HP5-MS capillary column (30 m × 0.25 μm i.d.; coating thickness, 0.25 μm) was used, and 1 μl of sample was injected in the pulsed splitless mode. Other GC-MS analyses were conducted with an Agilent 7820 gas chromatograph coupled with an Agilent 5977B MSD (mass selective detector, quadrupole type). In this case, the employed column was a fused-silica DB-5MS UI capillary column (30 m × 0.25 i.d.; coating thickness, 0.25 μm), and 1 μl of sample was injected in the pulsed splitless mode.

3.2.2. Liquid chromatography- tandem mass spectrometry (LC-MS/MS).

Samples were analyzed by using an Agilent liquid chromatography system (1200 Series) consisting of binary pump (G1312A), degasser (G1379B), and autosampler (G1329A), connected to a triple quadrupole API 2000 mass spectrometer (Applied Biosystems, Foster City, CA) using an electrospray ionisation interface in positive ionization mode (ESI^+), or in negative ionization mode (ESI^-) in some cases. Compounds were separated on a Zorbax Eclipse XDB-C18 (150 mm × 4.6 mm, 5 μm) column from Agilent (Santa Clara, CA).

3.2.3. Liquid chromatography-high resolution mass spectrometry (LC-HRMS).

The LC-ESI-MS system consisted of a Dionex Ultimate 3000RS U-HPLC (Thermo Fisher Scientific, Waltham, MA) coupled to a micrOTOF-QII

ultra high resolution time-of-flight mass spectrometer (UHR-TOF) with q-TOF geometry (Bruker Daltonics, Bremen, Germany). Chromatographic separation was performed on a Zorbax Eclipse XDB-C18 column (150 mm × 4.6 mm, 5 μm) from Agilent.

3.2.4. Nuclear magnetic resonance spectroscopy (NMR).

Most NMR spectra were obtained by using a Bruker Advance III spectrometer operating at 500 MHz for protons. For ^{1}H spectra, acquisition parameters were: spectral width 10000 Hz, relaxation delay 1 s, number of scans 16, acquisition time 3.277 s, and pulse width 90°, with a total acquisition time of 1 min 17 s. For ^{13}C spectra, acquisition parameters were: spectral width 27500 Hz, relaxation delay 2 s, acquisition time 1.188 s, and number of pulses depended on the concentration of the sample. All experiments were performed at 24 °C and 2D experiments (COSY, HMQC and HMBC) were carried out to determine the chemical structures of the isolated compounds. Only spectra of compounds **37-39** were obtained in a Bruker AC-300P operating at 300 MHz for protons.

3.2.5. Other equipment.

The following equipment was also used: mortar, mixer UltraTurrax T-25, rotary evaporator R210 (Büchi, Valinhos, Brazil), oven ULE 400 with forced convection (Memmert, Schwabach, Germany), block heater QBH2 (Grant, Cambridge, UK), vortex Reax 2000 (Heidolph, Schwabach, Germany), vacuum pump (Vacuubrand, Wertheim, Germany), stirrer heater (Selecta, Univeba, Barcelona, Spain), magnetic stirrer hotplate (Gallenkamp, Loughborough, UK), centrifuge Sorvall RC6 plus (Thermo Scientific), centrifuge Universal 16R (Hettich, Germany), heating/stirrer module Reacti-Therm III TS-18823 (Thermo Scientific), fraction collector 7000 ultrorac (LKB), fraction collector Model 203 (Gilson, Middleton, WI),

and analytical precision balances (Sartorius, Goettingen, Germany). In addition, a glass bowl, a heating mantle and a thermocouple were also used for frying experiments with samples of onion.

3.3. Studied systems.

3.3.1. Formation of carbonyl-phenol adducts in the reaction of alkanals and phenolic compounds.

3.3.1.1. Synthesis and Characterization of Alkanal-Phenol Adducts.

The reaction was carried out by mixing the saturated aldehyde (3 mmol) and the phenolic compound (3 mmol) in methanol (10 ml) containing 400 µl of triethylamine and heating the mixture in closed test tubes under nitrogen at 60 ºC. At the end of the heating process, reactions mixtures were fractionated by column chromatography on silica gel 60 (230-400 mesh; Macherey-Nagel) using mixtures of hexane and diethyl ether as eluent. The separation was controlled by GC-MS using the analytical conditions described in section 3.4.2.1. Different reactions were studied (see section 4.1).

In addition, a study of the reaction between pentanal and 2-methylresorcinol was carried out in order to determine the reaction pathway between alkanals and phenolic compounds. In this case, reaction was carried out as described above but the products present in the reaction mixture were stabilized by acetylation. Briefly, after the heating process, the reaction mixture was cooled at room temperature for 15 min and taken to dryness using a rotary evaporator. The dried sample was acetylated by adding 100 ml of anhydrous pyridine and 50 ml of acetic anhydride, and then left in the dark for 22 h at room temperature. After that time, 160 ml of water and 160 ml of chloroform were added and the mixtures were stirred for 10 s. After phase separation, the aqueous layer was removed and discarded. The resulting organic phase was firstly washed three times with 250 ml of 5% hydrochloric

acid until the pyridine was removed and then, with water to remove the hydrochloric acid. The resulting organic extract was treated with sodium sulfate to eliminate the remaining moisture, then taken to dryness, and, finally, fractionated by column chromatography on silica gel 60 (230-400 mesh; Macherey-Nagel) using mixtures of hexane and diethyl ether as eluent to isolate the produced compounds. The separation was controlled by GC-MS, using the analytical conditions described in section 3.4.2.1.

The formed compounds were isolated and characterized by 1D and 2D NMR and MS, using the analytical conditions described in sections 3.2.4 and 3.4.2.1, respectively.

3.3.1.2. Effect of Aldehyde Chain Length on the Formation of Alkanal-Phenol Adducts.

Mixtures of one phenolic compound (80 µmol) and four lineal alkanals (propanal, butanal, pentanal, and hexanal, 20 µmol of each) in 500 µl of methanol containing 20 µl of triethylamine were heated at 60 ºC under nitrogen. At different reaction times, reaction mixtures were cooled at room temperature (15 min), 15 µl of the internal standard (a solution of 54.8 mg of methyl heptanoate in 25 ml of methanol) was added, and the formation of the corresponding adducts was studied by GC-MS using the analytical conditions described in section 3.4.2.1. The phenolic compounds assayed were resorcinol, 2-methylresorcinol, 2,5-dimethylresorcinol, and orcinol.

3.3.1.3. Effect of Aldehyde Branching on the Formation of Alkanal-Phenol Adducts.

Two different studies were carried out. Firstly, mixtures of 2-methylresorcinol (40 µmol) and two alkanals (butanal and 2-methylpropanal, 20 µmol of each) in 500 µl of methanol containing 20 µl of triethylamine were heated at 60 ºC under nitrogen. In the second study, mixtures of 2-

methylresorcinol (60 µmol) and three alkanals (pentanal, 2-methylbutanal, and 3-methylbutanal, 20 µmol of each) in 500 µl of methanol containing 20 µl of triethylamine were heated at 60 ºC under nitrogen. At different reaction times, reaction mixtures were cooled at room temperature (15 min), 15 µl of the internal standard (a solution of 54.8 mg of methyl heptanoate in 25 ml of methanol) was added, and the formation of the corresponding adducts was studied by GC-MS using the analytical conditions described in section 3.4.2.1.

3.3.2. Formation of carbonyl-phenol adducts in the reaction of epoxyalkenals and phenolic compounds.

For analytical studies, mixtures of the epoxyalkenal (40 µmol in 40 µL of methanol) and the phenolic compound (30 µmol in 170 µL of water) in 0.3 M buffer (300 µl) were heated in closed test tubes at 100 ºC for 30 min under nitrogen. The solvent employed in most of experiments was 0.3 M sodium phosphate buffer, pH 8. In addition, two buffers were employed when studying the effect of reaction pH: sodium phosphate, pH 6–8, and sodium borate, pH 8–9. At the end of the heating process, samples were cooled at room temperature for 15 min, 1.2 ml of ethanol added, and taken to dryness using a flow of nitrogen.

Dried samples were then acetylated by adding 30 µl of internal standard (a solution of 36.64 mg of *cis*-3-nonen-1-ol in 5 ml of anhydrous pyridine), 1 mL of anhydrous pyridine, and 500 µl of acetic anhydride, and then left in the dark for 20 h at room temperature. After that time, 2 ml of water and 2 ml of chloroform were added and the mixtures were stirred for 10 s. After phase separation, the aqueous layer was removed and discarded. The resulting organic phase was firstly washed three times with 2 ml of 5% hydrochloric acid until the pyridine was removed and then, with 2 ml of water to remove the hydrochloric acid. The resulting organic extracts were treated with sodium sulfate to eliminate the remaining moisture and then studied by GC-MS using the analytical conditions described in section 3.4.2.2.

For preparative studies, the reaction conditions were the same but the reaction was carried out using 2.4 mmol of phenolic compound, 3.4 mmol of epoxyalkenal, and 24 ml of 0.3 M sodium phosphate buffer, pH 8. Acetylation of the heated and dried mixtures was carried out with 80 ml of anhydrous pyridine and 40 ml of acetic anhydride. Acetylated compounds were extracted with chloroform, and the pyridine was removed as described above. The mixtures of acetylated compounds obtained were fractionated by column chromatography on silica gel 60 (230-400 mesh; Macherey-Nagel,) using mixtures of hexane and diethyl ether as eluent, and the separation was controlled by GC-MS using the analytical conditions described in section 3.4.2.2. The compounds formed in the different assayed reactions (see section 4.2) were isolated and characterized by 1D and 2D NMR and MS, using the analytical conditions described in sections 3.2.4 and 3.4.2.2, respectively.

3.3.3. Formation of carbonyl-phenol adducts in the reaction of oxoalkenals and phenolic compounds.

For analytical purposes, mixtures of the oxoalkenal (40 µmol in 40 µL of methanol) and the phenolic compound (30 µmol in 170 µL of water) in 0.3 M buffer (300 µl) were heated in closed test tubes at 100 ºC for 30 min under nitrogen. The solvent employed in most of experiments was 0.3 M sodium phosphate buffer, pH 8. In addition, three buffers were employed when studying the effect of reaction pH: sodium citrate, pH 5; sodium phosphate, pH 6–8; and sodium borate, pH 8–9. In reactions involving fumaraldehyde, the commercial fumaraldehyde bis(dimethyl acetal) was previously treated with Dowex 50WX8 to release the dialdehyde as indicated in section 3.1.1 and, then, treated with the phenolic compound for 30 min at 37 ºC under nitrogen in 0.3 M sodium phosphate buffer, pH 7. When reactions were carried out in methanol/triethylamine, the phenolic compound was dissolved in methanol and a total volume of 500 µL of methanol and 20 µL of triethylamine was employed. In all cases, at the end of the heating process,

samples were cooled at room temperature for 15 min and either submitted to acetylation or reduction.

Samples to be acetylated were treated with 1.2 mL of ethanol and then taken to dryness using a flow of nitrogen. Once dried, the internal standard was added (30 µL of a solution of 36.64 mg of cis-3-nonen-1-ol in 5 mL of anhydrous pyridine) and samples were acetylated as described in section 3.3.2. Acetylated samples were studied by GC-MS using the analytical conditions described in section 3.4.2.3.

Samples to be reduced were treated with excess of sodium borohydride for 1 h at room temperature and, then, extracted twice with ethyl acetate. Reduced samples were studied by GC-MS using the analytical conditions described in section 3.4.2.3.

For preparative purposes, identical reaction conditions were used but higher amounts of reagents were employed: 2.4 mmol of phenolic compound, 3.4 mmol of oxoalkenal, and 24 mL of 0.3 M sodium phosphate buffer, pH 8, in most experiments. Reactions involving the reduction of the produced adducts were carried out using an amount of aldehyde four times higher than that of phenol. Either acetylated or reduced samples were fractionated by column chromatography on silica gel 60 (230-400 mesh; Macherey-Nagel) using mixtures of hexane and diethyl ether as eluent. The separation was controlled by GC-MS using the analytical conditions described in section 3.4.2.3. The compounds formed in the different assayed reactions (see section 4.3) were isolated and characterized by 1D and 2D NMR and MS, using the analytical conditions described in sections 3.2.4 and 3.4.2.3, respectively.

3.3.4. Formation of carbonyl-phenol adducts in the reaction of alkenals and quercetin.

A mixture of quercetin (200 µmol) and acrolein, crotonaldehyde, or (*E*)-2-pentenal (400 µmol) in methanol (2 ml) containing 290 µmol of triethylamine, was heated under nitrogen at 100 °C for 3.5 h (acrolein), 10 h

(crotonaldehyde), or 96 h ((*E*)-2-pentenal), respectively. At the end of the heating time, the reaction mixture was fractionated on a Sephadex LH-20 column using methanol/water (80/20, v/v) as eluent at a flow rate of 15 ml/h. Eluted products were detected by MS/MS using direct injection and the analytical conditions described in section 3.4.2.4. The compounds formed in the different assayed reactions (see section 4.5) were isolated and characterized by 1D and 2D NMR and LC-HRMS, using the analytical conditions described in sections 3.2.4 and 3.4.2.4, respectively.

3.3.5. Thermal degradation of unsaturated aldehydes.

Two different procedures were followed depending on whether the formed compounds were going to be either identified or quantified.

The identification of thermal degradation products of the studied aldehydes was carried out by GC-MS after derivatization with *O*-(2,3,4,5,6-pentafluorobenzyl)hydroxylamine hydrochloride, according to a previously described procedure (Zamora et al., 2006a), which was modified. Briefly, the aldehyde (4 μmol) was either heated alone or in the presence of 200 μl of 50 mM buffer pH 8, for 1 h at 200 ºC in a closed test tube under either nitrogen or air. Two buffers were employed: sodium phosphate and sodium borate. At the end of the heating process, samples were cooled (5 min at room temperature and 10 min at −20 ºC) and derivatized with 400 μl of a freshly prepared solution of *O*-(2,3,4,5,6-pentafluorobenzyl)hydroxylamine hydrochloride (10 mg/ml in methanol). The resulting solution was stirred and incubated for 1 h at 37 ºC. Finally, reactions were studied by GC-MS, using the analytical conditions described in section 3.4.1.1.

Quantification of the compounds produced was carried out by LC-MS/MS after derivatization with dansylhydrazine according to a previously described procedure (Zamora et al., 2014), which was also modified. In short, a solution of the aldehyde (0–80 μmol) in tetrahydrofuran (80 μl) was treated with 0.2 M buffer (420 μl) and, then, heated for the indicated time and

temperature in a closed test tube under air. The solvent employed in most of experiments was 0.2 M sodium phosphate buffer, pH 8. In addition, three buffers were employed when studying the effect of reaction pH: sodium citrate, pH 2.15-5; sodium phosphate, pH 6–8; and sodium borate, pH 9–12. At the end of the heating process, samples were cooled (5 min at room temperature and 10 min at −20 ºC). Fifty microliters of these cooled samples were diluted with 350 μl of methanol, and treated with 50 μl of the internal standard (a solution of 88 μmol of formaldehyde-d_2 in 2 ml of methanol), 150 μl of trifluoromethanesulfonic acid solution (3% in methanol), and 200 μl of dansylhydrazine solution (4 mg/ml in methanol). The resulting solution was incubated for 15 min at 100 ºC, then maintained for 1 h at 25 ºC, and finally diluted with 200 μl of eluent A (a 30:70 mixture of 0.2% formic acid in acetonitrile and 4 mM ammonium acetate), and analyzed by LC-MS/MS using the analytical conditions described in section 3.4.1.1.

3.3.6. Deep-frying experiments.

Deep-frying experiments were carried out in rapeseed oil (100 g) containing acrolein, crotonaldehyde, and (*E*)-2-pentenal (2.7 μmol/g of oil of each aldehyde), which were added before heating the oil. The oil was first preheated for 9 min to achieve 160 °C and, then, heated in the presence, or absence, of thin slices of onions (5 g) for further 3 min. At the end of the heating time, the heated oils were analyzed for aldehyde contents by ^{1}H NMR using the procedure described in section 3.4.1.2. The fried onions were also analyzed to identify aldehyde-quercetin adducts.

Aldehyde-quercetin adducts were firstly extracted and concentrated according to the following procedure: samples of onions (5 g each) were homogenized in water (20 ml) and hexane (50 ml). The resulting mixture was centrifuged at 7500*g* for 10 min at room temperature. The organic layer was discarded and other 50 ml of hexane were added. The mixture was homogenized again and centrifuged at 7500*g* for 10 min. The organic layer

was discarded and methanol (80 ml) was added. The mixture was newly homogenized and centrifuged at 7500*g* for 10 min. The supernatant was collected and the solid was extracted with 100 ml of methanol/water (80/20, v/v). The resulting mixture was centrifuged at 7500*g* for 10 min and the supernatant was collected. Both supernatants were combined, concentrated to about 4 ml using a rotatory evaporator (30 °C, 16 mbar) and fractionated on a Sephadex LH-20 column using methanol/water (80/20, v/v) as eluent at a flow rate of 15 mL/h. Fractions obtained were analyzed by LC-HRMS, using the analytical conditions described in section 3.4.2.5. The different carbonyl-phenol adducts were identified by comparison with adducts synthesized as described in section 3.3.4, which were used as reference compounds. The same procedure was used to analyze commercially prepared crispy fried onions.

3.4. Analytical determinations.

3.4.1. Determination of aldehydes.

3.4.1.1. Aldehydes produced by thermal degradation of alkadienals amd 2-alkenals.

Thermal degradation products of the studied aldehydes (2-pentenal, 2-octenal, 2,4-heptadienal and 2,4-decadienal) were determined using the samples prepared in section 3.3.5.

Samples for identification purposes were analyzed by GC-MS. In this case, working conditions were as follows: carrier gas, helium (1 ml/min at constant flow); injector temperature, 250 ºC; oven temperature, from 70 (1 min) to 240 ºC at 5 ºC/min and, then, to 325 ºC at 10 ºC/min; transfer line to MSD, 280 ºC; ionisation EI, 70 eV. Reaction products were identified by

comparison of mass spectra and retention times to those of authentic standards.

On the other hand, samples for quantification purposes were analyzed by LC-MS/MS. Working conditions were as follow: as eluent A, a 30:70 mixture of 0.2% formic acid in acetonitrile and 4 mM ammonium acetate was used. As eluent B, a 0.2% formic acid solution in acetonitrile was employed. The mobile phase was delivered at 0.5 ml/min using the following gradient: for 0–13 min, the content of mobile phase B was 7%; for 13–20 min, the content of mobile phase B was increased linearly from 7% to 60%; for 20–30 min, the content of mobile phase B was 60%; for 30–32 min, the content of mobile phase B was increased linearly from 60% to 90%; for 32–42 min, the content of mobile phase B was 90%; and for 42–45 min, the content of mobile phase B was decreased linearly from 90% to 7%. Mass spectrometric acquisition was performed using multiple reaction monitoring (MRM). The nebulizer gas (synthetic air), the curtain gas (nitrogen), and the heater gas (synthetic air) were set at 40, 25, and 50 (arbitrary units), respectively. The collision gas (nitrogen) was set at 3 (arbitrary units). The heater gas temperature was set at 500 ºC and the electrospray capillary voltage to 5.5 kV. The fragment ions in MRM mode were produced by collision-activated dissociation of selected precursor ions in the collision cell of the triple quadrupole and the selected products analyzed with the second analyzer of the instrument. Three transitions were acquired for the identification of each dansylhydrazone derivative. To establish the appropriate MRM conditions for the individual compounds, the mass spectrometric conditions were optimized using infusion with a syringe pump to select the most suitable ion transitions for the target analytes. Precursor and product ions used for quantification and confirmation purposes, and operating conditions are summarized in **Table 3**.

Table 3. *Optimization of MRM transitions for detection of aldehydes.*

Aldehyde	Monitored transition	DP	FP	EP	CEP	CE	CXP
Formaldehyde-d_2	280.0→156.1	26	360	8	18	47	6
	280.0→115.2	26	360	8	18	67	4
	280.0→171.1	26	360	8	18	31	6
Formaldehyde	278.1→170.1	26	370	10	18	35	6
	278.1→128.1	26	370	10	18	71	4
	278.1→115.2	26	370	10	18	77	4
Propanal	306.2→156.0	26	370	10.5	14	53	6
	306.2→115.1	26	370	10.5	14	71	4
	306.2→171.1	26	370	10.5	14	31	6
2-Pentenal	332.2→156.1	26	370	10	14	55	6
	332.2→171.1	26	370	10	14	37	6
	332.2→115.1	26	370	10	14	79	4
2-Methyl-2-pentenal	346.2→156.1	21	370	6.5	26	57	6
	346.2→171.1	21	370	6.5	26	39	8
	346.2→115.1	21	370	6.5	26	79	6
2,4-Heptadienal	358.1→170.1	21	370	8	16	29	6
	358.1→171.1	21	370	8	16	35	6
	358.1→115.2	21	370	8	16	79	4
Hexanal	348.1→156.1	26	370	10.5	16	61	6
	348.1→115.1	26	370	10.5	16	83	4
	348.1→171.2	26	370	10.5	16	41	6
2-Octenal	374.1→156.1	26	350	11.5	14	61	6
	374.1→171.1	26	350	11.5	14	39	6
	374.1→115.1	26	350	11.5	14	83	4
2,4-Decadienal	400.1→170.0	21	370	10.5	16	33	6
	400.1→171.1	21	370	10.5	16	37	6
	400.1→95.1	21	370	10.5	16	37	6

Abbreviations: DP, declustering potential; FP, focusing potential; EP, entrance potential; CEP, collision cell entrance potential; EC, collision energy; CXP, collision cell exit potential.

Quantification of the different aldehydes was carried out by preparing five standard curves of aldehyde mixtures in 500 μl of the mixture tetrahydrofuran/sodium phosphate buffer, pH 8, and following the whole procedure described above. For each curve, seven different concentration levels of each aldehyde (0–2 nmol) were used. Aldehyde contents were directly proportional to aldehyde/IS area ratios ($r > 0.99$, $p < 0.0001$). All data given are the mean of, at least, three independent experiments.

3.4.1.2. Aldehydes in heated oils.

Aldehydes content in oil samples subjected to deep-frying experiments described in section 3.3.6 was determined by ^{1}H NMR analogously to the analysis of oil components developed by Sopelana et al. (2013). Briefly, oil samples (200 mg) were diluted with $CDCl_3$ (400 μl), which contained 0.2% of nondeuterated chloroform, and their spectra were obtained by ^{1}H NMR, using the analytical conditions described in section 3.2.4. Quantification of the three aldehydes (acrolein, crotonaldehyde, and (*E*)-2-pentenal) was carried out by considering the area of the $CHCl_3$ signal (at δ 7.29 ppm) as internal standard. The proton of the aldehyde group appeared as a doublet that was independent for each one of the three analyzed aldehydes and appeared far from other signals in the spectrum. The signals of the aldehydic proton appeared at δ 9.55 (d, J = 7.4 Hz) for acrolein, 9.47 (d, J = 7.9 Hz) for crotonaldehyde, and 9.49 (d, J = 7.7 Hz) for (*E*)-2-pentenal. Four samples were analyzed for each heated oil and each sample was measured three times. Therefore, the aldehyde content for each analyzed oil was the mean value of 12 determinations.

3.4.2. Determination of carbonyl-phenol adducts.

3.4.2.1. Adducts formed with alkanals.

Alkanal-phenol adducts were determined in the samples prepared according to the procedure described in section 3.3.1 by GC-MS. Working conditions were as follows: carrier gas, helium (1 mL/min at constant flow); injector temperature, 250 °C; transfer line to MSD, 280 °C; ionization EI, 70 eV; ion source temperature, 230 °C. Two oven temperatures were programmed. For acetylated derivatives, the oven temperature was programmed from 100 °C (1 min) to 300 °C at 15 °C/min and, then, 5 min at 300 °C. For nonacetylated derivatives, the oven temperature was programmed from 40 °C (1 min) to 240 °C at 12 °C/min, then to 300 °C at 20 °C/min, and, finally, 5 min at 300 °C. The flow velocities employed were 30 cm/s for acetylated compounds and 37 cm/s for nonacetylated compounds.

Quantification of alkanal-phenol adducts was carried out by preparing standard curves of the isolated adducts in the 515 µl of solution employed in samples prepared in section 3.3.1. Seven different concentration levels were used. Adduct content was directly proportional to the aldehyde/internal standard area ratio ($r > 0.98$, $p < 0.001$). The coefficients of variation were less than 10 %. When one adduct was not available, such as the adducts derived from either orcinol or butanal, the calibration curve used was that of the adduct with the closest chemical structure.

3.4.2.2. Adducts formed with epoxyalkenals.

Epoxyalkenal-phenol adducts were determined in the samples prepared according to the procedure described in section 3.3.2 by GC-MS. The following working conditions were employed: carried gas, helium (0.8 ml/min at constant pressure); injector, 250 °C; oven temperature programmed from 100 °C (1 min) to 300 °C at 15 °C/min and then 5 min at 300 °C;

transfer line to MSD, 280 °C; ionization EI, 70 eV; ion source temperature, 230 °C; mass range 50–550 amu.

The quantification of aldehyde-phenol adducts was carried out by preparing standard curves of the isolated adducts (**20a**, **20b**, **25a**, **25b**) in the reaction between 4,5-epoxy-2-heptenal and 2-methylresorcinol. For each curve, six different concentration levels were used. Adduct content was directly proportional to the adduct/internal standard area ratio ($r > 0.99$, $p < 0.001$). The coefficients of variation were <10%. Because the reaction between 4,5-epoxy-2-heptenal and 2-methylresorcinol produced four isomers of 1-ethyl-8-methyl-3,4,4a,9a-tetrahydro-1*H*-pyrano[3,4-*b*]benzofuran-3,7-diyl diacetates (**25a, 25b, 25c** and **25d**) and only two of them could be isolated and employed for preparing the corresponding standard curves (**25a** and **25b**), the quantification of the other two isomers (**25c**, **25d**) was carried out by employing a calibration curve that was the media of the other two. This approximation should be considered satisfactory because the calibration curves of the adducts **25a** and **25b** were very similar between them.

3.4.2.3. Adducts formed with oxoalkenals.

Oxoalkenal-phenol adducts were determined in the samples prepared according to the procedure described in section 3.3.3 by GC-MS. Working conditions employed were similar to those described in section 3.4.2.2.

Adducts were quantified by preparing standard curves of the isolated adducts (**29-31**) in the reaction between 4-oxo-2-hexenal and 2-methylresorcinol. Six different concentration levels were used. Adduct content was directly proportional to the adduct/internal standard area ratio ($r > 0.99$, $p < 0.001$). The coefficients of variation were <10%.

3.4.2.4. Adducts formed with alkenals in model systems.

Two different methods were used in the determination of aldehyde-quercetin adducts in model systems, prepared according to the procedure described in section 3.3.4.

On the one hand, these adducts were analyzed by MS/MS using direct injection. It was used in order to detect the eluted products in the gel filtration separation carried out using a Sephadex LH-20 column, which was described in section 3.3.4. Working conditions for MS/MS analyses were as follows: the nebulizer gas and the curtain gas were set at 19 and 10 (arbitrary units), respectively. The electrospray capillary voltage was set to −4.5 kV, the declustering potential was −50 V, the focusing potential was −400 V and the entrance potential was −10 V.

In addition, aldehyde-quercetin adducts were analyzed by LC-HRMS, in order to characterize the adducts synthesized as reference compounds. Working conditions were as follows: as eluent A, a mixture of acetonitrile containing 0.2% formic acid and 4 mM ammonium formiate (30/70, v/v) was used. As eluent B, acetonitrile containing 0.2% formic acid was employed. The flow rate was 0.5 mL/min in linear gradient mode: 0−13 min 7% B, 13−20 min from 7 to 60% B, 20−30 min 60% B, 30− 32 min from 60 to 90% B, 32−42 min 90% B, 42−45 min from 90 to 7% B. A split postcolumn with a flow rate of 0.25 mL/min was inserted directly into the mass spectrometer ESI source. The scan range applied was *m/z* 50−1500 and mass resolving power was always over 18,000 ($m/\Delta m$). The instrument was operated in the negative ion mode. Mass spectra and data were obtained by broadband Collision Induced Dissociation (bbCID) mode, providing MS and MS/MS spectra simultaneously. Collision energy was estimated dynamically based on appropriate values for the mass and stepped across a ± 10% magnitude range to ensure good quality fragmentation spectra. The instrument control was performed using Compass 1.3 for micrOTOF-QII + Focus Option Version 3.0 (Bruker Daltonics).

3.4.2.5. Adducts formed with alkenals in fried onions.

Aldehyde-quercetin adducts were analyzed by LC-HRMS, in order to detect their presence in onions fried in the laboratory and commercially prepared crispy fried onions. Fried onion samples were prepared for their analysis according to the procedure described in section 3.3.6. Working conditions for LC-HRMS analyses were similar to those described in section 3.4.2.4.

3.5. Statistical analyses.

All quantitative data given are mean ± standard deviation (SD) values of, at least, three independent experiments. Statistical comparisons among different groups were made using analysis of variance. When significant *F* values were obtained, group differences were evaluated by the Tukey test (Snedecor & Cochran, 1980). Statistical differences among the amounts of aldehydes remaining in the oils after heating in the presence or in the absence of onions were evaluated by the Student *t*-test. Statistical comparisons were carried out using Origin® v. 7.0 (OriginLab Corporation, Northampton, MA). The significance level is $p < 0.05$ unless otherwise indicated.

4. RESULTS

This part will describe the reaction between phenolic compounds and alkanals (section 4.1), epoxyalkenals (section 4.2), and oxoalkenals (section 4.3). In addition, the thermal decomposition suffered by unsaturated aldehydes was also investigated to understand the complex mixtures of carbonyl-phenol adducts formed in the reaction between phenolics and lipid-derived unsaturated aldehydes (section 4.4). Finally, section 4.5 will be dedicated to the study of the presence of carbonyl-phenol adducts in food products. Besides, sections 4.1 to 4.3 have been divided into different subsections to try to achieve the specific objectives proposed in section 2. Thus, the isolation and characterization of the formed carbonyl-phenol adducts will be firstly discussed. Then, the role of reaction conditions on the formation of carbonyl-phenol adducts will be analyzed. Finally, the SAR of both phenolics and carbonyl compounds for these reactions will be examined. The reaction pathways proposed for the formation of the different carbonyl-phenol adducts will be discussed in the Discussion section.

4.1. Alkanal-trapping ability of phenolic compounds.

This section firstly describes the reaction of lipid-derived flavor-relevant alkanals and phenolic compounds. In addition, reactions with glyoxal are also reported for comparison purposes. The carbonyl-phenol adducts produced in the different reactions were isolated and characterized by NMR and MS. Because a large number of alkanals are available, in addition to the isolation and characterization of the formed products, the SAR of both phenolics and carbonyl compounds for these reactions were also investigated.

4.1.1. Characterization of the adducts produced in the reaction between alkanals and phenolic compounds.

Two kinds of studies were carried out. Firstly, a reaction mixture between pentanal and 2-methylresorcinol was acetylated and fractionated by column chromatography to isolate products and intermediates that could be employed to identify the reaction pathway by which the reaction is produced. The results obtained in this study will be presented in subsection 4.1.1.1. Secondly, the adducts formed in the reaction among a wide variety of saturated aldehydes and phenolics were isolated and characterized in order to obtain standards that could be employed in the studies of SAR. These results will be described in subsection 4.1.1.2.

4.1.1.1. Compounds isolated and characterized in the reaction of pentanal and 2-methylresorcinol after acetylation of the reaction mixture.

In order to determine the different compounds produced between alkanals and phenolic compounds, a preliminary study between pentanal and 2-methylresorcinol was carried out. In this study, a mixture of pentanal and 2-methylresorcinol in methanol was heated under nitrogen for 72 h at 60 ºC. Afterwards, reaction products were stabilized by acetylation to avoid both reaction reversion and further polymerizations. Thus, the different adducts produced could be identified by GC-MS previously to be isolated by column chromatography and characterized by NMR and MS. The total ion chromatogram obtained by GC-MS of the reaction mixture is shown in **Figure 40**.

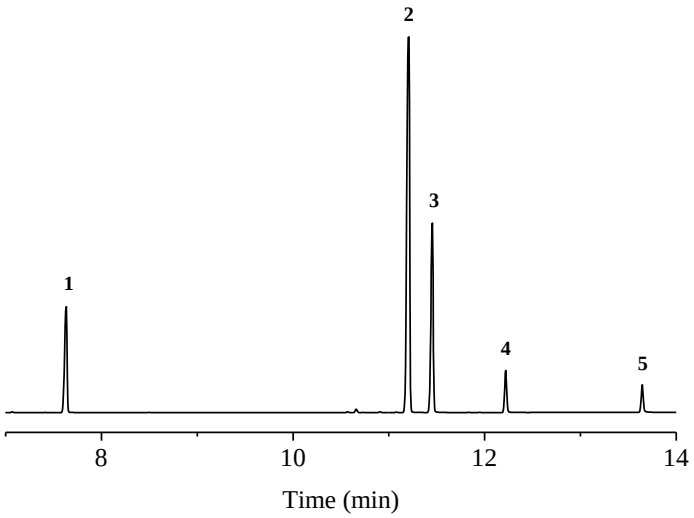

Figure 40. *Total ion chromatogram obtained by GC-MS of the reaction between pentanal and 2-methylresorcinol after acetylation. Only the portion corresponding to the phenolic and epoxyalkenal/phenol adducts is shown. Chemical structures for the identified compounds are given in* ***Figure 41***.

Compound **1** was the product of acetylation of 2-methylresorcinol (2-methyl-1,3-phenylene diacetate). The other compounds were isolated by column chromatography and characterized by 1D and 2D NMR and MS. Their structures are shown in **Figure 41**.

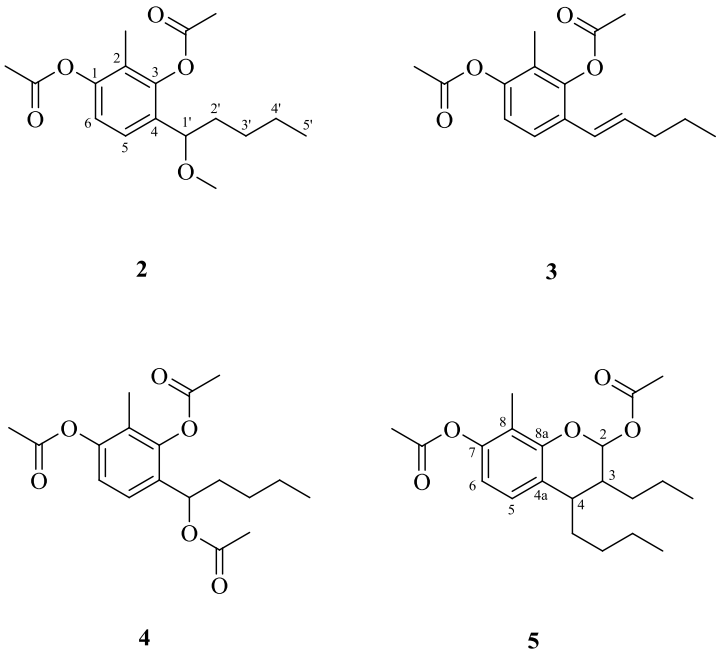

***Figure 41**. Chemical structures of the compounds isolated and characterized by NMR and MS in the reaction between pentanal and 2-methylresorcinol.*

The chromatographic, spectroscopic, and spectrometric data of the isolated and characterized compounds are the following:

4-(1-Methoxypentyl)-2-methyl-1,3-phenylene diacetate (**2**). Yield: 13.8%. Retention time: 11.21 min. ^{1}H NMR ($CDCl_3$): δ (ppm) 0.90t (3H, *J* = 7.1 Hz, H5'), 1.29m and 1.41m (2H, H3'), 1.32m (2H, H4'), 1.62m and 1.75m (2H, H2'), 1.98s (3H, CH_3C2), 2.33s (3H, CH_3CO), 2.33s (3H, CH_3CO), 3.17s (3H, CH_3O), 4.15dd (1H, *J* = 5.0 Hz, *J* = 8.0 Hz, H1'), 7.00d (1H, *J* = 8.1 Hz, H6), and 7.26d (1H, *J* = 8.1 Hz, H5). ^{13}C NMR ($CDCl_3$): δ (ppm) 10.11 ($\underline{C}H_3$C2), 13.97 (C5'), 20.74 ($\underline{C}H_3$CO), 20.79 ($\underline{C}H_3$CO), 22.52 (C4'), 28.07 (C3'), 36.63 (C2'), 56.97 (CH_3O), 79.05 (C1'), 119.93 (C6), 123.66 (C2), 124.97 (C5), 132.36 (C4), 148.03 (C3), 148.89 (C1), 168.89 (CO), and 168.92 (CO). MS, *m/z* (%, ion structure): 308 (0.02, M^+), 277 (0.02,

$M^+ - CH_3O$), 265 (3, $M^+ - CH_3CO$), 251 (50, $M^+ - CH_3CH_2CH_2$), 234 (19, $C_{13}H_{14}O_4$), 209 (76, 251 – CH_2CO), 192 (70, 234 – CH_2CO), and 167 (100, 209 – CH_2CO).

2-Methyl-4-(pent-1-en-1-yl)-1,3-phenylene diacetate (**3**). Yield: 5.2%. Retention time: 11.46 min. ^{1}H NMR ($CDCl_3$): δ (ppm) 0.96t (3H, *J* = 7.3 Hz, H5'), 1.50sx (2H, *J* = 7.3 Hz, H4'), 1.99s (3H, CH_3C2), 2.20qd (2H, *J* = 7.3 Hz, *J* = 1.2 Hz, H3'), 2.33s (3H, CH_3CO), 2.37s (3H, CH_3CO), 6.18dt (1H, *J* = 15.8 Hz, *J* = 6.8 Hz, H2'), 6.31d (1H, *J* = 15.8 Hz, H1'), 6.94d (1H, *J* = 8.5 Hz, H6), and 7.37d (1H, *J* = 8.5 Hz, H5). ^{13}C NMR ($CDCl_3$): δ (ppm) 10.11 ($\underline{C}H_3$C2), 13.64 (C5'), 20.49 ($\underline{C}H_3CO$), 20.80 ($\underline{C}H_3CO$), 22.38 (C4'), 35.37 (C3'), 119.83 (C6), 123.10 (C1'), 123.55 (C2), 123.94 (C5), 128.83 (C4), 133.85 (C2'), 146.94 (C3), 148.50 (C1), 168.58 (CO), and 169.03 (CO). MS, *m/z* (%, ion structure): 276 (17, M^+), 234 (38, $M^+ - CH_2CO$), 192 (100, 234 – CH_2CO), and 163 (97, 192 – CH_3CH_2).

4-(1-Acetoxypentyl)-2-methyl-1,3-phenylene diacetate (**4**). Yield: 3.2%. Retention time: 12.22 min. ^{1}H NMR ($CDCl_3$): δ (ppm) 0.90t (3H, *J* = 7.1 Hz, H5'), 1.24m and 1.34m (2H, H3'), 1.34m (2H, H4'), 1.79m and 1.92m (2H, H2'), 1.98s (3H, CH_3C2), 2.04s (3H, $\underline{C}H_3$COOC1'), 2.34s (3H, CH_3CO), 2.38s (3H, CH_3CO), 5.87br (1H, H1'), 6.99d (1H, *J* = 8.4 Hz, H6), and 7.29d (1H, *J* = 8.4 Hz, H5). ^{13}C NMR ($CDCl_3$): δ (ppm) 10.24 ($\underline{C}H_3$C2), 13.90 (C5'), 20.59 ($\underline{C}H_3$COOC1), 20.82 ($\underline{C}H_3CO$), 21.06 ($\underline{C}H_3CO$), 22.34 (C4'), 27.78 (C3'), 34.44 (C2'), 70.95 (C1'), 119.92 (C6), 124.17 (C2), 125.43 (C5), 130.46 (C4), 147.77 (C3), 149.41 (C1), 168.60 (CO), and 168.86 (CO). MS, *m/z* (%, ion structure): 336 (0.2, M^+), 277 (1, $M^+ - CH_3COO$), 276 (0.4, $M^+ - CH_3COOH$), 234 (16, 276 – CH_2CO), 192 (100, 234 – CH_2CO), and 163 (62, 192 – CH_3CH_2).

4-Butyl-8-methyl-3-propylchroman-2,7-diyl diacetate (**5**). Yield: 2.9%. Retention time: 13.65 min. ^{1}H NMR ($CDCl_3$): δ (ppm) 0.92t (3H, *J* = 7.2 Hz, $C\underline{H}_3CH_2$), 0.95t (3H, *J* = 7.0 Hz, $C\underline{H}_3CH_2$), 1.4m (8H, $CH_3C\underline{H}_2$, $CH_3C\underline{H}_2$, $CH_3CH_2C\underline{H}_2$, and $CH_3CH_2C\underline{H}_2$), 2.02s (3H, CH_3C8), 2.06s (3H, CH_3CO), 2.33s (3H, CH_3CO), 2.55dd (1H, *J* = 5.5 Hz and *J* = 9.9 Hz, H3), 2.80dt (2H, *J* = 5.3 Hz and *J* = 7.7 Hz, C<u>H</u>2C4), 2.95dt (1H, *J* = 4.8 Hz and *J* = 7.5 Hz, H4), 6.37dd (1H, *J* = 1.3 Hz and *J* = 1.9 Hz, H2), 6.67d (1H, *J* = 8.3 Hz, H6), and 6.98d (1H, *J* = 8.3 Hz, H7). ^{13}C NMR ($CDCl_3$): δ (ppm) 9.23 (CH_3C8), 14.01 ($\underline{C}H_3CH_2$), 14.23 ($\underline{C}H_3CH_2$), 20.13 ($CH_3\underline{C}H_2$), 20.83 (CH_3CO), 21.19 (CH_3CO), 23.01 ($CH_3\underline{C}H_2$), 27.48 ($CH_3CH_2\underline{C}H_2$), 29.97 ($CH_3CH_2\underline{C}H_2$), 33.83 (C4), 36.72 ($\underline{C}H_2$C4), 37.45 (C3), 93.90 (C2), 114.86 (C6), 118.60 (C8), 122.55 (C4a), 127.31 (C5), 148.54 (C7), 150.45 (C8a), 169.35 (CO), and 169.64 (CO). MS, *m/z* (%, ion structure): 362 (7, M^+), 320 (8, $M^+ - CH_2CO$), 303 (3, $M^+ - CH_2COO$), 302 (1, $M^+ - CH_2COOH$), 260 (9, 302 – propene), 259 (22, 302 – $CH_3CH_2CH_2$), 245 (19, 302 – $CH_3CH_2CH_2CH_2$), 217 (32, 260 – $CH_3CH_2CH_2$), and 203 (100, 260 – $CH_3CH_2CH_2CH_2$).

4.1.1.2. <u>Compounds isolated and characterized in the different alkanal/phenolic compound reaction mixtures assayed.</u>

In order to prepare the adducts needed for the SAR studies, a number of reactions involving different saturated aldehydes and phenolic compounds were carried out and the corresponding carbonyl-phenol adducts were analyzed and characterized. Thus, the adducts produced in the reactions between propanal, 2-methylbutanal, pentanal and hexanal with resorcinol were isolated and characterized. In the same way, the adducts produced in the reactions between propanal, 2-methylbutanal, 3-metilbutanal, pentanal and hexanal with 2-methylresorcinol were isolated and characterized as well.

Furthermore, analogous reactions between glyoxal and resorcinol or 2-methylresorcinol, and the reaction between resorcinol and 2-methyl-2-pentenal were also studied for comparison purposes.

Reactions were carried out analogously to the reaction between pentanal and 2-methylresorcinol discussed in subsection 4.1.1.1, but formed compounds were isolated without acetylation. In all studied reactions, only major reaction products were isolated and characterized. **Figure 42** shows the adducts isolated in the different assayed reactions.

The chromatographic, spectroscopic, and spectrometric data of the isolated and characterized compounds are the following:

The reaction between resorcinol and propanal produced *4-(1-methoxypropyl)benzene-1,3-diol* (**6**). The reaction was heated for 48 h at 60 ºC and compound **6** was isolated using hexane-diethyl ether (7:3) as eluent. Retention time: 18.18 min. ^{1}H NMR (CD_3OD): δ (ppm) 0.88t (3H, *J* = 7.5 Hz, H3'), 1.67m and 1.77m (2H, H2'), 3.22s (3H, CH_3O), 4.42t (1H, *J* = 6.7 Hz, H1'), 6.29d (1H, *J* = 2.3 Hz, H2), 6.31dd (1H, *J* = 2.3 Hz, *J* = 8.2 Hz, H6), and 6.96d (1H, *J* = 8.2 Hz, H5). ^{13}C NMR (CD_3OD): δ (ppm) 9.15 (C3'), 28.98 (C2'), 55.24 (CH_3O), 80.31 (C1'), 102.07 (C2), 106.39 (C6), 118.25 (C4), 127.61 (C5), 156.17 (C3), and 157.21 (C1). MS, *m/z* (%, ion structure): 150 (100, $M^+ - CH_3OH$), 133 (19, 150 – OH), and 123 (36, $C_7H_7O_2$).

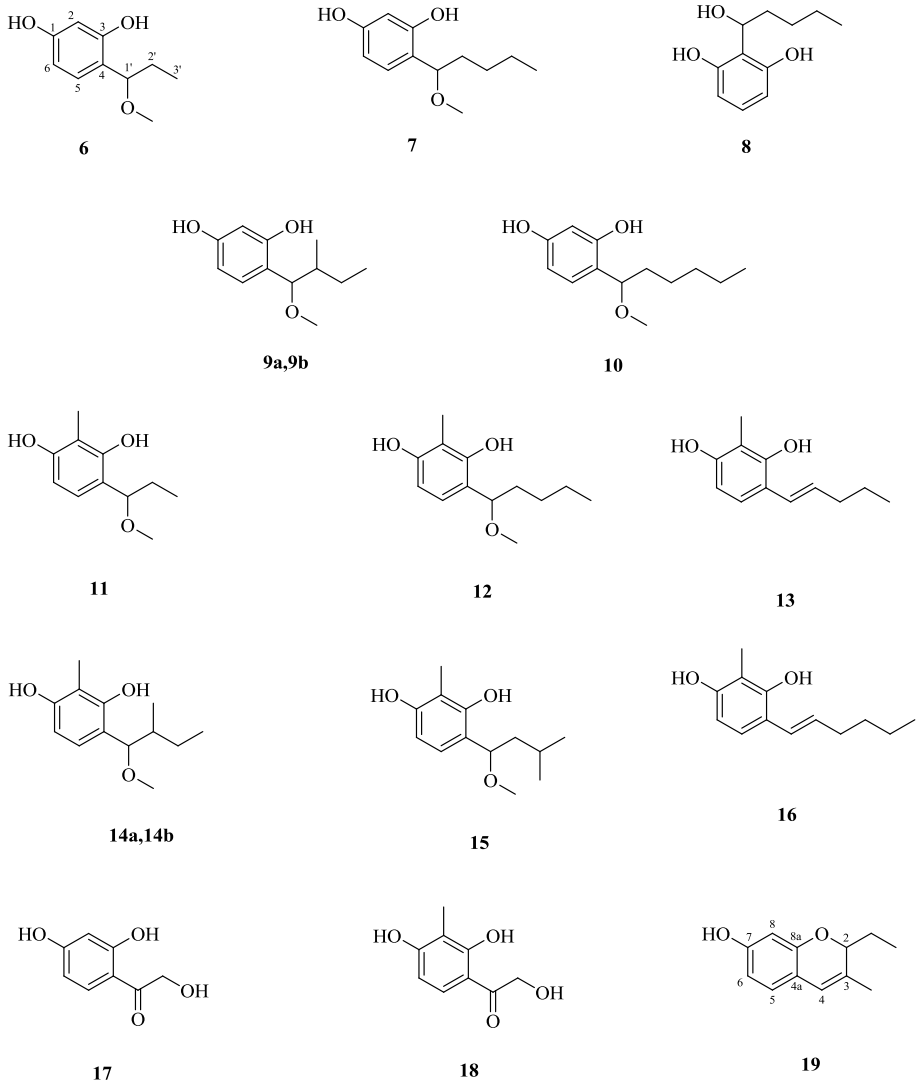

Figure 42. *Chemical structures of the carbonyl-phenol adducts isolated and characterized by NMR and MS in the different assayed reactions between alkanals and phenolics. The aldehyde and the phenolic compound involved in the formation of each adduct is described in the text.*

The reaction between resorcinol and pentanal produced *4-(1-methoxypentyl)benzene-1,3-diol* (**7**) and *2-(1-hydroxypentyl)benzene-1,3-diol*

(**8**). The reaction was heated for 72 h at 60 ºC and the compounds were isolated using hexane-diethyl ether (3:1) as eluent. Retention time of compound **7**: 20.04 min. Retention time of compound **8**: 18.87 min. ^{1}H NMR (CD_3OD) of compound **7**: δ (ppm) 0.90t (3H, *J* = 7.2 Hz, H5'), 1.35m (4H, H3' and H4'), 1.65m and 1.75m (2H, H2'), 3.21s (3H, CH_3O), 4.50t (1H, *J* = 6.6 Hz, H1'), 6.28d (1H, *J* = 2.4 Hz, H2), 6.31dd (1H, *J* = 2.4 Hz, *J* = 8.2 Hz, H6), and 6.96d (1H, *J* = 8.2 Hz, H5). ^{13}C NMR (CD_3OD) of compound **7**: δ (ppm) 13.02 (C5'), 22.26 (C4'), 27.73 (C3'), 35.92 (C2'), 55.14 (CH_3O), 78.31 (C1'), 102.03 (C2), 106.40 (C6), 118.55 (C4), 127.52 (C5), 156.14 (C3), and 157.20 (C1). MS of compound **7**, *m/z* (%, ion structure): 178 (38, M^+ – CH_3OH), and 149 (100, 178 – CH_3CH_2). ^{1}H NMR (CD_3OD) of compound **8**: δ (ppm) 0.92t (3H, *J* = 7.2 Hz, H5'), 1.36m (2H, H4'), 1.36m and 1.49m (2H, H3'), 1.78m and 1.81m (2H, H2'), 5.22dd (1H, *J* = 5.4 Hz, *J* = 7.7 Hz, H1'), 6.27d (2H, *J* = 8.1 Hz, H4 and H6), and 6.87t (1H, *J* = 8.1 Hz, H5). ^{13}C NMR (CD_3OD) of compound **8**: δ (ppm) 13.03 (C5'), 22.27 (C4'), 27.48 (C3'), 36.17 (C2'), 68.95 (C1'), 106.76 (C4 and C6), 115.54 (C2), 127.54 (C5), and 155.72 (C1 and C3). MS of the dehydrated product formed from compound **8**, *m/z* (%, ion structure): 178 (48, M^+), 149 (100, M^+ – CH_3CH_2), and 123 (56, $C_7H_7O_2$).

The reaction between resorcinol and 2-methylbutanal produced *4-(1-methoxy-2-methylbutyl)benzene-1,3-diol* (**9a** and **9b**). This compound has two chiral centers at C1' and C2'. Therefore, it was produced as two pairs of diastereomers, which have been named **9a** and **9b**. Their retention times were 18.64 and 18.86 min. The reaction was heated for 48 h at 60 ºC and the compounds were isolated using hexane-diethyl ether (7:3) as eluent. ^{1}H NMR (CD_3OD) of compound **9a**: δ (ppm) 0.73d (3H, *J* = 6.9 Hz, CH_3C2'), 0.92t (3H, *J* = 7.5 Hz, C4'), 1.21m and 1.76m (2H, H3'), 1.73m (2H, H2'), 3.19s (3H, CH_3O), 4.24d (1H, *J* = 7.8 Hz, H1'), 6.28d (1H, *J* = 2.4 Hz, H2), 6.32dd (1H, *J* = 2.4 Hz, *J* = 8.2 Hz, H6), and 6.92d (1H, *J* = 8.2 Hz, H5). ^{13}C NMR

(CD_3OD) of compound **9a**: δ (ppm) 10.19 (C4'), 14.26 (CH_3C2'), 24.98 (C3'), 40.21 (C2'), 55.44 (CH_3O), 83.13 (C1'), 101.93 (C2), 106.16 (C6), 117.37 (C4), 128.46 (C5), 156.60 (C3), and 157.09 (C1). MS of compound **9a**, *m/z* (%, ion structure): 178 (100, $M^+ - CH_3OH$), 163 (71, 178 – CH_3), 149 (84, 178 – CH_3CH_2), and 123 (75, $C_7H_7O_2$). ^{1}H NMR (CD_3OD) of compound **9b**: δ (ppm) 0.86t (3H, *J* = 7.5 Hz, C4'), 0.95d (3H, *J* = 6.7 Hz, CH_3C2'), 1.10m and 1.37m (2H, H3'), 1.73m (2H, H2'), 3.20s (3H, CH_3O), 4.28d (1H, *J* = 6.9 Hz, H1'), 6.28d (1H, *J* = 2.4 Hz, H2), 6.32dd (1H, *J* = 2.4 Hz, *J* = 8.2 Hz, H6), and 6.93d (1H, *J* = 8.2 Hz, H5). ^{13}C NMR (CD_3OD) of compound **9b**: δ (ppm) 10.51 (C4'), 13.90 (CH_3C2'), 25.53 (C3'), 40.18 (C2'), 55.60 (CH_3O), 82.98 (C1'), 101.96 (C2), 106.26 (C6), 117.54 (C4), 128.26 (C5), 156.40 (C3), and 157.17 (C1). MS of compound **9b**, *m/z* (%, ion structure): 178 (100, $M^+ - CH_3OH$), 163 (80, 178 – CH_3), 149 (95, 178 – CH_3CH_2), and 123 (81, $C_7H_7O_2$).

The reaction between resorcinol and hexanal produced *4-(1-methoxyhexyl)benzene-1,3-diol* (**10**). The reaction was heated for 3 h at 100 ºC and compound **10** was isolated using hexane-diethyl ether (75:25) as eluent. Retention time: 12.08 min. ^{1}H NMR (CD_3OD): δ (ppm) 0.88t (3H, *J* = 6.9 Hz, H6'), 1.27m (6H, H3', H4', and H5'), 1.66m (2H, H2'), 3.21s (3H, CH_3O), 4.48t (1H, *J* = 6.7 Hz, H1'), 6.26dd (1H, *J* = 2.5 Hz, *J* = 8.1 Hz, H6), 6.30d (1H, *J* = 2.5 Hz, H2), and 6.94d (1H, *J* = 8.1 Hz, H5). ^{13}C NMR (CD_3OD): δ (ppm) 14.40 (C6'), 23.70 (C5'), 26.58 (C4'), 32.94 (C3'), 37.62 (C2'), 56.51 (CH_3O), 79.93 (C1'), 103.33 (C6), 107.74 (C2), 119.93 (C4), 128.82 (C5), 157.55 (C3), and 158.60 (C1). MS, *m/z* (%, ion structure): 192 (34, $M^+ - CH_3OH$), 163 (2, 192 – CH_3CH_2), and 149 (100, 192 – $CH_3CH_2CH_2$).

The reaction between 2-methylresorcinol and propanal produced *4-(1-methoxypropyl)-2-methylbenzene-1,3-diol* (**11**). The reaction was heated for 72 h at 60 ºC and compound **11** was isolated using hexane-diethyl ether (9:1)

as eluent. Retention time: 18.52 min. ^{1}H NMR (CD_3OD): δ (ppm) 0.88t (3H, *J* = 7.5 Hz, H3'), 1.68m and 1.83m (2H, H2'), 2.07s (3H, CH_3C2), 3.29s (3H, CH_3O), 4.23t (1H, *J* = 6.9 Hz, H1'), 6.33d (1H, *J* = 8.2 Hz, H6), and 6.96d (1H, *J* = 8.2 Hz, H5). ^{13}C NMR (CD_3OD): δ (ppm) 7.08 ($\underline{C}H_3C2$), 9.32 (C3'), 28.84 (C2'), 55.60 (CH_3O), 80.81 (C1'), 106.04 (C6), 111.36 (C2), 116.85 (C4), 125.02 (C5), 153.92 (C3), and 155.41 (C1). MS, *m/z* (%, ion structure): 164 (100, $M^+ - CH_3OH$), 149 (42, 164 – CH_3), 147 (17, 164 – OH), and 137 (20, $C_8H_9O_2$).

The reaction between 2-methylresorcinol and pentanal produced *4-(1-methoxypentyl)-2-methylbenzene-1,3-diol* (**12**) and 2-methyl-4-(pent-1-en-1-yl)benzene-1,3-diol (**13**). The reaction was heated for 72 h at 60 ºC and the compounds were isolated using hexane-diethyl ether (85:15) as eluent. Retention time of compound **12**: 20.28 min. Retention time of compound **13**: 20.38 min. ^{1}H NMR (CD_3OD) of compound **12**: δ (ppm) 0.89t (3H, *J* = 7.2 Hz, H5'), 1.23m and 1.38m (2H, H3'), 1.31m (2H, H4'), 1.65m and 1.82m (2H, H2'), 2.08s (3H, CH_3C2), 3.28s (3H, CH_3O), 4.31t (1H, *J* = 6.9 Hz, H1'), 6.33d (1H, *J* = 8.2 Hz, H6), and 6.69d (1H, *J* = 8.2 Hz, H5). ^{13}C NMR (CD_3OD) of compound **12**: δ (ppm) 7.09 (CH_3C2), 13.04 (C5'), 22.23 (C4'), 27.84 (C3'), 35.72 (C2'), 55.52 (CH_3O), 83.31 (C1'), 106.05 (C6), 111.36 (C2), 117.15 (C4), 124.89 (C5), 153.89 (C3), and 155.41 (C1). MS of compound **12**, *m/z* (%, ion structure): 192 (36, $M^+ - CH_3OH$), and 163 (100, 192 – CH_3CH_2). ^{1}H NMR (CD_3OD) of compound **13**: δ (ppm) 0.95t (3H, *J* = 7.4 Hz, H5'), 1.50sx (2H, *J* = 7.4 Hz, H4'), 2.08s (3H, CH_3C2), 2.18qd (2H, *J* = 1.4 Hz, *J* = 7.2 Hz, H3'), 5.98dt (1H, *J* = 7.2 Hz, *J* = 15.7 Hz, H2'), 6.33d (1H, *J* = 8.4 Hz, H6), 6.63d (1H, *J* = 15.7 Hz, H1'), and 7.03d (1H, *J* = 8.4 Hz, H5). ^{13}C NMR (CD_3OD) of compound **13**: δ (ppm) 7.48 (CH_3C2), 12.74 (C5'), 22.62 (C4'), 35.27 (C3'), 106.98 (C6), 111.33 (C2), 117.90 (C4), 123.04 (C5), 125.02 (C1'), 127.45 (C2'), 152.39 (C3), and 154.86 (C1). MS

of compound **13**, *m/z* (%, ion structure): 192 (35, M^+), and 163 (100, M^+ – CH_3CH_2).

The reaction between 2-methylresorcinol and 2-methylbutanal produced *4-(1-methoxy-2-methylbutyl)-2-methylbenzene-1,3-diol* (**14a** and **14b**). Analogously to compounds **9a** and **9b**, this compound also has two chiral centers at C1' and C2'. Therefore, it was produced as two pairs of diastereomers, which have been named **14a** and **14b**. Their retention times were 19.05 and 19.27 min. The reaction was heated for 72 h at 60 ºC and the compounds were isolated using hexane-diethyl ether (85:15) as eluent. ^{1}H NMR (CD_3OD) of compound **14a**: δ (ppm) 0.71d (3H, *J* = 6.9 Hz, CH_3C2'), 0.84t (3H, *J* = 7.4 Hz, C4'), 1.20m and 1.80m (2H, H3'), 1.79m (1H, H2'), 2.07s (3H, CH_3C2), 3.28s (3H, CH_3O), 4.01d (1H, *J* = 8.1 Hz, H1'), 6.32d (1H, *J* = 8.2 Hz, H6), and 6.65d (1H, *J* = 8.2 Hz, H5). ^{13}C NMR (CD_3OD) of compound **14a**: δ (ppm) 7.09 (CH_3C2), 10.52 (C4'), 14.60 (CH_3C2'), 25.10 (C3'), 39.78 (C2'), 55.99 (CH_3O), 88.17 (C1'), 105.79 (C6), 111.23 (C2), 115.60 (C4), 126.11 (C5), 154.22 (C3), and 154.33 (C1). MS of compound **14a**, *m/z* (%, ion structure): 192 (82, M^+ – CH_3OH), 177 (48, 192 – CH_3), 163 (100, 192 – CH_3CH_2), and 137 (49, $C_8H_9O_2$). ^{1}H NMR (CD_3OD) of compound **14b**: δ (ppm) 0.92t (t, 3H, *J* = 6.9 Hz, C4'), 0.99d (d, 3H, *J* = 6.7 Hz, CH_3C2'), 1.05m and 1.30m (2H, H3'), 1.72m (1H, H2'), 2.07s (3H, CH_3C2), 3.29s (3H, CH_3O), 4.07d (1H, *J* = 7.5 Hz, H1'), 6.33d (1H, *J* = 8.2 Hz, H6), and 6.66d (1H, *J* = 8.2 Hz, H5). ^{13}C NMR (CD_3OD) of compound **14b**: δ (ppm) 7.09 (CH_3C2), 10.16 (C4'), 14.15 (CH_3C2'), 25.65 (C3'), 40.39 (C2'), 56.12 (CH_3O), 87.98 (C1'), 105.87 (C6), 111.23 (C6), 115.83 (C4), 125.88 (C5), 154.17 (C3), and 155.41 (C1). MS of compound **14b**, *m/z* (%, ion structure): 192 (90, M^+ – CH_3OH), 177 (45, 192 – CH_3), 163 (100, 192 – CH_3CH_2), and 137 (49, $C_8H_9O_2$).

The reaction between 2-methylresorcinol and 3-methylbutanal produced *4-(1-methoxy-3-methylbutyl)-2-methylbenzene-1,3-diol* (**15**). The

reaction was heated for 48 h at 60 ºC and compound **15** was isolated using hexane-diethyl ether (85:15) as eluent. Retention time: 19.97 min. ^{1}H NMR (CD_3OD): δ (ppm) 0.92d (3H, *J* = 6.6 Hz, C4'), 0.94d (3H, *J* = 6.6 Hz, CH_3C3'), 1.46m and 1.76m (2H, H3'), 1.67hp (1H, *J* = 6.6 Hz, H3'), 2.08s (3H, CH_3C2), 3.27s (3H, CH_3O), 4.42dd (1H, *J* = 6.0 Hz, *J* = 8.2 Hz, H1'), 6.34d (1H, *J* = 8.2 Hz, H6), and 6.71d (1H, *J* = 8.2 Hz, H5). ^{13}C NMR (CD_3OD): δ (ppm) 7.09 (CH_3C2), 21.42 (CH_3C3'), 22.07 (C4'), 24.53 (C3'), 45.26 (C2'), 55.43 (CH_3O), 81.33 (C1'), 106.14 (C6), 111.40 (C2), 117.45 (C4), 124.70 (C5), 153.92 (C3), and 155.41 (C1). MS, *m/z* (%, ion structure): 192 (67, $M^+ - CH_3OH$), 177 (83, 192 – CH_3), 175 (19, 192 – OH), and 137 (100, $C_8H_9O_2$).

The reaction between 2-methylresorcinol and hexanal produced *4-(hex-1-en-1-yl)-2-methylbenzene-1,3-diol* (**16**). The reaction was heated for 24 h at 100 ºC and compound **16** was isolated using hexane-diethyl ether (80:20) as eluent. Retention time: 13.55 min. ^{1}H NMR (CD_3OD): δ (ppm) 0.93t (3H, *J* = 7.3 Hz, H6'), 1.40m (4H, H4' and H5'), 2.06s (3H, CH_3C2), 2.18qd (2H, *J* = 1.5 Hz, *J* = 7.1 Hz, H3'), 5.96dt (1H, *J* = 7.1 Hz, *J* = 15.7 Hz, H2'), 6.32d (1H, *J* = 8.3 Hz, H6), 6.60dt (1H, *J* = 1.5 Hz, 15.7 Hz, H1'), and 7.01d (1H, *J* = 8.3 Hz, H5). ^{13}C NMR (CD_3OD): δ (ppm) 8.87 (CH_3C2), 14.39 (C6'), 23.36 (C5'), 33.16 (C4'), 34.21 (C3'), 108.29 (C6), 112.61 (C2), 119.26 (C4), 124.36 (C5), 126.15 (C1'), 128.93 (C2'), 153.72 (C3), and 156.19 (C1). MS, *m/z* (%, ion structure): 206 (39, M^+), 191 (1, $M^+ - CH_3$), 177 (100, $M^+ - CH_3CH_2$), 163 (100, $M^+ - CH_3CH_2CH_2$), and 137 (19, $C_8H_9O_2$).

The reaction between resorcinol and glyoxal produced *1-(2,4-dihydroxyphenyl)-2-hydroxyethan-1-one* (**17**). The reaction, using a glyoxal-resorcinol ratio of 4:1, was heated for 3 h at 100 ºC and compound **17** was isolated using hexane-diethyl ether (1:3) as eluent. Retention time: 12.18 min. ^{1}H NMR (CD_3OD): δ (ppm) 4.80s (2H, CH_2OH), 6.28d (1H, *J* = 2.3 Hz, H2), 6.35dd (1H, *J* = 2.3 Hz, *J* = 8.7 Hz, H6), and 7.59d (1H, *J* = 8.7 Hz, H5). ^{13}C

NMR (CD_3OD): δ (ppm) 65.21 (CH_2OH), 103.70 (C2), 109.39 (C6), 111.84 (C4), 132.15 (C5), 165.80 (C3), 166.53 (C1), and 202.57 (CO). MS, *m/z* (%, ion structure): 168 (15, M^+), and 137 (100, $M^+ - CH_2OH$).

The reaction between 2-methylresorcinol and glyoxal produced *1-(2,4-dihydroxy-3-methylphenyl)-2-hydroxyethan-1-one* (**18**). The reaction, using a glyoxal-2-methylresorcinol ratio of 4:1, was heated for 3 h at 100 ºC and compound **18** was isolated using hexane-diethyl ether (2:5) as eluent. Retention time: 12.57 min. ^{1}H NMR (CD_3OD): δ (ppm) 2.01s (3H, CH_3C2), 4.78s (2H, CH_2OH), 6.35d (1H, *J* = 8.8 Hz, H6), and 7.36d (1H, *J* = 8.8 Hz, H5). ^{13}C NMR (CD_3OD): δ (ppm) 7.54 ($\underline{C}H_3C2$), 64.72 (CH_2OH), 108.24 (C6), 111.15 (C4), 112.43 (C2), 128.56 (C5), 163.59 (C3), 166.98 (C1), and 202.70 (CO). MS, *m/z* (%, ion structure): 182 (15, M^+), and 151 (100, $M^+ - CH_2OH$).

The reaction between resorcinol and 2-methyl-2-pentenal produced *2-ethyl-3-methyl-2H-chromen-7-ol* (**19**). The reaction was heated for 72 h at 100 ºC and compound **19** was isolated using hexane-diethyl ether (3:1) as eluent. Retention time: 11.65 min. ^{1}H NMR (CD_3OD): δ (ppm) 0.99t (3H, *J* = 7.3 Hz, $C\underline{H}_3CH_2$), 1.65m (2H, CH_2C2), 1.78s (3H, CH_3C3), 4.49dd (1H, *J* = 3.8 Hz, *J* = 7.7 Hz, H2), 6.07s (1H, H4), 6.19d (1H, *J* = 2.7 Hz, H8), 6.24dd (1H, *J* = 2.7 Hz, *J* = 8.0 Hz, H6), and 6.70d (1H, *J* = 8.5 Hz, H5). ^{13}C NMR (CD_3OD): δ (ppm) 9.92 ($\underline{C}H_3CH_2$), 19.55 (CH_3C3), 26.73 (CH_2C2), 81.19 (C2), 103.87 (C8), 108.68 (C6), 116.42 (C4a), 119.99 (C4), 127.19 (C5), 131.61 (C3), 154.12 (C8a), and 158.78 (C7). MS, *m/z* (%, ion structure): 190 (12, M^+), and 161 (100, $M^+ - CH_3CH_2$).

Comparative mass spectral data for all these compounds are given in **Table 4**.

Table 4. *Selected Mass Spectral Data of Compounds 6–19*[a].

Compound	Ion structure				
	M^+	$M^+ - CH_3OH$	$M^+ - CH_3OH - R$	$M^+ - CH_2OH$	$M^+ - R$
6		150 (100)			
7		178 (38)	149 (100)		
8[b]		178 (48)	149 (100)		
9a		178 (100)	163 (71)		
9b		178 (100)	163 (80)		
10		192 (34)	149 (100)		
11		164 (100)			
12		192 (36)	163 (100)		
13	192 (35)				163 (100)
14a[c]		192 (82)	177 (48)		
14b[c]		192 (90)	177 (45)		
15		192 (67)	177 (83)		
16	206 (39)				163 (100)
17	168 (15)			137 (100)	
18	182 (15)			151 (100)	
19	190 (12)				161 (100)

[a]Values are *m/z* (%). R is the alkyl chain with the exception of C-1 to C-3. [b]The ions for this compound were $M^+ - H_2O$ and $M^+ - H_2O - CH_3CH_2$. [c]The base ion for these compounds was $M^+ - CH_3OH - CH_3CH_2$.

As can be observed in **Figure 42**, when resorcinol was involved (compounds **6**-**10**), most reactions occurred at the C4 of the phenolic compound, and only when using pentanal, the corresponding adduct at C2 could be isolated and characterized (compound **8**). In addition, all adducts involving C4 were similar and corresponded to the methoxylated adduct. On the contrary, the adduct at C2 was the hydroxylated adduct.

When 2-methylresorcinol was involved (compounds **11**-**16**), the methoxylated adduct was also the compound isolated in all assayed reactions

with the exception of its reaction with hexanal. In addition, when this phenolic compound was used, two olefins were also produced to a significant extent: those corresponding to the reactions with pentanal and hexanal (compounds **13** and **16**, respectively). On the other hand, the hydroxylated derivative could not be isolated in any reaction.

All these reactions always implied the formation of a new chiral center and the corresponding racemic mixture was produced. Therefore, when the aldehyde had a chiral center, as in the case of 2-methylbutanal, the formed adduct had two chiral centers and 2 pairs of diastereomers were produced (compounds **9a**, **9b**, and **14a**, **14b**).

Glyoxal is a dialdehyde, but it reacted similarly to other saturated aldehydes and the addition of the phenolic C4 to one of the carbonyl carbons was produced to form compounds **17** and **18** from resorcinol and 2-methylresorcinol respectively. However, the structure was stabilized by shifting of the carbonyl group, so that this group could be conjugated with the aromatic ring.

The reaction product between resorcinol and 2-methyl-2-pentenal, which is the aldolic condensation product of propanal, was also isolated and characterized (compound **19**). Its structure is shown in **Figure 42**.

4.1.2. The structure-activity relationships (SAR) of aldehydes and phenolic compounds in the formation of carbonyl-phenol adducts.

Previous studies (Salazar et al., 2014) showed that phenolic compounds having two hydroxyl groups at *meta* positions were required for exhibiting carbonyl-trapping ability and, therefore, to produce carbonyl-phenol adducts to a significant extent. In order to know other structural characteristics that promoted the formation of carbonyl-phenol adducts, different reactions involving a series of linear and branched aldehydes were studied.

As shown in **Figures 43-45**, the amount of carbonyl-phenol adducts always increased linearly as a function of time for the first 96 h of incubation at 60 ºC. However, some adducts were produced to a higher extent than others.

Figure 43 shows the formation of carbonyl-phenol adducts in the reaction between linear alkanals (propanal, butanal, pentanal, and hexanal) and phenolic compounds: resorcinol (**Figure 43A**), 2-methylresorcinol (**Figure 43B**), 2,5-dimethylresorcinol (**Figure 43C**), and orcinol (**Figure 43D**). As can be observed, resorcinol had a lower reactivity than other phenolics. In addition, the highest amount of adducts was formed with orcinol, whereas yields for 2-methylresorcinol and 2,5-dimethylresorcinol were very similar. These results are likely a consequence of the electronic and steric effects of methyl groups in the phenolic compound.

For all assayed phenolics, the formation of carbonyl-phenol adducts mostly followed the same order: propanal < butanal < pentanal ≈ hexanal. This behavior seemed to be related to an easier formation of aldol products in shorter aldehydes under the employed reaction conditions. Thus, carbonyl-phenol adducts of 2-methyl-2-pentenal (the product of aldolic condensation of propanal) with phenolic compounds were detected to a high extent, although they were not quantified (data not shown).

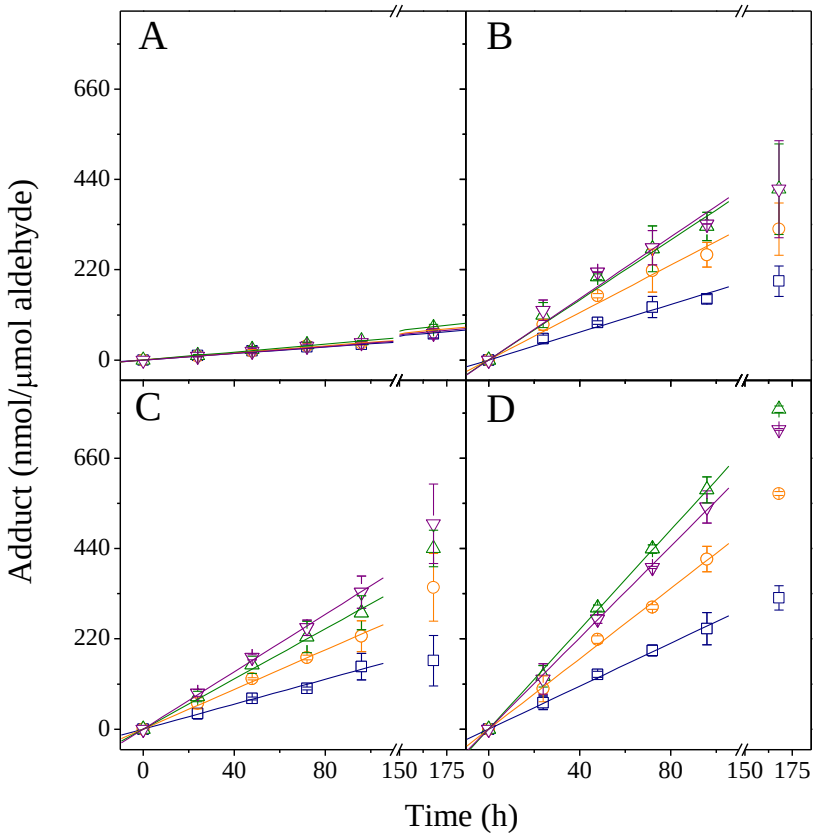

Figure 43. *Time-course of carbonyl-phenol adduct formation in the reactions of: (A), resorcinol; (B), 2-methylresorcinol; (C), 2,5-dimethylresorcinol; and (D), orcinol; with propanal (□), butanal (○), pentanal (△), or hexanal (▽). Reactions were carried out by heating a mixture of the corresponding phenolic compound (80 µmol) and the four linear alkanals (20 µmol of each) in 500 µl of methanol containing 20 µl of triethylamine at 60 ºC under nitrogen for the indicated times.*

Adduct concentration always increased linearly for the first 96 h. Reaction rates were calculated by using the equation

$$[\text{adduct}] = k \cdot t$$

where [adduct] is the concentration of the adduct, k is the rate constant, and t is the time. Reaction rates for the formation of adducts of **Figure 43** are collected in **Table 5**.

***Table 5**. Effect of Aldehyde Chain Length on the Rate Constants of Carbonyl-Phenol Adduct Formation*

Phenol	**Aldehyde**	**Rate constant** [(mmol adduct)·(mol aldehyde)$^{-1}$·h^{-1}]
Resorcinol	Propanal	0.40 ± 0.01
	Butanal	0.43 ± 0.01
	Pentanal	0.48 ± 0.01
	Hexanal	0.41 ± 0.01
2-Methylresorcinol	Propanal	1.69 ± 0.08
	Butanal	2.89 ± 0.13
	Pentanal	3.65 ± 0.17
	Hexanal	3.75 ± 0.21
2,5-Dimethylresorcinol	Propanal	1.52 ± 0.05
	Butanal	2.41 ± 0.04
	Pentanal	3.05 ± 0.06
	Hexanal	3.49 ± 0.04
Orcinol	Propanal	2.62 ± 0.04
	Butanal	4.29 ± 0.07
	Pentanal	6.06 ± 0.07
	Hexanal	5.56 ± 0.06

Figure 44 and **Figure 45** show the effect of aldehyde branching on the formation of carbonyl-phenol adducts. The presence of a methyl group at position 2 of the aldehyde always decreased the formation of the carbonyl-phenol adducts. Thus, a higher amount of butanal/2-methylresorcinol adduct

than of 2-methylpropanal/2-methylresorcinol adduct was produced when aldehydes having four carbon atoms were studied (**Figure 44**).

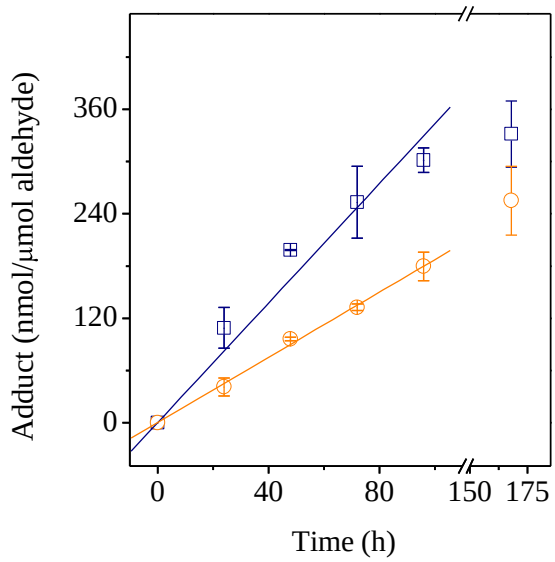

Figure 44. *Time-course of carbonyl-phenol adduct formation in the reactions of butanal (□) and 2-methylpropanal (○) with 2-methylresorcinol. Reaction was carried out by heating a mixture of 2-methylresorcinol (40 µmol) and the two alkanals (20 µmol of each) in 500 µl of methanol containing 20 µl of triethylamine at 60 ºC under nitrogen for the indicated times.*

Aldehydes having five carbon atoms exhibited two different behaviors (**Figure 45**). Thus, pentanal produced a higher amount of adducts than 2-methylbutanal. On the other hand, similar amounts of adducts were produced by both pentanal and 3-methylbutanal.

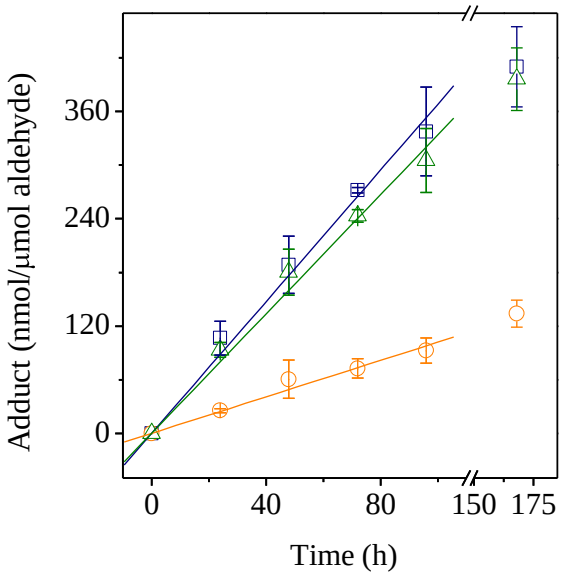

Figure 45. *Time-course of carbonyl-phenol adduct formation in the reactions of pentanal (□), 2-methylbutanal (○), and 3-methylbutanal (△) with 2-methylresorcinol. Reaction was carried out by heating a mixture of 2-methylresorcinol (60 µmol) and the three alkanals (20 µmol of each) in 500 µl of methanol containing 20 µl of triethylamine at 60 ºC under nitrogen for the indicated times.*

Reaction rates for adduct formation between branched aldehydes and phenolic compounds were calculated as described above and they are collected in **Table 6**.

Table 6. *Effect of Aldehyde Branching on the Rate Constants of Carbonyl-Phenol Adduct Formation*

Phenol	**Aldehyde**	**Rate constant** [(mmol adduct)·(mol aldehyde)$^{-1}$·h^{-1}]
2-Methylresorcinol	Butanal	3.44 ± 0.20
	2-Methylpropanal	1.87 ± 0.03
2-Methylresorcinol	Pentanal	3.68 ± 0.11
	2-Methylbutanal	1.02 ± 0.05
	3-Methylbutanal	3.34 ± 0.11

These results are a consequence of the steric hindrance introduced by the methyl group at position 2 of the aldehyde. In addition, this methyl group inhibited the formation of the 2-alkenal produced by aldol condensation and no carbonyl-phenol adducts involving two molecules of 2-methylbutanal were observed.

4.2. Epoxyalkenal-trapping ability of phenolic compounds.

This section describes the isolation and characterization of the carbonyl-phenol adducts produced in the reaction of 4,5-epoxy-2-alkenals and phenolic compounds. In addition, the reaction conditions that promote the formation of the corresponding adducts are also reported.

4.2.1. Characterization of the adducts produced in the reaction between epoxyalkenals and phenolic compounds.

The reaction between epoxyalkenals and phenolic compounds is very fast and rapidly produces a complex mixture of compounds (Hidalgo et al., 2017). Different attempts were carried out to isolate the produced compounds,

but all of them were unsuccessful because of the high reactivity of the formed adducts, which spontaneously suffered further reactions, including polymerizations. Only after their stabilization, they could be isolated and characterized. This stabilization was achieved by acetylation of the hydroxyl groups present in the formed adducts. As observed in **Figure 46**, acetylation allowed that carbonyl-phenol adducts could be easily identified by GC-MS. This technique was employed to control the chromatographic separation of the formed adducts. The compounds isolated and characterized in these reactions are described in subsections 4.2.1.1, 4.2.1.2, and 4.2.1.3.

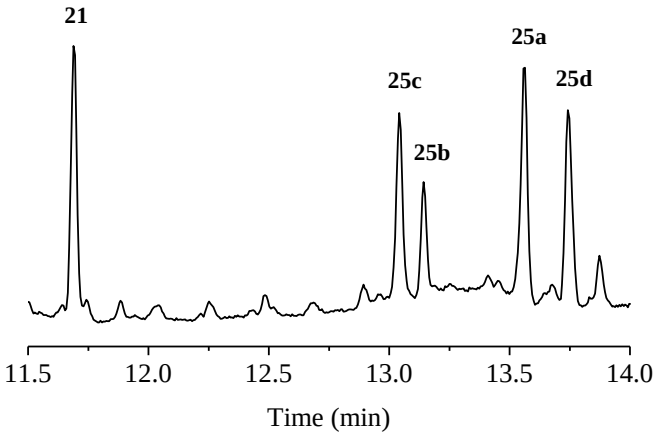

***Figure 46**. Total ion chromatogram obtained by GC-MS of the reaction between 4,5-epoxy-2-heptenal and 2-methylresorcinol after acetylation. Only the portion corresponding to epoxyalkenal/phenol adducts is shown. Chemical structures for the identified compounds are given in **Figure 47**.*

Two different kinds of adducts were isolated by column chromatography and characterized by 1D and 2D NMR and MS (**Figure 47**).

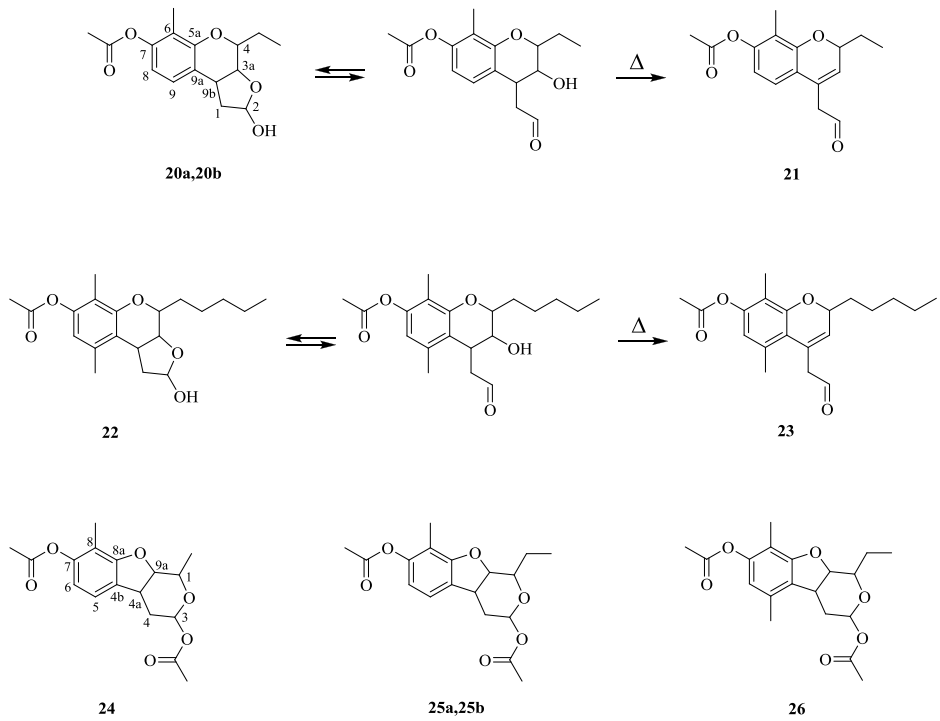

Figure 47. *Chemical structures of the carbonyl-phenol adducts isolated and characterized by NMR and MS in the different assayed reactions between epoxyalkenals and phenolics. The aldehyde and the phenolic compound involved in the formation of each adduct is described in the text.*

Differently to the adducts produced between alkanals and phenolics, which were the result of a single addition of the phenolic compound to the alkanal, the adducts produced with epoxyalkenals resulted more complex, and structures could only be determined by using 2D NMR. Thus, COSY, HMQC and HMBC experiments were carried out. Main HMBC couplings exhibited by compounds **20a** and **25a** are shown in **Figure 48**. HMBC couplings of compounds **20b**, **22** were identical to those of compound **20a**. HMBC couplings of compounds **24**, **25b**, and **26** were identical to those of compound **25a**.

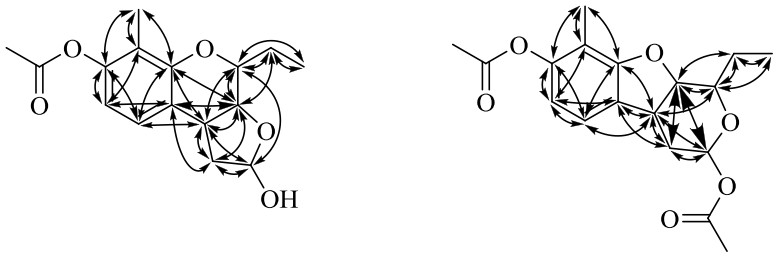

(20a) **(25a)**

***Figure 48**. HMBC couplings exhibited by compounds **20a** and **25a**.*

The first type of adducts isolated in reactions between epoxyalkenals and phenolic compounds were 1,3a,4,9b-tetrahydro-2*H*-furo[2,3-*c*]chromen-7-yl acetates (compounds **20a**, **20b** and **22**). This cyclic form was the only observed in solution by NMR. However, because the hemiacetalic hydroxyl group was not acetylated, when these compounds were studied by GC-MS, the cyclic hemiacetal was opened and the free hydroxyl group suffered a dehydration to produce the corresponding 4-(2-oxoethyl)-2*H*-chromen-7-yl acetate (compounds **21** and **23**).

Compounds **20a**, **20b** and **22** had only one acetyl group and two phenolic protons (or one in the case of compound **22**), indicating that one phenolic hydroxyl group and one of the phenolic protons were involved in the reaction with the epoxyalkenal. The epoxyalkenal chain could be easily identified in the adduct by means of a COSY experiment. The study of its chain showed that its epoxy, double bond and carbonyl groups were also involved in the reaction. The final characterization of their structures was carried out by using HMQC and HMBC experiments. In particular, HMBC showed long distance couplings, which were employed for the unequivocal identification of the formed structures.

Two isomers (**20a** and **20b**) were isolated in the reaction between 4,5-epoxy-2-heptenal and 2-methylresorcinol. This is consequence of the different chiral centers present in the molecule (C4, C3a, and C9b). Two of them (C3a

and C4) corresponded to the epoxy carbons of the epoxyalkenal (C4 and C5) and were already present in the aldehyde. Because the initial alkadienal (2,4-heptadienal) was *trans*,*trans* and the epoxidation was *syn*, the obtained epoxyalkenal should be a mixture of the isomer *4R*,5*R* and its enantiomer. Supposing that the formation of the adduct did not imply a racemization, the creation of the new chiral center at C9b would explain the existence of the two isomers **20a** and **20b**. In addition, C2 is also chiral, although it is not fixed and the interconversion between the two absolute configurations of this carbon might be produced. The ^{1}H NMR spectra of both isomers were quite similar. The most significant differences, as expected, corresponded to the protons belonging to chiral carbons C4, C3a, C9b, and C2. One difference was the chemical shift of protons H4 and H9b, which were interchanged in compounds **20a** and **20b** as confirmed by HMQC experiments. Other differences were the coupling constants, which were particularly different for H2. After dehydration, both compounds produced the same compound **21**.

The second type of adducts produced in these reactions were 3,4,4a,9a-tetrahydro-1*H*-pyrano[3,4-*b*]benzofuran-3,7-diyl diacetates (**24-26**). Compounds **24-26** had two acetyl groups and two phenolic protons (or one in the case of compound **26**), indicating that, at least, one of the phenolic protons was involved in the reaction with the epoxyalkenal. The epoxyalkenal chain could also be easily identified in the adduct by means of a COSY experiment. The study of its chain showed that epoxy, double bond and carbonyl groups of the epoxyalkenal were also involved in the reaction. The final characterization of the structures was carried out by using HMQC and HMBC experiments.

Analogously to the above described for compounds **20a** and **20b**, the reaction between 4,5-epoxy-2-heptenal and 2-methylresorcinol produced several compounds of this type (**25a, 25b, 25c** and **25d)**. In this case, four isomers were detected by GC-MS (**Figure 46**), two of which (**25a** and **25b**) could be isolated and characterized. The existence of these 4 isomers is a consequence of the presence in the molecule of 4 chiral carbons: C1, C9a, C4a, and C3. Two of them (C1 and C9a) were already present in the initial

epoxyalkenal, but C4a and C3 were created in the reaction with the phenol and C3 was fixed in the later acetylation.

The ^{1}H NMR spectra of stereoisomers **25a** and **25b** were similar between them and the main differences were again the chemical shifts and coupling constants of protons close to chiral carbons. Thus, for example, the acetyl group of C3 was different for the two isomers. On the other hand, the acetyl group of C7, which is quite far from the chiral centers, was identical for the two isomers. These differences were also observed in the mass spectra. Thus, although the fragmentation pattern was identical for the two isomers, the intensities of the produced fragments were different. Nevertheless, all compounds **24**-**26** had very similar fragmentation patterns by MS.

Although only a limited number of compounds could be isolated and characterized in the studied reactions, no other compounds having different mass fragmentation patterns were formed in the studied reactions to a significant extent. Therefore, it can be concluded that the reaction between epoxyalkenals and phenolic compounds mainly produces in a first step 1,3a,4,9b-tetrahydro-2*H*-furo[2,3-*c*]chromene-2,7-diols (**27**) and 3,4,4a,9a-tetrahydro-1*H*-pyrano[3,4-*b*]benzofuran-3,7-diols (**28**) (**Figure 49**). These compounds have reactive hydroxyl and carbonyl groups that can be involved in further reactions, which is in agreement with the reactivity observed for the formed adducts.

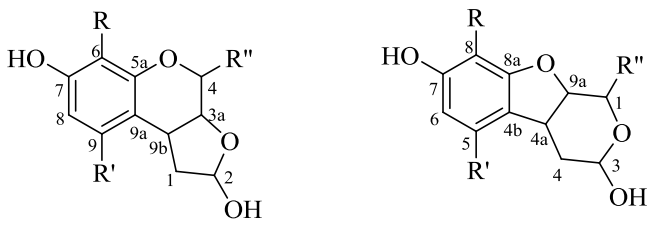

27 **28**

Figure 49*. Chemical structures of adducts produced in the reaction between epoxyalkenals and phenolics.*

The spectroscopic and spectrometric data of the carbonyl-phenol adducts isolated and characterized in the different epoxyalkenal-phenol reactions assayed are collected in the next subsections.

4.2.1.1. Compounds isolated and characterized in the reaction of 4,5-epoxy-2-heptenal and 2-methylresorcinol.

The reaction between 4,5-epoxy-2-heptenal and 2-methylresorcinol produced five carbonyl-phenol adducts (**Figure 46**). Four of them could be isolated and characterized. Their spectroscopic and spectrometric data are the following:

4-Ethyl-2-hydroxy-6-methyl-1,3a,4,9b-tetrahydro-2H-furo[2,3-c]chromen-7-yl acetate (**20a** and **20b**). Two diastereomers of this compound could be isolated and characterized. ^{1}H NMR ($CDCl_3$) of compound **20a**: δ (ppm) 1.04t (3H, *J* = 7.4 Hz, $C\underline{H}_3CH_2$), 1.65qu (2H, *J* = 7.4 Hz, $CH_3C\underline{H}_2$), 2.02s (3H, $C\underline{H}_3C6$), 2.21m and 2.29m (2H, H1), 2.33s (3H, CH_3CO), 3.52m (1H, H4), 3.89q,br (1H, *J* = 7.5 Hz, H9b), 4.65t (1H, *J* = 9.3 Hz, H3a), 6.07dd (1H, *J* = 2.7 Hz and 5.2 Hz, H2), 6.59d (1H, *J* = 8.0 Hz, H8), and 6.97d (1H, *J* = 8.0 Hz, H9). ^{13}C NMR ($CDCl_3$) of compound **20a**: δ (ppm) 9.19 ($\underline{C}H_3C6$), 9.45 ($\underline{C}H_3CH_2C4$), 20.76 (CH_3CO), 26.22 ($CH_3\underline{C}H_2C4$), 29.58 (C1), 36.56 (C9b), 74.33 (C4), 82.31 (C3a), 92.17 (C2), 113.51 (C6), 114.39 (C8), 120.90 (C9), 125.77 (C9a), 149.71 (C7), 158.60 (C5a), 169.39 ($CH_3\underline{C}O$). ^{1}H NMR ($CDCl_3$) of compound **20b**: δ (ppm) 1.06t (3H, *J* = 7.4 Hz, $C\underline{H}_3CH_2$), 1.64qu (2H, *J* = 7.4 Hz, $CH_3C\underline{H}_2$), 2.02s (3H, $C\underline{H}_3C6$), 1.95m and 2.30m (2H, H1), 2.32s (3H, CH_3CO), 3.51m (1H, H9b), 3.84dt (1H, *J* = 3.9 Hz, *J* = 8.7 Hz, *J* = 8.7 Hz, H4), 4.58t (1H, *J* = 9.3 Hz, H3a), 6.15dd (1H, *J* = 5.9 Hz and 8.5 Hz, H2), 6.55d (1H, *J* = 8.0 Hz, H8), and 6.96d (1H, *J* = 8.0 Hz, H9). ^{13}C NMR ($CDCl_3$) of compound **20b**: δ (ppm) 9.24 ($\underline{C}H_3C6$), 9.55 ($\underline{C}H_3CH_2C4$), 20.74 (CH_3CO), 26.36 ($CH_3\underline{C}H_2C4$), 30.56 (C1), 37.42 (C9b), 71.81 (C4), 84.16 (C3a), 91.92 (C2), 113.39 (C6), 114.13 (C8), 121.30 (C9), 126.16 (C9a),

149.65 (C7), 159.16 (C5a), 169.35 ($CH_3\underline{C}O$). These compounds suffered a dehydration when studied by GC-MS and were converted into 2-ethyl-8-methyl-4-(2-oxoethyl)-2*H*-chromen-7-yl acetate (**21**). MS, *m/z* (%, ion structure): 274 (19, M^+), 232 (33, $M^+ - CH_2CO$), 204 (15, 232 – ethene), 203 (100, 232 – CH_3CH_2), 189 (11, 204 – CH_3), 175 (19, 204 – CHO), 174 (31, 204 – HCHO) and 161 (13, 204 – CH_2CHO).

1-Ethyl-8-methyl-3,4,4a,9a-tetrahydro-1H-pyrano[3,4-b]benzofuran-3,7-diyl diacetate (**25a** and **25b**). Two diastereomers of this compound could be isolated and characterized. ^{1}H NMR ($CDCl_3$) of compound **25a**: δ (ppm) 0.91t (3H, *J* = 7.4 Hz, $C\underline{H}_3CH_2$), 1.57m and 1.78m (2H, CH_2C1), 1.99s (3H, CH_3C8), 2.15s (3H, CH_3CO), 2.29m (2H, H4), 2.32s (3H, CH_3CO), 3.05d (1H, *J* = 3.9 Hz, H4a), 4.29d (1H, *J* = 8.3 Hz, H9a), 4.75dt (1H, *J* = 3.8 Hz, *J* = 8.1 Hz, H1), 5.83d (1H, *J* = 3.3 Hz, H3), 6.56d (1H, *J* = 8.1 Hz, H6), and 6.83d (1H, *J* = 8.1 Hz, H5). ^{13}C NMR ($CDCl_3$) of compound **25a**: δ (ppm) 8.99 ($\underline{C}H_3C8$), 9.78 ($\underline{C}H_3CH_2$), 20.77 ($\underline{C}H_3CO$), 21.11 ($\underline{C}H_3CO$), 23.93 ($C\underline{H}_2C1$), 30.19 (C4), 37.72 (C4a), 73.76 (C1), 89.85 (C9a), 99.34 (C3), 113.74 (C6), 118.61 (C8), 123.52 (C5), 126.15 (C4b), 149.18 (C7), 150.59 (C8a), 169.31 ($CH_3\underline{C}O$), and 170.62 ($CH_3\underline{C}O$). MS of compound **25a**, *m/z* (%, ion structure): 334 (4, M^+), 292 (1, $M^+ - CH_2CO$), 274 (2, 278 – H_2O), 245 (55, 274 – CHO), 232 (16, 274 – CH_2CO), 217 (2, 232 – CH_3), 203 (100, 232 – CH_3CH_2), 191 (18, 232 – C_3H_5), 190 (5, 232 – CH_2CO), 189 (15, 232 – CH_2CHO), 175 (8, 190 – CH_3), and 161 (39, 190 – CH_3CH_2). ^{1}H NMR ($CDCl_3$) of compound **25b**: δ (ppm) 0.85t (3H, *J* = 7.5 Hz, $C\underline{H}_3CH_2$), 1.65m and 1.76m (2H, CH_2C1), 1.98s (3H, CH_3C8), 2.03s (3H, CH_3CO), 2.25dd (2H, *J* = 2.4 Hz, *J* = 3.2 Hz, H4), 2.31s (3H, CH_3CO), 3.20dd (1H, *J* = 3.0 Hz, *J* = 5.1 Hz, H4a), 4.22dd (1H, *J* = 3.2 Hz, *J* = 8.5 Hz, H9a), 4.47ddd (1H, *J* = 4.1 Hz, *J* = 6.5 Hz, *J* = 8.5 Hz, H1), 5.80br (1H, H3), 6.55d (1H, *J* = 8.1 Hz, H6), and 6.68d (1H, *J* = 8.1 Hz, H5). ^{13}C NMR ($CDCl_3$) of compound **25b**: δ (ppm) 8.62 ($\underline{C}H_3CH_2$), 9.07 ($\underline{C}H_3C8$), 20.78 ($\underline{C}H_3CO$), 21.00 ($\underline{C}H_3CO$), 24.37 ($C\underline{H}_2C1$), 32.87 (C4), 38.40 (C4a), 73.94 (C1), 87.95 (C9a), 99.13 (C3),

113.75 (C6), 118.24 (C8), 122.00 (C4b), 125.11 (C5), 149.52 (C7), 150.15 (C8a), 169.30 ($CH_3\underline{C}O$), and 169.61 ($CH_3\underline{C}O$). MS of compound **25b**, *m/z* (%, ion structure): 334 (4, M^+), 292 (2, $M^+ - CH_2CO$), 274 (3, 278 – H_2O), 245 (18, 274 – CHO), 232 (28, 274 – CH_2CO), 217 (1, 232 – CH_3), 203 (100, 232 – CH_3CH_2), 191 (10, 232 – C_3H_5), 190 (7, 232 – CH_2CO), 189 (43, 232 – CH_2CHO), 175 (11, 190 – CH_3), and 161 (17, 190 – CH_3CH_2).

4.2.1.2. Compounds isolated and characterized in the reaction of 4,5-epoxy-2-decenal and 2,5-dimethylresorcinol.

The reaction between 4,5-epoxy-2-decenal and 2,5-dimethylresorcinol produced similar carbonyl-phenol adducts to the reaction between 4,5-epoxy-2-heptenal and 2-methylresorcinol described above (subsection 4.2.1.1). One of them could be isolated and characterized. Its spectroscopic and spectrometric data are the following:

2-Hydroxy-6,9-dimethyl-4-pentyl-1,3a,4,9b-tetrahydro-2H-furo[2,3-c]chromen-7-yl acetate (**22**). ^{1}H NMR ($CDCl_3$): δ (ppm) 0.89t (3H, *J* = 6.8 Hz, $C\underline{H}_3CH_2$), 1.30 m (6H, $CH_3C\underline{H}_2C\underline{H}_2C\underline{H}_2$), 1.58m (2H, $C\underline{H}_2C4$), 1.85m and 2.36m (2H, H1), 1.98s (3H, $C\underline{H}_3C6$), 2.23s (3H, CH_3C9), 2.31s (3H, CH_3CO), 3.42m (1H, H9b), 3.95ddd (1H, *J* = 1.3 Hz, *J* = 4.4 Hz, *J* = 5.6 Hz, H4), 4.54t (1H, *J* = 8.9 Hz, H3a), 6.16dd (1H, *J* = 6.1 Hz and 9.1 Hz, H2), and 6.37s (1H, H8). ^{13}C NMR ($CDCl_3$): δ (ppm) 9.04 ($\underline{C}H_3C6$), 13.97 ($\underline{C}H_3CH_2$), 18.15 ($\underline{C}H_3C9$), 20.95 (CH_3CO), 22.48 ($CH_3\underline{C}H_2$), 25.12 ($CH_3CH_2CH_2\underline{C}H_2$), 29.00 (C1), 29.74 ($\underline{C}H_2C4$), 31.61 ($CH_3CH_2\underline{C}H_2$), 37.04 (C9b), 71.85 (C4), 84.61 (C3a), 92.03 (C2), 110.49 (C6), 115.18 (C8), 124.63 (C9), 132.17 (C9a), 149.52 (C7), 159.03 (C5a), 169.45 ($CH_3\underline{C}O$). This compound suffered a dehydration when studied by GC-MS and was converted into 8-methyl-4-(2-oxoethyl)-2-pentyl-2*H*-chromen-7-yl acetate (**23**). MS, *m/z* (%, ion structure): 330 (27, M^+), 288 (59, $M^+ - CH_2CO$), 273 (5, 288 – CH_3), 259 (10, 288 – CH_3CH_2), 245 (12, 288 – $CH_3CH_2CH_2$), 218 (15, 288 – pentene), 217 (100,

288 – $CH_3CH_2CH_2CH_2CH_2$), 189 (41, 218 – CHO), 188 (67, 218 – HCHO), 175 (69, 218 – CH_2CHO), and 151 (84).

Differently to the reaction between 4,5-epoxy-2-heptenal and 2-methylresorcinol, in the reaction between 4,5-epoxy-2-decenal and 2,5-dimethylresorcinol only isomer **22** could be isolated and characterized. According to the chemical shifts of protons H4 and H9b, this compound was similar to compound **20b**. However, isomer **22** differed from isomer **20b** in the coupling constants of H4, which were lower in compound **22**. On the other hand, the mass spectrum of the dehydrated compound **23** was similar to the mass spectra of compound **21**.

4.2.1.3. Compounds isolated and characterized in the reaction of 4,5-epoxy-2-hexenal and 2-methylresorcinol.

The reaction between 4,5-epoxy-2-hexenal and 2-methylresorcinol produced similar carbonyl-phenol adducts to the reaction between 4,5-epoxy-2-heptenal and 2-methylresorcinol described above (subsection 4.2.1.1). One of them could be isolated and characterized. Its spectroscopic and spectrometric data are the following:

1,8-Dimethyl-3,4,4a,9a-tetrahydro-1H-pyrano[3,4-b]benzofuran-3,7-diyl diacetate (**24**). ^{1}H NMR ($CDCl_3$): δ (ppm) 1.26d (3H, *J* = 6.6 Hz, CH_3C1), 1.99s (3H, CH_3C8), 2.08s (3H, CH_3CO), 2.28m (2H, H4), 2.32s (3H, CH_3CO), 3.12d (1H, *J* = 3.9 Hz, H4a), 4.24d (1H, *J* = 7.8 Hz, H9a), 4.79dt (1H, *J* = 7.8 Hz, *J* = 6.6 Hz, H1), 5.84d (1H, *J* = 3.2 Hz, H3), 6.57d (1H, *J* = 8.1 Hz, H6), and 6.85d (1H, *J* = 8.1 Hz, H5). ^{13}C NMR ($CDCl_3$): δ (ppm) 8.99 ($\underline{C}H_3$C8), 16.81 ($\underline{C}H_3$C1), 20.82 ($\underline{C}H_3CO$), 21.31 ($\underline{C}H_3CO$), 30.21 (C4), 37.57 (C4a), 69.77 (C1), 91.39 (C9a), 99.35 (C3), 113.77 (C6), 118.64 (C8), 123.50 (C5), 126.17 (C4b), 149.18 (C7), 150.59 (C8a), 169.35 ($CH_3\underline{C}O$), and 170.31 ($CH_3\underline{C}O$). MS, *m/z* (%, ion structure): 320 (8, M^+), 278 (1, $M^+ - CH_2CO$), 260

(8, 278 – H_2O), 245 (43, 260 – CH_3), 232 (5, 260 – CO), 218 (38, 260 – CH_2CO), 203 (100, 218 – CH_3), 190 (50, 218 – CH_3CH), 176 (9, 218 – CH_2CO), 175 (43, 218 – CH_3CO), and 161 (66, 176 – CH_3).

The isolated isomer **24** was similar to compound **25a** because it had similar coupling constants.

4.2.1.4. Compounds isolated and characterized in the reaction of 4,5-epoxy-2-heptenal and 2,5-dimethylresorcinol.

The reaction between 4,5-epoxy-2-heptenal and 2,5-dimethylresorcinol produced similar carbonyl-phenol adducts to the reaction between 4,5-epoxy-2-heptenal and 2-methylresorcinol described above (subsection 4.2.1.1). One of them could be isolated and characterized. Its spectroscopic and spectrometric data are the following:

1-Ethyl-5,8-dimethyl-3,4,4a,9a-tetrahydro-1H-pyrano[3,4-b]benzofuran-3,7-diyl diacetate (**26**). ^{1}H NMR (DMSO-d_6): δ (ppm) 0.83t (3H, *J* = 7.4 Hz, C$\underline{H}_3CH_2$), 1.48m and 1.69m (2H, CH_2C1), 1.82s (3H, CH_3C8), 2.11s (3H, CH_3CO), 2.19s (3H, CH_3C5), 2.26m (2H, H4), 2.27s (3H, CH_3CO), 3.31m (1H, H4a), 4.07d (1H, *J* = 8.0 Hz, H9a), 4.68dt (1H, *J* = 3.5 Hz, *J* = 8.2 Hz, H1), 5.88d (1H, *J* = 3.2 Hz, H3), and 6.47s (1H, H6). ^{13}C NMR (DMSO-d_6): δ (ppm) 9.22 ($\underline{C}H_3$C8), 9.62 ($\underline{C}H_3CH_2$), 18.22 ($\underline{C}H_3$C5), 20.93 ($\underline{C}H_3CO$), 21.23 ($\underline{C}H_3CO$), 23.88 (C$\underline{H}_2$C1), 30.07 (C4), 33.34 (C4a), 73.53 (C1), 89.92 (C9a), 99.27 (C3), 115.35 (C8), 115.74 (C6), 125.42 (C5), 131.76 (C4b), 148.48 (C7), 150.42 (C8a), 169.40 ($CH_3\underline{C}O$), and 170.57 ($CH_3\underline{C}O$). MS, *m/z* (%, ion structure): 348 (28, M^+), 306 (10, M^+ – CH_2CO), 288 (1, 292 – H_2O), 259 (53, 288 – CHO), 246 (49, 288 – CH_2CO), 231 (3, 246 – CH_3), 217 (100, 246 – CH_3CH_2), 205 (35, 246 – C_3H_5), 204 (14, 246 – CH_2CO), 203 (75, 246 – CH_2CHO), 189 (9, 204 – CH_3), 176 (96, 204 – ethene), 175 (80, 204 – CH_3CH_2), and 161 (20, C_3H_5).

The isolated isomer **26** was similar to compound **25a** because it had similar coupling constants.

4.2.2. Effect of reaction conditions on the formation of epoxyalkenal-phenol adducts in the reaction of 4,5-epoxy-2-heptenal and 2-methylresorcinol.

The effect of reaction conditions (pH, reactant concentration, time, and temperature) on the reaction between 4,5-epoxy-2-heptenal and 2-methylresorcinol was studied to determine the reaction conditions that favored the formation of carbonyl-phenol adducts. As shown in **Figure 46**, five adducts were observed by GC-MS after acetylation of the reaction mixture: one of them was a 4-(2-oxoethyl)-2*H*-chromen-7-yl acetate (compound **21**), and the other four adducts were 3,4,4a,9a-tetrahydro-1*H*-pyrano[3,4-*b*]-benzofuran-3,7-diyl diacetates (compounds **25a**, **25b**, **25c**, and **25d**). The effect of reaction conditions on the formation of all of them was studied.

Phenol disappearance and adduct formation was pH-dependent (**Figure 50**). Adducts were not formed at pH < 6. However, the formation of some adducts (**21**, **25a**, and **25c**) was already significant at pH 7, and the concentration of most of them increased at higher pH values. For most adducts, there were not significant differences between the amount formed at pH 8 in the presence of either phosphate or borate, therefore confirming that it was the pH and not the employed buffer the responsible for the formation of these compounds.

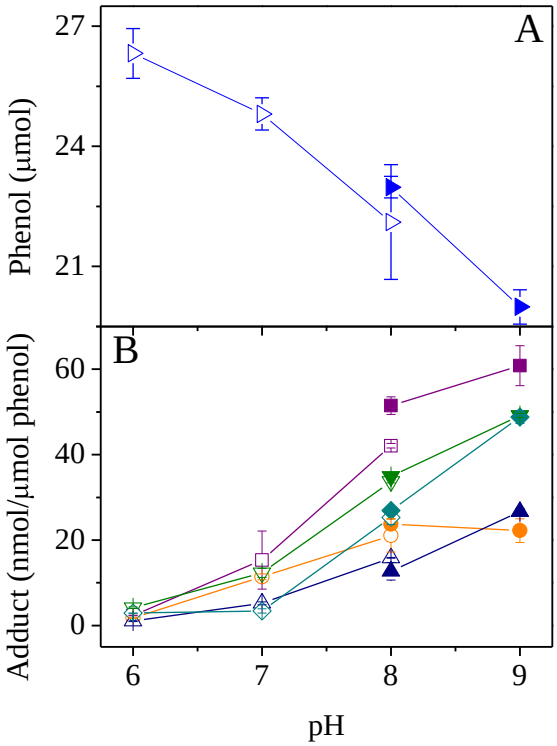

Figure 50. *Effect of reaction pH on: (A), phenol disappearance; and (B), formation of carbonyl-phenol adducts. Reactions were carried out by heating a mixture of 4,5-epoxy-2-heptenal (40 µmol) and 2-methylresorcinol (30 µmol, ▷,▶) in 300 µl of 0.3 M buffer for 30 min at 100 ºC under nitrogen. The carbonyl-phenol adducts produced were compounds* ***21*** *(□,■),* ***25a*** *(▽,▼),* ***25b*** *(△,▲),* ***25c*** *(○,●), and* ***25d*** *(◇,◆). Two buffers were employed: 0.3 M sodium phosphate buffer (open symbols) and 0.3 M sodium borate buffer (closed symbols).*

Figure 51 shows the effect of increasing amounts of 4,5-epoxy-2-heptenal on the disappearance of the phenolic compound and the formation of epoxyalkenal-phenol adducts. The addition of increasing amounts of aldehyde produced the linear (r = –0.996, p = 0.0003) disappearance of the phenolic compound (**Figure 51A**). The highest amount of epoxyalkenal tested (40

µmol) produced the disappearance of the 26% of the phenolic compound present (7.89 ± 1.38 µmol of the phenol disappeared). This disappearance was parallel to the appearance of the adducts **21** and **25a**, **25b**, **25c**, **25d**. (**Figure 51B**). The amount of all of them increased linearly as a function of the amount of epoxyalkenal added and were inversely correlated ($r > 0.98$, $p < 0.003$) to the disappearance of the phenol.

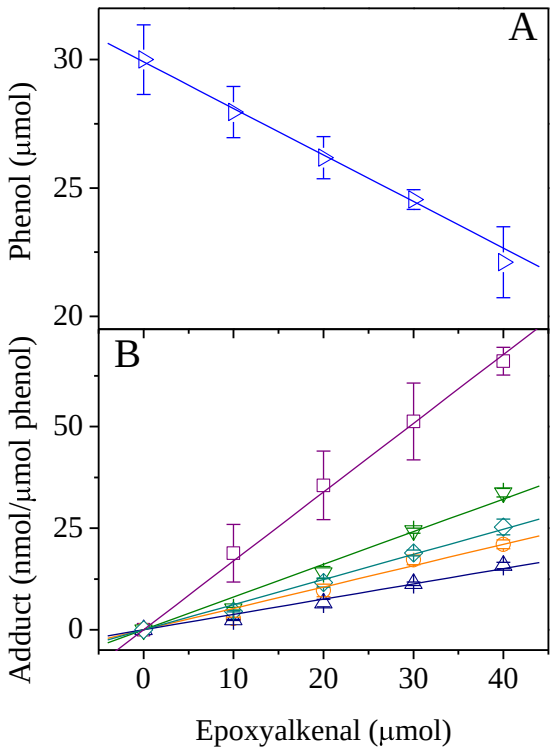

Figure 51. *Effect of epoxyalkenal concentration on: (A), phenol disappearance; and (B), formation of carbonyl-phenol adducts. Reactions were carried out by heating a mixture of 4,5-epoxy-2-heptenal at the indicated concentrations and 2-methylresorcinol (30 µmol, ▷) in 300 µl of 0.3 M sodium phosphate buffer, pH 8, for 30 min at 100 ºC under nitrogen. The carbonyl-phenol adducts produced were compounds* ***21*** *(□),* ***25a*** *(▽),* ***25b*** *(△),* ***25c*** *(○), and* ***25d*** *(◇).*

An analogous behavior was observed when increasing amounts of phenol were added (**Figure 52**). Thus, the addition of increasing amounts of phenol produced the linear increase ($r > 0.98$, $p < 0.002$) of the concentration of produced adducts **21** and **25a**, **25b**, **25c**, **25d** (**Figure 52B**), therefore confirming that formation of adducts required the participation of both epoxyalkenal and phenolic compound.

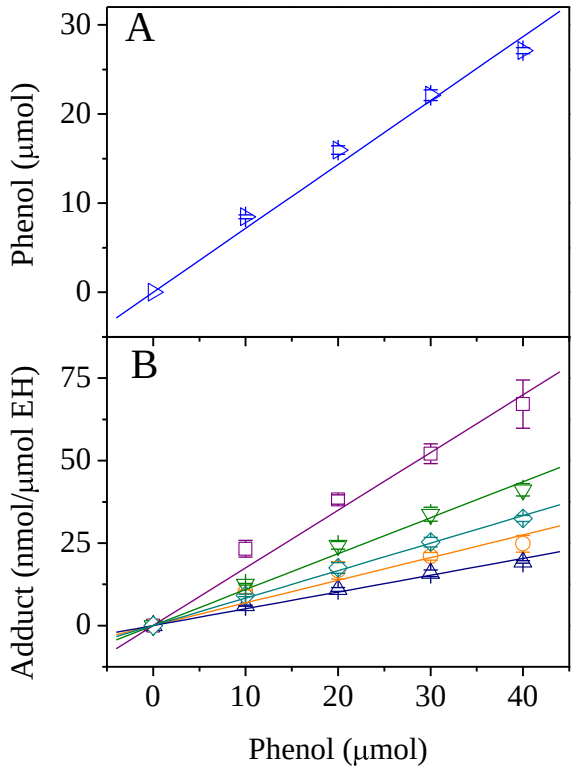

Figure 52. *Effect of phenol concentration on: (A), remaining phenol; and (B), formation of carbonyl-phenol adducts. Reactions were carried out by heating a mixture of 4,5-epoxy-2-heptenal (40 μmol) and 2-methylresorcinol (▷) at the indicated concentrations in 300 μl of 0.3 M sodium phosphate buffer, pH 8, for 30 min at 100 ºC under nitrogen. The carbonyl-phenol adducts produced were compounds* ***21*** *(□),* ***25a*** *(▽),* ***25b*** *(△),* ***25c*** *(○), and* ***25d*** *(◇). EH, 4,5-epoxy-2-heptenal.*

Phenol disappearance and adduct formation also depended on reaction times and temperatures (**Figures 53-58)**.

In general, phenol disappearance (**Figure 53**) and adduct formation (**Figures 54-58**) increased with time and temperature, although there were differences among the different adducts.

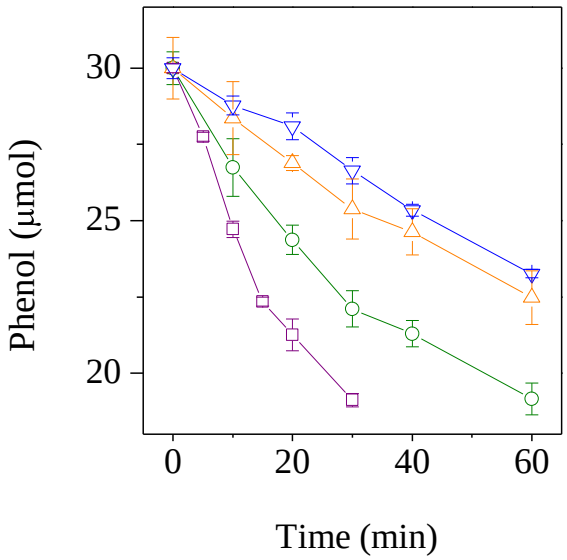

Figure 53. *Effect of reaction time and temperature on the phenol disappearance. Reactions were carried out by heating a mixture of 4,5-epoxy-2-heptenal (40 µmol) and 2-methylresorcinol (30 µmol) in 300 µl of 0.3 M sodium phosphate buffer, pH 8, at the indicated times and temperatures under nitrogen. The assayed temperatures were: 120 (□), 100 (○), 80 (△), and 60 ºC (▽).*

Thus, adduct **21** was produced similarly at 60–100 ºC but its concentration increased considerably at 120 ºC (**Figure 54**). At this temperature, its maximum concentration was achieved after only 20 min heating.

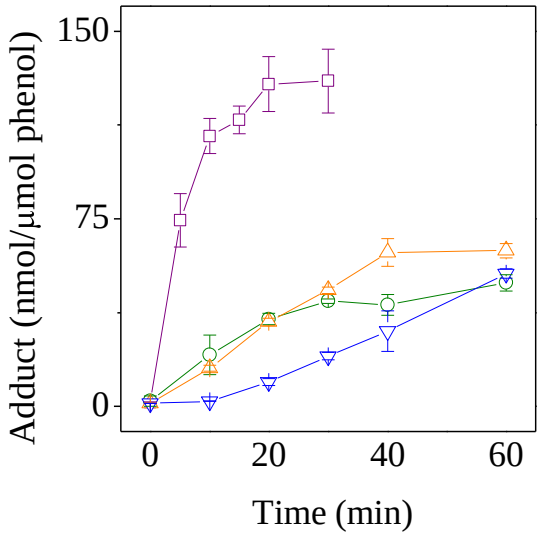

Figure 54. *Effect of reaction time and temperature on the formation of compound* ***21****. Reactions were carried out by heating a mixture of 4,5-epoxy-2-heptenal (40 µmol) and 2-methylresorcinol (30 µmol) in 300 µl of 0.3 M sodium phosphate buffer, pH 8, at the indicated times and temperatures under nitrogen. The assayed temperatures were: 120 (□), 100 (○), 80 (△), and 60 ºC (▽).*

The concentration of adduct **25c** exhibited a great dependence on the assayed temperature. Thus, the maximum concentration of this compound was obtained at low temperature because at temperatures higher than 80 ºC it suffered a significant decomposition (**Figure 55**).

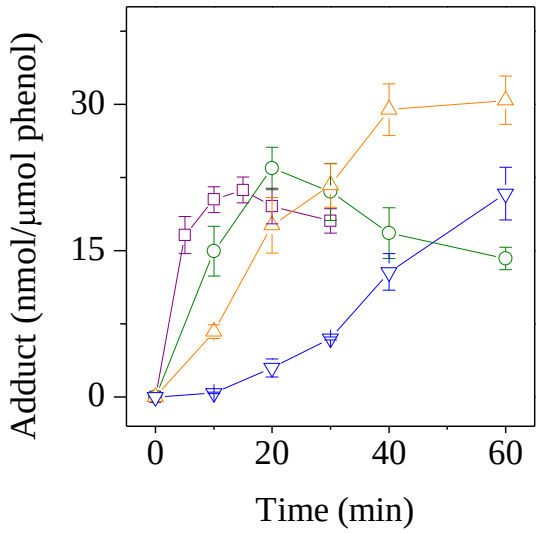

Figure 55. *Effect of reaction time and temperature on the formation of compound* ***25c****. Reactions were carried out by heating a mixture of 4,5-epoxy-2-heptenal (40 µmol) and 2-methylresorcinol (30 µmol) in 300 µl of 0.3 M sodium phosphate buffer, pH 8, at the indicated times and temperatures under nitrogen. The assayed temperatures were: 120 (□), 100 (○), 80 (△), and 60 ºC (▽).*

Adducts **25a** and **25b** (**Figures 56 and 57**, respectively), exhibited a similar behavior among them as a function of time and temperature. Thus, they were produced to a similar extent at 80 and 100 ºC, but the amount at which they were produced decreased significantly ($p < 0.05$) at 60 ºC and increased significantly ($p < 0.05$) at 120 ºC.

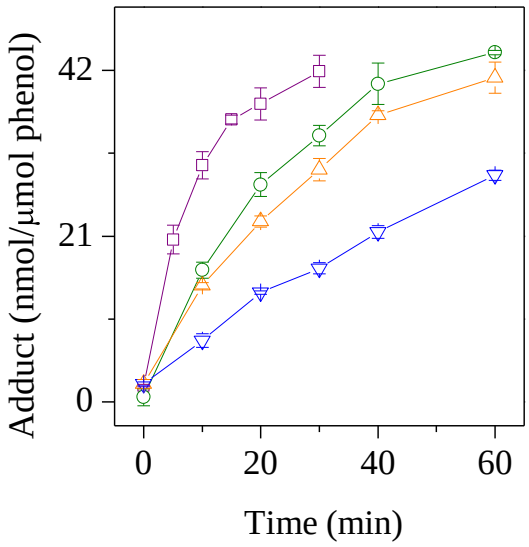

Figure 56. *Effect of reaction time and temperature on the formation of compound* ***25a****. Reactions were carried out by heating a mixture of 4,5-epoxy-2-heptenal (40 µmol) and 2-methylresorcinol (30 µmol) in 300 µl of 0.3 M sodium phosphate buffer, pH 8, at the indicated times and temperatures under nitrogen. The assayed temperatures were: 120 (□), 100 (○), 80 (△), and 60 ºC (▽).*

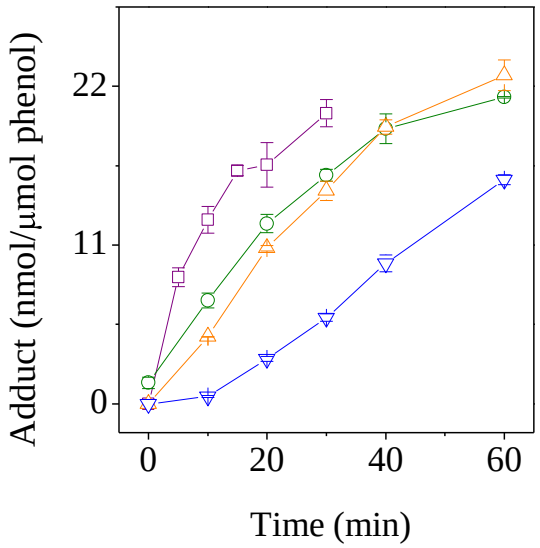

Figure 57. *Effect of reaction time and temperature on the formation of compound* ***25b****. Reactions were carried out by heating a mixture of 4,5-epoxy-2-heptenal (40 µmol) and 2-methylresorcinol (30 µmol) in 300 µl of 0.3 M sodium phosphate buffer, pH 8, at the indicated times and temperatures under nitrogen. The assayed temperatures were: 120 (□), 100 (○), 80 (△), and 60 ºC (▽).*

Finally, the adduct **25d** was the most temperature-dependent (**Figure 58**). It was almost not produced at 60 ºC and its concentration increased considerably when heating temperature increased. Thus, adducts **21**, **25a**, and **25d** were the main products at 120 ºC. On the other and, adduct **25d** was the adduct produced to a lower extent at 60 ºC.

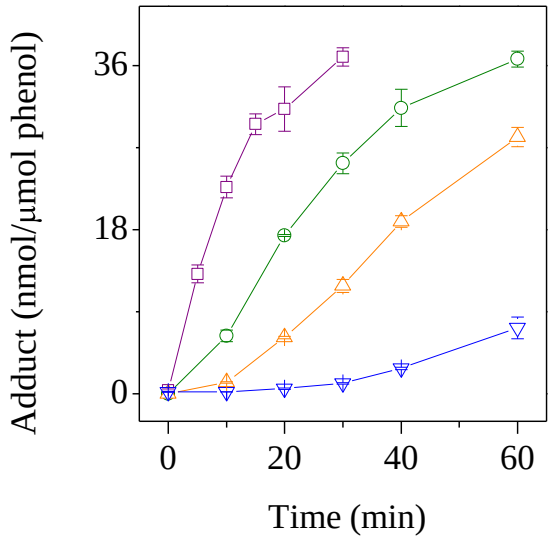

Figure 58. *Effect of reaction time and temperature on the formation of compound* ***25d****. Reactions were carried out by heating a mixture of 4,5-epoxy-2-heptenal (40 µmol) and 2-methylresorcinol (30 µmol) in 300 µl of 0.3 M sodium phosphate buffer, pH 8, at the indicated times and temperatures under nitrogen. The assayed temperatures were: 120 (□), 100 (○), 80 (△), and 60 ºC (▽).*

4.3. Oxoalkenal-trapping ability of phenolic compounds.

This section describes the trapping of 4-oxo-2-alkenals by phenolics. Both, the isolation and characterization of the carbonyl-phenol adducts formed in these reactions, and the conditions that promote their formation are reported.

4.3.1. Characterization of the adducts produced in the reaction between oxoalkenals and phenolic compounds.

The reaction between oxoalkenals and phenolic compound is complex and different oxoalkenal-phenol adducts are produced in a short time period.

Nevertheless, these adducts are not stable enough to be isolated and characterized since they are not final compounds and spontaneously suffer further reactions such as polymerization. As a consequence of this, the formed adducts had to be stabilized previously to their isolation and characterization. Two ways of stabilization were used: the acetylation of produced carbonyl-phenol adducts and the reduction of the formed adducts with sodium borohydride.

Once they were stabilized, the different carbonyl-phenol adducts produced could be easily identified by GC-MS. **Figure 59** shows the GC-MS chromatogram obtained for the acetylated reaction mixture. An analogous chromatogram was obtained for the reaction mixture reduced with sodium borohydride (data not shown). As observed in **Figure 59**, a very similar chromatographic pattern was always obtained independently of the oxoalkenal or the phenolic compound involved.

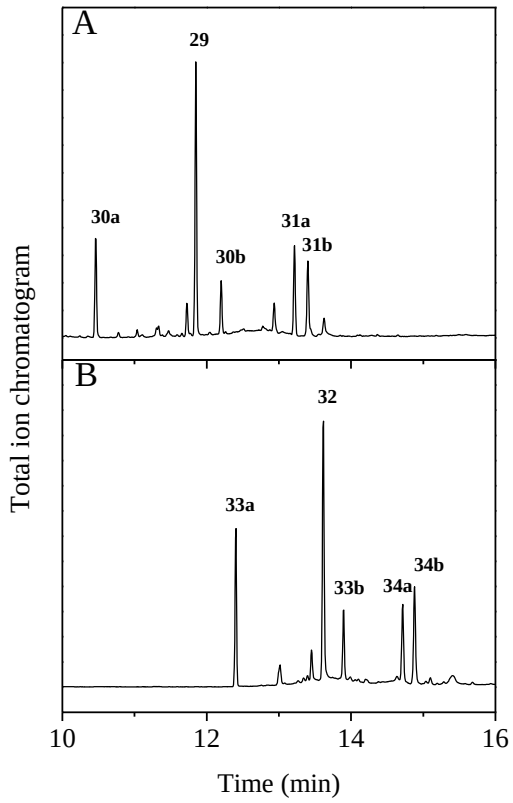

Figure 59. *Total ion chromatograms obtained by GC-MS of the reaction between 2-methylresorcinol and: (A), 4-oxo-2-hexenal, and (B), 4-oxo-2-nonenal, after acetylation. Only the portion corresponding to oxoalkenal/phenol adducts is shown. Chemical structures for the identified compounds are given in* ***Figure 60****.*

Figure 60 shows the chemical structures of the compounds isolated and characterized in the different assayed reactions. Their spectroscopic and spectrometric data are collected in subsections 4.3.1.1 to 4.3.1.5.

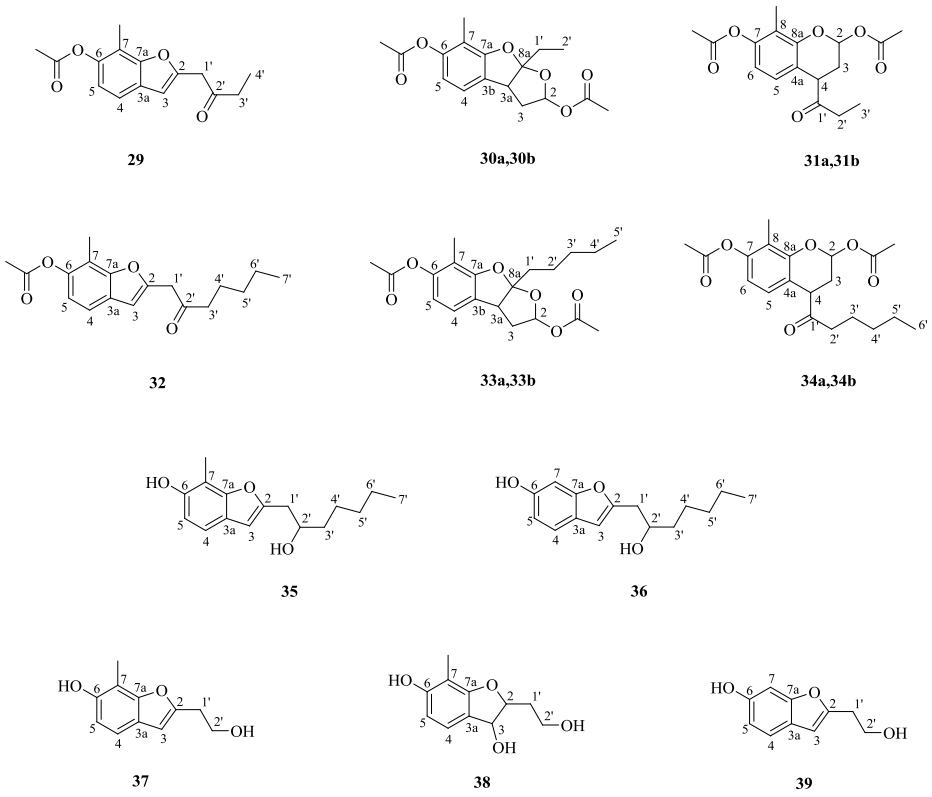

Figure 60. *Chemical structures of carbonyl-phenol adducts isolated and characterized by NMR and MS in the different assayed reactions between oxoalkenals and phenolics. The aldehyde and the phenolic compound involved in the formation of each adduct is described in the text.*

The compounds having a higher response by GC-MS (see, for example, compounds **29** and **32** in **Figure 59**) were always produced although the reactions were carried out in either buffer or methanol/triethylamine. In addition, they were the only adducts that were always isolated for all aldehydes and phenolic compounds assayed, and they were also isolated by employing different ways of stabilization for produced adducts. This compound was a benzofuran-6-ol that was produced by reaction of the oxoalkenal with both one of the hydroxyl groups of the phenol and its contiguous aromatic carbon. The final structure depended on the procedure

employed for its stabilization. Thus, acetylation carried out in adducts **29** and **32**, protected the free phenolic group and avoided that further reactions between this free hydroxyl group at position C6 and the carbonyl group at C2' of other molecules could take place. Similarly, the reduction of the carbonyl group in adducts **35-37**, and **39**, inactivated the carbonyl group at C2' by producing the corresponding hydroxyl group. The absence of a carbonyl group in adducts **35-37** and **39** was likely the reason for their relative stability.

It is also noteworthy the isolation of adduct **38**. This is an intermediate in the formation of adduct **37**. Thus, when compound **38** was heated softly, it was converted into adduct **37** (data not shown). This intermediate could not be isolated in other reactions, more likely because the dehydration was favored by the extension of the conjugation in the benzofuran ring and, therefore, took place rapidly even under soft reaction conditions.

When the reaction was acetylated, two other adducts could be isolated and characterized. Both adducts had several chiral centers. Therefore, different diastereomers were produced as a function of the number of chiral centers created in the reaction.

The first adduct was a 2,3,3a,8a-tetrahydrofuro[2,3-*b*]benzofuran-2,6-diol (compounds **30a**, **30b**, **33a**, and **33b**). Analogously to the benzofuran-6-ols discussed above (compounds **29**, **32**, **35**, **36**, **37**, and **39**), the formation of these adducts also involved the reaction of the oxoalkenal with both one of the hydroxyl groups and its contiguous aromatic carbon. The produced compound was a hemiacetal that could not be isolated from the reduced reaction mixtures. On the other hand, the acetylation protected both the aromatic hydroxyl group and the hemiacetal. Therefore, the existing hydroxyl and carbonyl groups were deactivated and the adduct could be isolated and characterized.

This adduct has three chiral centers (C2, C3a and C8a). Therefore, four diastereomers should be produced. However, only two of them (compounds **30a** and **30b** in **Figure 59A**, and compounds **33a** and **33b** in

Figure 59B) could be isolated and characterized, most likely because only these two diastereomers were produced to a high extent. Both diastereomers had very similar NMR spectra, but, surprisingly, their MS were quite different. The reason should be related to the different configuration of the reactive groups. Thus, compounds **30a** and **33a** lost rapidly acetic acid and the molecular ion could not be detected. On the other hand, compounds **30b** and **33b** lost acetic acid more difficultly and a more complex fragmentation scheme could be observed (see MS data in subsection 4.3.1.1 and 4.3.1.2). Although they could not be isolated, the other two diastereomers could be also present in the reaction mixture. Thus, in **Figure 59A**, the compound appearing at retention time 11.73 min had a mass spectrum very similar to that of diastereomer **30a**, and the compound appearing at retention time 12.94 min had a mass spectrum very similar to that of diastereomer **30b** (data not shown). These two compounds might be hypothesized to be the non-isolated diastereomers of the produced 2,3,3a,8a-tetrahydrofuro[2,3-*b*]benzofuran-2,6-diols.

The third isolated and characterized adduct was a chromane-2,7-diol (compounds **31a**, **31b**, **34a**, and **34b**). This adduct was also produced between the oxoalkenal and both, one of the hydroxyl groups and its contiguous aromatic carbon. This compound was also a hemiacetal and, analogously to the above discussed for 2,3,3a,8a-tetrahydrofuro[2,3-*b*]benzofuran-2,6-diols (compounds **30a**, **30b**, **33a**, and **33b**), this compound could not be isolated from the reduced reaction mixtures. On the other hand, it could be isolated and characterized after acetylation. This was likely a consequence of the stabilization obtained by acetylation. The introduced acetyl groups protected the phenolic group and inhibited the reactivity of the carbonyl group in the stabilized hemiacetal.

Differently to compounds **30a**, **30b**, **33a**, and **33b**, the produced chromane-2,7-diols have two chiral centers (C2 and C4), and two diastereomers should be produced. Both diastereomers could be isolated and characterized. They had very similar NMR and MS spectra.

Therefore, it can be concluded that the reaction between oxoalkenals and phenolic compounds mainly produces in a first step benzofuran-6-ols (**40**), 2,3,3a,8a-tetrahydrofuro[2,3-*b*]benzofuran-2,6-diols (**41**), and chromane-2,7-diols (**42**) (**Figure 61**). These compounds have reactive hydroxyl and carbonyl groups that can be involved in further reactions, which is in agreement with the reactivity observed for the formed adducts.

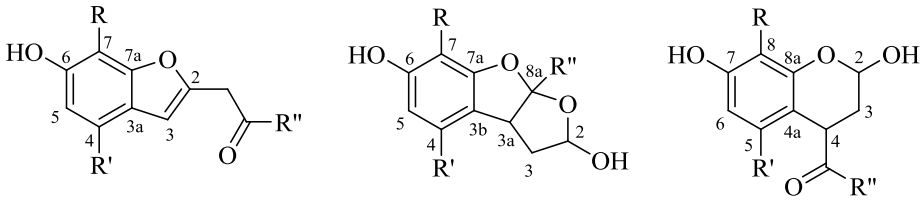

40 **41** **42**

Figure 61. *Chemical structures of adducts produced in the reaction between oxoalkenals and phenolics.*

The spectroscopic and spectrometric data of the carbonyl-phenol adducts isolated and characterized in the different oxoalkenal-phenol reactions assayed are collected in the next subsections.

4.3.1.1. *Compounds isolated and characterized in the reaction of 4-oxo-2-hexenal and 2-methylresorcinol.*

The reaction was carried out in sodium phosphate buffer, pH 8, and later acetylated. Five compounds (**29**-**31**) could be isolated and characterized. The total ion chromatogram of the reaction mixture is shown in **Figure 59A**.

7-Methyl-2-(2-oxobutyl)benzofuran-6-yl acetate (**29**). ^{1}H NMR ($CDCl_3$): δ (ppm) 1.09t (3H, *J* = 7.3 Hz, H4'), 2.33s (3H, CH_3C7), 2.37s (3H, CH_3CO), 2.58q (2H, *J* = 7.3 Hz, H3'), 3.87br (2H, H1'), 6.59t,br (1H, *J* = 0.7 Hz, H3), 6.92d (1H, *J* = 8.3 Hz, H5), and 7.34d (1H, *J* = 8.3 Hz, H4). ^{13}C

NMR ($CDCl_3$): δ (ppm) 7.60 (C4'), 9.28 (CH_3C7), 20.78 ($C\underline{H}_3CO$), 35.41 (C3'), 42.64 (C1'), 105.51 (C3), 114.30 (C7), 117.21 (C5), 117.73 (C4), 126.60 (C3a), 146.02 (C6), 152.08 (C2), 154.20 (C7a), 169.66 (CH_3CO), and 205.92 (CH_2CO). MS, *m/z* (%, ion structure): 260 (7, M^+), 218 (17, M^+ – CH_2CO), and 189 (100, 218 – CH_3CH_2CO).

*8a-Ethyl-7-methyl-2,3,3a,8a-tetrahydrofuro[2,3-b]benzofuran-2,6-diyl diacetat*e (**30a** and **30b**). Two diastereomers of this compound could be isolated and characterized. ^{1}H NMR ($CDCl_3$) of compound **30a**: δ (ppm) 1.05t (3H, *J* = 7.4 Hz, H2'), 2.03q (2H, *J* = 7.4 Hz, H1'), 2.05s (3H, CH_3C7), 2.10s (3H, CH_3CO), 2.33s (3H, CH_3CO), 2.43t (1H, *J* = 5.1 Hz, H3, signal a), 2.46dd (1H, *J* = 3.9 Hz, *J* = 8.8 Hz, H3, signal b), 3.79dd (1H, *J* = 4.7 Hz, *J* = 8.8 Hz, H3a), 6.33dd (1H, *J* = 4.4 Hz, *J* = 5.2 Hz, H2), 6.60d (1H, *J* = 8.0 Hz, H5), and 6.98d (1H, *J* = 8.0 Hz, H4). ^{13}C NMR ($CDCl_3$) of compound **30a**: δ (ppm) 8.02 (C2'), 9.29 (CH_3C7), 20.75 (CH_3CO), 21.16 (CH_3CO), 31.11 (C1'), 39.30 (C3), 46.68 (C3a), 97.99 (C2), 113.58 (C7), 114.64 (C5), 121.30 (C4), 123.15 (C8a), 126.03 (C3b), 149.89 (C6), 157.32 (C7a), 169.35 (CO), and 169.82 (CO). MS, *m/z* (%, ion structure) of compound **30a**: 260 (25, M^+ – CH_3COOH), 218 (49, 260 – CH_2CO), 203 (41, 218 – CH_3), and 189 (100, 218 – CH_2CH_3). ^{1}H NMR ($CDCl_3$) of compound **30b**: δ (ppm) 1.04t (3H, *J* = 7.4 Hz, H2'), 2.02q (2H, *J* = 7.4 Hz, H1'), 2.05s (3H, CH_3C7), 2.10s (3H, CH_3CO), 2.32s (3H, CH_3CO), 2.44m (2H, H3), 3.77dt (1H, *J* = 9.1 Hz, *J* = 0.9 Hz, H3a), 6.35d (1H, *J* = 5.0 Hz, H2), 6.60d (1H, *J* = 7.9 Hz, H5), and 6.99d (1H, *J* = 7.9 Hz, H4). ^{13}C NMR ($CDCl_3$) of compound **30b**: δ (ppm) 7.91 (C2'), 9.22 (CH_3C7), 20.72 (CH_3CO), 21.16 (CH_3CO), 30.32 (C1'), 39.72 (C3), 46.35 (C3a), 98.88 (C2), 112.92 (C7), 114.32 (C5), 120.97 (C4), 124.00 (C8a), 126.66 (C3b), 149.76 (C6), 157.51 (C7a), 169.36 (CO), and 170.20 (CO). MS of compound **30b**, *m/z* (%, ion structure): 320 (13, M^+), 261 (19, M^+ – CH_3COO), 260 (20, M^+ – CH_3COOH), 219 (32, 261 – CH_2CO),

218 (95, 260 – CH_2CO), 203 (37, 218 – CH_3), 190 (11, $C_{11}H_{10}O_3$), 189 (59, 218 – CH_2CH_3), 179 (55, $C_{10}H_{11}O_3$), and 161 (100, $C_{10}H_9O_2$).

8-Methyl-4-propionylchromane-2,7-diyl diacetate (**31a** and **31b**). The two diastereomers of this compound could be isolated and characterized. ^{1}H NMR ($CDCl_3$) of compound **31a**: δ (ppm) 1.10t (3H, *J* = 7.2 Hz, H3'), 2.02s (3H, CH_3C8), 2.11s (3H, CH_3CO), 2.16dd (1H, *J* = 4.1 Hz, *J* = 5.8 Hz, H3, signal a), 2.18dd (1H, *J* = 4.1 Hz, *J* = 5.8 Hz, H3, signal b), 2.34s (3H, CH_3CO), 2.55q (1H, *J* = 7.2 Hz, H2', signal a), 2.88q (1H, *J* = 7.2 Hz, H2', signal b), 4.02dd (1H, *J* = 5.8 Hz, *J* = 10.4 Hz, H4), 6.63t (1H, *J* = 3.4 Hz, H2), 6.68d (1H, *J* = 8.4 Hz, H6), and 6.84d (1H, *J* = 8.4 Hz, H5). ^{13}C NMR ($CDCl_3$) of compound **31a**: δ (ppm) 7.87 (C3'), 9.20 ($\underline{C}H_3$C8), 20.79 (CH_3CO), 21.17 (CH_3CO), 28.14 (C3), 33.95 (C2'), 44.55 (C4), 89.34 (C2), 115.27 (C6), 116.87 (C4a), 119.84 (C8), 125.43 (C5), 149.24 (C7), 150.09 (C8a), 169.24 ($CH_3\underline{C}O$), 169.47 ($CH_3\underline{C}O$), and 207.82 (CH_2CO). MS of compound **31a**, *m/z* (%, ion structure): 320 (1, M^+), 278 (0.1, M^+ – CH_2CO), 261 (4, M^+ – CH_3COO), 260 (6, M^+ – CH_3COOH), 236 (0.1, 278 – CH_2CO), 219 (7, 261 – CH_2CO), 218 (8, 260 – CH_2CO), 203 (24, 260 – CH_3CH_2CO), 179 (10, 236 – CH_3CH_2CO), and 161 (100, 218 – CH_3CH_2CO or 203 – CH_2CO). ^{1}H NMR ($CDCl_3$) of compound **31b**: δ (ppm) 1.05t (3H, *J* = 7.2 Hz, H3'), 2.04s (3H, CH_3C8), 2.11s (3H. CH_3CO), 2.22ddd (1H, *J* = 2.4 Hz, *J* = 7.3 Hz, *J* = 14.3 Hz, H3, signal a), 2.34s (3H, CH_3CO), 2.47q (1H, *J* = 7.1 Hz, H2', signal a), 2.56q (1H, *J* = 7.1 Hz, H2', signal b), 2.81dt (1H, *J* = 2.4 Hz, *J* = 14.3 Hz, H3, signal b), 3.53dd (1H, *J* = 2.0 Hz, *J* = 7.2 Hz, H4), 6.57t (1H, *J* = 2.5 Hz, H2), 6.75d (1H, *J* = 8.3 Hz, H6), and 7.00d (1H, *J* = 8.3 Hz, H5). ^{13}C NMR ($CDCl_3$) of compound **31b**: δ (ppm) 7.69 (C3'), 9.26 ($\underline{C}H_3$C8), 20.80 (CH_3CO), 21.17 (CH_3CO), 27.98 (C3), 34.34 (C2'), 44.33 (C4), 89.56 (C2), 115.11 (C6), 116.49 (C4a), 119.54 (C8), 128.36 (C5), 149.35 (C7), 149.94 (C8a), 169.24 ($CH_3\underline{C}O$), 169.46 ($CH_3\underline{C}O$), and 207.44 (CH_2CO). MS of compound **31b**, *m/z* (%, ion structure): 320 (1, M^+), 278 (0.1, M^+ – CH_2CO), 261 (3, M^+ – CH_3COO), 260 (2, M^+ – CH_3COOH), 236 (0.1, 278 –

CH_2CO), 219 (7, 261 – CH_2CO), 218 (6, 260 – CH_2CO), 203 (24, 260 – CH_3CH_2CO), 179 (11, 236 – CH_3CH_2CO), and 161 (100, 218 – CH_3CH_2CO or 203 – CH_2CO).

4.3.1.2. Compounds isolated and characterized in the reaction of 4-oxo-2-nonenal and 2-methylresorcinol.

This reaction was studied both after acetylation and after reduction with sodium borohydride. When the reaction was carried out with 4-oxo-2-nonenal in sodium phosphate buffer, pH 8, and later acetylated, five compounds (**32**-**34**), analogous to the above described for the reaction between 4-oxo-2-hexenal and 2-methylresorcinol, could be isolated and characterized (total ion chromatogram of the reaction mixture is shown in **Figure 59B**). When the reaction was carried out in methanol/triethylamine and was later reduced with sodium borohydride only one compound (compound **35**) could be isolated and characterized. Compound **35** was analogous to compound **32**.

7-Methyl-2-(2-oxoheptyl)benzofuran-6-yl acetate (**32**). ^{1}H NMR ($CDCl_3$): δ (ppm) 0.90t (3H, *J* = 7.1 Hz, H7'), 1.30m (4H, H5' and H6'), 1.62 qu (2H, *J* = 7.4 Hz, H4'), 2.34s (3H, CH_3C7), 2.37s (3H, CH_3CO), 2.54t (2H, *J* = 7.4 Hz, H3'), 3.86s (2H, H1'), 6.59t,br (1H, *J* = 0.8 Hz, H3), 6.92d (1H, *J* = 8.3 Hz, H5), and 7.34d (1H, *J* = 8.3 Hz, H4). ^{13}C NMR ($CDCl_3$): δ (ppm) 9.28 (CH_3C7), 13.88 (C7'), 20.78 ($C\underline{H}_3CO$), 22.42 (C6'), 23.28 (C4'), 31.24 (C5'), 42.12 (C3'), 42.93 (C1'), 105.50 (C3), 114.30 (C7), 117.21 (C5), 117.72 (C4), 126.07 (C3a), 146.01 (C6), 152.08 (C2), 154.19 (C7a), 169.65 (CH_3CO), and 205.53 (CH_2CO). MS, *m/z* (%, ion structure): 302 (8, M^+), 260 (21, M^+ – CH_2CO), 231 (2, M^+ – $CH_3CH_2CH_2CH_2CH_2$), 203 (2, M^+ – $CH_3CH_2CH_2CH_2CH_2CO$), and 161 (100, 260 – $CH_3CH_2CH_2CH_2CH_2CO$).

7-Methyl-8a-pentyl-2,3,3a,8a-tetrahydrofuro[2,3-b]benzofuran-2,6-diyl diacetate (**33a** and **33b**). Two diastereomers of this compound could be isolated and characterized. ^{1}H NMR ($CDCl_3$) of compound **33a**: δ (ppm) 0.91t (3H, *J* = 7.1 Hz, H5'), 1.35m (4H, H3' and H4'), 1.50m (2H, H2'), 1.97m (2H, H1'), 2.05s (3H, CH_3C7), 2.09s (3H, CH_3CO), 2.32s (3H, CH_3CO), 2.42t (1H, *J* = 5.0 Hz, H3, signal a), 2.45dd (1H, *J* = 3.9 Hz, *J* = 8.9 Hz, H3, signal b), 3.79dd (1H, *J* = 4.6 Hz, *J* = 8.8 Hz, H3a), 6.32dd (1H, *J* = 4.1 Hz, *J* = 5.1 Hz, H2), 6.60d (1H, *J* = 8.0 Hz, H5), and 6.97d (1H, *J* = 8.0 Hz, H4). ^{13}C NMR ($CDCl_3$) of compound **33a**: δ (ppm) 9.31 (CH_3C7), 13.97 (C5'), 20.75 (CH_3CO), 21.16 (CH_3CO), 22.47 (C4'), 23.26 (C2'), 31.77 (C3'), 38.11 (C1'), 39.25 (C3), 47.17 (C3a), 97.95 (C2), 113.58 (C7), 114.62 (C5), 121.30 (C4), 122.77 (C8a), 126.01 (C3b), 149.90 (C6), 157.28 (C7a), 169.28 (CO), and 169.73 (CO). MS, *m/z* (%, ion structure) of compound **33a**: 302 (30, M^+ – CH_3COOH), 273 (12, 302 – CH_3CH_2), 260 (66, 302 – CH_2CO), 231 (100, 302 – $CH_3CH_2CH_2CH_2CH_2$ or 260 – CH_3CH_2), 203 (73, 260 – $CH_3CH_2CH_2CH_2$), 190 (8, 260 – pentene) and 189 (4, 260 – $CH_3CH_2CH_2CH_2CH_2$). ^{1}H NMR ($CDCl_3$) of compound **33b**: δ (ppm) 0.91t (3H, *J* = 7.1 Hz, H5'), 1.35m (4H, H3' and H4'), 1.50m (2H, H2'), 1.97m (2H, H1'), 2.05s (3H, CH_3C7), 2.09s (3H, CH_3CO), 2.32s (3H, CH_3CO), 2.44m (2H, H3), 3.78d (1H, *J* = 9.3 Hz, H3a), 6.34d (1H, *J* = 4.7 Hz, H2), 6.60d (1H, *J* = 8.0 Hz, H5), and 6.97d (1H, *J* = 8.0 Hz, H4). ^{13}C NMR ($CDCl_3$) of compound **33b**: δ (ppm) 9.31 (CH_3C7), 13.98 (C5'), 20.73 (CH_3CO), 21.17 (CH_3CO), 22.44 (C4'), 23.19 (C2'), 31.74 (C3'), 37.42 (C1'), 39.69 (C3), 46.81 (C3a), 98.92 (C2), 112.92 (C7), 114.29 (C5), 120.96 (C4), 123.62 (C8a), 126.66 (C3b), 149.77 (C6), 157.47 (C7a), 169.30 (CO), and 169.74 (CO). MS, *m/z* (%, ion structure) of compound **33b**: 362 (7, M^+), 320 (0.3, M^+ – CH_2CO), 303 (14, M^+ – CH_3COO), 302 (24, M^+ – CH_3COOH), 278 (0.2, 320 – CH_2CO), 261 (26, 303 – CH_2CO), 260 (100, 302 – CH_2CO), 231 (44, 260 – CH_3CH_2), 217 (7, 260 – $CH_3CH_2CH_2$), 203 (55, 260 – $CH_3CH_2CH_2CH_2$), 179 (28, $C_{10}H_{11}O_3$), 175 (38), and 161 (68, $C_{10}H_9O_2$).

4-Hexanoyl-8-methylchromane-2,7-diyl diacetate (**34a** and **34b**). The two diastereomers of this compound could be isolated and characterized. ^{1}H NMR ($CDCl_3$) of compound **34a**: δ (ppm) 0.90t (3H, *J* = 7.3 Hz, H6'), 1.35m (4H, H4' and H5'), 1.49m (2H, H3'), 2.02s (3H, CH_3C8), 2.10s (3H, CH_3CO), 2.15dd (1H, *J* = 4.0 Hz, *J* = 5.8 Hz, H3, signal a), 2.17dd (1H, *J* = 4.0 Hz, *J* = 5.8 Hz, H3, signal b), 2.33s (3H, CH_3CO), 2.53t (2H, *J* = 7.4 Hz, H2'), 4.01dd (1H, *J* = 5.8 Hz, *J* = 10.5 Hz, H4), 6.63t (1H, *J* = 3.4 Hz, H2), 6.68d (1H, *J* = 8.4 Hz, H6), and 6.84d (1H, *J* = 8.4 Hz, H5). ^{13}C NMR ($CDCl_3$) of compound **34a**: δ (ppm) 9.20 ($\underline{C}H_3C8$), 13.88 (C6'), 20.77 (CH_3CO), 21.15 (CH_3CO), 22.44 (C5'), 23.40 (C3'), 28.12 (C3), 31.38 (C4'), 40.65 (C2'), 44.69 (C4), 89.33 (C2), 115.24 (C6), 116.81 (C4a), 119.80 (C8), 125.76 (C5), 149.24 (C7), 150.09 (C8a), 169.16 ($CH_3\underline{C}O$), 169.40 ($CH_3\underline{C}O$), and 210.36 (CH_2CO). MS of compound **34a**, *m/z* (%, ion structure): 362 (0.3, M^+), 303 (3, M^+ – CH_3COO), 302 (3, M^+ – CH_3COOH), 261 (4, 303 – CH_2CO), 260 (6, 302 – CH_2CO), 203 (39, 260 – $CH_3CH_2CH_2CH_2$) and 161 (100, 260 – $CH_3CH_2CH_2CH_2CH_2CO$). ^{1}H NMR ($CDCl_3$) of compound **34b**: δ (ppm) 0.88t (3H, *J* = 7.3 Hz, H6'), 1.38m (4H, H4' and H5'), 1.48m (2H, H3'), 2.04s (3H, CH_3C8), 2.10s (3H. CH_3CO), 2.22ddd (1H, *J* = 2.4 Hz, *J* = 7.3 Hz, *J* = 14.3 Hz, H3, signal a), 2.32s (3H, CH_3CO), 2.46m (2H, H2'), 2.78dt (1H, *J* = 2.6 Hz, *J* = 14.3 Hz, H3, signal b), 3.53dd (1H, *J* = 2.3 Hz, *J* = 7.3 Hz, H4), 6.56t (1H, *J* = 2.6 Hz, H2), 6.74d (1H, *J* = 8.4 Hz, H6), and 6.99d (1H, *J* = 8.4 Hz, H5). ^{13}C NMR ($CDCl_3$) of compound **34b**: δ (ppm) 9.26 ($\underline{C}H_3C8$), 13.90 (C6'), 20.75 (CH_3CO), 21.16 (CH_3CO), 22.55 (C5'), 23.39 (C3'), 27.83 (C3), 31.39 (C4'), 43.68 (C2'), 44.63 (C4), 89.58 (C2), 115.09 (C6), 116.40 (C4a), 119.50 (C8), 128.35 (C5), 149.31 (C7), 149.96 (C8a), 169.21 ($CH_3\underline{C}O$), 169.78 ($CH_3\underline{C}O$), and 207.44 (CH_2CO). MS of compound **34b**, *m/z* (%, ion structure): 362 (0.2, M^+), 303 (3, M^+ – CH_3COO), 302 (2, M^+ – CH_3COOH), 261 (4, 303 – CH_2CO), 260 (7, 302 – CH_2CO), 203 (34, 260 – $CH_3CH_2CH_2CH_2$) and 161 (100, 260 – $CH_3CH_2CH_2CH_2CH_2CO$).

2-(2-Hydroxyheptyl)-7-methylbenzofuran-6-ol (**35**). ^{1}H NMR (CD_3OD): δ (ppm) 0.92t (3H, *J* = 6.9 Hz, H7'), 1.35m (6H, H4', H5', and H6'), 1.56m (2H, H3'), 2.32s (3H, CH_3C7), 2.87d (2H, *J* = 6.4 Hz, H1'), 3.97m (1H, H2'), 6.38s (1H, H3), 6.69d (1H, *J* = 8.3 Hz, H5), and 7.09d (1H, *J* = 8.3 Hz, H4). ^{13}C NMR (CD_3OD): δ (ppm) 7.28 ($\underline{C}H_3C7$), 13.03 (C7'), 22.30 (C6'), 24.99 (C4'), 31.63 (C5'), 36.31 (C1'), 36.51 (C3'), 69.66 (C2'), 103.30 (C3), 106.94 (C7), 110.79 (C5), 116.48 (C4), 121.01 (C3a), 151.85 (C6), 154.68 (C2), and 154.86 (C7a). MS, *m/z* (%, ion structure): 262 (44, M^+), 191 (56, $M^+ - CH_3CH_2CH_2CH_2CH_2$), 162 (64, $C_{10}H_{10}O_2$), 161 (47, $C_{10}H_9O_2$), and 149 (100, $C_9H_9O_2$).

4.3.1.3. Compounds isolated and characterized in the reaction of 4-oxo-2-nonenal and resorcinol.

This reaction was carried out in methanol/triethylamine and was later reduced with sodium borohydride. Only compound **36** could be isolated and characterized.

2-(2-hydroxyheptyl)benzofuran-6-ol (**36**). ^{1}H NMR (CD_3OD): δ (ppm) 0.92t (3H, *J* = 6.9 Hz, H7'), 1.34m (6H, H4', H5', and H6'), 1.51m (2H, H3'), 2.85d (2H, *J* = 6.2 Hz, H1'), 3.95m (1H, H2'), 6.40d (1H, *J* = 0.8 Hz, H3), 6.70dd (1H, *J* = 2.0 Hz, *J* = 8.4 Hz, H5), 6.84d (1H, *J* = 2.0 Hz, H7), and 7.27d (1H, *J* = 8.4 Hz, H4). ^{13}C NMR (CD_3OD): δ (ppm) 13.04 (C7'), 22.29 (C6'), 25.00 (C4'), 31.60 (C5'), 36.24 (C1'), 36.56 (C3'), 69.63 (C2'), 97.10 (C7), 102.79 (C3), 111.12 (C5), 119.87 (C4), 121.40 (C3a), 154.42 (C6), 154.84 (C2), and 155.79 (C7a). MS, *m/z* (%, ion structure): 248 (30, M^+), 177 (48, $M^+ - CH_3CH_2CH_2CH_2CH_2$), 148 (57, $C_9H_8O_2$), 147 (46, $C_9H_7O_2$), and 135 (100, $C_8H_7O_2$).

4.3.1.4. Compounds isolated and characterized in the reaction of fumaraldehyde and 2-methylresorcinol.

This reaction was carried out in sodium phosphate buffer, pH 7.0, and was later reduced with sodium borohydride. Two compounds (**37** and **38**) were isolated and characterized.

2-(2-Hydroxyethyl)-7-methylbenzofuran-6-ol (**37**). ^{1}H NMR (CD_3OD): δ (ppm) 1.98s (3H, CH_3C7), 2.94t (2H, *J* = 7.0 Hz, H1'), 3.88t (2H, *J* = 7.0 Hz, H2'), 6.35s (1H, H3), 6.68d (1H, *J* = 8.5 Hz, H5), and 7.04d (1H, *J* = 8.5 Hz, H4). ^{13}C NMR (CD_3OD): δ (ppm) 8.60 (CH_3C7), 33.03 (C1'), 61.72 (C2'), 104.30 (C3), 108.42 (C7), 112.10 (C5), 118.10 (C4), 124.45 (C3a), 153.22 (C6), 155.65 (C2), and 155.85 (C7a). MS of the trimethylsilyl derivative, *m/z* (%, ion structure): 336 (32, M^+), 321 (13, $M^+ - CH_3$), 233 (100, M+ – CH_2OTMSi), and 73 (41, TMSi).

2-(2-Hydroxyethyl)-7-methyl-2,3-dihydrobenzofuran-3,6-diol (**38**). ^{1}H NMR (CD_3OD): δ (ppm) 2.02s (3H, CH_3C7), 2.04m (2H, H1'), 3.45t (2H, *J* = 7.0 Hz, H2'), 5.23t (1H, *J* = 5.8 Hz, H2), 5.50d (1H, *J* = 5.8 Hz, H3), 6.35d (1H, *J* = 8.1 Hz, H5), and 6.94d (1H, *J* = 8.1 Hz, H4). ^{13}C NMR (CD_3OD): δ (ppm) 8.53 (CH_3C7), 35.64 (C1'), 65.94 (C2'), 84.66 (C3), 87.97 (C2), 107.12 (C7), 108.75 (C5), 116.81 (C3a), 124.01 (C4), 158.61 (C6), and 162.22 (C7a). MS of the trimethylsilyl derivative, *m/z* (%, ion structure): 426 (12, M^+), 411 (27, $M^+ - CH_3$), 336 (9, M+ – TMSiOH), 323 (39, M^+ – CH_2OTMSi), 321 (27, 336 – CH_3), 308 (31, $M^+ - CH_3CH_2OTMSi$), 307 (39), 293 (22, 308 – CH_3), 247 (21, 336 – TMSiO), 233 (31, 336 – $TMSiOCH_2$), and 73 (100, TMSi).

4.3.1.5. Compounds isolated and characterized in the reaction of fumaraldehyde and resorcinol.

This reaction was carried out in sodium phosphate buffer, pH 7.0, and was later reduced with sodium borohydride. Only compound **39** was isolated and characterized.

2-(2-Hydroxyethyl)benzofuran-6-ol (**39**). ^{1}H NMR (CD_3OD): δ (ppm) 2.92dt (2H, *J* = 0.8 Hz, *J* = 6.9 Hz, H1'), 3.86t (2H, *J* = 6.9 Hz, H2'), 6.38d (1H, *J* = 0.8 Hz, H3), 6.68dd (1H, *J* = 2.2 Hz, *J* = 8.4 Hz, H5), 6.84dd (1H, *J* = 0.8 Hz, *J* = 2.2 Hz, H7), and 7.24d (1H, *J* = 8.4 Hz, H4). ^{13}C NMR (CD_3OD): δ (ppm) 33.14 (C1'), 61.31 (C2'), 98.73 (C7), 104.10 (C3), 112.77 (C5), 121.55 (C4), 123.00 (C3a), 156.12 (C6), 156.33 (C2), and 157.46 (C7a). MS, *m/z* (%, ion structure): 178 (47, M^+), and 147 (100, $M^+ - CH_2OH$).

4.3.2. Effect of reaction conditions on the formation of oxoalkenal-phenol adducts in the reaction of 4-oxo-2-hexenal and 2-methylresorcinol.

The effects of pH, reactant concentration, time, and temperature on the reaction between 4-oxo-2-hexenal and 2-methylresorcinol were studied to find out the reaction conditions that favored the formation of carbonyl-phenol adducts. As shown in **Figure 59A**, five adducts were observed by GC-MS after acetylation of the reaction mixture: one of them was a *benzofuran-6-yl acetate* (compound **29**), other two adducts were 2,3,3a,8a-tetrahydrofuro[2,3-b]benzofuran-2,6-diyl diacetates (compounds **30a** and **30b**), and the other two adducts were chromane-2,7-diyl diacetates (compounds **31a** and **31b**). The effect of reaction conditions on the formation of all of them was studied.

The effect of pH is shown in **Figure 62**. Most adducts were produced to a higher extent at pH 7-8 and their concentration decreased to a higher pH

values. Only the concentration of compound **29** increased slightly from pH 8 to pH 9, although its concentration at pH 9 was lower than that at pH 7.

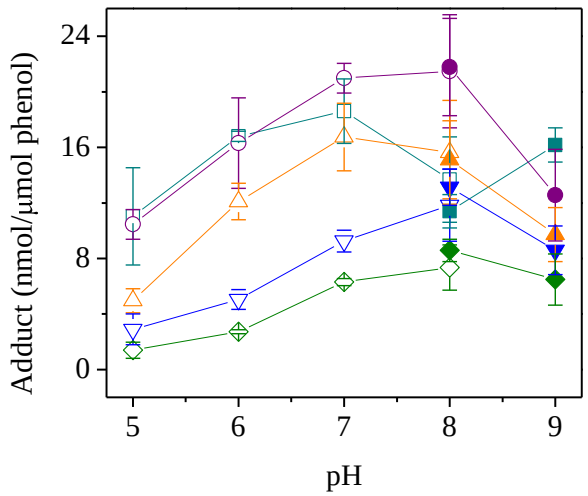

Figure 62. *Effect of reaction pH on the formation of carbonyl-phenol adducts. Reactions were carried out by heating a mixture of 4-oxo-2-hexenal (40 µmol) and 2-methylresorcinol (30 µmol) in 300 µl of 0.3 M buffer for 30 min at 100 ºC under nitrogen. The carbonyl-phenol adducts produced were compounds* ***29*** *(□,■),* ***30a*** *(○,●),* ***30b*** *(△,▲),* ***31a*** *(▽,▼), and* ***31b*** *(◇,◆). Three buffers were employed: 0.3 M sodium citrate buffer, pH 5, sodium phosphate, pH 6–8 (open symbols), and 0.3 M sodium borate buffer,pH 8–9 (closed symbols).*

As expected, adduct concentration depended on the concentration of both the oxoalkenal and the phenolic compound, and increased when the concentration of any of them increased (**Figures 63** and **64**, respectively). Adduct concentration exhibited a great dependence on the oxoalkenal concentration (**Figure 63**) and this dependence was less relevant in relation to the concentration of the phenolic compound (**Figure 64**). In relation to the aldehyde, the different adducts exhibited different behaviors. Thus, compound **29** increased linearly ($r = 0.999$, $p < 0.0001$) as a function of the concentration

of the oxoalkenal (**Figure 63**). On the contrary, compound **30a** was mostly favored at low concentrations of oxoalkenal, and its diastereomer compound **30b** was mostly favored at high concentrations of oxoalkenal. In fact, considering the concentrations of diastereomers **30a** and **30b** altogether, their concentration increased linearly (r = 0.995, p < 0.0001) as a function of the concentration of the oxoalkenal. In relation to compounds **31a** and **31b**, both compounds were favored at high concentrations of the aldehyde and, when considered altogether, their concentration seemed to follow an exponential growth (r^2 = 0.999) as a function of the concentration of the oxoalkenal.

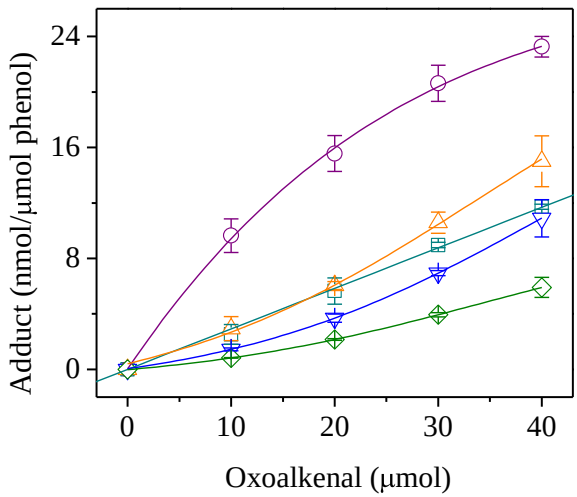

Figure 63. *Effect of oxoalkenal concentration on the formation of carbonyl-phenol adducts. Reactions were carried out by heating a mixture of 4-oxo-2-hexenal at the indicated concentrations and 2-methylresorcinol (30 µmol) in 300 µl of 0.3 M sodium phosphate buffer, pH 8, for 30 min at 100 ºC under nitrogen. The carbonyl-phenol adducts produced were compounds* ***29*** *(□),* ***30a*** *(○),* ***30b*** *(△),* ***31a*** *(▽), and* ***31b*** *(◇).*

Different to this behavior, an increase in the concentration of the phenolic compound only seemed to favor the formation of compound **29**, which increased linearly (r = 0.993, p = 0.0001) as a function of the

concentration of the phenolic compound (**Figure 64**). On the contrary, the concentration of compounds **30-31** seemed to achieve the maximum value when 30 µmol of 2-methylresorcinol were added and further additions of 2-methylresorcinol did not produce increases in the formed amounts of these adducts.

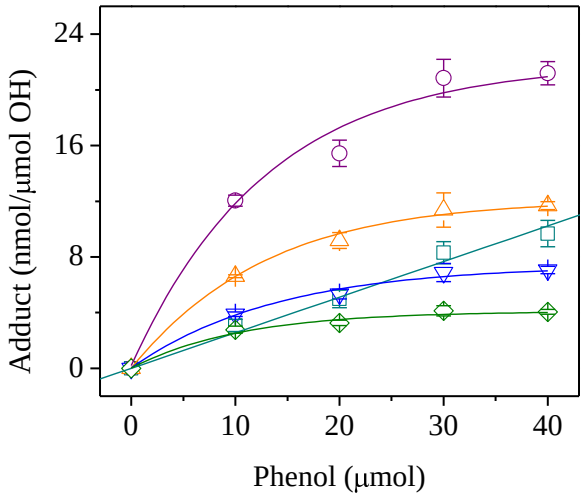

Figure 64. *Effect of phenol concentration on the formation of carbonyl-phenol adducts. Reactions were carried out by heating a mixture of 4-oxo-2-hexenal (40 µmol) and 2-methylresorcinol at the indicated concentrations in 300 µl of 0.3 M sodium phosphate buffer, pH 8, for 30 min at 100 ºC under nitrogen. The carbonyl-phenol adducts produced were compounds* ***29*** *(□),* ***30a*** *(○),* ***30b*** *(△),* ***31a*** *(▽), and* ***31b*** *(◇). OH, 4-oxo-2-hexenal.*

Figures 65-69 show the effect of reaction time and temperature on adduct formation. As can be observed, concentration of all adducts exhibited a great dependence on both time and temperature.

In general, the formation of the adducts was very fast, and a significant concentration of them was observed after very short reaction times. In addition, high temperatures (140 ºC) and long heating times (1 h) mostly promoted their disappearance. On the contrary, low temperatures (60 ºC) seemed to promote their formation as a function of the heating time. An intermediate temperature (100 ºC) mostly promoted their formation at low reaction times (20 min) and, then, their degradation at higher reaction times (1 h). Although there were exceptions, the highest amount of the different adducts was usually obtained after 20 min when heated at 100 ºC and after 60 min when heated at 60 ºC.

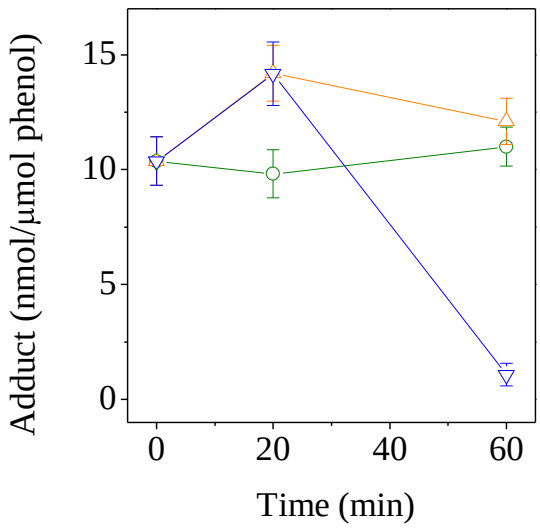

Figure 65. *Effect of reaction time and temperature on the formation of compound* ***29****. Reactions were carried out by heating a mixture of 4-oxo-2-hexenal (40 µmol) and 2-methylresorcinol (30 µmol) in 300 µl of 0.3 M sodium phosphate buffer, pH 8, at the indicated times and temperatures under nitrogen. The assayed temperatures were: 60 (○), 100 (△), and 140 ºC (▽).*

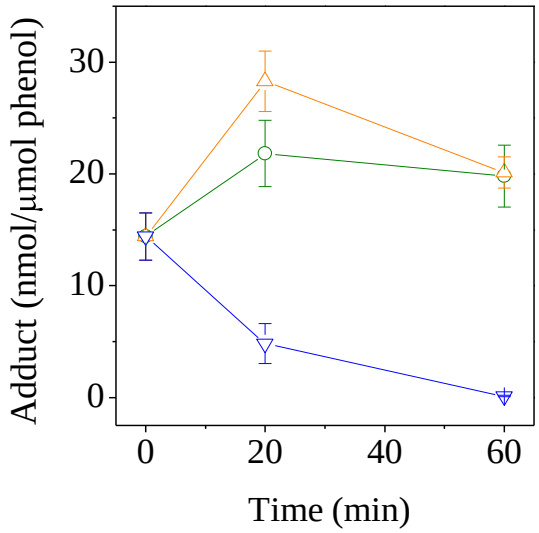

***Figure 66**. Effect of reaction time and temperature on the formation of compound **30a**. Reactions were carried out by heating a mixture of 4-oxo-2-hexenal (40 µmol) and 2-methylresorcinol (30 µmol) in 300 µl of 0.3 M sodium phosphate buffer, pH 8, at the indicated times and temperatures under nitrogen. The assayed temperatures were: 60 (○), 100 (△), and 140 ºC (▽).*

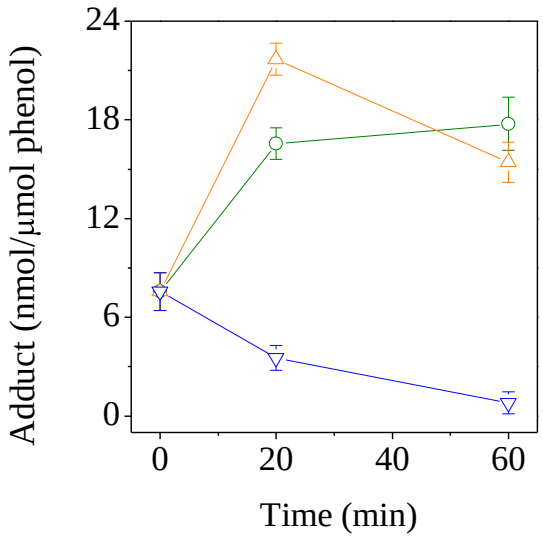

Figure 67. *Effect of reaction time and temperature on the formation of compound* ***30b****. Reactions were carried out by heating a mixture of 4-oxo-2-hexenal (40 µmol) and 2-methylresorcinol (30 µmol) in 300 µl of 0.3 M sodium phosphate buffer, pH 8, at the indicated times and temperatures under nitrogen. The assayed temperatures were: 60 (○), 100 (△), and 140 ºC (▽).*

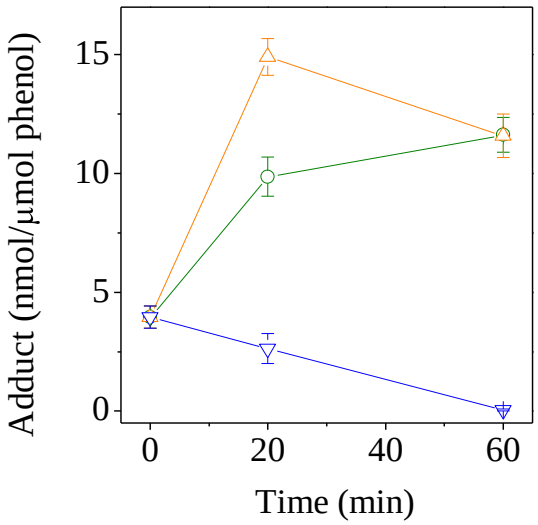

Figure 68. *Effect of reaction time and temperature on the formation of compound* ***31a****. Reactions were carried out by heating a mixture of 4-oxo-2-hexenal (40 µmol) and 2-methylresorcinol (30 µmol) in 300 µl of 0.3 M sodium phosphate buffer, pH 8, at the indicated times and temperatures under nitrogen. The assayed temperatures were: 60 (○), 100 (△), and 140 ºC (▽).*

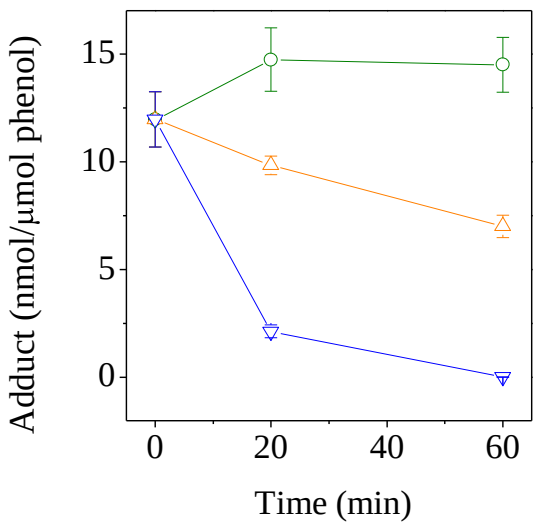

Figure 69. *Effect of reaction time and temperature on the formation of compound* ***31b****. Reactions were carried out by heating a mixture of 4-oxo-2-hexenal (40 µmol) and 2-methylresorcinol (30 µmol) in 300 µl of 0.3 M sodium phosphate buffer, pH 8, at the indicated times and temperatures under nitrogen. The assayed temperatures were: 60 (○), 100 (△), and 140 ºC (▽).*

4.4. Thermal degradation of unsaturated aldehydes.

In addition to the above described reactions of phenolics with alkanals (section 4.1), epoxyalkenals (section 4.2), and oxoalkenals (section 4.3), the carbonyl-phenol adducts produced with some other lipid-derived aldehydes were also studied, but carbonyl-phenol adducts were not produced to a high extent because the studied aldehydes resulted unstable and suffered degradative reactions upon heating. These reactions produced new aldehydes that were able to react with the phenolic compounds producing the corresponding carbonyl-phenol adducts. These reactions complicated considerably the compounds produced in carbonyl-phenol reaction mixtures.

In an attempt to both clarify the stability of 2-alkenals and 2,4-alkadienals upon thermal treatment and to characterize the compounds produced as a consequence of their degradation, this section describes the identification and quantification of the thermal degradation products of 2-alkenals and 2,4-alkadienals. As models of 2-alkenals and 2,4-alkadienals, 2-pentenal and 2,4-heptadienal, respectively, were selected as oxidation products of ω3 fatty acid chains, and 2-octenal and 2,4-decadienal, respectively, were selected as oxidation products of ω6 fatty acid chains.

4.4.1. Thermal degradation of 2-alkenals and 2,4-alkadienals.

2-Alkenals and 2,4-alkadienals were more or less stable upon heating depending on the presence of both air and buffers. **Figure 70** shows the chromatograms obtained by GC-MS after 1 h heating at 200 ºC for the four assayed aldehydes: 2-pentenal (chromatograms **a**–**d**), 2-octenal (chromatograms **e**–**h**), 2,4-heptadienal (chromatograms **i**–**l**), and 2,4-decadienal (chromatograms **m**–**p**). The first chromatogram of each series (chromatograms **a**, **e**, **i**, and **m**) corresponds to the aldehyde with no solvent added and heated under nitrogen. The second chromatogram of each series (chromatograms **b**, **f**, **j**, and **n**) corresponds to the aldehyde with no solvent added and heated under air. The third chromatogram of each series (chromatograms **c**, **g**, **k**, and **o**) corresponds to the solution of the aldehyde in a buffer that was heated under nitrogen. The fourth chromatogram of each series (chromatograms **d**, **h**, **l**, and **p**) corresponds to the solution of the aldehyde in a buffer that was heated under air. Although two buffers were used in the different experiments, because the results obtained using either sodium phosphate buffer, pH 8, or sodium borate buffer, pH 8, were identical, only the chromatograms obtained using sodium phosphate buffer are shown in **Figure 70** (chromatograms **c**, **d**, **g**, **h**, **k**, **l**, **o**, and **p**).

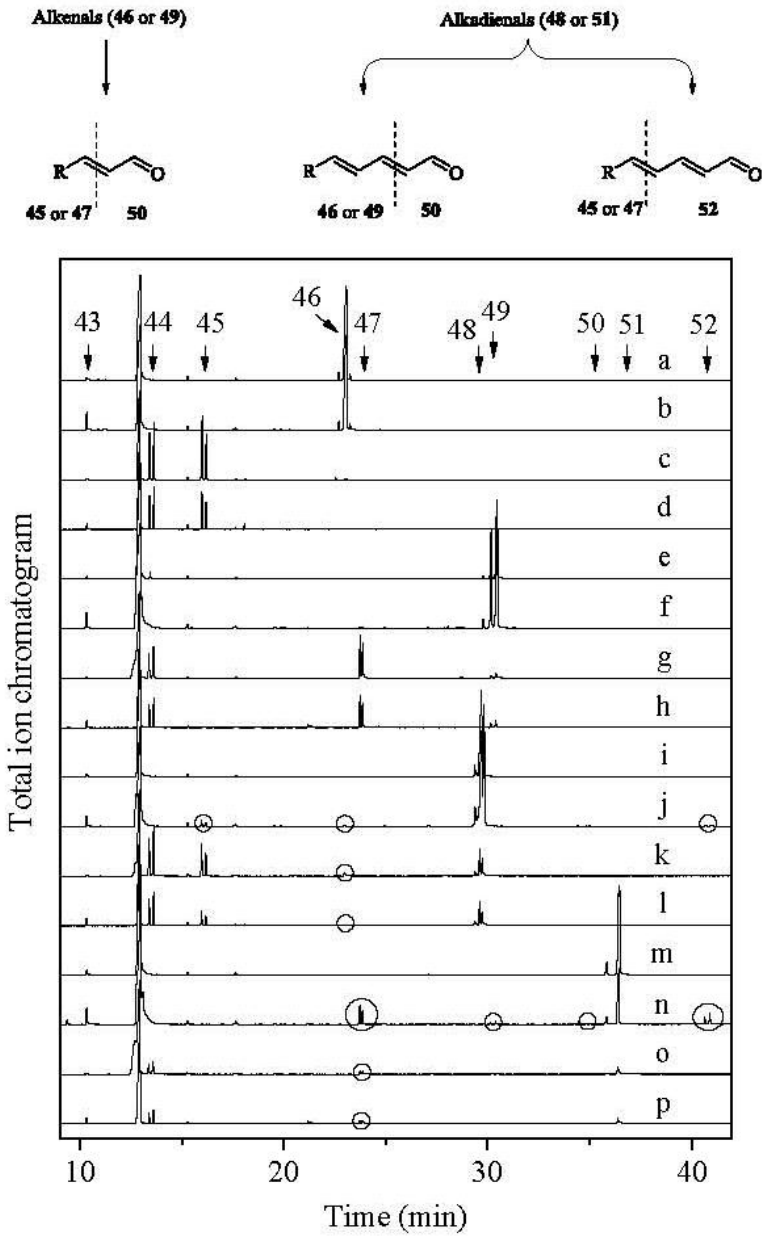

***Figure 70**. Total ion chromatograms obtained by GC-MS for: 2-pentenal (**a**-**d**), 2-octenal (**e**-**h**), 2,4-heptadienal (**i**-**l**), and 2,4-decadienal (**m**-**p**). All samples were heated for 1 h at 200 ºC and, then, derivatized with O-(2,3,4,5,6-pentafluorobenzyl)hydroxylamine hydrochloride. Compounds identified were: formaldehyde (**43**), acetaldehyde (**44**), propanal (**45**), 2-pentenal (**46**), hexanal (**47**), 2,4-heptadienal (**48**), 2-octenal (**49**), glyoxal (**50**), 2,4-decadienal (**51**), and fumaraldehyde (**52**).*

2-Alkenals and 2,4-alkadienals mostly remained unchanged in the absence of both buffer and air. Thus, 2-pentenal (**46**) with no solvent added was relatively stable after heating under nitrogen (chromatogram **a**). Something similar occurred for 2-octenal (**49**, chromatogram **e**), 2,4-heptadienal (**48**, chromatogram **i**), and 2,4-decadienal (**51**, chromatogram **m**).

When the aldehyde with no solvent added was heated in the presence of air, the most significant change produced was the appearance of formaldehyde (**43**, chromatograms **b**, **f**, **j**, and **n**, for the heating of 2-pentenal, 2-octenal, 2,4-heptadienal, and 2,4-decadienal, respectively, under air). In addition, the formation of minute amounts of glyoxal (**50**) and fumaraldehyde (**52**) were also observed in chromatograms **j** and **n** corresponding to the thermal degradation of 2,4-heptadienal and 2,4-decadienal, respectively. Furthermore, the formation of trace amounts of 2-pentenal (**46**) and propanal (**45**) in chromatogram **j**, and of 2-octenal (**49**) and hexanal (**47**) in chromatogram **n** were also observed.

Aldehydes suffered a higher decomposition in the presence of buffer. However, dialdehydes glyoxal (**50)** and fumaraldehyde (**52)** were not observed under these reaction conditions, and formaldehyde (**43**) was detected to a lower extent than when the buffer was absent. On the other hand, shorter aldehydes were produced to a higher extent and a similar decomposition was observed in the presence and in the absence of air. Thus, 2-pentenal (**46**) disappeared completely after 1 h at 200 ºC (chromatograms **c** and **d** for nitrogen and air, respectively) and the formation of propanal (**45**) and acetaldehyde (**44**) was observed. Something similar occurred for 2-octenal (**49**). It almost disappeared and the formation of hexanal (**47**) and acetaldehyde (**44**) was observed (chromatograms **g** and **h** for nitrogen and air, respectively). Results for 2,4-heptadienal (**48**) show slightly more stability and the initial aldehyde could still be detected after 1 h heating at 200 ºC (chromatograms **k** and **l** for nitrogen and air, respectively). In addition, 2,4-heptadienal decomposition produced propanal (**45**), acetaldehyde (**44**) and small amounts of 2-pentenal (**46**). Finally, decomposition of 2,4-decadienal

(**51**) (chromatograms **o** and **p** for nitrogen and air, respectively) mostly produced hexanal (**47**) and acetaldehyde (**44**).

With the exception of formaldehyde (**43**) and acetaldehyde (**44**), the formed aldehydes corresponded to the breakage of the different double bonds present in the initial aldehyde as indicated in **Figure 70**. Thus, 2-alkenals (**46** or **49**) produced the corresponding alkanals propanal (**45**) or hexanal (**47**), respectively. In addition, 2,4-alkadienals (**48** or **51**) produced both 2-alkenals (**46** or **49**, respectively) and alkanals (**45** or **47**, respectively). These reactions were accompanied by the formation of both glyoxal (**50**) and fumaraldehyde (**52**), although these last compounds seemed to be easily decomposed when buffer was present. The next subsections will describe this thermal breakage suffered by the different assayed aldehydes.

4.4.2. Thermal degradation of 2-pentenal.

As discussed above, the breakage of 2-pentenal produced propanal, in addition to formaldehyde and acetaldehyde. This reaction should be accompanied by formation of glyoxal, although this compound was not detected when the reaction was carried out in the presence of buffer. 2-Pentenal decomposition in buffer solution and the formation of the corresponding propanal is shown in **Figures 71-74**. Propanal was formed to an extent that depended on the concentration of 2-pentenal and the reaction conditions.

Figure 71 shows that propanal formation took place over a wide pH-range with a maximum around pH 8. Thus, propanal was produced with a yield >8% at pH 5-11.

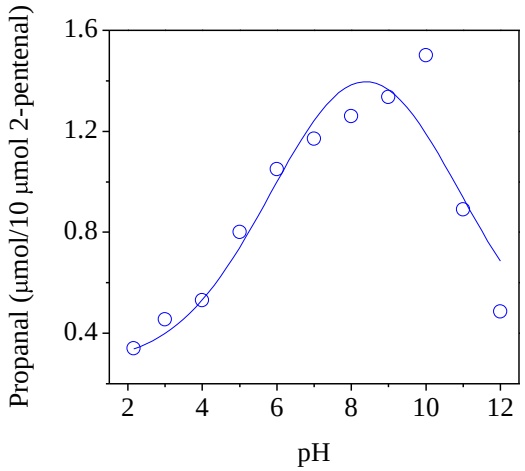

Figure 71. *Effect of reaction pH on the formation of propanal by thermal decomposition of 2-pentenal. Reactions were carried out by heating a solution of 2-pentenal (10 μmol) in 420 μl of 0.2 M buffer for 1 h at 200 ºC. Three buffers were employed: 0.2 M sodium citrate buffer, pH 2.15-5; sodium phosphate, pH 6–8; and 0.2 M sodium borate buffer, pH 9–12.*

The amount of propanal produced increased linearly (r = 0.993, p < 0.0001) as a function of 2-pentenal concentration (**Figure 72**). The slope of the obtained line (0.125) indicates the reaction yield (12.5%), which was constant over the assayed concentration range (0–80 μmol of 2-pentenal).

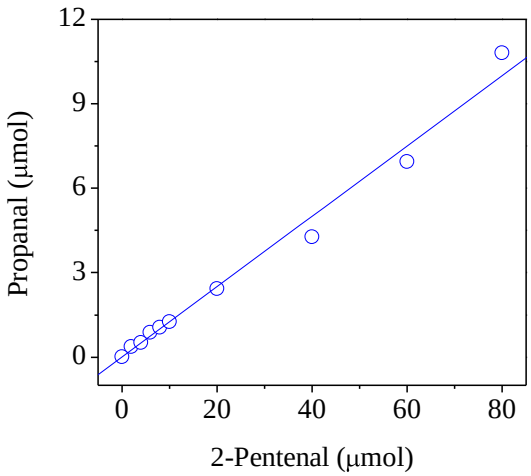

Figure 72. *Effect of 2-pentenal concentration on the formation of propanal by thermal decomposition of 2-pentenal. Reactions were carried out by heating a solution of 2-pentenal at the indicated concentrations in 420 μl of 0.2 M sodium phosphate buffer, pH 8, for 1 h at 200 ºC.*

2-Pentenal concentration decreased exponentially as a function of heating time and temperature (**Figure 73**), and 2-pentenal disappearance was produced more rapidly at a higher temperature. Thus, less than 10% of initial 2-pentenal was observed after 25 min at 200 ºC and after 45 min at 160 ºC. When 2-pentenal was heated at 120 ºC, 17% of the initial aldehyde was still present after 60 min.

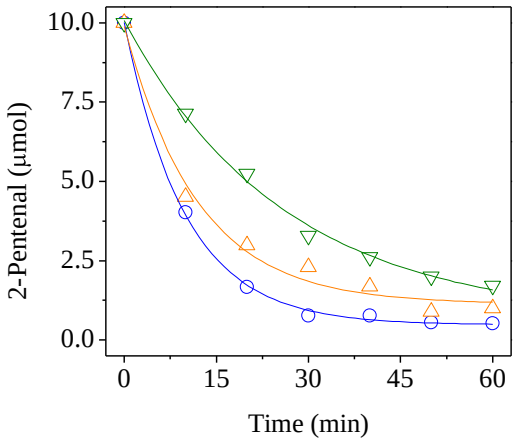

Figure 73. *Time-course of 2-pentenal disappearance by thermal decomposition. Reactions were carried out by heating a solution of 2-pentenal (10 µmol) in 420 µl of 0.2 M sodium phosphate buffer, pH 8, at the indicated times and temperatures. The assayed temperatures were 200 (○), 160 (△), or 120 ºC (▽).*

This disappearance of 2-pentenal was parallel to the formation of propanal (**Figure 74**). Propanal concentration only increased linearly (r > 0.994, p < 0.0067) for most temperatures at the beginning of the heating, in accordance to the exponential degradation observed for 2-pentenal. In fact, there was an inverse correlation (r > 0.935, p < 0.002) between the concentrations of 2-pentenal and propanal as a function of heating time at the three assayed temperatures.

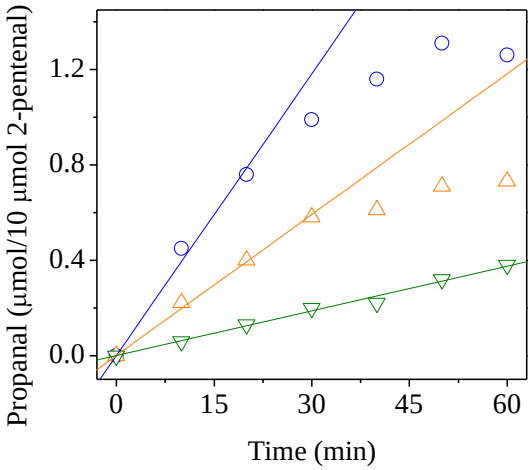

Figure 74. *Time-course of propanal formation by thermal decomposition of 2-pentenal. Reactions were carried out by heating a solution of 2-pentenal (10 µmol) in 420 µl of 0.2 M sodium phosphate buffer, pH 8, at the indicated times and temperatures. The assayed temperatures were 200 (○), 160 (△), or 120 ºC (▽).*

Reaction rates for propanal formation were higher at higher temperatures. These reaction rates were calculated from the initial times at which the concentration of propanal increased linearly as a function of heating time (**Figure 74**) by using the equation:

$$[\text{propanal}] = kt$$

where k is the rate constant and t is the time. These rate constants were used in an Arrhenius plot for the calculation of the activation energy (E_a) of propanal formation by heating 2-pentenal. The determined E_a was 25.2 kJ/mol.

4.4.3. Thermal degradation of 2-octenal.

2-Octenal exhibited a behavior analogous to that of 2-pentenal, and hexanal formation also depended on 2-octenal concentration and reaction conditions (**Figures 75-78**).

The effect of pH is shown in **Figure 75**. Thus, hexanal was mainly produced at basic pH, with a maximum around pH 10. Differently to the formation of propanal (**Figure 71**), the formation of hexanal was promoted at a narrower pH interval.

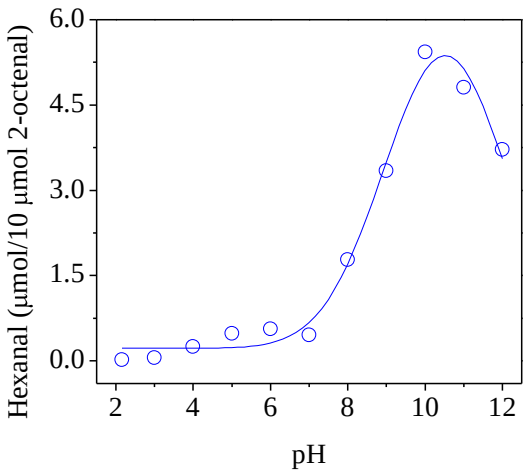

Figure 75. *Effect of reaction pH on the formation of hexanal by thermal decomposition of 2-octenal. Reactions were carried out by heating a solution of 2-oxtenal (10 µmol) in 420 µl of 0.2 M buffer for 1 h at 200 ºC. Three buffers were employed: 0.2 M sodium citrate buffer, pH 2.15-5; sodium phosphate, pH 6–8; and 0.2 M sodium borate buffer,pH 9–12.*

The amount of hexanal formed increased linearly (r = 0.999, p < 0.0001) as a function of 2-octenal concentration (**Figure 76**). The slope of the obtained line (0.180) indicated the reaction yield (18.0%), which was constant over the assayed range (0–80 µmol of 2-octenal). This yield was slightly

higher than that found for the formation of propanal from 2-pentenal (**Figure 72**).

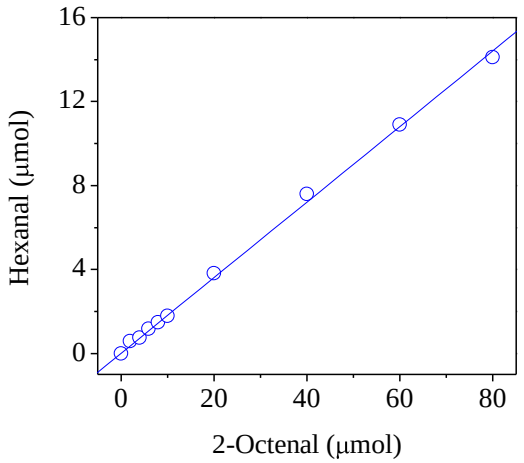

Figure 76. *Effect of 2-octenal concentration on the formation of hexanal by thermal decomposition of 2-octenal. Reactions were carried out by heating a solution of 2-octenal at the indicated concentrations in 420 μl of 0.2 M sodium phosphate buffer, pH 8, for 1 h at 200 ºC.*

Analogously to 2-pentenal, 2-octenal also disappeared exponentially as a function of reaction time and this disappearance was produced more rapidly at a higher temperature (**Figure 77**). Less than 10% of the initial 2-octenal was found after 40 min heating at 200 ºC, 50 min heating at 160 ºC, and about 60 min when heating at 120 ºC.

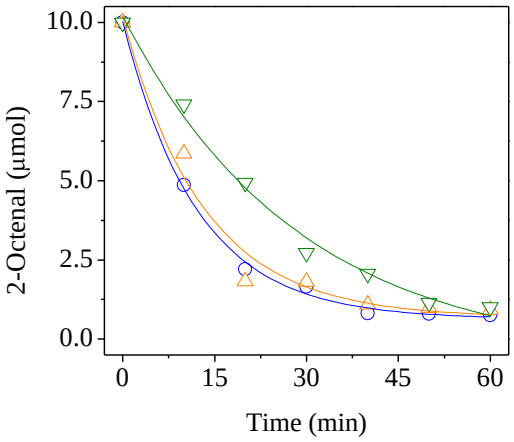

Figure 77. *Time-course of 2-octenal disappearance by thermal decomposition. Reactions were carried out by heating a solution of 2-octenal (10 µmol) in 420 µl of 0.2 M sodium phosphate buffer, pH 8, at the indicated times and temperatures. The assayed temperatures were 200 (○), 160 (△), or 120 ºC (▽).*

Hexanal concentration increased linearly ($r > 0.971$, $p < 0.00097$) as a function of reaction time, and reaction rates were higher at higher temperatures (**Figure 78**). Reaction rates were calculated from the slopes of the adjusted lines as described previously. The determined E_a was 25.3 kJ/mol, which was very similar to the E_a obtained for propanal formation from 2-pentenal (see section 4.4.2).

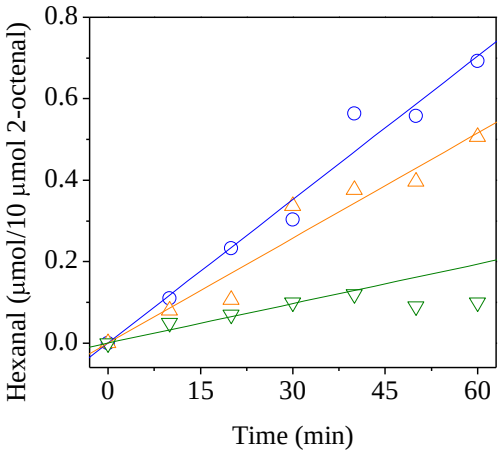

Figure 78. *Time-course of hexanal formation by thermal decomposition of 2-octenal. Reactions were carried out by heating a solution of 2-octenal (10 µmol) in 420 µl of 0.2 M sodium phosphate buffer, pH 8, at the indicated times and temperatures. The assayed temperatures were 200 (○), 160 (△), or 120 ºC (▽).*

4.4.4. Thermal degradation of 2,4-heptadienal.

When 2,4-heptadienal was heated in the presence of buffer, the formation of the two aldehydes corresponding to the breakage of either one or the other double bond was observed, although propanal was always formed to a higher extent than 2-pentenal (**Figures 79-83**). In addition, and analogously to 2-pentenal and 2-octenal thermal decomposition, aldehyde formation depended on the concentration of 2,4-heptadienal and the reaction conditions.

The effect of reaction pH on the decomposition of 2,4-heptadienal is shown in **Figure 79**. Both, propanal and 2-pentenal were produced over a wide pH range with a maximum at about pH 7–8. There was no clear difference between the optimum pH values for the formation of any of them, although 2-pentenal seemed to be produced better at a pH slightly more acidic than propanal.

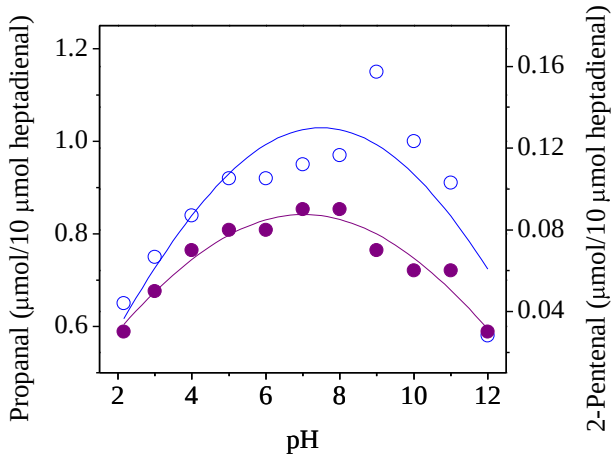

Figure 79. *Effect of reaction pH on the formation of propanal (○) and 2-pentenal (●) by thermal decomposition of 2,4-heptadienal. Reactions were carried out by heating a solution of 2,4-heptadienal (10 µmol) in 420 µl of 0.2 M buffer for 1 h at 200 ºC. Three buffers were employed: 0.2 M sodium citrate buffer, pH 2.15-5; sodium phosphate, pH 6–8; and 0.2 M sodium borate buffer,pH 9–12.*

Propanal and 2-pentenal concentrations increased when the concentration of 2,4-heptadienal increased (**Figure 80**). This increase was linear ($r = 0.995$, $p < 0.0001$) for 2-pentenal for the whole concentration range assayed (0–80 µmol of 2,4-heptadienal), and also for propanal ($r = 0.996$, $p < 0.0001$) but only in the 0–40 µmol range of 2,4-heptadienal. The slopes of the obtained lines (0.09774 and 0.00973) indicated reaction yields of 9.8% and 1.0% for propanal and 2-pentenal, respectively.

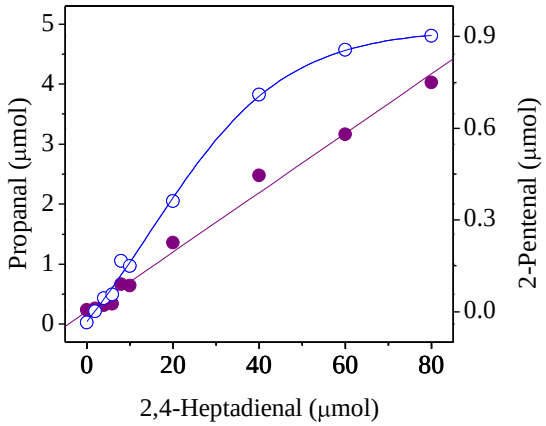

Figure 80. *Effect of 2,4-heptadienal concentration on the formation of propanal (○) and 2-pentenal (●) by thermal decomposition of 2,4-heptadienal. Reactions were carried out by heating a solution of 2,4-heptadienal at the indicated concentrations in 420 μl of 0.2 M sodium phosphate buffer, pH 8, for 1 h at 200 ºC.*

Analogously to the above discussed behavior of 2-alkenals, 2,4-heptadienal concentration decreased exponentially as a function of reaction time and this decrease was higher at higher temperatures (**Figure 81**).

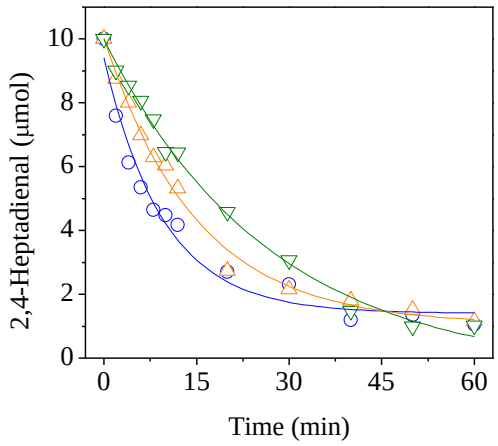

Figure 81. *Time-course of 2,4-heptadienal disappearance by thermal decomposition. Reactions were carried out by heating a solution of 2,4-heptadienal (10 µmol) in 420 µl of 0.2 M sodium phosphate buffer, pH 8, at the indicated times and temperatures. The assayed temperatures were 200 (○), 160 (△), or 120 ºC (▽).*

This decrease was parallel to the formation of both propanal (**Figure 82**) and 2-pentenal (**Figure 83**). The E_a required for the formation of both aldehydes was calculated by using the slopes of the obtained lines as described previously. The E_a for propanal and 2-pentenal formation were 25.2 and 22.5 kJ/mol, respectively.

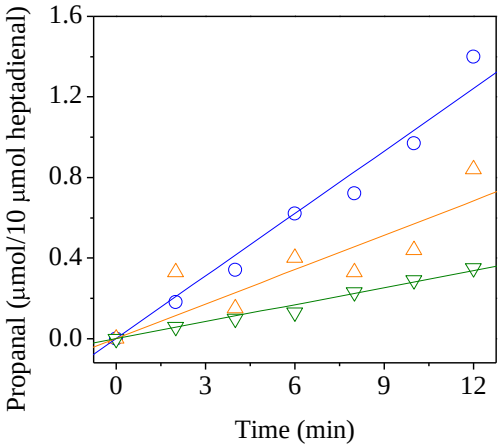

Figure 82. *Time-course of propanal formation by thermal decomposition of 2,4-heptadienal. Reactions were carried out by heating a solution of 2,4-heptadienal (10 µmol) in 420 µl of 0.2 M sodium phosphate buffer, pH 8, at the indicated times and temperatures. The assayed temperatures were 200 (○), 160 (△), or 120 ºC (▽).*

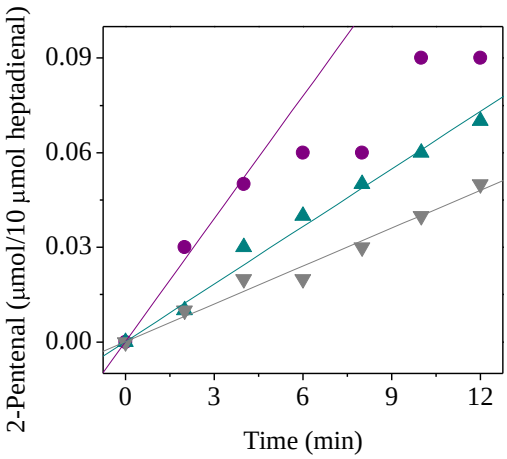

Figure 83. *Time-course of 2-pentenal formation by thermal decomposition of 2,4-heptadienal. Reactions were carried out by heating a solution of 2,4-heptadienal (10 µmol) in 420 µl of 0.2 M sodium phosphate buffer, pH 8, at the indicated times and temperatures. The assayed temperatures were 200 (●), 160 (▲), or 120 ºC (▼).*

4.4.5. Thermal degradation of 2,4-decadienal.

Analogously to the above described for 2,4-heptadienal, when 2,4-decadienal was heated, the formation of the two aldehydes corresponding to the breakage of either the first or the second double bond was observed and hexanal was always formed to a higher extent than 2-octenal (**Figures 84-88**). In addition, and analogously to the above described decompositions for the other aldehydes, the yields of hexanal and 2-octenal formation depended on the concentration of 2,4-decadienal and the reaction conditions.

The effect of reaction pH on the decomposition of 2,4-decadienal is shown in **Figure 84**. Analogously to the aldehydes produced in the decomposition of 2,4-heptadienal, hexanal and 2-octenal were produced over a wide pH range with a maximum at about pH 8 and there was no clear difference between the optimum pH values for the formation of both aldehydes. Nevertheless, and in accordance with the above observations for 2,4-heptadienal decomposition, the 2-alkenal seemed to be produced in a greater yield at a pH value slightly more acidic than the alkanal.

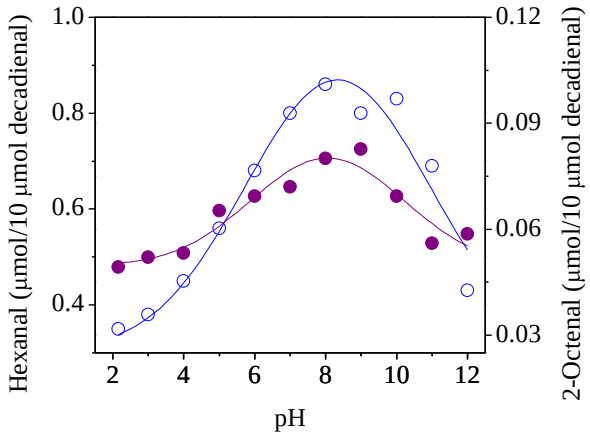

Figure 84. *Effect of pH on the formation of hexanal (○) and 2-octenal (●) by thermal decomposition of 2,4-decadienal. Reactions were carried out by heating a solution of 2,4-decadienal (10 µmol) in 420 µl of 0.2 M buffer for 1 h at 200 ºC. Three buffers were employed: 0.2 M sodium citrate buffer, pH 2.15-5; sodium phosphate, pH 6–8; and 0.2 M sodium borate buffer,pH 9–12.*

Hexanal and 2-octenal concentrations increased when the concentration of 2,4-decadienal increased (**Figure 85**). This increase was linear ($r > 0.998$, $p < 0.0001$) for both hexanal and 2-octenal for the whole concentration range assayed (0–80 µmol of 2,4-decadienal). The slopes of the obtained lines (0.1154 and 0.00821) indicated reaction yields of 11.5% and 0.8% for hexanal and 2-octenal, respectively.

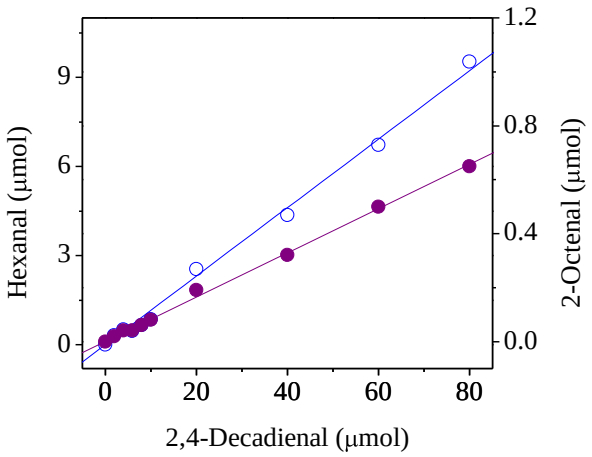

Figure 85. *Effect of 2,4-decadienal concentration on the formation of hexanal (○) and 2-octenal (●) by thermal decomposition of 2,4-decadienal. Reactions were carried out by heating a solution of 2,4-decadienal at the indicated concentrations in 420 μl of 0.2 M sodium phosphate buffer, pH 8, for 1 h at 200 ºC.*

As observed for other aldehydes, 2,4-decadienal concentration decreased exponentially as a function of reaction time and this decrease was higher at higher temperatures (**Figure 86**).

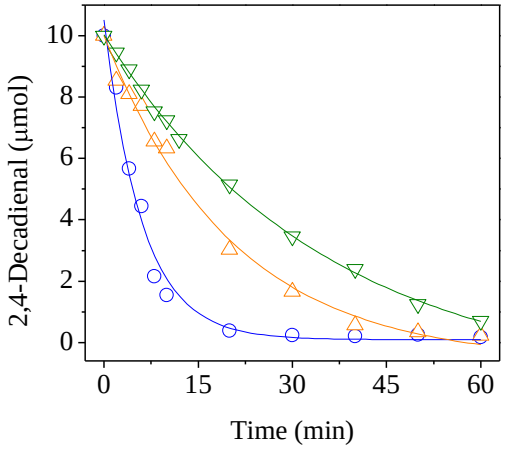

Figure 86. *Time-course of 2,4-decadienal disappearance by thermal decomposition. Reactions were carried out by heating a solution of 2,4-decadienal (10 µmol) in 420 µl of 0.2 M sodium phosphate buffer, pH 8, at the indicated times and temperatures. The assayed temperatures were 200 (○), 160 (△), or 120 ºC (▽).*

This decrease was parallel to the formation of both hexanal (**Figure 87**) and 2-octenal (**Figure 88**). The E_a required for the formation of both aldehydes was calculated by using the slopes of the obtained lines as described previously. The E_a for hexanal and 2-octenal formation were 21.3 and 29.6 kJ/mol, respectively.

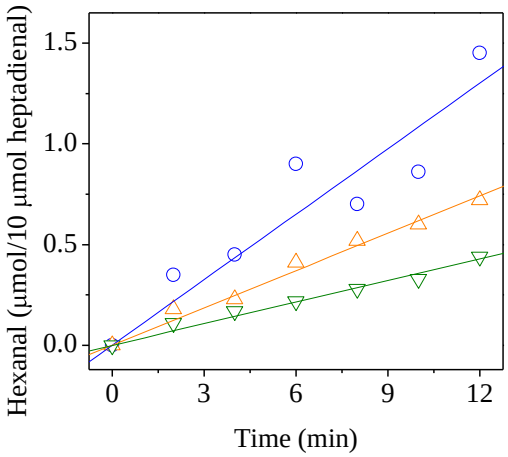

Figure 87. *Time-course of hexanal formation by thermal decomposition of 2,4-decadienal. Reactions were carried out by heating a solution of 2,4-decadienal (10 µmol) in 420 µl of 0.2 M sodium phosphate buffer, pH 8, at the indicated times and temperatures. The assayed temperatures were 200 (○), 160 (△), or 120 ºC (▽).*

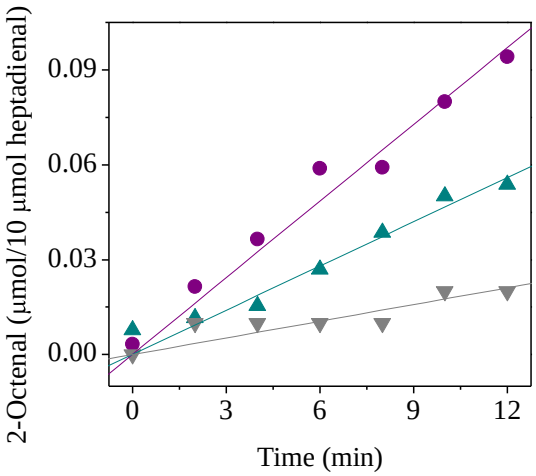

Figure 88. *Time-course of 2-octenal formation by thermal decomposition of 2,4-decadienal. Reactions were carried out by heating a solution of 2,4-decadienal (10 µmol) in 420 µl of 0.2 M sodium phosphate buffer, pH 8,at the indicated times and temperatures. The assayed temperatures were 200 (●), 160 (▲), or 120 ºC (▼).*

4.5. Carbonyl-trapping by phenols during the frying process.

The final section of Results part is dedicated to the study of the formation and presence of carbonyl-phenol adducts in food products. These studies were carried out with fried foods because the frying of foods produces short chain toxicologically relevant aldehydes, namely 2-propenal and (*E*)-2-butenal (acrolein and crotonaldehyde, respectively) in both frying oils and fried foods (Ewert et al., 2011; Granvogl, 2014; Ewert et al., 2014). However, the amounts of these compounds are much higher in the frying oils than in the fried foods (Granvogl, 2014).

The decreased content of lipid-derived aldehydes in fried foods might be a consequence of a limited absorption of these compounds by the foods, but also of a reaction of the generated aldehydes with some food components.

In an attempt to clarify this point, this section describes the formation of carbonyl-phenol adducts in both onions submitted to frying in rapeseed oil containing acrolein, crotonaldehyde, and (*E*)-2-pentenal as well as in commercially crispy fried onions.

These aldehydes were selected because of both their confirmed formation in oils submitted to frying (Ewert et al., 2011; Granvogl, 2014; Ewert et al., 2014) and the fact that the reaction mechanism of (*E*)-2-alkenals with phenolic compounds is now well understood (Hidalgo & Zamora, 2014). In addition, onion was chosen as a model food because its flavonoid composition and content are well-known (Price & Rhodes, 1997; Crozier et al., 1997; Price et al., 1997; Marotti & Piccaglia, 2002; Patil et al., 1995). Thus, the total flavonoids in red onions are about 140 mg/100 g of fresh weight, from which quercetin derivatives are about 85% of the total flavonoids. Therefore, the presence of adducts formed between these aldehydes and quercetin was investigated.

4.5.1. Formation of carbonyl-phenol adducts by reaction of acrolein, crotonaldehyde, or (*E*)-2-pentenal with quercetin.

The main adducts formed in the reactions of acrolein, crotonaldehyde, or (*E*)-2-pentenal with quercetin were synthesized and characterized in order to use them as reference compounds for the identification of these aldehyde-phenol adducts in both onions fried in the laboratory and commercially crispy fried onions.

The reaction between (*E*)-2-alkenals and phenols is complex, and different single compounds as well as polymers are produced (Hidalgo & Zamora, 2014). When the reaction was carried out with the flavonoid quercetin, the complexity of the reaction increased because this phenol has a higher number of reactive positions. However, the reactivity of some positions was found to be higher than that of others, and thus, only a limited number of adducts was produced.

The reaction between (*E*)-2-alkenals and quercetin took place as indicated in **Figure 89**.

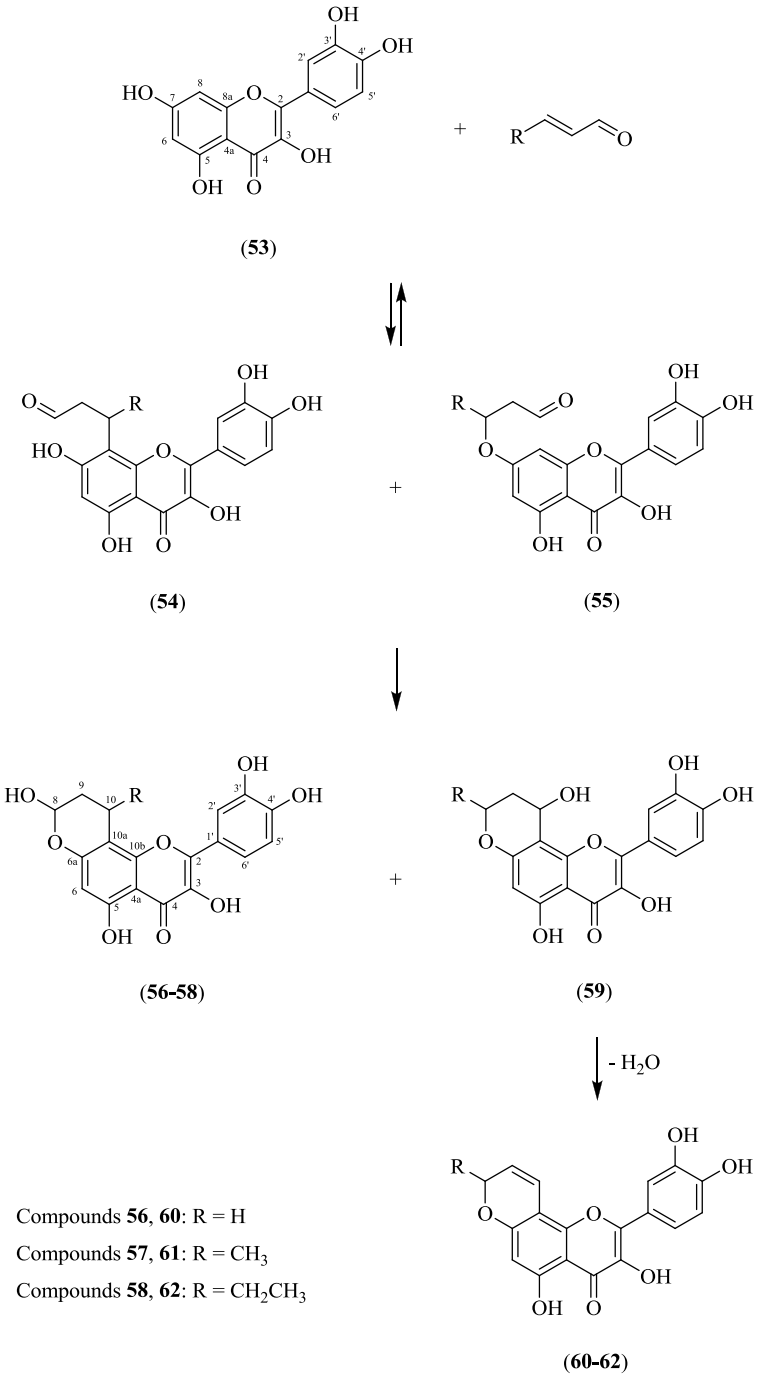

***Figure 89**. Formation mechanism of aldehyde-quercetin adducts. The aldehydes employed in this study were acrolein (R = H), crotonaldehyde (R = CH_3), and (E)-2-pentenal (R = CH_2CH_3).*

The first step was the addition of one aromatic carbon or one hydroxyl group with a high nucleophilicity in the phenol to the olefinic carbon at the β-position of the aldehyde. Quercetin (**53**) has different atoms susceptible for this addition: the carbons at positions 6 and 8, and all the hydroxyl groups. If the reaction takes place with an aromatic carbon of quercetin, an adduct similar to compound **54** is produced. If the reaction takes place with a hydroxyl group, an adduct similar to compound **55** is formed. The stabilization is different for compounds **54** and **55** and involves the other reactive groups that did not react in the first step. This first step is reversible, and only the adducts that can later be stabilized are able to be isolated.

Adducts **54** are stabilized by reacting with the contiguous hydroxyl group and forming the corresponding hemiacetals **56-58**. These compounds **56-58** have a molecular weight resulting from the addition of the molecular weights of quercetin and the respective carbonyl compounds. Theoretically, three isomers can be produced for each aldehyde, which would involve carbon 8 and hydroxyl 7, carbon 6 and hydroxyl 7, and carbon 6 and hydroxyl 5 of quercetin, respectively.

Adducts **55** are stabilized by addition of an aromatic carbon of quercetin to the carbonyl carbon of the aldehyde, resulting in the cyclic structure **59**, which is later dehydrated to yield the conjugated olefins **60**-**62**. These compounds **60-62** have a molecular weight resulting from the addition of the molecular weights of quercetin and the respective carbonyl compounds minus one molecule of water. Analogously to compounds **56-58**, three isomers can be produced for each aldehyde, which would involve carbon 8 and hydroxyl 7, carbon 6 and hydroxyl 7, and carbon 6 and hydroxyl 5 of quercetin, respectively.

When the reaction between the aldehydes and quercetin was carried out, the presence of both kinds of products (the hemiacetal and the conjugated olefin) could be observed. However, the ratio among them depended on the involved aldehyde.

Figure 90 shows the mass spectra of the reaction mixtures obtained for the three assayed aldehydes. Acrolein mostly produced the hemiacetal **56** [*m/z* 357 ($M^+ - 1$)] and only small amounts of the conjugated olefin **60** [*m/z* 339 ($M^+ - 1$)] (**Figure 90A**). In addition, an adduct involving 2 molecules of acrolein and 1 molecule of quercetin was also observed [*m/z* 413 ($M^+ - 1$)]. This is likely a consequence of the high reactivity of this aldehyde, which is able to react with several positions of the phenolic compound. For adducts involving one molecule of acrolein and one molecule of quercetin, the hemiacetal is a more stable compound than the conjugated olefin. This last compound is susceptible to polymerize because of the presence of the additional double bond. Besides, the conjugated olefin suffers the addition of methanol to produce a further adduct [*m/z* 371 ($M^+ - 1$)].

Differently from acrolein, the two adducts involving one molecule of crotonaldehyde and one molecule of quercetin were produced for crotonaldehyde (**Figure 90B**), although the hemiacetal [*m/z* 371 ($M^+ - 1$)] (compound **57**) seemed to be formed to a higher extent than the conjugated olefin [*m/z* 353 ($M^+ - 1$)] (compound **61**). Because of the reactivity of this olefin, the corresponding methanol adduct was also present in the reaction mixture [*m/z* 385 ($M^+ - 1$)].

The introduction of an additional methylene group into the aldehyde shifted the reaction toward the formation of the conjugated olefin as the main product [*m/z* 367 ($M^+ - 1$)] (compound **62**), although the hemiacetal **58** [*m/z* 385 ($M^+ - 1$)] was also formed to a significant extent (**Figure 90C**). As observed for the other conjugated olefins, the corresponding methanol adduct was also present in the reaction mixture [*m/z* 399 ($M^+ - 1$)].

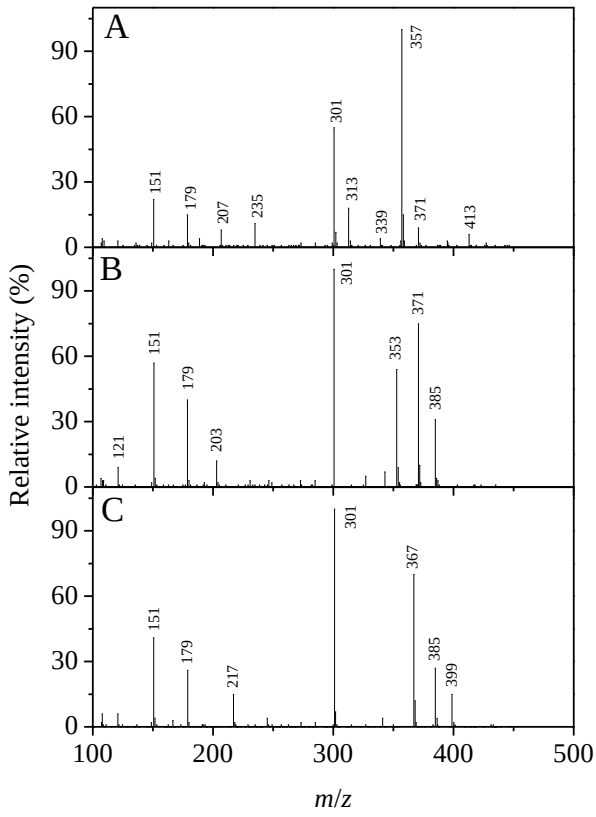

***Figure 90**. Mass spectra of the reaction mixtures between quercetin and: (A) acrolein; (B),crotonaldehyde; and (C), (E)-2-pentenal.*

The main adducts formed in the three reaction mixtures were isolated by column chromatography on Sephadex LH-20 and characterized by NMR and LC-HRMS. These compounds were the hemiacetals produced with acrolein and crotonaldehyde (compounds **56** and **57**, respectively) and the conjugated olefins produced with crotonaldehyde and (*E*)-2-pentenal (compounds **61** and **62**, respectively). The chemical structures for all these compounds are shown in **Figure 91**.

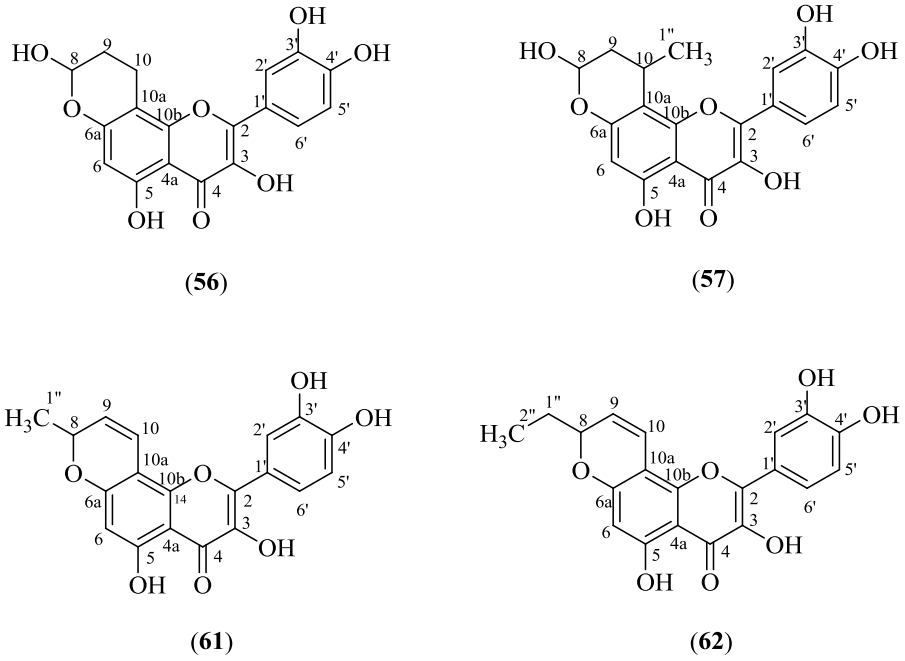

***Figure 91**. Chemical structures of the carbonyl-phenol adducts isolated and characterized by NMR and LC-HRMS in the different assayed reactions between 2-alkenals and quercetin. The aldehyde and the phenolic compound involved in the formation of each adduct is described in the text.*

Long distance NMR couplings were determined by HMBC experiments and allowed the unequivocal characterization of the formed structures. The observed HMBC couplings for the two kinds of produced adducts are shown in **Figure 92**. HMBC couplings of compounds **57** and **62** were identical to those of compounds **56** and **61**, respectively.

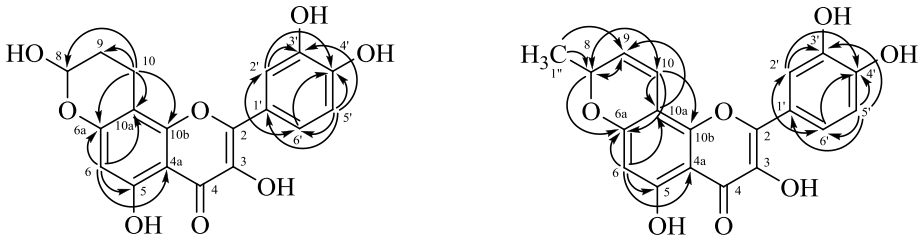

(**56**) (**61**)

Figure 92. *HMBC couplings exhibited by compounds* ***56*** *and* ***61***.

These adducts always involved carbon 8 and hydroxyl 7 in quercetin. The spectroscopic and spectrometric data of the different isolated and characterized compounds are the following:

2-(3,4-Dihydroxyphenyl)-3,5,8-trihydroxy-9,10-dihydro-4H,8H-pyrano[2,3-f]chromen-4-one (**56**). ^{1}H NMR (DMSO-d_6): δ (ppm) 1.97br (2H, H9), 2.88br (2H, H10), 3.38br (OH), 5.58br (1H, H8), 6.18s (1H, H6), 6.90d (1H, *J* = 8.5 Hz, H5′), 7.61dd (1H, *J* = 2.1 Hz, *J* = 8.5 Hz, H6′), 7.73d (1H, *J* = 2.1 Hz, H2′), 9.47br (OH), 12.30br (OH). ^{13}C NMR (DMSO-d_6): δ (ppm) 14.85 (C10), 26.87 (C9), 93.29 (C8), 98.89 (C6), 101.26 (C10a), 104.20 (C4a), 115.32 (C2′), 116.18 (C5′), 120.43 (C6′), 122.64 (C1′), 136.56 (C3), 145.64 (C3′), 147.26 (C2′), 148.27 (C4′), 153.10 (C10b), 158.59 (C6a), 158.78 (C5), 176.51 (C4). HRMS, m/z 357.06154 ($M^+ - 1$), error 0.2 ppm.

2-(3,4-Dihydroxyphenyl)-3,5,8-trihydroxy-10-methyl-9,10-dihydro-4H,8H-pyrano[2,3-f]chromen-4-one (**57**). ^{1}H NMR (DMSO-d_6): δ (ppm) 1.38d (3H, *J* = 7.0 Hz, H1″), 1.94br (2H, H9), 3.38br (OH), 3.41br (1H, H10), 5.50d br (1H, *J* = 7.9 Hz, H8), 6.18s (1H, H6), 6.91d (1H, *J* = 8.5 Hz, H5′), 7.60dd (1H, *J* = 2.2 Hz, *J* = 8.5 Hz, H6′), 7.73d (1H, *J* = 2.2 Hz, H2′), 9.52br (OH), 12.38br (OH). ^{13}C NMR (DMSO-d_6): δ (ppm) 19.02 (C10), 21.74 (C1′), 56.49 (C9), 92.76 (C8), 98.64 (C6), 104.38 (C4a), 105.74 (C10a), 115.27 (C2′), 116.20 (C5′), 120.25 (C6′), 122.61 (C1′), 136.56 (C3), 145.71 (C3′),

147.31 (C2), 148.27 (C4′), 153.44 (C10b), 158.88 (C6a), 159.16 (C5), 176.51 (C4). HRMS, m/z 371.07763 ($M^+ - 1$), error 0.9 ppm.

2-(3,4-Dihydroxyphenyl)-3,5-dihydroxy-8-methyl-4H,8H-pyrano-[2,3-f]chromen-4-one (**61**). ^{1}H NMR (DMSO-d_6): δ (ppm) 1.42d (3H, *J* = 6.6 Hz, H1″), 3.36br (OH), 5.15m (1H, H8), 5.83dd (1H, *J* = 3.2 Hz, *J* = 10.0 Hz, H9), 6.23s (1H, H6), 6.87dd (1H, *J* = 1.1 Hz, *J* = 10.0 Hz, H10), 6.91d (1H, *J* = 8.5 Hz, H5′), 7.62dd (1H, *J* = 2.2 Hz, *J* = 8.5 Hz, H6′), 7.73d (1H, *J* = 2.2 Hz, H2′), 9.52br (OH), 12.49br (OH), 12.65br (OH), 12.99br (OH). ^{13}C NMR (DMSO-d_6): δ (ppm) 21.56 (C1″), 72.88 (C8), 98.83 (C6), 101.63 (C10a), 104.48 (C4a), 115.21 (C2′), 116.00 (C10), 116.25 (C5′), 120.58 (C6′), 122.36 (C1′), 124.55 (C9), 136.61 (C3), 145.68 (C3′), 147.57 (C2), 148.39 (C4′), 150.47 (C10b), 159.24 (C6a), 160.71 (C5), 176.57 (C4). HRMS, m/z 353.0625 ($M^+ - 1$), error 4.8 ppm.

2-(3,4-Dihydroxyphenyl)-8-ethyl-3,5-dihydroxy-4H,8H-pyrano-[2,3-f]chromen-4-one (**62**). ^{1}H NMR (DMSO-d_6): δ (ppm) 0.97t (3H, *J* = 7.3 Hz, H2″), 1.74qu (2H, *J* = 7.3 Hz, H1″), 3.36br (OH), 4.98m (1H, H8), 5.83dd (1H, *J* = 3.4 Hz, *J* = 10.1 Hz, H9), 6.23s (1H, H6), 6.89dd (1H, *J* = 1.1 Hz, *J* = 10.1 Hz, H10), 6.91d (1H, *J* = 8.5 Hz, H5′), 7.61dd (1H, *J* = 2.2 Hz, *J* = 8.5 Hz, H6′), 7.72d (1H, *J* = 2.2 Hz, H2′), 9.52br (OH), 12.49br (OH), 12.65br (OH), 12.99br (OH). ^{13}C NMR (DMSO-d_6): δ (ppm) 9.23 (C2″), 28.39 (C1″), 77.49 (C8), 98.75 (C6), 101.69 (C10a), 104.39 (C4a), 115.21 (C2′), 116.24 (C5′), 116.40 (C10), 120.59 (C6′), 122.37 (C1′), 123.20 (C9), 136.52 (C3), 145.66 (C3′), 147.39 (C2), 148.35 (C4′), 150.42 (C10b), 159.47 (C6a), 160.69 (C5), 176.52 (C4). HRMS, m/z 367.0810 ($M^+ - 1$), error 3.6 ppm.

4.5.2. Fate of toxicologically relevant carbonyls during thermal heating of oils in the presence and in the absence of added food.

Oil samples containing acrolein, crotonaldehyde, and (*E*)-2-pentenal were submitted to frying in the presence and in the absence of onions and the contents of these aldehydes were determined by ^{1}H NMR in order to compare the amount of aldehydes remained in the oil after the frying process. Fresh rapeseed oil spiked with acrolein, crotonaldehyde, and (*E*)-2-pentenal (2.7 μmol/g of oil) was used in this study.

During the frying process, toxicologically relevant aldehydes are formed as a consequence of oxidation, but short chain aldehydes have a boiling point lower than the employed frying temperature and are evaporated, among other processes. Therefore, and independently of the presence or absence of food, the amounts of aldehydes present in the spiked oil (2.7 μmol/g of oil) at the end of the frying process were much reduced. Thus, the initial amount of aldehyde was lowered by 35% in the case of acrolein, but by more than 90% in the case of crotonaldehyde and (*E*)-2-pentenal (**Figure 93**). This surprising result (the boiling point of acrolein is lower than that of crotonaldehyde and (*E*)-2-pentenal) is likely a consequence of the higher formation of acrolein by oil oxidation in comparison to the other assayed aldehydes (Granvogl, 2014).

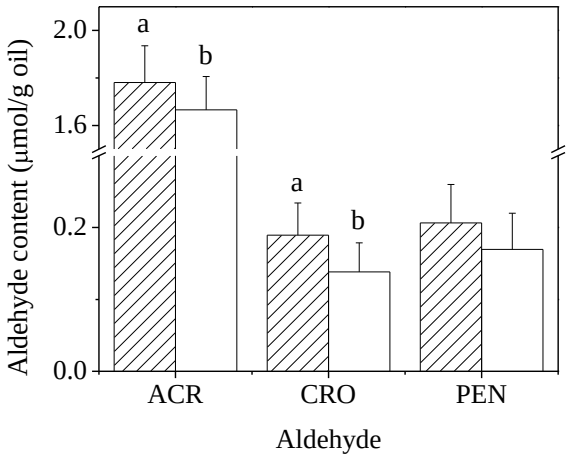

***Figure 93**. Aldehydes recovered from the oil after the frying process in the absence (striped bars) or in the presence (open bars) of onions. Bars for each aldehyde having different letters are significantly ($p < 0.05$) different. Four samples were analyzed for each heated oil and each sample was measured three times. Therefore, the aldehyde content for each analyzed oil was the mean value of 12 determinations. Abbreviations: ACR, acrolein; CRO, crotonaldehyde; PEN, (E)-2-pentenal.*

When the oil was heated in the presence of onions, only slight decreases in the aldehyde concentrations were observed compared to the aldehyde concentrations in the oils heated in the absence of onions (**Figure 93**). However, these decreases were significant ($p < 0.05$) for acrolein and crotonaldehyde, but they were not for (*E*)-2-pentenal.

4.5.3. Formation of aldehyde-phenol adducts in fried onions.

When the oil was heated in the absence of food, the above-described decrease of aldehydes was mainly a consequence of their evaporation. In fact, these aldehydes are considered as environmental pollutants and they have been detected, among others, in the exhaust of kitchens and thermally

processed oils (Ewert et al., 2011; Granvogl, 2014; Seaman et al., 2009; Umano & Shibamoto, 1987; Da Silva & de Paula Pereira, 2008).

However, when a food is present, in addition to aldehyde evaporation, the absorption of the aldehydes in the food and the reaction of these aldehydes with food components might also occur. In fact, trace amounts of these aldehydes have already been found in fried foods (Granvogl, 2014).

When the onions fried in the laboratory were analyzed for detection of the four adducts previously synthesized, adduct **62** was present in all analyzed samples (**Figure 94**). This compound, which is produced in the reaction between (*E*)-2-pentenal and quercetin, was unequivocally identified according to the retention time and HRMS of the corresponding standard. Error was <3 ppm. In addition, some samples showed the presence of compound **56** (produced with acrolein) and/or compound **57** (produced with crotonaldehyde), which were also identified analogously on the basis of retention times and HRMS. Thus, the sample shown in **Figure 94** exhibited trace amounts of compound **57**, but not of compounds **56** or **61**. Compounds **56** and **57** were present to a much lower extent than compound **62**. Compound **61** was not detected in any of the analyzed samples.

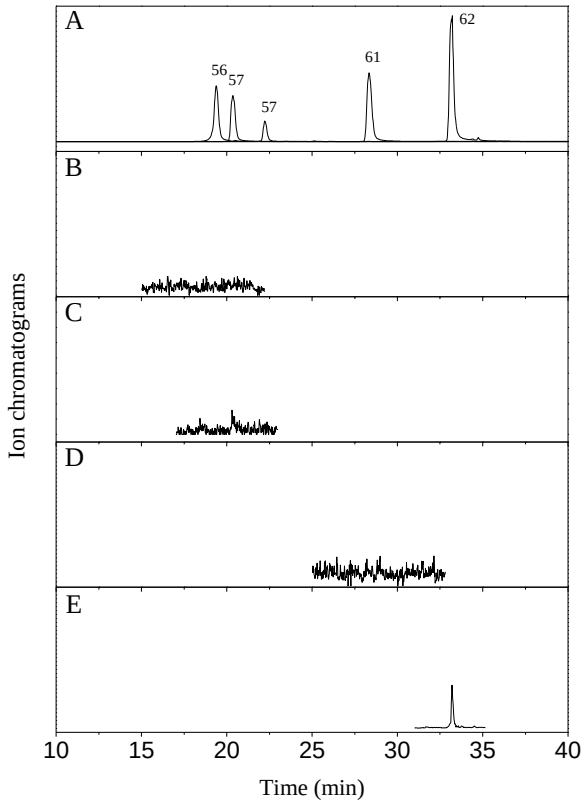

***Figure 94**. Trace chromatograms obtained by LC-HRMS of (A) a mixture of the four carbonyl-phenol adducts prepared in this study, and (B-E) the extract of an onion sample fried in the laboratory. The traces correspond to the exact masses ($M^+ - 1$) of (B) compound **56**; (C) compound **57**; (D) compound **61**; and (E) compound **62**.*

4.5.4. Identification of aldehyde-phenol adducts in commercially crispy fried onions.

Differently from the frying carried out in the laboratory, in which nonoxidized oils spiked with selected aldehydes were used and these oils were only heated for 9 min before adding the onions, the history of the oils employed as well as the process followed in the preparation of the commercially crispy fried onions is unknown. But in this case, all available

aldehydes, which were able to react with onion phenols, must originate from the frying oil. Interestingly, several carbonyl-quercetin adducts were present in the analyzed samples (see, for example, **Figure 95**). For commercially crispy fried onions, compound **56** was the main adduct detected, followed by compound **62**. As can be observed in the figure, only trace amounts of compound **57** could be found and compound **61** was absent in the different assayed samples. These compounds were identified on the basis of their retention times and HRMS determined for the obtained standards. Errors were always <5 ppm.

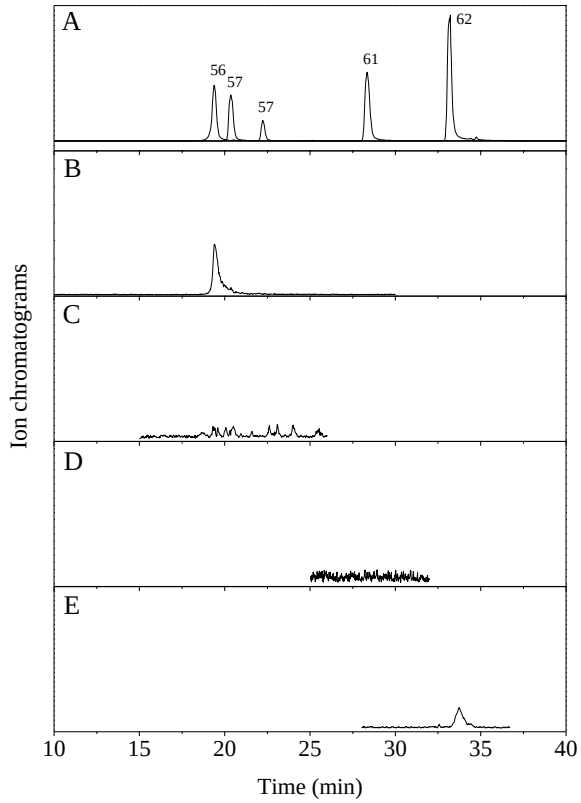

***Figure 95**. Trace chromatograms obtained by LC-HRMS of (A) a mixture of the four carbonyl-phenol adducts prepared in this study, and (B-E) the extract of a commercial crispy fried onion sample. The traces correspond to the exact masses ($M^+ - 1$) of (B) compound **56**; (C) compound **57**; (D) compound **61**; and (E) compound **62**.*

5. DISCUSSION

As discussed in the Introduction section, phenolics are able to chelate metal ions avoiding in this way the formation of free radicals. In addition, they are able to scavenge free radicals, inhibit the propagation of the free radical chain, and avoid the formation of a wide range of LOPs. Furthermore, the results obtained in this thesis confirm that phenolics have an additional protective role by inhibiting of the broadcasting of the lipid oxidative damage to other food macromolecules: they trap the reactive carbonyls produced in the lipid oxidative pathway. This trapping was observed for all assayed LOPs, but reactivities and structures of formed adducts depended on the involved reactive carbonyls.

5.1. The phenolic trapping of alkanals.

The carbonyl-phenol adducts formed in the reaction between phenolics and alkanals involve one phenolic carbon and the carbonyl carbon of the aldehyde. A reaction pathway that explains the formation of these compounds is collected in **Figure 96**.

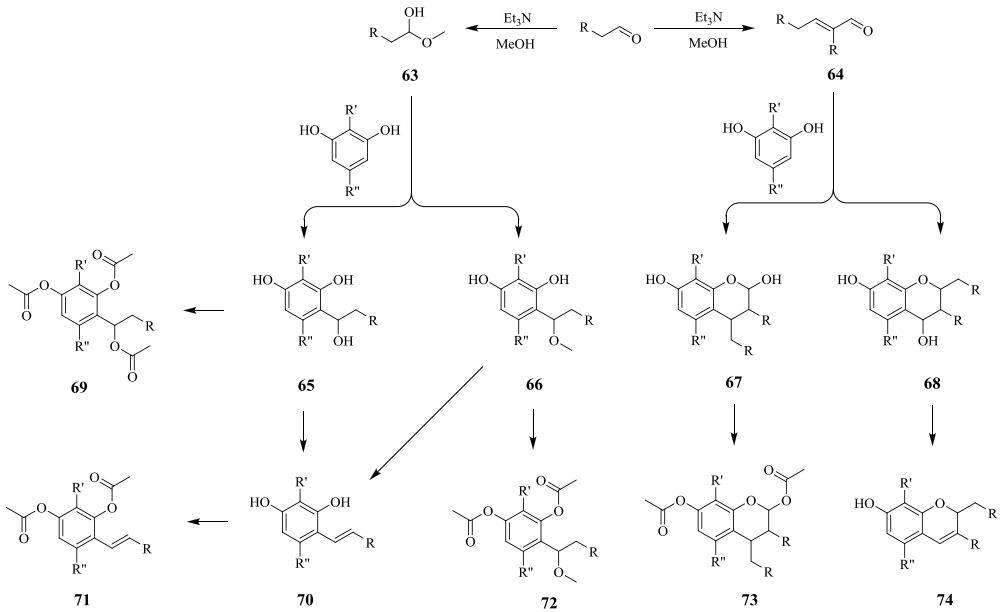

Figure 96. *Proposed reaction pathway for the reaction between alkanals and phenolic compounds. The assayed phenolic compounds were: resorcinol (R' = H and R'' = H), 2-methylresorcinol (R' = CH_3 and R'' = H), 2,5-dimethylresorcinol (R' = CH_3 and R'' = CH_3) and orcinol (R' = H and R'' = CH_3). The assayed alkanals were: propanal (R = CH_3), butanal (R = CH_2CH_3), pentanal (R = $CH_2CH_2CH_3$), and hexanal (R = $CH_2CH_2CH_2CH_3$). The alkanals 2-methylpropanal, 2-methylbutanal, and 3-methylbutanal were also used to study the effect of aldehyde branching on the formation of carbonyl-phenol adducts. Compounds having the structures of compounds* ***66***, ***69***, ***70***, ***71***, ***72***, ***73*** *and* ***74*** *have been isolated and characterized in alkanal/phenolic reaction mixtures.*

As described in the section 4.1.1, compounds **2**, **3**, **4**, and **5** (the analogues of compounds **72**, **71**, **69**, and **73**, respectively, in **Figure 96**) were isolated and characterized in the reaction between pentanal and 2-methylresorcinol. On the other hand, the analogue of acetate of compound **74** was not detected under the employed conditions. Nevertheless, compound **19** (**Figure 42** in section 4.1.1), which is the analogue of compound **74** when propanal is involved, was isolated in the reaction between 2-methyl-2-pentenal and resorcinol. The reason for the not appearance of the analogue of compound **74** in the reaction between pentanal and 2-methylresorcinol may be related to the instability of compound **74**. Thus, previous studies have suggested that adducts similar to compound **74** are more unstable than adducts similar to compound **67**, and disappear upon prolonged heating (Hidalgo & Zamora, 2014).

As shown in **Figure 96**, under the reaction conditions employed, saturated aldehydes can either react with methanol to produce the corresponding hemiacetal **63** or suffer an aldol condensation to produce the corresponding 2-alkenal **64**. Both compounds **63** and **64** react then with the phenolic compound.

In the case of the hemiacetal **63**, this reaction can be produced with the exit of either methanol or water. If the exit of methanol is produced, the carbonyl-phenol adduct **65** is formed. The presence of a hydroxyl group in this adduct makes possible its dehydration to produce the corresponding olefin **70**. After acetylation, adduct **70** produces compound **71** (this adduct corresponds to compound **3** isolated in the reaction of pentanal with 2-methylresorcinol), and adduct **65** forms compound **69** (this adduct corresponds to compound **4** isolated in the reaction of pentanal with 2-methylresorcinol). If the attack of the phenolic compound produces the exit of water, the carbonyl-phenol adduct **66** will have a methoxy group and, after acetylation, compound **72** (this adduct corresponds to compound **2** isolated in the reaction of pentanal with 2-methylresorcinol) will be formed. The loss of

methanol in adduct **66** would also be another route to produce compound **70** in a first step and, after acetylation, compound **71**.

The reaction of the product of aldolic condensation **64** with the phenolic compound is more complex because one of the phenolic carbons and, also, one of the phenolic hydroxyl groups are involved (Hidalgo & Zamora, 2014). Compound **73** (this adduct corresponds to compound **5** isolated in the reaction of pentanal with 2-methylresorcinol) is produced by addition of one phenolic carbon to the carbon-carbon double bond of the aldolisation product followed by the addition of one phenolic hydroxyl group to the carbonyl carbon to produce the corresponding hemiacetal **67** and **73** after acetylation. On the other hand, compound **74** is produced by addition of one phenolic hydroxyl group to the carbon-carbon double bond of the aldehyde and then addition of one phenolic carbon to the carbonyl carbon to produce a hydroxyl derivative **68**. The dehydration of this compound is the origin of compound **74**. The presence of a carbon-carbon double bond in this compound increases its susceptibility to further reactions, including polymerizations, and explains its relative instability (Hidalgo & Zamora, 2014).

Although all these compounds are produced, some carbonyl-phenol adducts are produced to a higher extent than others depending on the structure of the reactants and the reaction conditions. In addition, some of the reaction products are more stable than others. Thus, when reactions involving different saturated aldehydes and phenolic compounds were carried out in order to synthesize and characterize saturated aldehyde-phenol adducts, only major reaction products were isolated and characterized.

As shown in section 4.1.1, when resorcinol was involved most reactions occurred at the C4 of the phenolic compound, and only when using pentanal, the corresponding adduct at C2 could be isolated and characterized (compound **8** in **Figure 42**). In addition, all adducts involving C4 were similar and corresponded to the methoxylated adduct (the analogue of compound **66** in **Figure 96**). Neither the corresponding hydroxylated derivative (the

analogue of compound **65** in **Figure 96**) nor the olefin (the analogue of compound **70** in **Figure 96**) could be isolated. On the contrary, the adduct at C2 was the hydroxylated adduct (the analogue of compound **65** in **Figure 96**), and neither the methoxylated adduct (the analogue of compound **66** in **Figure 96**) nor the olefin (the analogue of compound **70** in **Figure 96**) could be isolated.

When 2-methylresorcinol was involved, the methoxylated adduct (the analogue of compound **66** in **Figure 96**) was also the compound isolated in all assayed reactions with the exception of its reaction with hexanal. In addition, when using this phenolic compound, two olefins (the analogue of compound **70** in **Figure 96**) were also produced to a significant extent: those corresponding to the reactions with pentanal and hexanal (compounds **13** and **16** in **Figure 42**, respectively). On the other hand, the hydroxylated derivative (the analogue of compound **65** in **Figure 96**) could not be isolated in any reaction.

All of these reactions always implied the formation of a new chiral center and the corresponding racemic mixture was produced. Therefore, when the aldehyde had a chiral center, as in the case of 2-methylbutanal, the formed adduct had two chiral centers and 2 pairs of diastereomers were produced (compounds **9a**, **9b** and **14a**, **14b** in **Figure 42**, that are the analogues of compound **66** in Figure **96**).

In general, above described results showed that alkanals reacted similarly with phenolic compounds and the preferred adduct was formed at position C4 of the phenol ring. This is likely a consequence of being C4 the carbon atom of the phenolic compound with the lowest steric hindrance among those with a high nucleophilicity in the phenolic ring.

Glyoxal is a dialdehyde, but it reacts similarly to other saturated aldehydes and the addition of the phenolic C4 to one of the carbonyl carbons was produced to form compounds **17** and **18** (**Figure 42)**. However, different from most suggested structures in many previous studies between phenolics and glyoxal, the structure determined by NMR indicated that the carbonyl

group was conjugated with the aromatic ring and the adduct was a primary alcohol. The formation of this product implies that an isomerization was produced. This isomerization also made difficult the addition of a second molecule of phenol to the carbonyl compound. For that reason, adducts involving two molecules of phenolics and one of glyoxal were not isolated.

The wide variety of carbonyl-phenol adducts isolated when alkanals were involved allowed to study the SAR of both phenolics and aldehydes for this reaction. Thus, in relation to resorcinol, this had a lower reactivity than other phenolics (section 4.1.2). On the other hand, orcinol produced carbonyl-phenol adducts to the highest extent. These results are likely a consequence of the electronic and steric effects of methyl groups in the phenolic compound. Thus, the introduction of a methyl group at C2 activates the phenolic ring and, for that reason, 2-methylresorcinol was more reactive than resorcinol. When a new methyl group was introduced at position 5 of the aromatic ring, the phenolic ring should be further activated but this group also introduced a steric hindrance. For that reason, reaction yields for 2-methylresorcinol and 2,5-dimethylresorcinol were very similar. However, when the methyl group at C2 was eliminated, as occurred in orcinol, the yield increased because the electronic effects of methyl groups are higher at *ortho* and *para* positions than at *meta* position (Wright et al., 2001).

The effect of the aldehyde chain length was also studied. As observed in **Figure 43**, and independently of the assayed phenol, the formation of carbonyl-phenol adducts mostly followed the same order: propanal < butanal < pentanal ≈ hexanal. This behavior is likely related to the high reactivity of shorter aldehydes that produced the formation of aldol products under the employed reaction conditions. As described above, these aldol products were later involved in the formation of carbonyl-phenol adducts as shown in **Figure 96**.

The existence of branchings in the aldehyde also played a role in the formation of carbonyl-phenol adducts. Thus, the presence of a methyl group at position 2 of the aldehyde always decreased the formation of carbonyl-

phenol adducts as a consequence of the steric hindrance introduced by this group (see section 4.1.2). This effect was not observed when the methyl group was present at the carbon 3 of the aldehyde.

All these results showed that these alkanals were trapped by phenolics, but this trapping depended on the electronic effects and steric hindrances of aldehydes and phenolics. In particular, to expect a high trapping, the nucleophilicity of the phenolic carbons should be high and the presence of groups that contribute to an increase of this nucleophilicity will increase the carbonyl trapping. On the other hand, any group that increase the steric hindrance of these positions without affecting nucleophilicity, will inhibit the reaction. The steric hindrance in the aldehyde also plays a major role. Thus, the presence of a branching at C2 of the aldehyde will make more difficult the formation of the corresponding carbonyl-phenol adducts.

5.2. The phenolic trapping of epoxyalkenals.

Analogously to alkanals, epoxyalkenals are also trapped by phenolics. In fact, this reaction is very fast as described previously (Hidalgo et al., 2017).

The reaction is complex because the adducts produced in a first step still have reactive groups that promote further reactions, included polymerizations. Therefore, the stabilization of these first adducts was required previously to their isolation and characterization. The carbonyl-phenol adducts produced in this first step between epoxyalkenals and phenolics were 1,3a,4,9b-tetrahydro-2*H*-furo[2,3-*c*]chromene-2,7-diols (**27**) and 3,4,4a,9a-tetrahydro-1*H*-pyrano[3,4-*b*]benzofuran-3,7-diols (**28**) (**Figure 97**).

A reaction pathway that explains the formation of these adducts is proposed in **Figure 97**.

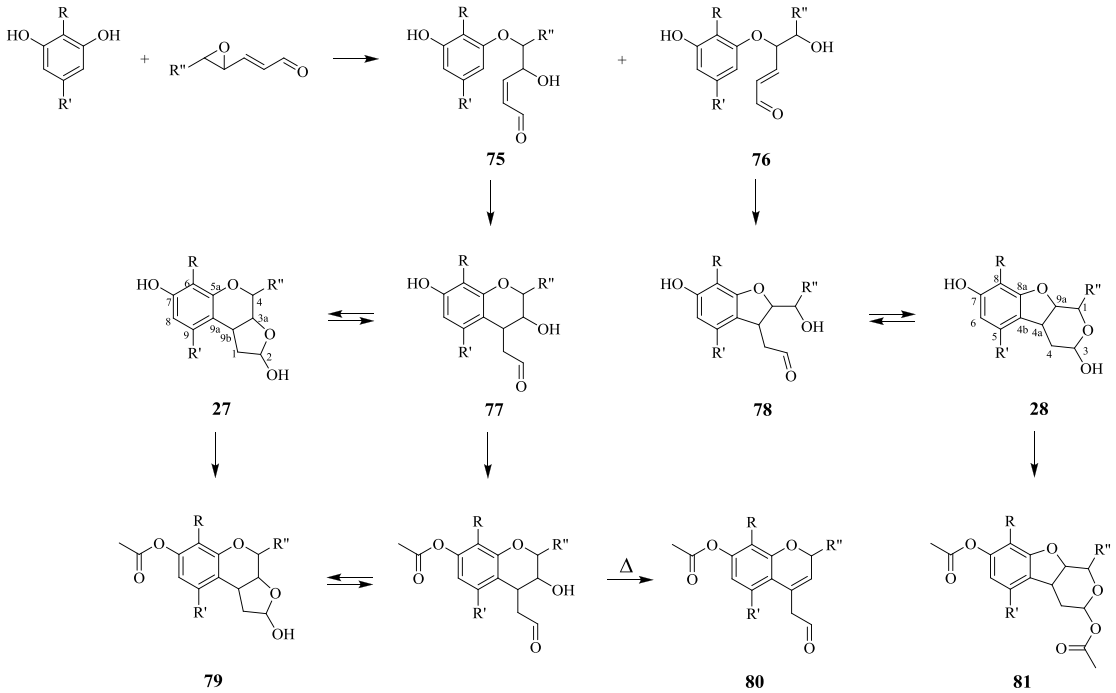

Figure 97. *Proposed reaction pathway for the reaction between epoxyalkenals and phenolic compounds. The assayed epoxyalkenals and phenolic compounds were: 2-methylresorcinol (R = CH_3 and R' = H), 2,5-dimethylresorcinol (R = CH_3 and R' = CH_3), 4,5-epoxy-2-hexenal (R'' = CH_3), 4,5-epoxy-2-heptenal (R'' = CH_2CH_3), and 4,5-epoxy-2-decenal (R'' = $CH_2CH_2CH_2CH_2CH_3$). Compounds having the structures of compounds **79** and **81** have been isolated and characterized in 4,5-epoxy-2-alkenal/phenolic reaction mixtures.*

The reaction is initiated by the opening of the epoxide ring of the aldehyde by one of the hydroxyl groups of the phenol. Two different compounds (**75** and **76**) are produced by addition of the phenolic to any of the two carbons of the epoxide. Because of the disposition of the groups in the phenol, the aromatic carbon at the α-position of the hydroxyl group that has reacted with the epoxide has a high nucleophilicity and it is added to the carbon-carbon double bond of compound **75** or **76**. Adducts **75** and **76** are α,β-unsaturated carbonyl compounds. Therefore, the addition of the aromatic carbon to the carbon-carbon double bond occurs at the β-carbon. The result is the formation of a six-membered ring in compound **77** when starting from compound **75**, and a five-membered ring in compound **78** when starting from compound **76**. Both adducts still have a carbonyl group and a hydroxyl group to an adequate distance to produce a cyclic hemiacetal. Therefore, the predominant forms of these adducts are 1,3a,4,9b-tetrahydro-2*H*-furo[2,3-*c*]chromene-2,7-diol (**27**) and 3,4,4a,9a-tetrahydro-1*H*-pyrano[3,4-*b*]benzofuran-3,7-diol (**28**) when starting from adducts **77** and **78**, respectively. Upon acetylation under soft conditions, compound **27** only suffers the acetylation of the phenolic hydroxyl group to produce adduct **79** (this adduct corresponds to compounds **20a**, **20b**, and **22** isolated in the reactions of 4,5-epoxy-2-heptenal and 4,5-epoxy-2-decenal with 2-methylresorcinol and 2,5-dimethylresorcinol). However, the hydroxyl group of the six-membered ring of the hemiacetal **28** is acetylated at the same time that the phenolic hydroxyl group to produce adduct **81** (this adduct corresponds to compounds **24**-**26** isolated in the reactions of 4,5-epoxy-2-heptenal and 4,5-epoxy-2-hexenal with 2-methylresorcinol and 2,5-dimethylresorcinol). When the acetylated compound **79** (compounds **20a, 20b** and **22**) was submitted to GC-MS, the hemiacetal ring was opened and a dehydration was produced to form the corresponding 4-(2-oxoethyl)-2*H*-chromen-7-yl acetate (adduct **80**), which were the adducts observed by GC-MS (compounds **21** and **23**). On the other hand, adduct **81** was completely

acetylated and was not transformed when studied by GC-MS (compounds **24-26**).

Although only two adducts were formed in the first steps of this reaction, the reaction mixtures were quite complex because of the existence of different isomers (**Figure 46**). According to the reaction pathway proposed in **Figure 97**, the initial epoxyalkenal is a mixture of 4*R*,5*R* plus its enantiomer. These two carbons have different numberings depending on the produced compounds. Thus, they are 3a*R*,4*R* plus its enantiomer if the numbering compound **27** is employed or 9a*R*,1*R* plus its enantiomer if the numbering compound **28** is used. The opening of the epoxide ring in compounds **75** and **76** implies the inversion of the stereochemistry of the carbon that suffers the attack of the phenolic hydroxyl group. As a result, compound **75** should be a mixture of 3a*S*,4*R* plus its enantiomer and compound **76** should be a mixture of 9a*R*,1*S* plus its enantiomer. The addition of the phenolic carbon to the carbon-carbon double bond creates a new chiral center. This means that compound **77** should be a mixture of 3a*S*,4*R*,9b*R*, 3a*S*,4*R*,9b*S* and their corresponding enantiomers. Something similar should be happening in compound **78**, which should be a mixture of 1*S*,4a*R*,9a*R*, 1*S*,4a*S*,9a*R*, and their corresponding enantiomers.

Acetylation does not change the stereochemistry of compound **27**, in which the stereochemistry of C2 is not fixed, and the later dehydration implies the loss of two chiral centers (C3a and C9b), and the formation of a carbon-carbon double bond with a fixed stereochemistry because of the six-membered ring. For that reason, compound **80** has only one chiral center, and only one dehydrated compound (compound **21**) was observed in the gas chromatogram of **Figure 46**.

On the other hand, acetylation of compound **28** fixes a new chiral center (C3). This means that compound **81** should be a mixture of 1*S*,3*R*,4a*R*,9a*R*, 1*S*,3*S*,4a*R*,9a*R*, 1*S*,3*R*,4a*S*,9a*R*, 1*S*,3*S*,4a*S*,9a*R*, and their corresponding enantiomers. For that reason, the gas chromatogram of **Figure 46** showed the existence of four peaks with the same mass spectra that

corresponded to compounds **25a**, **25b**, **25c**, and **25d**. Obviously, not all isomers have to be formed to the same extent, and those having less steric hindrance would be preferred. Thus, compound **25a** was the 3,4,4a,9a-tetrahydro-1*H*-pyrano[3,4-*b*]benzofuran-3,7-diol formed to a higher extent in the reaction between 4,5-epoxy-2-heptenal and 2-methylresorcinol at the different assayed temperatures (**Figure 56**).

The presence of hydroxyl and carbonyl groups in compounds **77** and **78** also explain the reactivity of these molecules and, therefore, the difficulty for their study. Saturated carbonyl compounds have been shown to react with phenolic compounds (see, for example, Totlani & Peterson, 2005) and also with amino compounds (Kitryte et al., 2012), but their reactivity is much reduced in comparison to that of epoxyalkenals (see, for example, Hidalgo et al., 2010). Therefore, phenolic compounds are able to reduce rapidly the high reactivity of epoxyalkenals, although the produced adducts still have functional groups having a potential reactivity with both phenolics and amino compounds.

Reaction pathway proposed in **Figure 97** is also in agreement with the effects of reaction conditions on adducts formation described in the section 4.2.2. Thus, both epoxyalkenal (**Figure 51**) and phenol (**Figure 52**) take part in the reaction; the basic pH (**Figure 50**) is needed for the addition of the aromatic carbon to the carbon-carbon double bond, as observed previously for 2-alkenals (Hidalgo & Zamora, 2014), because of the higher nucleophilicity of phenolic carbons at these pH values; and reaction times and temperatures are expected to favor the formation of adducts (**Figures 53-58**). However, many steps in **Figure 97** are reversible and the relative proportions among final products will change as a function of reaction conditions.

5.3. The phenolic trapping of oxoalkenals.

Analogously to alkanals and epoxyalkenals, phenolics also trap oxoalkenals. In addition, this is also a complex reaction and different adducts were produced to different extents that depended on reaction conditions. As described in section 4.3, three different carbonyl-phenol adducts were produced: benzofuran-6-ols (**40**), 2,3,3a,8a-tetrahydrofuro[2,3-*b*]benzofuran-2,6-diols (**41**), and chromane-2,7-diols (**42**) (**Figure 98**).

These adducts, which were produced in a first step, resulted unstable because of the presence of reactive groups in their structures. Therefore, they had to be stabilized, by either acetylation or reduction, previously to their isolation and characterization. A reaction pathway that explains the formation of these adducts is shown in **Figure 98**.

The reaction between oxoalkenals and phenolic compounds occurs similarly to the previously described reaction between 2-alkenals and phenolic compounds (Hidalgo & Zamora, 2014). Thus, both one hydroxyl group and its contiguous carbon in the phenolic compound (the carbon at the α-position in relation to the hydroxyl group) are involved, and the produced reaction is an addition of these nucleophilic groups to the carbon-carbon double bond of the oxoalkenal. Because the oxoalkenal has two carbonyls groups and the phenolic compound has two nucleophilic groups that can be added to the aldehyde, four adducts might be expected. Thus, the addition of the hydroxyl group of the phenol to the position either 2 or 3 of the oxoalkenal would produce compounds **82** and **83**, respectively; and the addition of the phenolic carbon to the position either 2 or 3 of the oxoalkenal would produce compounds **84** and **85**, respectively. For some reason, the isolated compounds were only derived from compounds **82** and **85**. The other two additions were either not produced or produced to a much lower extent and the formed compounds could not be isolated and characterized.

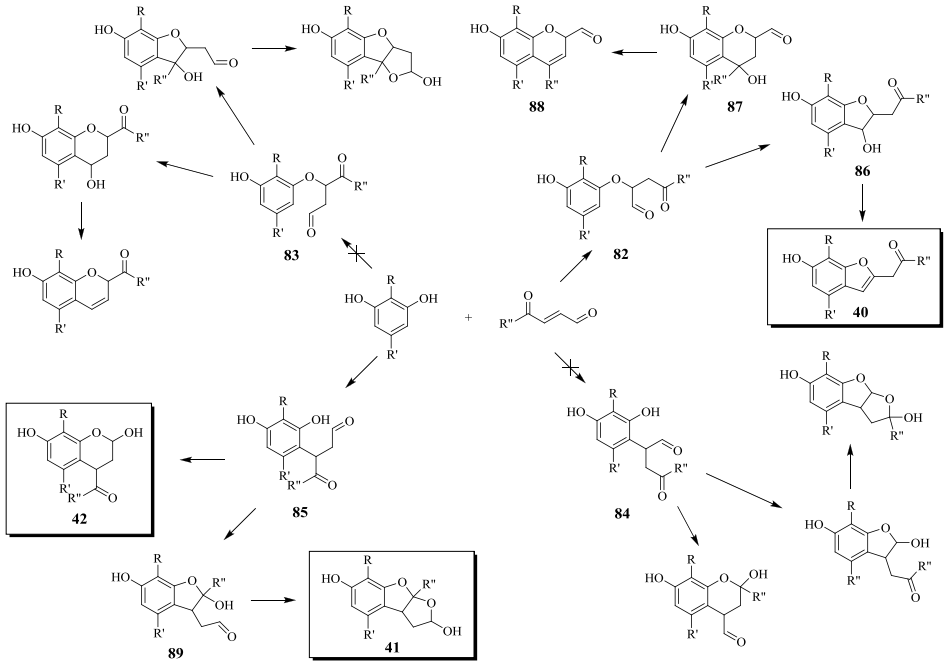

Figure 98. *Proposed reaction pathways for the reaction between 4-oxo-2-alkenals and phenolic compounds. The assayed oxoalkenals and phenolic compounds were: resorcinol (R = H and R' = H), 2-methylresorcinol (R = CH_3 and R' = H), fumaraldehyde (R'' = H), 4-oxo-2-hexenal (R'' = CH_2CH_3), and 4-oxo-2-nonenal (R'' = $CH_2CH_2CH_2CH_2CH_3$). Compounds having the structures of compounds* ***40***, ***41*** *and* ***42*** *have been isolated and characterized in 4-oxo-2-alkenal/phenolic reaction mixtures.*

Once the first addition was produced, the next step was the reaction of the unreacted nucleophilic group of the phenolic compound with the carbonyl compound that now is a saturated carbonyl compound and reacts like these compounds. Thus, for example, the aromatic carbon in compound **82** is added to the aldehyde group to produce the corresponding 2,3-dihydrobenzofuran-3,6-diol (**86**). This compound, which could be isolated in the reaction between 2-methylresorcinol and fumaraldehyde (compound **38**), suffers then a dehydration which is the origin of the different benzofuran-6-ols (adduct **40**) isolated in this study (compounds **29**, **32**, **35**, **36**, **37**, and **39** produced in the reactions of 4-oxo-2-hexenal, 4-oxo-2-nonenal and fumaraldehyde with resorcinol and 2-methylresorcinol).

Alternatively, the aromatic carbon in compound **82** might also be added to the ketone group to produce in a first step the corresponding 4,7-dihydroxychromane-2-carbaldehyde (**87**) and then, after dehydration, the corresponding 7-hydroxy-2*H*-chromene-2-carbaldehyde (**88**). None of these compounds could be detected. The reason might be both the lower reactivity of the ketone group, and therefore the attack of the aromatic carbon to this carbonyl carbon is not favored, and the instability of the produced compound having both an aldehyde and a phenolic group that can suffer later reactions.

The formation of the other products isolated and characterized are likely derived from adduct **85**. In this adduct, the phenolic hydroxyl group, which was not involved in its formation, can be added to either the aldehyde or the ketone group. The addition to the aldehyde group would produce the chromane-2,7-diol (**42**), which has been isolated and characterized (compounds **31a**, **31b**, **34a**, and **34b** isolated from the reactions of 4-oxo-2-hexenal and 4-oxo-2-nonenal with 2-methylresorcinol). On the other hand, the addition to the ketone group would produce the hemiacetal **89** in a first step and, then, after addition to the aldehyde group, the 2,3,3a,8a-tetrahydrofuro[2,3-*b*]benzofuran-2,6-diol (**41**). This compound has also be isolated and characterized (compounds **30a**, **30b**, **33a**, and **33b** isolated from the reactions of 4-oxo-2-hexenal and 4-oxo-2-nonenal with 2-

methylresorcinol). In fact, this adduct seems to be the main adduct produced under most assayed reaction conditions.

This proposed reaction pathway is also in agreement with the reaction conditions required for the formation of the adducts, which were described in section 4.3.2. Thus, the reaction mainly took place at neutral or slightly basic pH values because of the higher nucleophilicity of phenolic carbons at these pH values (**Figure 62**), although significant amounts of adducts could be found in the whole range of studied pH values (between 5 and 9). In addition, the concentration of the formed adducts depended on the concentration of both aldehyde and phenolic compound (**Figure 63-64**). Furthermore, they were only partially stable because of the presence of free carbonyl groups. Therefore, they disappeared when elevated heating temperatures or prolonged heating times were assayed (**Figure 65-69**).

These free reactive groups were present in all adducts and they had to be blocked to avoid further reactions. Thus, the benzofuran-6-ols had a carbonyl group in the chain at position C2'. This carbonyl group was converted into a hydroxyl group in compounds **35**–**39** after reduction. In addition, compounds **30a**, **30b**, **33a**, and **33b** were 2,3,3a,8a-tetrahydrofuro[2,3-*b*]benzofuran-2,6-diols with a carbonyl group in a hemiacetalic form, and compounds **31a**, **31b**, **34a**, and **34b** were chromane-2,7-diols also having a carbonyl group in a hemiacetalic form.

5.4. Lipid-derived aldehyde degradation under thermal conditions.

As described in previous sections, carbonyl-phenol reactions are very complex because different adducts are produced and many of them are only intermediate in further polymerizations reactions. Furthermore, reactions are complicated because of the formation of new chiral centers and therefore, production of complex mixtures of diastereomers. Moreover, some carbonyls produced in the course of lipid oxidation are labile, can be decomposed, and

the aldehydes produced are also able to react with phenolics producing more carbonyl-phenol adducts.

The studies carried out in this thesis also allow to understand some of the decomposition reactions suffered by lipid-derived reactive carbonyls. Thus, aldehydes were shown to be relatively stable in the absence of buffer and oxygen, but when aqueous solutions were employed, a rapid decomposition was observed. This decomposition was similar for 2-alkenals and 2,4-alkadienals and always produced shorter aldehydes, among other compounds. The aldehydes produced were formaldehyde, acetaldehyde and the corresponding carbonyl compounds produced as a consequence of the breakage of the carbon-carbon double bonds present in the molecule. Thus, because 2-alkenals only have one carbon-carbon double bond, the products formed were alkanals and glyoxal. The reaction was more complex for 2,4-alkadienals because these compounds have two carbon-carbon double bonds. The breakage of the double bond between C2 and C3 produced 2-alkenals and glyoxal, and the breakage of the double bond between C4 and C5 produced alkanals and fumaraldehyde.

As shown in sections from 4.4.2 to 4.4.5, the E_a for the breakage of the different carbon-carbon double bonds was always very similar and was about 25 kJ/mol. However, alkanals were produced to a much higher extent than 2-alkenals. Thus, 10–18% of the initial either 2-alkenal or 2,4-alkadienal was converted into alkanal after 1 h heating at 200 ºC and only about 1% of the initial 2,4-alkadienal was converted into 2-alkenal under the same reaction conditions. The lower amount of 2-alkenals found during 2,4-alkadienal degradation in relation to that of alkanals is likely a consequence of the degradation suffered by 2-alkenals, which also produce alkanals. However, alkanals were also produced directly from 2,4-alkadienals because fumaraldehyde was found in these reactions (**Figure 70**, chromatograms **j** and **n** for 2,4-heptadienal and 2,4-decadienal, respectively).

5.5. Lipid-derived carbonyls are trapped by phenolics under common food processing conditions.

Previous reactions produced large amounts of carbonyl-phenol adducts but, they were carried out under conditions far from those employed during usual cookery. To fill this gap, a final investigation was carried out to determine whether these carbonyl-phenol adducts are produced in the course of cooking and the produced lipid-derived carbonyls are incorporated into food products in the form of carbonyl-phenol adducts.

When quercetin (a major phenolic compound in onion) reacts with acrolein, crotonaldehyde, and (*E*)-2-pentenal (common LOPs produced during frying), two different kind of carbonyl-phenol adducts (hemiacetals and conjugated olefins) are produced. Some of these carbonyl-phenol adducts were found to be produced in onions fried in fresh rapeseed oil spiked with acrolein, crotonaldehyde, and (*E*)-2-pentenal. Thus, adduct **62 (**produced between quercetin and (*E*)-2-pentenal) was the major compound produced. In addition, trace amounts of adducts **56** and **57** (produced with acrolein and crotonaldehyde, respectively), but not of adduct **61** (a second adduct of crotonaldehyde), were also detected. The major presence of the adduct derived from (*E*)-2-pentenal in comparison to that derived from acrolein and crotonaldehyde might be a consequence of both the higher boiling point of (*E*)-2-pentenal and its lower reactivity. Thus, oils were heated for 9 min before adding the onions, and the aldehydes with a lower boiling point were evaporated more easily than aldehydes with a higher boiling point. In addition, the higher reactivity of acrolein and crotonaldehyde might lead to their faster reaction with other food components than with food phenols.

In contrast, compound **56** (the adduct formed with acrolein) was the major adduct present in commercially crispy fried onions. Compound **62** (the adduct formed with (*E*)-2-pentenal) was also present to a lower extent, and trace amounts of compound **57** (the adduct with crotonaldehyde), but not of compound **61** (the second adduct with crotonaldehyde), were also detected.

The difference in the amounts of adduct **56** found between the onions fried in the laboratory (only present in trace amounts in some samples) and those found in commercially crispy fried onions (the main carbonyl-phenol adduct) might be a consequence of the quality of the employed oils. In the laboratory, fresh nonoxidized oil was used (although spiked with a small amount of acrolein) and most acrolein was likely evaporated during oil heating before adding the onions. On the other hand, the oil employed for preparing the commercially crispy fried onions was likely more oxidized and acrolein was produced at the same time that the onions were fried.

5.6. Lipid-derived carbonyl trapping, an additional protective mechanism of food phenolics.

The results obtained in this thesis show the complexity of carbonyl-phenol reactions and explain why these reactions are still poorly understood. However, these results can contribute to a better understanding of these reactions. Thus, for saturated aldehydes or alkanals, only the addition of phenolic carbons to the carbonyl carbon has been described (Shao et al., 2008), and the results described in section 4.1 confirm such mechanism and allow to understand why specific aldehydes or phenolics are more prone to these reactions.

However, the case of alkanals is only an exception and the reaction of other lipid-derived reactive carbonyls with phenolics always involve an aromatic carbon and its contiguous hydroxyl group in the phenolic compound, as well as several functional groups in the LOP. Thus, in the case of 2-alkenals, the reaction can be initiated by addition of either the phenolic hydroxyl group or the phenolic carbon to the carbon-carbon double bond of the aldehyde (Hidalgo & Zamora, 2014). In the case of epoxyalkenals, the reaction is always initiated by the epoxide-ring opening produced by the phenolic hydroxyl group and then the later addition of the phenolic carbon to the carbon-carbon double bond of the initial aldehyde. Finally, for

oxoalkenals, the produced reaction always involves the carbon-carbon double bond and one of the carbonyl groups of the aldehyde as well as the phenolic hydroxyl group and the phenolic carbon. Because oxoalkenals have two carbonyl groups, the second carbonyl group either remains unreacted in the produced adduct or is partially stabilized by forming an hemiacetal.

All these results suggest a versatility of phenolic compounds, which are able to react differently with the diverse carbonyl compounds as a function of their structure. This provides an additional explanation for the differences observed in the scavenging of carbonyl compounds by phenolic compounds, which depends on the structures of both the lipid-derived carbonyl compounds and the phenolic compounds involved (Hidalgo et al., 2017).

To sum up, although carbonyl-phenol reactions only involve one aromatic carbon of the phenol when alkanals are implicated, for other LOPs, these reactions always involve one hydroxyl group and the contiguous aromatic carbon of the phenolic compound (Hidalgo & Zamora, 2014). Therefore, these two groups are usually needed for a positive trapping activity of the phenolic compound. Furthermore, both phenolic hydroxyl group and phenolic carbon need to have a high nucleophilicity and this is mostly produced when two hydroxyl groups are at *meta* position in the aromatic ring (Salazar et al., 2014). Therefore, the phenolic compounds with the highest nucleophilicity in these two positions are expected to exhibit the highest carbonyl-trapping ability.

However, a high nucleophilicity is not the only requisite so that the formed carbonyl-phenol adducts can be detected. Once formed the adduct, it will be more or less stable depending on the presence of additional reactive groups. Thus, alkanals and 2-alkenals produce stable compounds (Hidalgo, & Zamora, 2014). On the other hand, the most reactive LOPs, such as 4,5-epoxy-2-alkenals and 4-oxo-2-alkenals, produce unstable compounds because of the presence of additional reactive groups in the formed adducts. Therefore, these last adducts are likely involved in further reactions, including polymerizations.

In addition, under usual cooking conditions, lipid-derived aldehydes can suffer decompositions and the formation of additional aldehydes has been observed, which are also involved in the formation of new carbonyl-phenol adducts. As an extra difficulty of all these reactions, the formation of chiral centers is usually produced and the presence of mixtures of diastereomers should be expected.

For all these reasons, the complex mixtures of LOPs formed in the course of lipid oxidation in foods are expected to be further complicated in presence of phenolic compounds, because numerous carbonyl-phenol adducts are produced, including the formation of polymers. The formation of these mixtures complicates considerably the detection of the formed adducts. Nevertheless, the characterization of the carbonyl-phenol adducts carried out in this and in previous studies points out to the kinds of compounds that should be searched for in food products. In fact, some of these carbonyl-phenol adducts have been shown to be common components in processed foods. As discussed in the previous section, they are produced under usual cooking conditions and are present in cooked foods. However, the function(s) they might be playing in foods, in addition to the removal of reactive carbonyl compounds, remains to be investigated, although they are expected to contribute to food browning as well as changes in food flavors as a consequence of a potential selective sequestering of significant flavor components in processed foods (Kokkinidou & Peterson, 2014; Troise et al., 2014).

All the obtained results in this thesis suggest an additional protective role of food polyphenols in the lipid oxidation pathway. Thus, in addition to their well-known functions as free radical scavengers and chelators, the lipid-derived reactive carbonyls produced in the course of lipid reaction are removed by phenolics (**Figure 99**). This reaction produces in a first step the addition product of the phenolic compound to the lipid-derived reactive carbonyl. This addition product suffer then either a rapid stabilization by protecting its reactive groups, or polymerization.

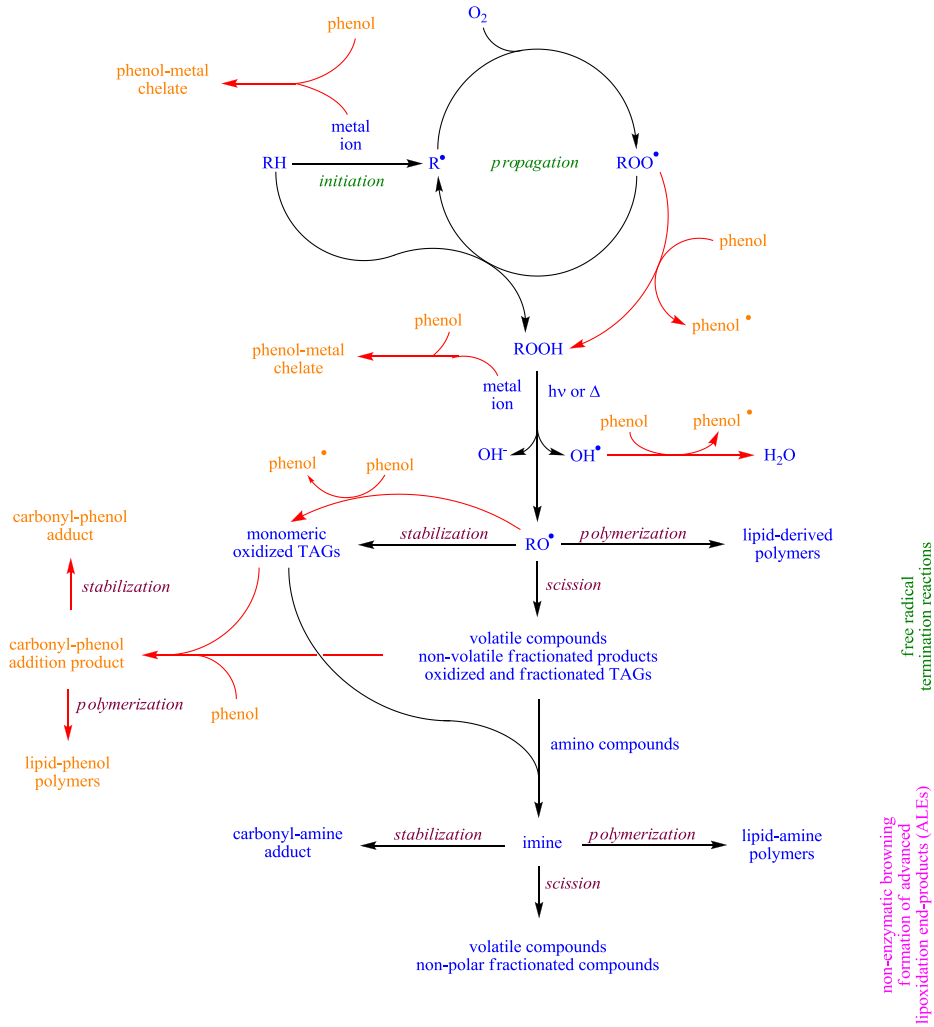

Figure 99. *The triple defensive barrier of phenolic compounds against the lipid oxidative damage in food products* (*Adapted from Zamora & Hidalgo, 2016).*

6. CONCLUSIONS

First. Phenolic compounds react differently with a wide range of lipid-derived carbonyl compounds producing the corresponding carbonyl-phenol adducts.

Second. The formation of carbonyl-phenol adducts depends on the structure of both the phenolic and the aldehyde involved. In relation to the phenolic compound, the presence of groups that increase the nucleophilicity of the phenolic carbons also increases the carbonyl-trapping ability of these compounds. On the other hand, the presence of groups that increase the steric hindrance of these positions without affecting nucleophilicity inhibits the formation of the corresponding carbonyl-phenol adducts. Analogously, the presence of branching at position 2 of the aldehyde also inhibits the formation of carbonyl-phenol adducts by steric hindrance.

Third. For alkanals and other saturated aldehydes, the carbon atoms in α-position to the phenolic hydroxyl groups have a high nucleophilicity and react with the carbonyl carbon of the aldehyde. In addition, these aldehydes can also suffer an aldolic condensation to produce the corresponding 2-alkenal, which is also trapped by phenolics.

Fourth. For epoxyalkenals, the reaction with the phenol is initiated by the epoxide-ring opening produced by a phenolic hydroxyl group and, then, the addition of the phenolic carbon to the carbon-carbon double bond of the initial aldehyde is produced. Finally, the aldehyde group is stabilized as a hemiacetal.

Fifth. For oxoalkenals, addition of either one of the phenolic hydroxyl groups or its carbon at α-position to the carbon-carbon double bond of the oxoalkenal is produced. The adduct is then stabilized by involving one of the carbonyl groups of the aldehyde, although the other carbonyl group remains free or is

stabilized as a hemiacetal when the spatial distribution of the reactive groups allows this additional reaction.

Sixth. The formation of carbonyl-phenol adducts reduces the reactivity of lipid-derived carbonyls by blocking their most reactive functional groups. However, some of these groups can remain in the first adducts produced, such as in epoxyalkenals and oxoalkenals. The adducts produced with these aldehydes are unstable and suffer further reactions, including polymerizations.

Seventh. Reaction conditions play a major role in carbonyl-phenol adduct formation. Thus, these reactions are mostly produced at neutral or slightly basic pH values and the formation of adducts increases with time and temperature. Nevertheless, the decomposition of some carbonyl-phenol adducts has been observed at high temperature for long reaction times.

Eighth. All these reactions are complicated because unsaturated aldehydes are decomposed rapidly under thermal conditions and the produced aldehydes can also be trapped by phenolics producing new carbonyl-phenol adducts.

Ninth. When submitted to heating in the presence of buffer and air, 2-alkenals are decomposed to yield alkanals and glyoxal, and 2,4-alkadienals are degraded to produce either 2-alkenals and glyoxal, or alkanals and fumaraldehyde.

Tenth. The E_a for the breakage of the different carbon-carbon double bonds in unsaturated aldehydes was found to be about 25 kJ/mol and was similar for both of them. However, alkanals were produced to a much higher extent than 2-alkenals.

Eleventh. The formation of carbonyl-phenol adducts has been shown to occur during food frying and these adducts have been found in fried foods.

Twelfth. All these results suggest that carbonyl-trapping by phenolics is a common protective function of phenolics in addition to their well-known functions as free radical scavengers or chelators.

Thirteenth. This carbonyl-trapping function seems to be playing a role in the removal of toxicologically relevant aldehydes produced as a consequence of lipid oxidation.

Fourteenth. The function(s) of the produced carbonyl-phenol adducts remain(s) to be investigated, although their contribution to food browning and flavor changes can be hypothesized as a consequence of both their involvement in polymerization reactions and the sequestering of significant flavor components.

7. REFERENCES

Abeywickrama, G., Debnath, S. C., Ambigaipalan, P., & Shahidi, F. (2016). Phenolics of selected cranberry genotypes (*Vaccinium macrocarpon Ait.*) and their antioxidant efficacy. *Journal of Agricultural and Food Chemistry*, 64, 9342−9351.

Andjelkovic, M., Van Camp, J., De Meulenaer, B., Depaemelaere, G., Socaciu, C., Verloo, M., & Verhe, R. (2006). Iron-chelation properties of phenolic acids bearing catechol and galloyl groups. *Food Chemistry*, 98, 23-31.

Bastos, L. C. S., Costa, E. A. A., & Pereira, P. A. P. (2017). Development, validation and application of an UFLC-DAD-ESI-MS method for determination of carbonyl compounds in soybean oil during continuous heating. *Food Chemistry*, 218, 518–524.

Belitz, H. D., Grosch, W., & Schieberle, P. (2009). Food Chemistry. 4th revised and extended edition, Springer-Verlag, Berlin, Germany.

Beretta, G., Furlanettob, S., Regazzoni, L., Zarrella, M., & Facino, R. M. (2008). Quenching of α,β-unsaturated aldehydes by green tea polyphenols: HPLC-ESI-MS/MS studies. *Journal of Pharmaceutical and Biomedical Analysis*, 48, 606-611.

Brewer, M. S. (2011). Natural antioxidants: sources, compounds, mechanisms of action, and potential applications. *Comprehensive Reviews in Food Science and Food Safety*, 10, 221-247.

Brewer, S. (2014). Effects of oxidation on sensory characteristics of food components during processing and storage. In: *Food Oxidants and Antioxidants: Chemical, Biological, and Functional Properties.* Bartosz, G., ed., CRC Press, Boca Raton, 159-186.

Bukhari, S. B., Memon, S., Mahroof-Tahir, M., & Bhanger, M. I. (2009). Synthesis, characterization and antioxidant activity copper-quercetin complex. *Spectrochimica Acta Part A: Molecular and Biomolecular Spectroscopy*, 71, 1901-1906.

Cai, Y. Z., Sun, M., Xing, J., Luo, Q., & Corke, H. (2006). Structure-radical scavenging activity relationships of phenolic compounds from traiditional Chinese medicinal plants. *Life Sciences*, 78, 2872-2888.

Cheng, K. W., Chen, F., & Wang, M. (2007). Inhibitory activities of dietary phenolic compounds on heterocyclic amine formation in both chemical model system and beef patties. *Molecular Nutrition & Food Research*, 51, 969-976.

Cheng, K. W., Wong, C. C., Chao, J., Lo, C., Chen, F., Chu, I. K., Che, C. M., Ho, C. T. & Wang, M. (2009). Inhibition of mutagenic PhIP formation by epigallocatechin gallate via scavenging of phenylacetaldehyde. *Molecular Nutrition & Food Research*, 53, 716-725.

Cheng, K. W., Wong, C. C., Cho, C. K., Chu, I. K., Sze, H. K., Lo, C., Chen, F., & Wang, M. (2008). Trapping of phenylacetaldehyde as a key mechanism responsible for naringenin´s inhibitory activity in mutagenic 2-amino-1-methyl-6-phenylimidazo[4,5-*b*]pyridine formation. *Chemical Research in Toxicology*, 21, 2026-2034.

Correddu, F., Nuda, A., Manca, M. G., Pulina, G., & Dalsgaard, T. K. (2015). Light-induced lipid oxidation in sheep milk: effects of dietary grap seed and linseed, alone or in combination, on milk oxidative stability. *Journal of Agricultural and Food Chemistry*, 63, 3980−3986.

Coultate, T. (2016). Lipids. In: *Food. The Chemistry of its components*. Coultate, T., eds., 6th ed., The Royal Society of Chemistry, Cambridge, 107-171.

Crozier, A., Jaganath, I. B., & Clifford, M. N. (2009). Dietary phenolics: chemistry, bioavailability and effects on health. *Natural Products Reports*, 26, 1001-1043.

Crozier, A., Lean, M. E. J., Mc Donald, M. S., & Black, C. (1997). Quantitative analysis of the flavonoid content of commercial tomatoes, onions, lettuce, and celery. *Journal of Agricultural and Food Chemistry*, 45, 590-595.

Da Silva, T. O., & de Paula Pereira, P. A. (2008). Influence of time, surface-to-volume ratio, and heating process (continuous or intermittent) on the emission rates of selected carbonyl compounds during thermal oxidation of palm and soybean oils. *Journal of Agricultural and Food Chemistry*, 56, 3129-3135.

Decker, E. A. (2008). Antioxidant mechanisms. In: *Food Lipids: Chemistry, Nutrition, and Biotechnology*. Akoh, C. C., & Min, D. B., eds., 3rd ed., CRC Press, Boca Raton, 409-433.

Delgado, R. M., Hidalgo, F. J., Zamora, R. (2016). Antagonism between lipid-derived reactive carbonyls and phenolic compounds in the Strecker degradation of amino acids. *Food Chemistry*, 194, 1143-1148.

Demir, E., Turna, F., Kaya, B., Creus, A., & Marcos, R. (2013). Mutagenic/recombinogenic effects of four lipid peroxidation products in Drosophila. *Food Chemistry*, 53, 221–227.

Erickson, M. C. (2008). Lipid oxidation of muscle foods. In: *Food Lipids: Chemistry, Nutrition, and Biotechnology*. Akoh, C. C., & Min, D. B., eds., 3rd ed., CRC Press, Boca Raton, 321-347.

Ewert, A., Granvogl, M., & Schieberle, P. (2011). Development of two stable isotope dilution assays for the quantitation of acrolein in heat-processed fats. *Journal of Agricultural and Food Chemistry*, 59, 3582–3589.

Ewert, A., Granvogl, M., & Schieberle, P. (2014). Isotope-labeling studies on the formation pathway of acrolein during heat processing of oils. *Journal of Agricultural and Food Chemistry*, 62, 8524-8529.

Frankel, E. N. (2005). *Lipid Oxidation*. 2nd ed., The Oily Press, Bridgwater.

Gardner, H. W. (1989). Oxygen radical chemistry of polyunsaturated fatty acids. *Free Radical Biology & Medicine*, 7, 65-86.

Gliszczynska-Swiglo, A., & Oszmianski, J. (2014). Antioxidant and prooxidant activity of food components. In: *Food Oxidants and Antioxidants: Chemical, Biological, and Functional Properties.* Bartosz, G., ed., CRC Press, Boca Raton, 375-432.

Granvogl, M. (2014). Development of three stable isotope dilution assays for the quantitation of (*E*)-2-butenal (crotonaldehyde) in heat-processed edible fats and oils as well as in food. *Journal of Agricultural and Food Chemistry*, 62, 1272–1282.

Guillen, M. D., & Goicoechea, E. (2008a). Formation of oxygenated α,β-unsaturated aldehydes and other toxic compounds in sunflower oil oxidation at room temperature in closed receptacles. *Food Chemistry,* 111, 157–164.

Guillen, M. D., & Goicoechea, E. (2008b). Toxic oxygenated α,β-unsaturated aldehydes and their study in foods: A review. *Critical Reviews in Food Science and Nutrition*, 48, 119-136.

Guillén, M. D., & Uriarte, P. S. (2012). Aldehydes contained in edible oils of a very different nature after prolonged heating at frying temperature:

Presence of toxic oxygenated α,β unsaturated aldehydes. *Food Chemistry*, 131, 915-926.

Heim, K. E., Tagliaferro, A. R., & Bolbiya, D. J. (2002). Flavonoid antioxidants: Chemistry, metabolism and structure-activity relationships. *Journal of Nutritional Biochemistry*, 13, 572-584.

Hermund, D. B., Karadag, A., Andersen, U., Jonsdottir, R., Kristinsson, H. G., Alasalvar, C., & Jacobsen, C. (2016). Oxidative stability of granola bars enriched with multilayered fish oil emulsion in the presence of novel brown seaweed based antioxidants. *Journal of Agricultural and Food Chemistry*, 64, 8359−8368.

Hidalgo, F. J., Delgado, R. M., Navarro, J. L., & Zamora, R. (2010). Asparagine decarboxylation by lipid oxidation products in model systems. *Journal of Agricultural and Food Chemistry*, 58, 10512–10517.

Hidalgo, F. J., Delgado, R. M., & Zamora, R. (2017). Protective effect of phenolic compounds on carbonyl-amine reactions produced by lipid-derived reactive carbonyls. *Food Chemistry*, 229, 388-395.

Hidalgo, F. J., Gallardo, E., & Zamora, R. (2005). Strecker type degradation of phenylalanine by 4-hydroxy-2-nonenal in model systems. *Journal of Agricultural and Food Chemistry*, 53, 10254-10259.

Hidalgo, F. J., León, M. M., & Zamora, R. (2016). Amino acid decarboxylations produced by lipid-derived reactive carbonyls in amino acid mixtures. *Food Chemistry*, 209, 256–261.

Hidalgo, F. J., & Zamora, R. (1993). Fluorescent pyrrole products from carbonyl-amine reactions. *Journal of Biological Chemistry*, 268, 16190–16197.

Hidalgo, F. J., & Zamora, R. (1995). In vitro production of long chain pyrrole fatty esters from carbonyl-amine reactions. *Journal of Lipid Research,* 36, 725–735.

Hidalgo, F. J., & Zamora, R. (2000a). The role of lipids in nonenzymatic browning. *Grasas y Aceites*, 51(1-2), 35-49.

Hidalgo, F. J., & Zamora, R. (2000b). Modification of bovine serum albumin structure following reaction with 4,5(*E*)-epoxy-2(*E*)-heptenal. *Chemical Research in Toxicology*, 13, 501–508.

Hidalgo, F. J., & Zamora, R. (2004). Strecker-type degradation produced by the lipid oxidation products 4,5-epoxy-2-alkenals. *Journal of Agricultural and Food Chemistry*, 52, 7126-7131.

Hidalgo, F. J., & Zamora, R. (2014). 2-Alkenal scavenging ability of *m*-diphenols. *Food Chemistry*, 160, 118-126.

Hidalgo, F. J., & Zamora, R. (2016). Amino acid degradations produced by lipid oxidation products. *Critical Reviews in Food Science and Nutrition*, 56, 1242–1252.

Hidalgo, F. J., & Zamora, R (2017). Food processing antioxidants. *Advances in Food and Nutrition Research*, 81, 31-64.

Janoszka, B. (2010). Heterocyclic amines and azaarenes in pan-fried meat and its gravy fried without additives and in the presence of onion and garlic. *Food Chemistry*, 120, 463-473.

Kasai, H., & Kawai, K. (2008). 4-Oxo-2-hexenal, a mutagen formed by ω-3 fat peroxidation: Occurrence, detection, and adduct formation. *Mutation Research,* 659, 56–59.

Kawai, K., Matsuno, K., & Kasai, H. (2006). Detection of 4-oxo-hexenal, a novel mutagenic product of lipid peroxidation, in human diet and cooking vapor. *Mutation Research*, 603, 186–192.

Khokhar, S., & Owusu Apenten, R. K. (2003). Iron binding characteristics of phenolic compounds: Some tentative structure-activity relations. *Food Chemistry*, 81, 133-140.

Kikugawa, K., Ido, Y., & Mikami, A. (1984). Studies on peroxidized lipids. VI. Fluorescent products derived from the reaction of primary amines, malondialdehyde and monofunctional aldehydes. *Journal of the American Oil Chemists' Society*, 61, 1574–1581.

Kim, S. Y., Li, J. L., Lim, N. R., Kang, B. S., & Park, H. J. (2016). Prediction of warmed-over flavor development in cooked chicken by colorimetric sensor array. *Food Chemistry*, 211, 440–447.

Kim, H. J., & Min, D. B. (2008). Chemistry of Lipid Oxidation. In: *Food Lipids: Chemistry, Nutrition, and Biotechnology*. Akoh, C. C., & Min, D. B., eds., 3rd ed., CRC Press, Boca Raton, 299-318.

Kitryte, V., Adams, A., Venskutonis, P. R., & De Kimpe, N. (2012). Impact of lipid oxidation-derived aldehydes and ascorbic acid on the antioxidant activity of model melanoidins. *Food Chemistry*, *135*, 1273–1283.

Kokkinidou, S., & Peterson, D. G. (2014). Control of Maillard-type off-flavor development in ultrahigh-temperature-processed bovine milk by phenolic chemistry. *Journal of Agricultural and Food Chemistry*, 62, 8023−8033.

Kolakowska, A. (2003). Lipid Oxidation in Food Systems. In: *Chemical and Functional Properties of Food Lipids*. Sikorski, Z. E., & Kolakowska, A., eds., CRC Press, Boca Raton, 133-166.

Kolakowska, A., & Sikorski, Z. E. (2003). The role of lipids in food quality. In: *Chemical and Functional Properties of Food Lipids.* Sikorski, Z. E., & Kolakowska, A., eds., CRC Press, Boca Raton, 1-8.

Lee, J., Xiao, L., Zhang, G., Ebeler, S. E., & Mitchell, A. E. (2014). Influence of storage on volatile profiles in roasted almonds (*Prunus dulcis*). *Journal of Agricultural and Food Chemistry*, 62, 11236−11245.

Lee, S. H., Oe, T., & Blair, I.A. (2002). 4,5-Epoxy-2(*E*)-decenal-induced formation of 1, N^2-etheno-2'-deoxyguanosine adducts. *Chemical Research in Toxicology*, 15, 300–304.

Leopoldini, M., Russo, N., Chiodo, S., & Toscano, M. (2006). Iron chelation by the powerful antioxidant flavonoid quercetin. *Journal of Agricultural and Food Chemistry*, 54, 6343-6352.

Leopoldini, M., Russo, N., & Toscano, M. (2011). The molecular basis of working mechanism of natural polyphenolic antioxidants. *Food Chemistry*, 125, 288-306.

Lindsay, R. C. (2017). Food additives. In: *Fennema´s Food Chemistry*. Damodaran, S., & Parkin, K. L., eds., 5th ed., CRC Press, Boca Raton, 803-864.

Liu, H., & Gu, L. (2012). Phlorotannins from brown algae (*Fucus versiculosus*) inhibited the formation of advanced glycation endproducts by scavenging reactive carbonyls. *Journal of Agricultural and Food Chemistry*, 60, 1326-1334.

Liu, Q., Raina, A.K., Smith, M.A., Sayre, L.M., & Perry, G. (2003). Hydroxynonenal, toxic carbonyls and Alzheimer disease. *Molecular Aspects of Medicine*, 24, 305–313.

Liu, S., Liu, F., Xue, Y., & Gao, Y. (2016). Evaluation on oxidative stability of walnut beverage emulsions. *Food Chemistry*, 203, 409–416.

Liu, W., Ma, H., Frost, L., Yuan, T., Dain, J. A., & Seeram, N. P. (2014). Pomegranate phenolics inhibit formation of advanced glycation endproducts by scavenging reactive carbonyl species. *Food & Function*, 5, 2996-3004.

Lo, C. Y., Hsiao, W. T., & Chen, X. Y. (2011). Efficiency of trapping methylglyoxal by phenols and phenolic acids. Journal of Food Science, 76, H90-H96.

Lo, C. Y., Li, S., Tan, D., Pan, M. H., Sang, S., & Ho, C. T. (2006). Trapping reactions of reactive carbonyl species with tea polyphenols in simulated physiological conditions. *Molecular Nutrition and Food Research*, 50, 118-1128.

Lv, L., Shao, X., Chen, H., Ho, C. T., & Sang, S. (2011). Genistein inhibits advanced glycation end product formation by trapping methylglyoxal. *Chemical Research in Toxicology*, 24, 579-586.

Malesev, D., & Kuntic, V. (2007). Investigation of metal-flavonoid chelates and the determination of flavonoids via metal-flavonoid complexing reactions. *Journal of the Serbian Chemical Society*, 72, 921-939.

Maqsood, S., Benjakul, S., Abushelaibi, A., & Alam, A. (2014). Phenolic compounds and plant phenolic extracts as natural antioxidants in prevention of lipid oxidation in seafood: A detailed review. *Comprehensive Reviews in Food Science and Food Safety*, 13, 1125-1140.

Mara Block, J., & Barrera-Arellano, D. (2012). Introducción a la química de lípidos. In: *Temas selectos en aceites y grasas*. Volumen 2-Química. Mara Block J., & Barrera-Arellano D., eds., Blucher, Sao Paulo, 1-36.

Marotti, M., & Piccaglia, R. (2002). Characterization of flavonoids in different cultivars of onion (*Allium cepa L.*). *Journal of Food Science*, 67, 1229−1232.

Márquez-Ruiz, G., Holgado, F., & Velasco, J. (2014). Mechanisms of oxidation in food lipids. In: *Food Oxidants and Antioxidants: Chemical, Biological, and Functional Properties.* Bartosz, G., ed., CRC Press, Boca Raton, 79-114.

McClements, D. J., & Decker, E. A. (2017). Lipids. In: *Fennema´s Food Chemistry*. Damodaran, S., & Parkin, K. L., eds., 5th ed., CRC Press, Boca Raton, 171-234.

Mesías, M., Navarro, M., Martínez-Saez, N., Ullate, M., del Castillo, M. D., & Morales, F. J. (2014). Antiglycative and carbonyl trapping properties of the water soluble fraction of coffee silverskin. *Food Research International*, 62, 1120-1126.

Mira, L., Fernandez, M. T., Santos, M., Rocha, R., Florencio, M. H., & Jennings, K. R. (2002). Interactions of flavonoids with iron and copper ions: A mechanism for their antioxidant activity. *Free Radical Research*, 36, 1199-1208.

Murkovic, M., Steinberger, D., & Pfannhauser, W. (1998). Antioxidant spices reduce the formation of heterocyclic amines in fried meat. *Z Lebensm Unters Forsch A*, 207, 477–480.

Muttucumaru, N., Powers, S. J., Elmore, J. S., Dodson, A., Briddon, A., Mottram, D. S., & Halford, N. G. (2017). Acrylamide-forming potential of potatoes grown at different locations, and the ratio of free asparagine to reducing sugars at which free asparagine becomes a limiting factor for acrylamide formation. *Food Chemistry*, 220, 76-86.

Navarro, M., & Morales, F. J. (2015). Mechanism of reactive carbonyl species trapping by hydroxytyrosol under simulated physiological conditions. *Food Chemistry*, 175, 92-99.

Nichols, D.S., & Sanderson, K. (2003). The nomenclature, structure, and properties of food lipids. In: *Chemical and functional properties of food lipids*. Sikorski, Z. E., & Kolakowska, A., eds., CRC Press, Boca Raton, 29-59.

O´Keefe, S. F. (2008). Nomenclature and classification of lipids, In: *Food Lipids, Chemistry, Nutrition, and Biotechnology*. Akoh, C. C., & Min, D. B., 3rd ed., CRC Press, Boca Raton, 3-37.

Pannala, A. S., Chan, T. S., O'Brien, P. J., & Rice-Evans, C. A. (2001). Flavonoid B-ring chemistry and antioxidant activity: Fast reactions kinetics. *Biochemical and Biophysical Research Communications*, 282, 1161-1168.

Patil, B. S., Pike, L. M., & Yoo, K. S. (1995). Variation in the quercetin content in different colored onions (*Allium cepa L.*). *Journal of the American Society for Horticultural Science*, 120, 909−913.

Peng, X., Cheng, K. W., Ma, J., Chen, B., Ho, C. T., Lo, C., et al. (2008). Cinnamon bark proanthocyanidins as reactive carbonyl scavengers to prevent the formation of advanced glycation endproducts. *Journal of Agricultural and Food Chemistry*, 56, 1907-1911.

Peng, X., Ma, J., Chen, F., & Wang, M. (2011). Naturally occurring inhibitors against the formation of advanced glycation end-products. *Food & Function*, 2, 289-301.

Persson, E., Graziani, G., Ferracane, R., Fogliano, V., & Skog, K. (2003). Influence of antioxidants in virgin olive oil on the formation of

heterocyclic amines in fried beefburgers. *Food and Chemical Toxicology*, 41, 1587-1597.

Picklo, M. J., Azenkeng, A., & Hoffmann, M. R. (2011). *trans*-4-Oxo-2-nonenal potently alters mitochondrial function. *Free Radical Biology & Medicine*, 50, 400-407.

Porter, N. A., Caldwell, S. E., & Mills, K. A. (1995). Mechanisms of free radical oxidation of unsaturated lipids. *Lipids*, 30, 277-290.

Price, K. R., Bacon, J. R., & Rhodes, M. J. C. (1997). Effect of storage and domestic processing on the content and composition of flavonol glucosides in onion (*Allium cepa*). *Journal of Agricultural and Food Chemistry*, 45, 938−942.

Price, K. R., & Rhodes, M. J. C. (1997). Analysis of the major flavonol glycosides present in four varieties of onion (*Allium cepa*) and changes in composition resulting from autolysis. *Journal of the Science of Food and Agriculture*, 74, 331-339.

Reische, D. W., Lillard, D. A., & Eitenmiller, R. R. (2008). Antioxidants. In: *Food Lipids: Chemistry, Nutrition, and Biotechnology*. Akoh, C. C., & Min, D. B., eds., 3rd ed., CRC Press, Boca Raton, 409-433.

Rouphael, Y., Bernardi, J., Cardarelli, M., Bernardo, L., Kane, D., Colla, G.,& Lucini, L. (2016). Phenolic compounds and sesquiterpene lactones profile in leaves of nineteen artichoke cultivars. *Journal of Agricultural and Food Chemistry*, 64, 8540−8548.

Sainsbury, J., Grypa, R., Ellingworth, J., Duodu, K. G., & De Kock, H. L. (2016). The effects of antioxidants and shelf life conditions on oxidation markers in a sunflower oil salad dressing emulsion (SOSDE). *Food Chemistry*, 213, 230–237.

Salazar, R., Arámbula-Villa, G., Hidalgo, F. J., & Zamora, R. (2014). Structural characteristics that determine the inhibitory role of phenolic compounds on 2-amino-1-methyl-6-phenylimidazo[4,5-*b*]pyridine (PhIP) formation. *Food Chemistry*, 151, 480-486.

Salazar, R., Arámbula-Villa, G., Vázquez-Landaverde, P. A., Hidalgo, F. J., & Zamora, R. (2012). Mitigating effect of amaranth (*Amarantus hypochondriacus*) protein on acrylamide formation in foods. *Food Chemistry*, 135, 2293–2298.

Sang, S., Shao, X., Bai, N., Lo, C. Y., Yang, C. S., & Ho, C. T. (2007). Tea polyphenol (-)-epigallocatechin-3-gallate: A new trapping agent of reactive dicarbonyl species. *Chemical Research in Toxicology*, 20, 1862-1870.

Satterfield, M., & Brodbelt, J. S. (2000). Enhanced detection of flavonoids by metal complexation and electrospray ionization mass spectrometry. *Analytical Chemistry*, 72, 5898-5906.

Sayre, L. M., Arora, P. K., Iyer, R. S., & Salomon, R. G. (1993). Pyrrole formation from 4-hydroxynonenal and primary amines. *Chemical Research in Toxicology*, 6, 19–22.

Schaich, K. M. (2013). Challenges in elucidating lipid oxidation mechanisms: When, where, and how do products arise? In: *Lipid Oxidation: Challenges in Food Systems*. Logan, A., Nienaber, U., & Pan, X., eds., AOCS Press, Urbana, Illinois, 1-52.

Seaman, V. Y., Bennett, D. H., & Cahill, T. M. (2009). Indoor acrolein emission and decay rates resulting from domestic cooking events. *Atmospheric Environment*, 43, 6199–6204.

Selvaraj, S., Krishnaswamy, S., Devashya, V., Sethuraman, S., & Krishnan U. M. (2014). Flavonoid-metal ion complexes: a novel class of therapeutic agents. *Medicinal Research Reviews*, 34, 677-702.

Senanayake, S. P. J. N. (2013). Green tea extract: Chemistry, antioxidant properties and food applications-A review. *Journal of Functional Foods*, 5, 1529-1541.

Shao, X., Bai, N., He, K., Ho, C. T., Yang, C. S., & Sang, S. (2008). Apple polyphenols, phloretin and phloridzin: New trapping agents of reactive dicarbonyl species. *Chemical Research in Toxicology*, 21, 2042-2050.

Shimozu, Y., Shibata, T., Ojika, M., & Uchida, K. (2009). Identification of advanced reaction products originating from the initial 4-oxo-2-nonenal-cysteine Michael adducts. *Chemical Research in Toxicology*, 22(5), 957–964.

Snedecor, G. W., & Cochran, W. G. (1980). *Statistical Methods*, 7th ed., Iowa State University Press: Ames, IA.

Sopelana, P., Arizabaleta, I., Ibargoitia, M. L., & Guillén, M. D. (2013). Characterisation of the lipidic components of margarines by ^{1}H Nuclear Magnetic Resonance. *Food Chemistry*, 141, 3357-3364.

Steel, C. J., Mara Block, J., Barrera-Arellano, D., & Mancini-Filho, J. (2012). Oxidación de lípidos. In: *Temas Selectos en Aceites y Grasas*. Volumen 2-Química. Mara Block J., & Barrera-Arellano D., eds., Blucher, Sao Paulo, 37-55.

Sulaiman, S. F., & Ooi, K. L. (2012). Polyphenolic and vitamin C contents and antioxidant activities of aqueous extracts from mature-green and ripe fruit fleshes of *Mangifera* sp. *Journal of Agricultural and Food Chemistry*, 60, 11832−11838.

Suyama, K., & Adachi, S. (1979). Reaction of alkanals and amino acids or primary amines. Synthesis of 1,2,3,5- and 1,3,4,5-substituted quaternary pyridinium salts. *Journal of Organic Chemistry*, 44, 1417–1420.

Tenyang, N., Ponka, R., Tiencheu, B., Djikeng, F. T., Azmeera, T., Karuna, M. S. L., Prasad, R. B. N., & Womeni, H. M. (2017). Effects of boiling and roasting on proximate composition, lipid oxidation, fatty acid profile and mineral content of two sesame varieties commercialized and consumed in Far-North region of Cameroon. *Food Chemistry,* 221, 1308–1316.

Totlani, V. M., & Peterson, D. G. (2005). Reactivity of epicatechin in aqueous glycine and glucose Maillard reaction models: Quenching of C2, C3, and C4 sugar fragments. *Journal of Agricultural and Food Chemistry*, 53, 4130-4135.

Totlani, V. M., & Peterson, D. G. (2006). Epicatechin carbonyl-trapping reactions in aqueous Maillard systems: Identification and structural elucidation. *Journal of Agricultural and Food Chemistry*, 54, 7311-7318.

Troise, A. D., Fiore, A., Colantuono, A., Kokkinidou, S., Peterson, D. G., & Fogliano, V. (2014). Effect of olive mill wastewater phenol compounds on reactive carbonyl species and Maillard reaction endproducts in ultrahigh-temperature-treated milk. *Journal of Agricultural and Food Chemistry*, 62, 10092−10100.

Uluata, S., McClements, D. J., & Decker, E. A. (2015). Physical stability, autoxidation, and photosensitized oxidation of ω-3 oils in nanoemulsions prepared with natural and synthetic surfactants. *Journal of Agricultural and Food Chemistry*, 63, 9333−9340.

Umano, K., & Shibamoto, T. (1987). Analysis of acrolein from heated cooking oils and beef fat. *Journal of Agricultural and Food Chemistry*, 35, 909-912.

Van Hecke, T., Vossen, E., Hemeryck, L. Y., Vanden Bussche, J., Vanhaecke, L., & De Smet, S. (2015). Increased oxidative and nitrosative reactions during digestion could contribute to the association between well-done red meat consumption and colorectal cancer. *Food Chemistry*, 187, 29–36.

Wang. Y, & Ho, C. T. (2012). Flavour chemistry of methylglyoxal and glyoxal. *Chemical Society Reviews*, 41, 4140-4149.

Wells-Knecht, K. J., Brinkmann, E., & Baynes, J. W. (1995). Characterization of an imidazolium salt formed from glyoxal and *N*α-hippuryllysine: A model for Maillard reaction crosslinks in proteins. *Journal of Organic Chemistry*, 60, 6246–6247.

Wright, J. S., Johnson, E. R., DiLabio, G. A. (2001). Predicting the activity of phenolic antioxidants: Theoretical method, analysis of substituent effects, and application to major families of antioxidants. *Journal of the American Chemical Society*, 123, 1173–1183.

Wu, C. H., Huang, S. M., Lin, J. A., & Yen G. C. (2011). Inhibition of advanced glycation endproduct formation by foodstuffs. *Food & Function*, 2, 224-234.

Xu, F., Oruna-Concha, M. J., & Elmore, J. S. (2016). The use of asparaginase to reduce acrylamide levels in cooked food. *Food Chemistry*, 210, 163-171.

Yoon, S. R., & Shim, S. M. (2015). Inhibitory effect of polyphenols in *Houttuynia cordata* on advanced glycation end-products (AGEs) by

trapping methylglyoxal. *LWT – Food Science and Technology,* 61, 158-163.

Zamora, R., Alaiz, M., & Hidalgo, F. J. (1999). Modification of histidine residues by 4,5-epoxy-2-alkenals. *Chemical Research in Toxicology*, 12, 654–660.

Zamora, R., Alcón, E., & Hidalgo, F. J. (2014). Ammonia and formaldehyde participate in the formation of 2-amino-1-methyl-6-phenylimidazo[4,5-*b*]pyridine (PhIP) in addition to create(ni)ne and phenylacetaldehyde. *Food Chemistry*, 155, 74-80.

Zamora, R., Delgado, R. M., & Hidalgo, F. J. (2009). Conversion of 3-aminopropionamide and 3-alkylaminopropionamides into acrylamide in model systems. *Molecular Nutrition and Food Research*, 53, 1512–1520.

Zamora, R., Delgado, R. M., & Hidalgo, F. J. (2010). Model reactions of acrylamide with selected amino compounds. *Journal of Agricultural and Food Chemistry,* 58, 1708–1713.

Zamora, R., Delgado, R. M., & Hidalgo, F. J. (2011). Amino phospholipids and lecithins as mitigating agents for acrylamide in asparagine/glucose and asparagine/2,4-decadienal model systems. *Food Chemistry*, 126, 104-108.

Zamora, R., Delgado, R. M., & Hidalgo, F. J. (2012). Chemical conversion of phenylethylamine into phenylacetaldehyde by carbonyl−amine reactions in model systems. *Journal of Agricultural and Food Chemistry,* 60, 5491−5496.

Zamora, R., Gallardo, E., & Hidalgo, F. J. (2006b). Amine degradation by 4,5-epoxy-2-decenal in model systems. *Journal of Agricultural and Food Chemistry*, 54, 2398-2404.

Zamora, R., Gallardo, E., & Hidalgo, F. J. (2007). Strecker degradation of phenylalanine initiated by 2,4-decadienal or methyl 13-oxooctadeca-9,11-dienoate in model systems. *Journal of Agricultural and Food Chemistry*, 55, 1308-1314.

Zamora, R., Gallardo, E., & Hidalgo, F. J. (2008). Model studies on the degradation of phenylalanine initiated by lipid hydroperoxides and their secondary and tertiary oxidation products. *Journal of Agricultural and Food Chemistry*, 56, 7970–7975.

Zamora, R., Gallardo, E., Navarro, J. L., & Hidalgo, F. J. (2005). Strecker-type degradation of phenylalanine by methyl 9,10-epoxy-13-oxo-11-octadecenoate and methyl 12,13-epoxy-9-oxo-11-octadecenoate. *Journal of Agricultural and Food Chemistry*, 53, 4583-4588.

Zamora, R., & Hidalgo, F. J. (2005). 2-Alkylpyrrole formation from 4,5-epoxy-2-alkenals.*Chemical Research in Toxicology*, 18, 342–348.

Zamora, R., & Hidalgo, F. J. (2008). Contribution of lipid oxidation products to acrylamide formation in model systems. *Journal of Agricultural and Food Chemistry*, 56, 6075–6080.

Zamora, R., & Hidalgo, F. J. (2011). The Maillard reaction and lipid oxidation. *Lipid Technology*, 23(3), 59-62.

Zamora, R., & Hidalgo, F. J. (2015). 2-Amino-1-methyl-6-phenylimidazo[4,5-*b*]pyridine (PhIP) formation and fate: an example of the coordinate contribution of lipid oxidation and Maillard reaction to the production and elimination of processing-related food toxicants. *RSC Advances*, 5, 9709–9721.

Zamora, R., & Hidalgo, F. J. (2016). The triple defensive barrier of phenolic compounds against the lipid oxidation-induced damage in food products. *Trends in Food Science & Technology*, 54, 165-174.

Zamora, R., León, M. M., & Hidalgo, F. J. (2015). Oxidative versus non-oxidative decarboxylation of amino acids: Conditions for the preferential formation of either Strecker aldehydes or amines in amino acid/lipid-derived reactive carbonyl model systems. *Journal of Agricultural and Food Chemistry,* 63, 8037−8043.

Zamora, R., Navarro, J. L., Gallardo, E., & Hidalgo, F. J. (2006a). Chemical conversion of α-amino acids into α-keto acids by 4,5-epoxy-2-decenal. *Journal of Agricultural and Food Chemistry,* 54, 6101-6105.

Zarkovic, N. (2003). 4-Hydroxynonenal as a bioactive marker of pathophysiological processes. *Molecular Aspects of Medicine*, 24, 281–291.

Zeng, Z., Ma, J., Liu, B., & Jiang, H. (2015). Amino acid-catalyzed formation of 2-vinylfuran from lipid-derived 4-oxo-2-hexenal. *Food Chemistry,* 188, 591–595.

Zheng, Z. P., Yan, Y., Xia, J., Zhang, S., Wang, M., Chen, J., & Xu, Y. (2016). A phenylacetaldehyde-flavonoid adduct, 8-*C*-(*E*-phenylethenyl)-norartocarpetin, exhibits intrinsic apoptosis and MAPK pathways-related anticancer potential on HepG2, SMMC-7721 and QGY-7703. *Food Chemistry*, 197, 1085-1092.

Zhu, Q., Liang, C. P., Cheng, K. W., Peng, X., Lo, C. Y., Shahidi, F., Chen, F., Ho, C. T., & Wang, M. (2009b). Trapping effects of green and black tea extracts on peroxidation-derived carbonyl substances of seal blubber oil. *Journal of Agricultural and Food Chemistry*, 57, 1065-1069.

Zhu, Q., Zheng, Z. P., Cheng, K. W., Wu, J. J., Zhang, S., Tang, Y. S., Sze, K. H., Chen, J., Chen, F., & Wang, M. (2009a). Natural polyphenols as direct trapping agents of lipid peroxidation-derived acrolein and 4-hydroxy-*trans*-2-nonenal. *Chemical Research in Toxicology*, 22, 1721-1727.